Karagozian & Case, Inc.
700 N. Brand Blvd., Suite 700
Glendale, CA 91203-3215
818-240-1919
www.kcse.com

TR-18-06.2

RESULTS FROM PHASE 2 BLAST TESTS OF FULL-SCALE CROSS-LAMINATED TIMBER STRUCTURES

Mark K. Weaver, S.E.[1]
Charles Newberry, P.E.[2]
Casey O'Laughlin, P.E.[3]
Lisa Podesto, P.E.[4]

[1] *Karagozian & Case, Inc. – Glendale, CA*
[2] *RTL Networks Inc. – Tyndall AFB, FL*
[3] *Jacobs Technology SLG – Fort Walton Beach, FL*
[4] *WoodWorks – Washington, DC*

October 9, 2020

The work upon which this publication is based was funded in part through a grant awarded by the FPL Coalition for Advanced Wood Structures. (Award number "17-JV-11111133-02")

EXECUTIVE SUMMARY

UFC 4-010-01 requires that inhabited Department of Defense buildings constructed of mass timber structural systems be analyzed for blast loads. As of the summer of 2015, there was a lack of test data documenting mass timber system response under the strain rates imposed by blast loads, particularly of cross-laminated timber (CLT) systems. To address this knowledge gap, a series of quasi-static laboratory and arena blast tests were performed on CLT panels and structures without axial load. Three different CLT grades (i.e., V1, E1, and V4) were investigated during these tests.

Based on this effort (i.e., the Phase 1 testing), a follow-on series of tests was planned and executed (i.e., the Phase 2 testing). These follow-on tests are the subject of the report that follows. The overarching objectives of this Phase 2 effort were to investigate:

- the response of axially-loaded CLT construction exposed to blast loads; and

- the response of alternative (from those tested in Phase 1) mass timber panel and connection configurations exposed to blast loads.

Towards this end, two distinct series of tests were performed as part of the Phase 2 effort:

- A total of twenty-four quasi-static laboratory tests were used to investigate the flatwise bending response of axially-loaded CLT panels in their major strength direction under a uniformly-applied transverse quasi-static load. These tests varied the applied axial load, CLT grade, number of panel plies, and panel length and were performed using the Air Force Civil Engineer Center's load tree testing apparatus.

- Four arena blast tests (in addition to the three tests performed in Phase 1) were performed on three existing full-scale CLT structures constructed at Tyndall Air Force Base. The first two tests were used to demonstrate the ability of axially-loaded CLT panels to resist blast loads while the second two tests were used to demonstrate the ability of alternative mass timber configurations (i.e., 5-ply panels, alternative connection types, nail-laminated timber) to resist blast loads. In both test series, the first shot was intended to keep the panels elastic and the second shot was intended to rupture panels. Ruptured panels were removed and replaced prior to performing the first test in each series.

Based on the results of these tests, the following observations and associated remarks are offered:

- Increasing axial load corresponded with decreasing CLT panel flatwise bending resistance. This finding is consistent with current NDS design equations. However, the bending and axial compression interaction equation included in Chapter 15 of the NDS consistently underpredicted the peak panel strength recorded during the laboratory tests by between 120 and 220 percent. This underprediction occurred even though average, or 50th percentile, design values were used in place of the typical code-specified five-percent exclusion design values.

- Increased panel strengths (i.e., over that associated with pin-roller boundary conditions) in the presence of axial load is expected due to the following structural phenomena:

    - Partial end restraint due to applied axial load.

    - Strengthening of finger joints and other imperfections prone to rupture in bending due to applied axial load.

    - At higher axial loads, plastic response on the bottom face of panel due to combined axial and flexural compressive stress.

    - Compression membrane action and/or axial load arching.

    - Axial compressive stress capacity exceeding that indicated in the manufacturer's literature and ANSI/APA PRG 320.

- Although this increased panel strength may safely be ignored when sizing an axially-loaded CLT panel for blast loads, it could conceivably lead to larger connection forces, particularly in the overstressed condition. As such, it is recommended that a safety factor of 1.8 be applied to *tested* connection capacities absent a more refined analysis that explicitly considers the strength-enhancing aspects of axial load.

- CLT panels exhibited an ability to safely resist superimposed axial loads following rupture. The recommended maximum displacement ductility for both load bearing and non-load bearing CLT panels exposed to blast loads is two.

- Single degree-of-freedom (SDOF) analysis methods are well-suited to approximate the displacement response of CLT panels both with and without axial load exposed to far-field blast loads.

- The static and dynamic increase factors used to approximate the expected ultimate resistance showed good correlation with the arena blast test results.

Based on the tests performed, the displacement ductility, μ, response limits listed below are recommended when designing load bearing and non-load bearing CLT construction for far-field blast loads. These response limits correspond to the qualitative damage levels defined in PDC-TR 06-08.

Stress Type	**Superficial Damage**	**Moderate Damage**	**Heavy Damage**	**Hazardous Failure**	**Blowout**
Bending (without axial load)	$\mu < 1.0$	$1.0 \le \mu < 1.5$	$1.5 \le \mu < 1.75$	$1.75 \le \mu < 2.0$	$\mu \ge 2.0$
Bending (with axial load)	$\mu < 1.0$	$1.0 \le \mu < 1.5$	$1.5 \le \mu < 1.75$	$1.75 \le \mu < 2.0$	$\mu \ge 2.0$
Flatwise shear	$\mu < 1.0$	$1.0 \le \mu < 1.5$	$1.5 \le \mu < 1.75$	$1.75 \le \mu < 2.0$	$\mu \ge 2.0$

TABLE OF CONTENTS

LIST OF FIGURES

LIST OF TABLES

LIST OF ACRONYMS

AFB	Air Force Base
AFCEC	Air Force Civil Engineering Center
AG	Accelerometer
ASD	Allowable Stress Design
CCSD	Conventional Construction Standoff Distance
CLT	Cross-Laminated Timber
DG	Displacement Gage
DIF	Dynamic Increase Factor
DoD	Department of Defense
FF	Incident (Free-Field) Pressure Gage
K-B	Kingery-Bulmash
MOR	Modulus of Rupture
MSR	Machine Stress Rated
NDS	National Design Specification for Wood Construction
NLT	Nail-Laminated Timber
RP	Reflected Pressure Gage
SDOF	Single-Degree-of-Freedom
SIF	Static Increase Factor
SPF	Spruce-Pine-Fir
SST	Simpson Strong-Tie
STS	Self-Tapping Screw
UMaine	University of Maine

CHAPTER 1

INTRODUCTION

As part of a Forest Products Laboratory Coalition for Advanced Wood Structures Grant, WoodWorks, Karagozian and Case, Inc., and the Air Force Civil Engineer Center (AFCEC) partnered via a Cooperative Research and Development Agreement to extend the Phase 1 work pertaining to the blast resistance of mass timber panels documented in Ref. [1] as part of a follow-on Phase 2 effort. The overarching objectives of this Phase 2 effort were to investigate the response of:

- axially-loaded cross-laminated timber (CLT) construction exposed to far-field blast loads; and

- alternative mass timber panel and connection configurations exposed to far-field blast loads.

This report documents the technical approach, test setup, results obtained, and conclusions generated from these Phase 2 tests.

1.1 BACKGROUND

1.1.1 Phase 1 Summary

UFC 4-010-01 [2] requires that inhabited Department of Defense (DoD) buildings constructed of mass timber structural systems be analyzed for blast loads. As of the summer of 2015, there was a lack of test data documenting mass timber system response under the strain rates imposed by blast loads. Thus, the primary objective of the Phase 1 effort was to perform testing that would demonstrate the capability of mass timber systems to resist blast loads. To achieve this primary objective, the following project objectives were defined:

- To develop analytical methodologies to analyze mass timber panels for blast loads.

- To conduct static and dynamic testing on mass timber systems as a means to obtain data to validate and/or improve the analytical methodologies developed.

- To document the capabilities afforded by the developed analytical methodologies.

- To obtain test data in a form that could serve as a reference for structural engineers interested in designing mass timber structural systems to resist blast loads.

Two mass timber systems were investigated as part of the Phase 1 effort: CLT and nail-laminated timber (NLT). Grades V1, E1, and V4 CLT as well as 2x4 and 2x6 Spruce-Pine-Fir (SPF) NLT were tested. The general process followed for each entailed the following steps:

- Develop a preliminary resistance function for use in a single-degree-of-freedom (SDOF) analysis model.

- Perform testing to investigate the post-peak response of an individual mass timber panel under a quasi-static, uniformly-applied, out-of-plane load.

- Compare the results of the quasi-static testing with the preliminary resistance function to refine the preliminary resistance function.

- Use this refined resistance function to design test articles for inclusion in blast tests intended to gather phenomenology data and demonstrate the capacity of mass timber structures subjected to blast loads.

- Perform blast tests and document the results of this testing.

- Assess the efficacy of the developed resistance function based on the results of the blast testing.

The quasi-static panel testing was performed at the University of Maine in Orono for both CLT and NLT panels. The NLT blast testing was performed using BakerRisk's shock tube facility in La Vernia, Texas, and the CLT blast testing was performed at Tyndall Air Force Base (AFB) in Panama City, Florida. The test setup, procedures, and results from these testing efforts are documented in Ref. [1]. Based on the results of these tests, the following general conclusions were made:

- Mass timber structural systems can effectively resist blast loads while remaining in the elastic range with little noticeable damage.

- The post-peak response of mass timber panels is relatively brittle. However, for CLT systems, the presence of multiple plies allows for measurable residual strength following initial panel rupture. Additionally, the two-way action inherent in CLT systems provides a means for load distribution across the panel. NLT systems do not have this advantage of cross lamination and thus do not exhibit these post-peak response benefits.

- Provided that fastener penetration is of adequate depth, significant blast loads can be resisted and transferred through CLT connections that are both simple and quick to install. An added benefit is that dowel-type connection limit states associated with CLT construction are often ductile in nature due to the propensity for the wood to crush and/or the steel connections to yield when loaded in shear beyond their respective elastic limits.

- The results of the blast testing indicated that SDOF dynamic analysis can be used to approximate peak displacements of 3-ply CLT panels without openings within the elastic range. As such, based on CLT characteristic design values and SDOF dynamic analysis calculations, conventional construction standoff distances (CCSDs) for primary gathering / billeting facilities constructed with of CLT were proposed. These proposed CCSDs for CLT construction, which are included in Ref. [1], assumed a displacement ductility, μ, response limit of 1.

1.1.2 Identified Areas for Expanded Application at End of Phase 1

Based on post-test analysis involving the results obtained from the Phase 1 testing, the SDOF resistance function generated in response to the Phase 1 testing showed promise as an appropriate method to design CLT panels to resist far-field blast loads. However, to demonstrate repeatable results, the Phase 1 arena test plan intentionally limited test parameter variation. To validate the robustness of the developed resistance function, it was deemed important to expand the understanding of these results by introducing variation to the parameters used in Phase 1 arena tests. Areas for opportunity included the following:

- Consideration of load bearing CLT panels. The testing performed in Phase 1 (i.e., both quasi-static and arena blast) focused on panels with minimal axial load. In practice, CLT panels will likely be load bearing elements.

- Consideration of other forms of panel connections. The connections used in Phase 1 consisted primarily of hot-rolled steel angles with self-tapping screws. While this is one possible connection option, pre-fabricated angle clips and connections involving self-tapping screws only are also potential connection options commonly used in CLT construction.

- Consideration of CLT panels with more than three plies. While the Phase 1 laboratory testing investigated the response of 5-ply CLT panels to a uniformly-applied, quasi-static load, the arena blast tests only had 3-ply CLT panels exposed to blast loads. In practice, CLT panels with ply numbers exceeding three may also serve as the exterior wall structural system.

- Consideration of NLT panels. While the Phase 1 laboratory testing investigated the response of NLT panels to a uniformly-applied, quasi-static load, the arena blast tests did not include NLT panels.

1.2 PHASE 2 TESTING OVERVIEW

1.2.1 Objectives

Based on the areas identified in Section 1.1.2 for extending the Phase 1 work, a series of follow-on tests were programmed for Phase 2. The overarching objectives of these tests were to demonstrate:

- the ability of loaded CLT construction to resist blast loads generated by high explosives and still support their tributary dead load following the event; and

- the ability of alternative mass timber configurations (i.e., other than those tested in Phase 1) to resist blast loads generated by high explosives. The alternative mass timber configurations considered included: (1) 5-ply CLT panels, (2) alternative connection configurations that utilized pre-fabricated brackets and self-tapping screws, and (3) NLT panels.

1.2.2 Phase 2 Tests

To address the stated objectives, two distinct series of tests were performed as part of the Phase 2 effort:

- A total of twenty-four quasi-static laboratory tests investigated the out-of-plane bending response of axially-loaded CLT panels in their major strength direction under a uniformly-applied transverse quasi-static load. These tests varied the applied axial load, CLT grade, number of panel plies, and panel length. The tests were performed using AFCEC's load tree testing apparatus.

- A total of four arena-type blast tests were performed. In these tests, the responses were measured for three full-scale CLT structures, which had previously been constructed and tested (in Phase 1) at Tyndall AFB. The first two tests were used to demonstrate the ability of axially-loaded CLT to resist blast loads. The second two tests were used to demonstrate the ability of alternative mass timber configurations to resist blast loads. In both test series, the first shot was designed to obtain an elastic response for the panels and the second shot was designed so that the panels would rupture. Before the existing three CLT structures were tested, any panels that were damaged in the previous test were removed and replaced. Table 1-1 provides an overview of the parameters that were varied during the four arena tests.

Table 1-1. Summary of Arena Test Parameters.

Test	Existing Structure CLT Grade[1]	Front Panel Description[2]	Peak 1st Floor Front Panel Axial Load[3] [plf]	Connection Description
4 & 5	V1	3-ply Grade V1 CLT	2,600	Existing[4]
	E1	3-ply Grade E1 CLT	2,175	
	V4	3-ply GradeV4 CLT	1,550	
6 & 7	V1	5-ply Grade V1 CLT	775	Existing[4]
	E1	3-ply Grade E1 CLT	525	Screws only (1st floor) Pre-fabricated brackets (2nd floor)
	V4	2x4 SPF No. 2 NLT	450	Existing[4]

1 These grades are defined in Ref. [5] and [7].
2 New versions of these panels were used for the Phase 2 tests.
3 Estimates to the nearest 25 pounds.
4 "Existing" indicates connections used during Phase 1 testing.

1.3 REPORT OUTLINE

The remainder of this report is divided into five chapters:

- Chapter 2 describes the test setup, instrumentation, results obtained, and conclusions associated with the quasi-static laboratory tests on axially-loaded CLT panels.

- Chapter 3 describes the setup for the blast tests. This includes descriptions of the CLT test structures, explosive charges, and instrumentation employed.

- Chapter 4 documents the results obtained from each of the four blast tests, which includes visual observations and the gage data for each test.

- Chapter 5 assesses the capability of an SDOF model to compute the response of CLT panels exposed to blast loads. These analysis results are compared with the blast testing gage data to evaluate their efficacy.

- Chapter 6 presents general conclusions made as a result of this testing effort, recommendations for design criteria involving blast resistant CLT panels, and suggestions for future work.

Additionally, five appendices are provided that contain references, plots and photograph results from the quasi-static testing, as-built drawings of the structures tested in Tests 4 through 7, and the quick look report prepared by AFCEC for the arena blast testing.

CHAPTER 2

LABORATORY TESTING

Quasi-static tests were conducted to investigate the flatwise bending response of axially-loaded CLT panels in their major strength direction under a uniformly-applied load. Axial load and CLT panel grade, ply number, and length were varied in these tests performed. These laboratory tests were conducted using AFCEC's load tree apparatus. This chapter documents the test setup, results, and conclusions pertaining to these tests.

2.1 BACKGROUND

The 2018 version of the *National Design Specification for Wood Construction* (NDS) [3] includes a CLT chapter (i.e., Chapter 10) that specifies adjustment factors for the various reference design values (e.g., F_bS_{eff}, $F_cA_{parallel}$). However, this chapter does not address the combined axial compression and bending loading scenario specifically for CLT panels. Equations included in the *CLT Handbook* [4] to address this scenario, which is a modified version of equation 15.4-1 in the NDS, are listed as equations (1) through (3) below:

$$\left(\frac{P}{F_c' A_{parallel}}\right)^2 + \frac{M + P\Delta\left(1 + 0.234\frac{P}{P_{cE}}\right)}{F_b' S_{eff}\left(1 - \frac{P}{P_{cE}}\right)} \leq 1.0 \tag{1}$$

$$P_{cE} = \frac{\pi^2 EI'_{app-min}}{l_e^2} \tag{2}$$

$$EI_{app-min} = 0.5184 EI_{app} \tag{3}$$

where:

P	=	Applied axial load
M	=	Applied bending moment
Δ	=	Eccentricity of axial load measured perpendicular to the plane of the panel
l_e	=	Effective column length
EI_{app}	=	Apparent bending stiffness (see Equation 10.4-1 of the NDS [3])
F_c	=	Allowable stress design (ASD) reference compression design value parallel to grain
$A_{parallel}$	=	Area of cross section of CLT layers with fibers parallel to the load direction

F_bS_{eff} = ASD reference flatwise bending design value

Variables with a prime indicate that these values have been adjusted according to the adjustment factors defined in the NDS [3]. The reference design values shown in these equations are defined in manufacturer's literature or ANSI/APA PRG 320 [5].

For a given axial load, equation (1) can be reorganized to compute the ASD bending moment capacity, M_{ASD}:

$$M_{ASD} = F_b' S_{eff}\left(1 - \frac{P}{P_{cE}}\right)\left[1 - \left(\frac{P}{F_c' A_{parallel}}\right)^2\right] - P\Delta\left(1 + 0.234\frac{P}{P_{cE}}\right) \quad (4)$$

If pin-roller boundary conditions are assumed, equation (5) can be used with equation (4) to compute the maximum ASD uniform load, r_{ASD}, that can be resisted by the axial load bearing CLT panel:

$$r_{ASD} = \frac{8M_{ASD}}{l_e^2} \quad (5)$$

To transform ASD values to 50th percentile values, the $F_b'S_{eff}$ and $F_c'A_{parallel}$ capacities can be multiplied by the static increase factor (SIF) for bending, SIF_b, and compressive stress parallel to grain, SIF_c, respectively, defined in PDC-TR 18-02 [14]. Additionally, the load duration factor, C_D, defined in the NDS [3] can be used to adjust for the actual load duration (e.g., 1.6 for a 10-minute load duration). Finally, EI_{app} can be substituted for $EI_{app\text{-}min}$, as the 0.5184 reduction factor shown in equation (3) is used to transform an average value to a minimum value [4]. Thus, assuming the axial load eccentricity is zero, pin-roller boundary conditions, and a ten-minute load duration, the expected ultimate uniform load resistance, r_u, for an axial load bearing CLT panel is:

$$r_u = \frac{8 * SIF_b * 1.6 * F_b' S_{eff}}{l_e^2}\left(1 - \frac{P l_e^2}{\pi^2 EI_{app}'}\right)\left[1 - \left(\frac{P}{SIF_c * 1.6 * F_c' A_{parallel}}\right)^2\right] \quad (6)$$

2.2 TEST SETUP

A total of twenty-four CLT panels were tested. Panels were either 12 or 14 feet long in the major strength direction and either 48 inches wide (3-ply panels) or 16 inches wide (5-ply panels). Different panel widths were used to ensure the testing apparatus could break the panel. The test matrix listing the different configurations tested is presented as Table 2-1. The axial loads included in the test matrix were meant to bound and be representative of loads that a load bearing CLT wall could potentially experience.

Panel characteristics, including individual board characteristics and finger jointing, were consistent with those tested at the University of Maine in the Phase 1 testing [6]. Each ply for every panel tested was $1^3/_8$ inches thick, which resulted in 3-ply panels that were $4^1/_8$ inches thick and 5-ply panels that were $6^7/_8$ inches thick. All panels had a moisture content of less than 15 percent at the time of testing.

Table 2-1. Quasi-Static Testing Specimen Matrix.

Grade	Ply No.	L [in]	b [in]	QTY	$\%F_c^{*}$ [1,2]	Axial Load [2,3] [k]
V1	3	144	48	9	2@0, 5, 3@10, 20, 30, 40	2@0, 15, 3@29, 58, 86, 115
V1	5	144	16	6	0, 5, 10, 20, 30, 40	0, 8, 15, 29, 43, 58
E1	3	144	48	3	3@10	39
V4	3	144	48	3	3@10	22
V1	3	168	48	3	3@10	29

1 F_c^* refers to the ASD reference axial compressive stress, F_c, noted in manufacturer's literature [7] or ANSI/APA PRG 320 [5] multiplied by all applicable NDS adjustment factors except the column stability factor, C_p. F_c^* is 2,160 psi, 2,880 psi, and 1,600 psi for the Grades V1, E1, and V4 CLT panels, respectively. These values assume a load duration factor, C_D, of 1.6.

2 For the 0% F_c^* cases, although no axial load was applied to the CLT panel by the horizontally-oriented actuator, its load platens were fixed translationally. Thus, the platens passively imparted axial load to the panel as it was displaced upward (i.e., see Appendix B for axial load versus time measurement).

3 Axial loads were determined by multiplying F_c^* by $A_{parallel}$ (i.e., 132 in^2 for the 3-ply panels and 66 in^2 for the 5-ply panels), and the noted percentage F_c^*, and then rounding this value up to the nearest 1,000 pounds.

The load tree testing apparatus at AFCEC was used to perform these tests (Figure 2-1). The load tree uses actuator-controlled cylindrical steel tubes to apply a progressively-increasing uniform out-of-plane load by pulling test panels upwards while simultaneously applying a constant axial load via another actuator.

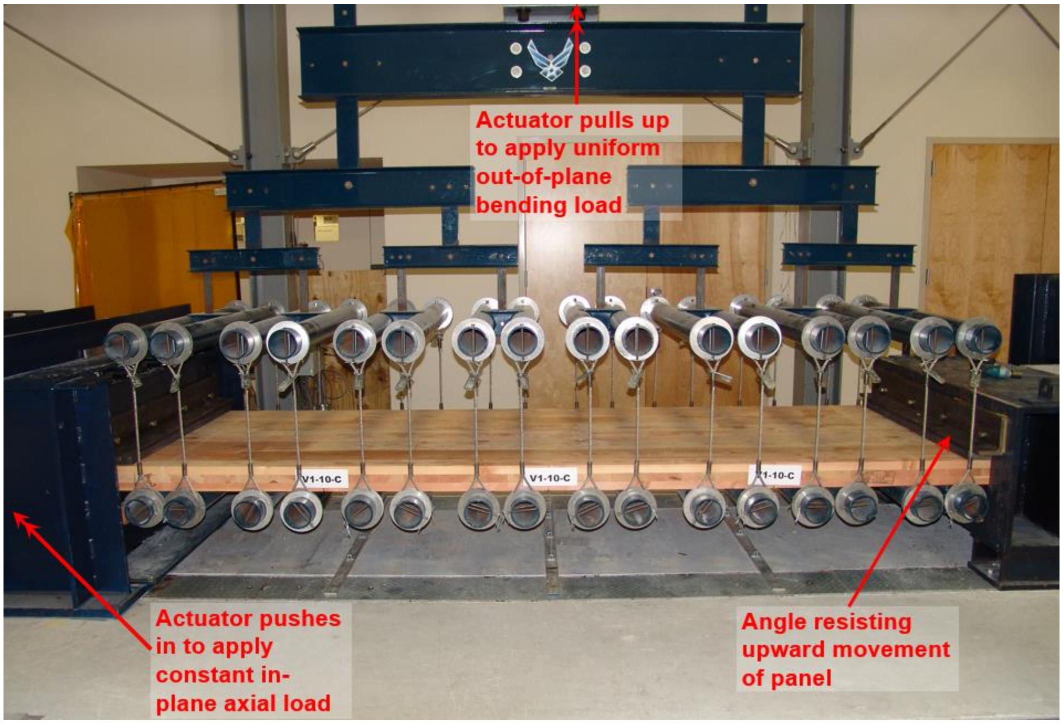

Figure 2-1. Load Tree Testing Apparatus.

Panel ends were supported by an L6x4x3/4 angle with its long leg oriented vertically. As such, the unsupported span, l_e, for the 12-foot long test panels was 136 inches and for the 14-foot long test panels was 160 inches. This angle and its connection were designed to remain elastic for all tests performed. To support the panel prior to beginning the test, an L6x4x3/8 steel angle (i.e., for test V1-10-A) or a 2x4 wood block (i.e., for the remainder of the tests) was used. The distance between the bottom of the L6x4x3/4 angle and top of the bottom angle/block was equal to 9.5 inches to ensure no rotational restraint, apart from that imparted by the applied axial load, was included in the test setup. For the 3-ply panels tested, a 1.5-inch thick shim plate was used to center the panel on the horizontally-oriented actuator applying the axial load.

Inherent with the utilization of a bearing angle is the introduction of an artificial restraint at the ends of the panel. The source of this artificial restraint is shown schematically in Figure 2-2. Essentially, the uniform load applied by the load tree directly beneath the angle, W_{LT}, and the friction force associated with the axial load between the panel and the load platen, F_N, combine to generate an artificial restraining moment, M_A, about the tip of the bearing angle. This moment serves to augment the peak strength of the panel but would not necessarily be indicative of the as-installed condition. As such, the peak strengths shown in this chapter include a correction to account for this artificial restraining moment.

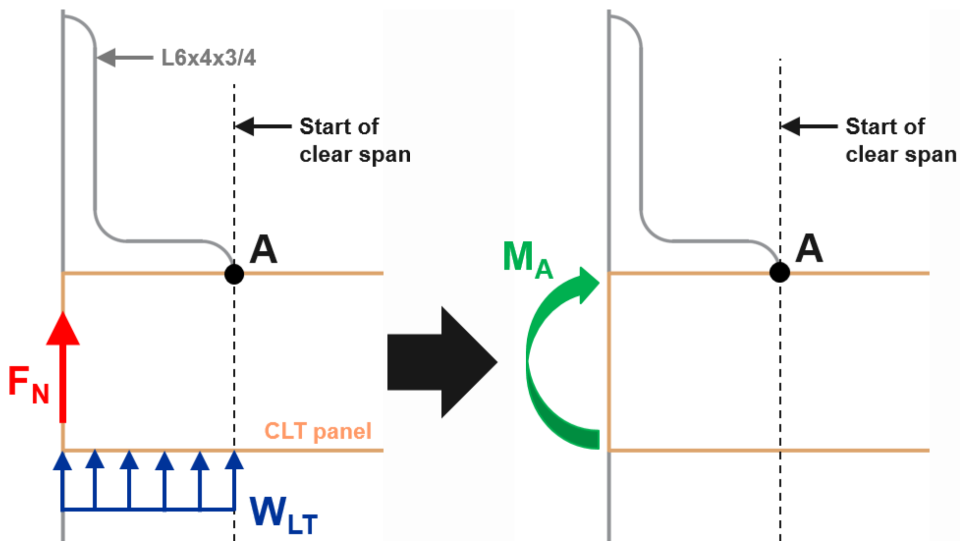

Figure 2-2. Artificial Restraining Moment Diagram.

Panel displacements were measured at quarter points; three string potentiometers were used at each quarter point for the 48-inch wide panels and one string potentiometer was used at each quarter point for the 16-inch wide panels. Load cells were used to measure applied in-plane (via actuator) and out-of-plane (via steel tubes) forces. Additionally, video of the panel's profile was recorded for each test.

Tests were initiated by loading the panels in the in-plane (axial) direction up to the prescribed axial load shown in Table 2-1 at a maximum rate of 1,000 pounds per minute. Once the axial load was reached, the panels were then displaced upward at a rate of 0.5-inch/min (i.e., as measured at the top of the load tree) using the collection of steel tubes. Axial load was maintained in the panel via force control except for panels with an axial load of 0% F_c^*, as was mentioned in footnote 2 in Table 2-1. Tests were typically completed within 15 minutes.

2.3 RESULTS

The peak measured uniform load resistance of panels ranged from 5.6 to 8.6 psi for the 12-foot 3-ply panels, from 3.9 to 5.9 psi for the 14-foot 3-ply panels, and from 16.0 to 18.2 psi for the 5-ply panels. These strengths were obtained by dividing the load measured at the actuator responsible for pulling up the panels by the total panel area (i.e., 6,912 in^2 for the 12-foot 3-ply panels, 8,064 in^2 for the 14-foot 3-ply panels, and 2,304 in^2 for the 5-ply panels). Table 2-2 lists the measured peak panel strengths as well as the observed panel damage.

Table 2-2. Summary of Quasi-Static Test Results.

ID		Grade	Ply No.	Clear Span [in]	$\%F_c^*$	Peak Strength [psi]	Observed Damage Associated with Peak Strength
Test	Panel ID						
S1	V1-00-A	V1	3	136	0	7.85	Bending rupture and rolling shear simultaneously
S2	V1-00-B					8.01	Bending rupture
S3	V1-05-A				5	8.58	Bending rupture with late time rolling shear
S4	V1-10-A				10	6.65	Bending rupture
S5	V1-10-B					7.05	Bending rupture
S6	V1-10-C					6.99	Bending rupture
S7	V1-20-A				20	7.03	Bending rupture
S8	V1-30-A				30	6.47	Bending rupture
S9	V1-40-A				40	5.59	Bending rupture
S10	5V1-00-A		5		0	17.01	Bending rupture
S11	5V1-05-A				5	16.26	Top ply detachment followed by rupture
S12	5V1-10-A				10	18.21	Rolling shear
S13	5V1-20-A				20	17.81	Top ply detachment followed by rupture
S14	5V1-30-A				30	16.96	Top ply detachment followed by rupture
S15	5V1-40-A				40	15.96	Top ply detachment followed by rupture
S16	E1-10-A	E1	3		10	6.02	Bending rupture
S17	E1-10-B					5.71	Bending rupture
S18	E1-10-C					5.87	Bending rupture
S19	V4-10-A	V4				5.89	Bending rupture
S20	V4-10-B					5.55	Bending rupture
S21	V4-10-C					5.75	Bending rupture
S22	V1-10-14-A	V1		160		3.93	Bending rupture
S23	V1-10-14-B					5.93	Bending rupture
S24	V1-10-14-C					5.37	Bending rupture

Panel rupture typically occurred near mid-span at knots, finger joints, or sloped grain (Figure 2-3a). This result was consistent with findings in the Phase 1 tests and expected because these material imperfections engender stress concentrations. (It should be noted that the grading of the constituent lumber in CLT panels accounts for the frequency of these imperfections.) No visual signs of wood crushing were observed, although the out-of-plane pressure versus displacement plots appeared to indicate that some occurred for the higher axial loads.

For a few tests with lower axial loads, planar (or rolling) shear damage appeared to occur (Figure 2-3b). Additionally, in most of the 5-ply panel tests, portions of the top-most ply detached from the crosswise ply near panel mid-span prior to rupturing in tension (Figure 2-3c). Whether or not the "rolling shear" noted in Table 2-2 is instead more aptly characterized as "top ply detachment followed by rupture" could be argued.

For all tests with an axial load greater than or equal to 10% F_c^*, (i.e., except for the Grade V4 panels) damage to either the top or side of the panel was observed near the support. (It is suspected that the Grade V4 panels did not exhibit this damage because it had the smallest ASD reference axial compressive stress value (i.e., 1,000 psi) and thus the smallest applied axial load of any grade at 10% F_c^*. This damage consisted of crushing due to the concentrated compressive stress imparted by the bearing support angle (Figure 2-3d) or splitting due to the tension perpendicular to grain stress associated with the friction force applied by the load platen (Figure 2-3e and f).

(a) Bending rupture (V1-10-B).

(b) Rolling shear (5V1-10-A).

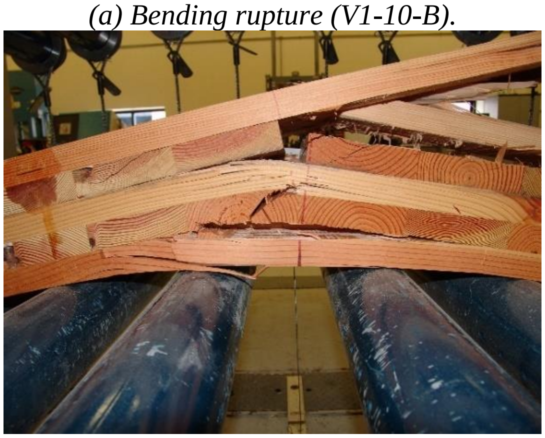

(c) Top ply detachment followed by rupture (5V1-20-A).

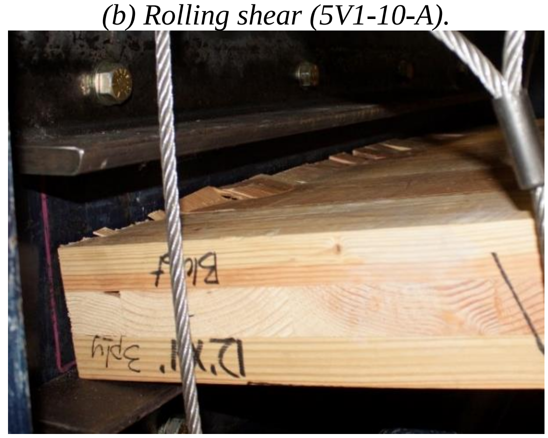

(d) Crushing at top of panel (V1-10-A).

Figure 2-3. Examples of Observed Damage.

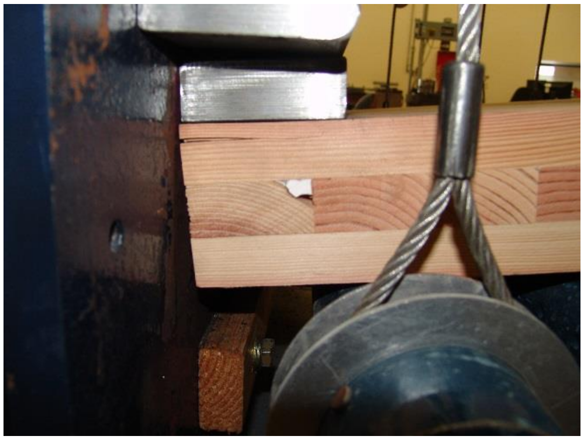

(e) Splitting at side of panel (V1-20-A).

(f) Splitting at end of panel (E1-10-A).

Figure 2-3. Examples of Observed Damage. (Cont'd)

The plots included in this chapter often include a gray "S-S" reference line. This reference line represents the theoretical expected elastic response of the panel specimen assuming idealized pin-roller boundary conditions and ignoring the effects of axial load. Apart from the dynamic increase factor (DIF) being set equal to 1.6, the process by which this reference line was generated is consistent with the approach outlined in Section 5.2.

The out-of-plane pressure versus mid-span displacement plot for the 12-foot 3-ply Grade V1 panels with an applied axial load of 10% F_c^* is shown in Figure 2-4. This plot displays some common characteristics observed throughout the test data obtained. While the initial stiffness of the panel exceeds that associated with pin-roller boundary conditions, at approximately 0.5 inches of displacement its stiffness transitions to that of the S-S reference line. This suggests that this initial stiffness anomaly is related to the non-ideal condition at the panel's support. Upon reaching peak strength at approximately 4 inches of displacement, the panels exhibit a sudden drop in capacity of various magnitudes until they have negligible out-of-plane load carrying capacity.

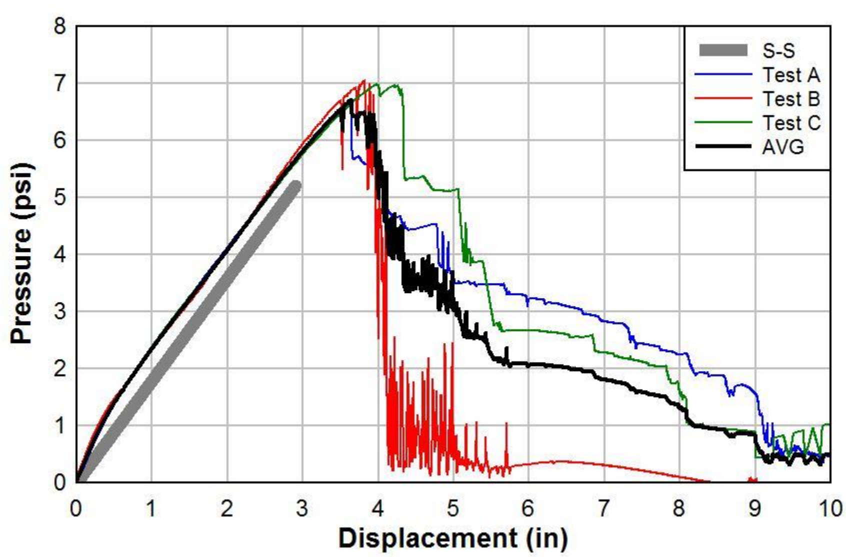

Figure 2-4. Typical Uncorrected Out-of-Plane Pressure vs. Displacement Plot [12-Foot 3-Ply Grade V1].

To account for the artificial restraining moment introduced by the bearing angle, a strength correction was computed as discussed in Section 2.1 and illustrated in Figure 2-2. This correction factor was subtracted from the measured peak strengths shown in Table 2-2 to obtain corrected peak strengths. Table 2-3 records the corrected peak strength of each panel as well as the computations used to derive this correction. Figure 2-5 illustrates the impact of this correction on the data for the 12-foot 3-ply Grade V1 panels with 10% F_c^* axial load.

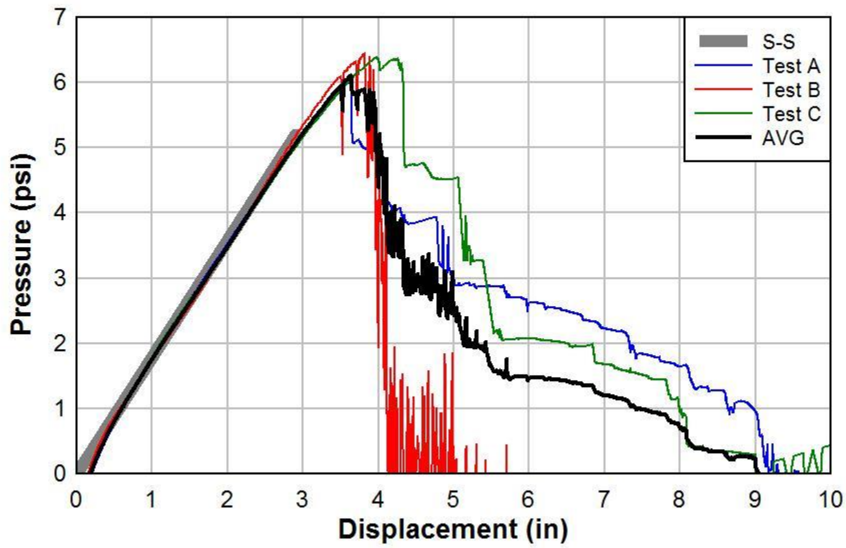

Figure 2-5. Typical Corrected Out-of-Plane Pressure vs. Displacement Plot [12-Foot 3-Ply Grade V1].

By subtracting out the resistance associated with the artificial restraining moment, the loading stiffness of the axially-loaded panel aligns well with that associated with pin-roller boundary conditions. It is also interesting to note that the damage exemplified in Figure 2-3d through Figure 2-3f enabled the panel to rotate relatively freely about point "A" in Figure 2-2 during the course of the test.

For several panels, the computed theoretical correction, r_{A_TH}, was so large that at no point did the corrected curve intersect with the S-S reference line, which is not physically possible. This phenomenon is illustrated in Figure 2-6. (A simple reason for this divergence of the theoretical from the actual could simply be the damage observed at the end of the panel, which would partially relieve the artificial restraint depicted by the free-body diagram included in Figure 2-2. Also, the assumed coefficient of friction between wood and steel was 0.60, but this assumption is merely an approximation of the actual coefficient of friction.) When this phenomenon occurred, the out-of-plane pressure versus displacement curve was offset in the y-direction such that the S-S reference line was tangent with the measured test data. The net movement downward of the test data is the actual correction, r_{A_ACT}, listed in Table 2-3. It is acknowledged that this correction process is approximate at best; however, it provides a means to interpret the peak strength data obtained in a consistent fashion without the obfuscation associated with the artificial restraining moment. It should also be noted that the simple theoretical model well approximates the observed artificial strength increase in most cases, as illustrated by the general good agreement of r_{A_TH} and r_{A_ACT} in Table 2-3.

Table 2-3. Summary of Peak Strengths with Correction.

Panel ID	$\%F_c$*	Peak Strength [psi]	W_{LT} [1] [k/in]	F_N [2] [k]	M_{A_TH} [3] [k-in]	r_{A_TH} [4] [psi]	r_{A_ACT} [5] [psi]	Corrected Peak Strength [6] [psi]
V1-00-A	0	7.85	0.38	0.0	3.0	0.03	0.03	7.82
V1-00-B		8.01	0.38	0.0	3.1	0.03	0.03	7.98
V1-05-A	5	8.58	0.41	9.0	39.3	0.35	0.35	8.23
V1-10-A	10	6.65	0.32	17.4	72.2	0.65	0.60	6.05
V1-10-B		7.05	0.34	17.4	72.3	0.65	0.60	6.45
V1-10-C		6.99	0.34	17.4	72.3	0.65	0.60	6.39
V1-20-A	20	7.03	0.34	34.8	141.9	1.28	0.80	6.23
V1-30-A	30	6.47	0.31	51.6	208.9	1.88	1.25	5.22
V1-40-A	40	5.59	0.27	69.0	278.1	2.51	1.00	4.59
5V1-00-A	0	17.01	0.27	0.0	2.2	0.06	0.06	16.95
5V1-05-A	5	16.26	0.26	4.8	21.3	0.58	0.58	15.68
5V1-10-A	10	18.21	0.29	9.0	38.3	1.04	1.04	17.17
5V1-20-A	20	17.81	0.28	17.4	71.9	1.94	1.94	15.87
5V1-30-A	30	16.96	0.27	25.8	105.4	2.85	2.85	14.11
5V1-40-A	40	15.96	0.26	34.8	141.2	3.82	3.45	12.51
E1-10-A	10	6.02	0.29	23.4	95.9	0.86	0.70	5.32
E1-10-B		5.71	0.27	23.4	95.8	0.86	0.70	5.01
E1-10-C		5.87	0.28	23.4	95.9	0.86	0.70	5.17
V4-10-A		5.89	0.28	13.2	55.1	0.50	0.50	5.39
V4-10-B		5.55	0.27	13.2	54.9	0.49	0.49	5.06
V4-10-C		5.75	0.28	13.2	55.0	0.50	0.50	5.25
V1-10-14-A		3.93	0.19	17.4	71.1	0.46	0.46	3.47
V1-10-14-B		5.93	0.28	17.4	71.9	0.47	0.47	5.46
V1-10-14-C		5.37	0.26	17.4	71.7	0.47	0.47	4.90

1. Uniform load applied by the load tree; equal to "Peak Strength" multiplied by the width of the panel.
2. Friction force associated with the applied axial load; equal to the axial load (see Table 2-1) multiplied by a wood-steel coefficient of friction of 0.6.
3. Moment about point "A" in Figure 2-2 due to W_{LT} and F_N.
4. Theoretical peak strength correction; equal to $8M_{A\_TH} / bl_e^2$.
5. Smaller of r_{A_TH} or the largest y-direction offset to make the measured test data be tangent with the S-S reference line.
6. Equal to "Peak Strength" minus r_{A_ACT}.

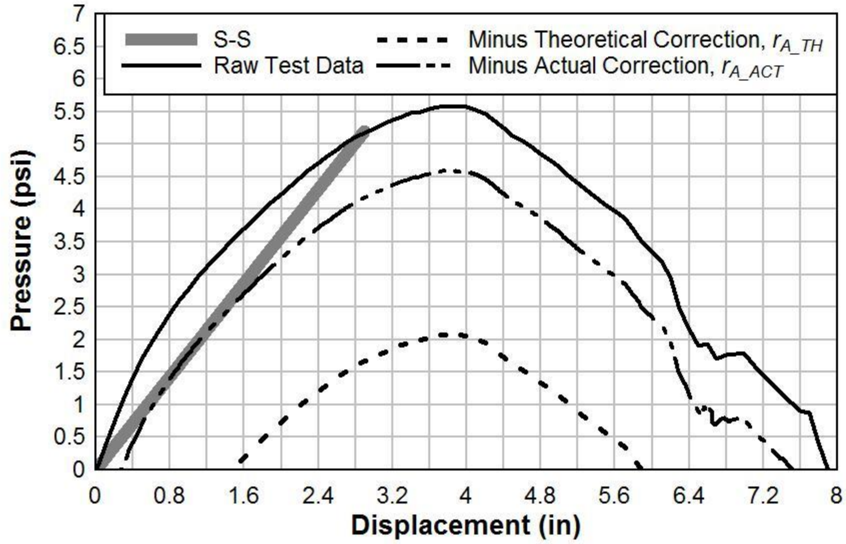

Figure 2-6. Theoretical vs. Actual Correction Divergence (V1-40-A).

Data documenting each test performed is included in Appendix B. For each test, two plots are included:

(1) applied axial load versus time, and

(2) applied uncorrected out-of-plane load versus mid-span displacement.

Photographs documenting the post-test condition of panel specimens are included as well.

The remainder of this chapter presents results according to the parameters varied in the test matrix (i.e., CLT grade, axial load, and panel length).

2.3.1 CLT Grade Variation

Figure 2-7 plots the average mid-span out-of-plane pressure versus displacement data for the 12-foot 3-ply panels resisting an axial load of 10% F_c^*. Both uncorrected and corrected plots are included. Several comments are made concerning the plots in Figure 2-7:

(1) The loading stiffness in the corrected plots aligns well with the S-S reference line for the Grades V1 and E1 panels. However, the Grade V4 panels' loading stiffness does not align well with the S-S reference line. Upon reviewing the photographs for the Grade V4 panels, it is apparent that limited damage occurred at the end of these panels, which would help explain why the loading stiffness does not fully transition to run parallel with the S-S reference line for this grade and axial load combination (Figure 2-8).

(2) The post-peak response of the Grade E1 panels appear to be more ductile and less prone to sudden drops in capacity than that of the Grade V1 and V4 panels. The plots in Appendix B and Figure 2-9 illustrate this observation more clearly.

(3) For all tests, the peak strength exceeds that associated with pin-roller boundary conditions.

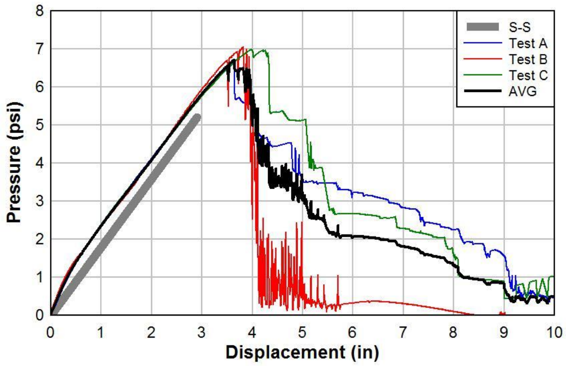

(a) Grade V1 (Uncorrected).

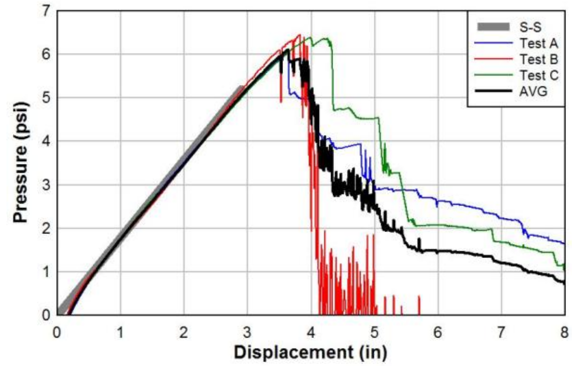

(b) Grade V1 (Corrected).

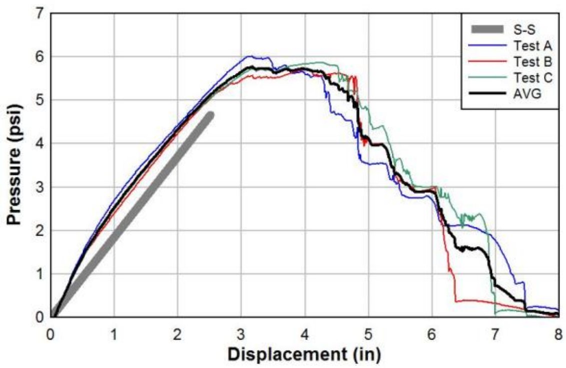

(c) Grade E1 (Uncorrected).

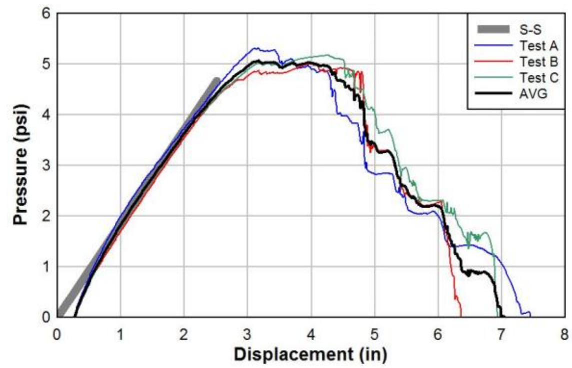

(d) Grade E1 (Corrected).

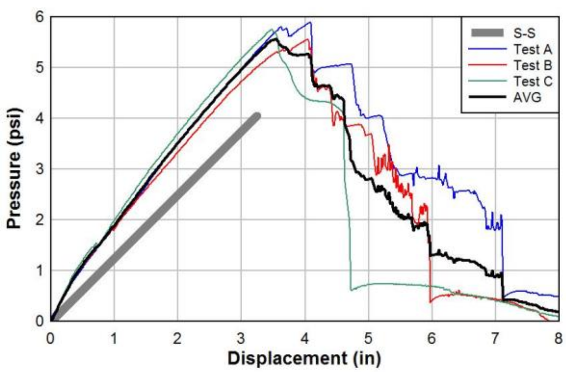

(e) Grade V4 (Uncorrected).

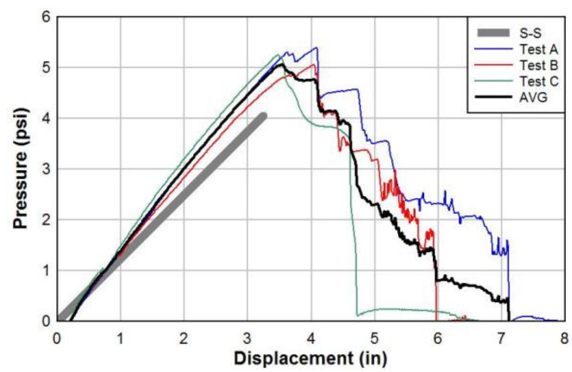

(f) Grade V4 (Corrected).

Figure 2-7. Pressure-Displacement Plots for 12-Foot 3-Ply Panels (Axial Load: 10%F_c^*).

(a) V4-10-A.

(b) V4-10-C.

Figure 2-8. Typical Grade V4 End of Panel Damage (Axial Load: 10%F_c^*).

(4) For the Grade E1 and V4 panels, a point was reached at which the panels had no residual capacity. Although not shown in Figure 2-7, this phenomenon was exhibited by the Grade V1 CLT as well, albeit at larger displacements.

(5) The CLT grades with visually graded lumber in their major strength direction ply (i.e., V1 and V4) were comparable in strength to the CLT grade with machine stress rated (MSR) lumber in its major strength direction (i.e., E1) even though the ASD bending moment capacities reported by manufacturer's literature [7] and ANSI/APA PRG 320 [5] for Grades V1 and V4 are less than half of that of Grade E1.

Representative photographs of the typical localized top of panel damage at mid-span incurred during these tests are included in Figure 2-9a, Figure 2-9b, and Figure 2-9c for the Grade V1, E1, and V4 panels, respectively.

(a) Grade V1 (V1-10-B).

(b) Grade E1 (E1-10-A).

(c) Grade V4 (V4-10-C).

Figure 2-9. Photographs of Panel Mid-Span Damage by CLT Grade (Axial Load: 10%F_c^*).

These photographs illustrate the phenomenon noted in comment (2) above, namely that the Grade E1 panels exhibited greater post-peak residual capacity and fewer sudden drops in capacity. Instead of the points of rupture localizing at finger joints or knots, as was typically observed in the Phase 1 testing and for the CLT composed of solely visually graded lumber, it appears a "hinge" is formed at panel mid-span and that the wood ruptures near this hinge. Finger joint orientation combined with modulus of rupture (MOR) variability could at least partially account for this difference in post-peak response. Whereas the Grade V1 and V4 panels have finger joints consisting of vertical grooves (Figure 2-10a), the Grade E1 panels have finger joints consisting of horizontal grooves (Figure 2-10b). The presence of axial load could serve to better "lock" the finger joints and minimize the potential for this discontinuity to serve as a point of failure. This combined with the lower MOR variation for MSR lumber could serve to localize failure and force rupture in sections of wood absent imperfection, which may enable more incremental, rather than large sudden, drops in flatwise bending capacity.

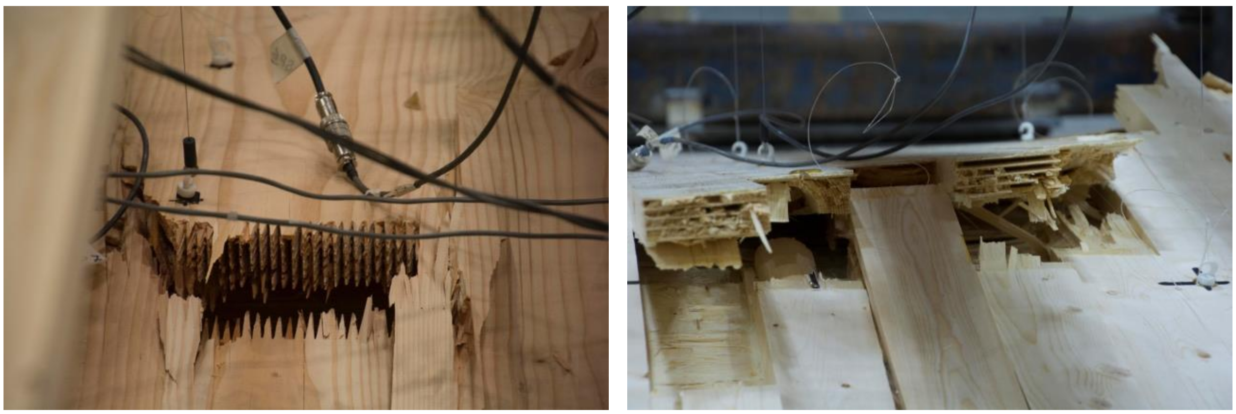

(a) Grade V1 (Grade V4 similar). *(b) Grade E1.*

Figure 2-10. Finger Joint Orientation in Panels.

2.3.2 Axial Load Variation

Figure 2-11 plots the average mid-span out-of-plane pressure versus displacement data for the 12-foot 3-ply and 5-ply panels resisting various axial loads. Both uncorrected and corrected plots are included. Several comments are made concerning the plots in Figure 2-11:

(1) Based on the results in Table 2-3 and these plots, it is apparent that greater axial load generally corresponds with reduced flatwise bending strength. This finding is in keeping with the equation (6). It is interesting to note that a small amount of axial load appears to relatively significantly augment the strength of the panel over that associated with pin-roller boundary conditions.

(2) This observation that a small amount of axial load is potentially helpful could be tied to several structural phenomena: (1) compression membrane action (i.e., for the 0% F_c^* case), (2) panel arching due to axial load (i.e., for the 5% F_c^* case), (3) effective increase of tension bending stress due to a pre-compression load, and (4) partial end restraint due to applied axial load.

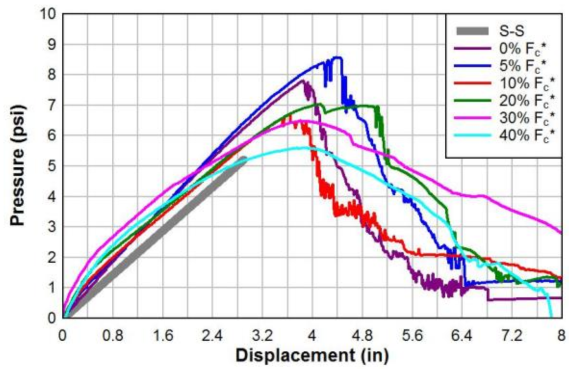

(a) 3-Ply (Uncorrected).

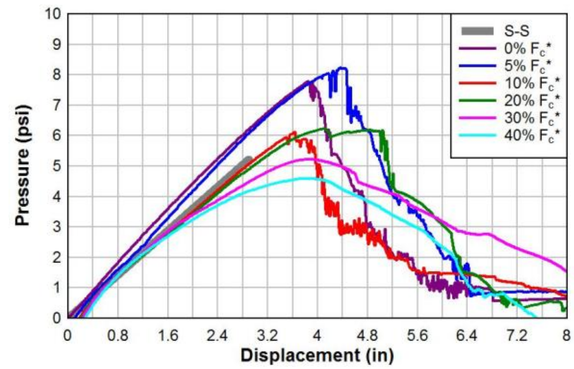

(b) 3-Ply (Corrected).

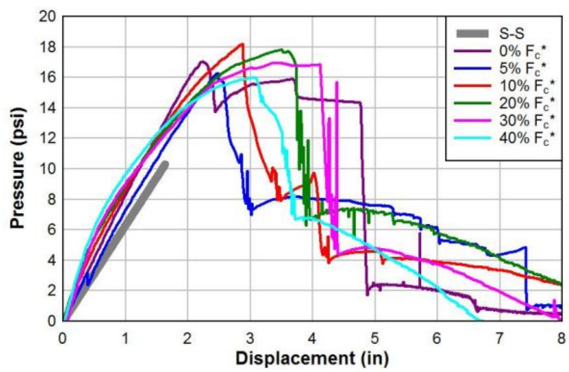

(c) 5-Ply (Uncorrected).

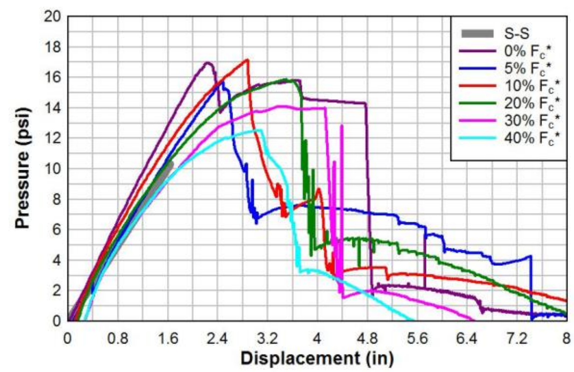

(d) 5-Ply (Corrected).

Figure 2-11. Pressure-Displacement Plots for 12-Foot Grade V1 CLT Panels at Various Axial Loads.

(3) The loading stiffness for the 0% F_c^* and 5% F_c^* cases for both 3-ply and 5-ply panels, as well as the 10% F_c^* case for 5-play panels, is noticeably higher than that for the remaining cases. Not surprisingly, these are the cases in which negligible localized damage was observed at panel ends (Figure 2-12a) when compared to other tests (Figure 2-12b).

(4) The greater the axial load, the earlier (in terms of out-of-plane displacement) the stiffness begins to decrease prior to reaching peak strength. This result may be associated with the bottom of the panel crushing under high levels of compression stress. Although no visible signs of crushing were observed following the tests, it is interesting to compare the damage patterns at the top of the panel at mid-span across several axial loads. Figure 2-12c and Figure 2-12d provides photographs for top of panel damage for 10% F_c^* and 40% F_c^*, respectively. Comparing the photographs indicates that the damage associated with 40% F_c^* is localized around a central "hinge" at panel mid-span while the 10% F_c^* failure is concentrated at finger joints and other material imperfections.

(5) Furthermore, comparing the softening stiffnesses following peak response with axial load indicates there is more ductility associated with the higher axial load failures, further supporting the supposition that a relatively ductile compression crushing response is controlling over a more brittle tension rupture response.

(6) The panel in 5V1-05-A appears to exhibit a partial premature failure, which could explain why this panel's strength appears to be abnormally low as compared to that of the remaining 5-ply panels.

(7) It is interesting to note that the theoretical artificial restraining moment matches well for most of the 5-ply panels unmodified while the simple theoretical model greatly overrepresents the restraining moment for the 3-ply panels at higher axial loads (Table 2-3). Panel thickness clearly is related to the percentage of the theoretical artificial restraining moment that can develop.

(a) 3-ply, 5% F_c^*.

(c) 3-ply, 10% F_c^*.

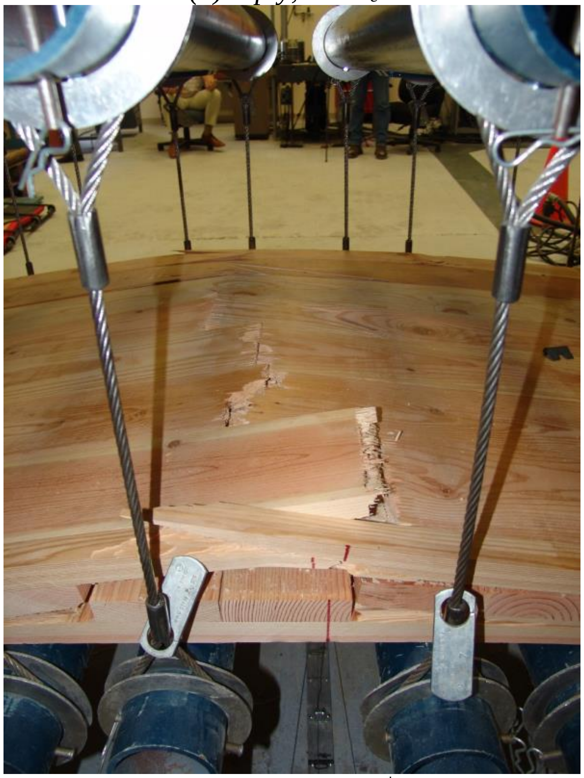

(c) 3-ply, 10% F_c^*.

(d) 3-ply, 40% F_c^*.

Figure 2-12. Photographs for 12-Foot Grade V1 CLT Panels at Various Axial Loads .

2.3.3 Panel Length Variation

Figure 2-13 plots the average mid-span out-of-plane pressure versus displacement data for the 14-foot 3-ply panels resisting an axial load of 10% F_c^*. Both uncorrected and corrected plots are included. Many of the same trends previously noted are apparent in this pressure-displacement plot as well. One unique aspect is the presence of a partial premature failure that leads to a corrected peak panel strength that is less than that associated with pin-roller boundary conditions. Out of the twenty-four tests performed, this phenomenon was only observed in this test.

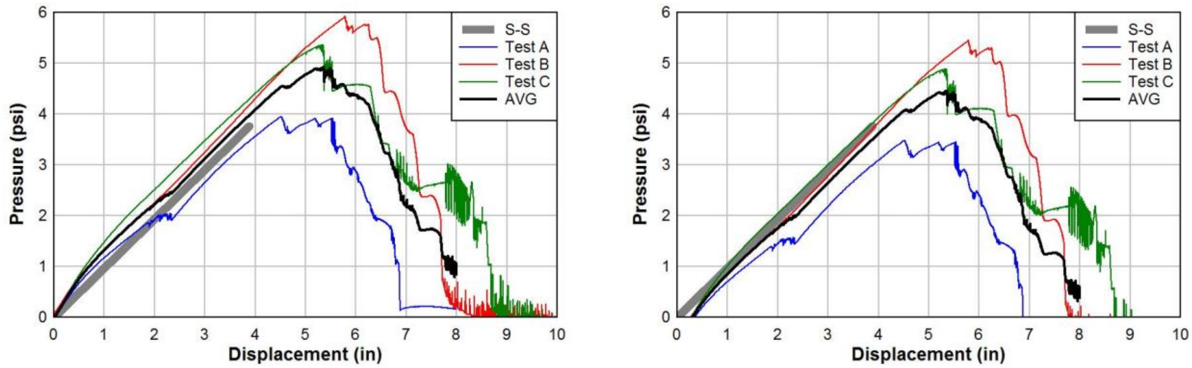

(a) Uncorrected. (b) Corrected.

Figure 2-13. Pressure-Displacement Plots for 14-Foot 3-Ply Panels (Axial Load: 10%F_c^*).

2.4 COMPARISONS WITH PHASE 1 QUASI-STATIC TESTING

This section compares the results of this quasi-static testing effort, which displaced axially-loaded CLT panels upward at a constant rate, with the Phase 1 quasi-static testing that displaced non-axially-loaded CLT panels upward at a constant rate. It should be noted that the panel lengths differed between the two efforts (i.e., 10 feet for Phase 1 versus 12 or 14 feet for Phase 2).

To assist in making comparisons, the Phase 1 pressure-displacement plots are reproduced in Figure 2-14. As with the other plots in this chapter, a reference line indicating the theoretical expected response of the panel assuming an idealized pin-roller boundary condition is included as well.

Several comments can be made concerning these comparisons of the Phase 1 and 2 plots:

(1) Generally, panels with axial load exhibited larger ratios of measured to theoretical expected ultimate resistances than for those without axial load. Table 2-4 tabulates this ratio for the Phase 1 and 2 testing. Two notable exceptions were the 30% F_c^* and 40% F_c^* cases.

(2) Panel softening (i.e., loss of capacity observed with increasing accrual of plastic strain) appeared to be more gradual in panels with measurable axial load than for those without axial load.

(3) A point was reached at which the axially-loaded CLT panels completely lost out-of-plane capacity. No such point was observed for panels without axial load (i.e., there was always

a measurable residual capacity up until the potentiometers ran out of stroke at roughly 10 inches of out-of-plane displacement).

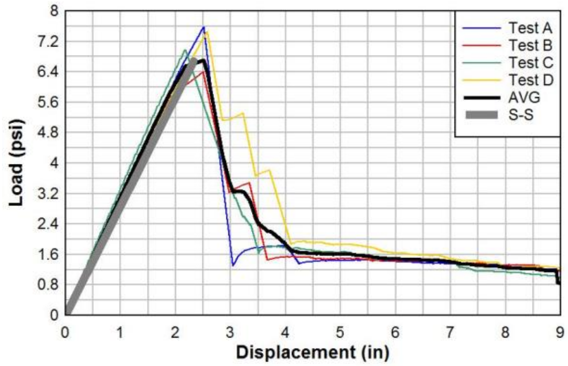

(a) 3-Ply Grade V1.

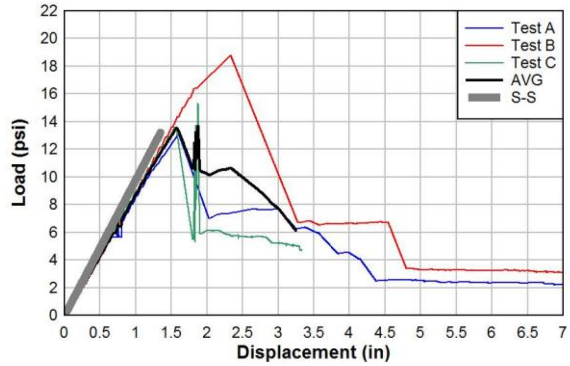

(b) 5-Ply Grade V1.

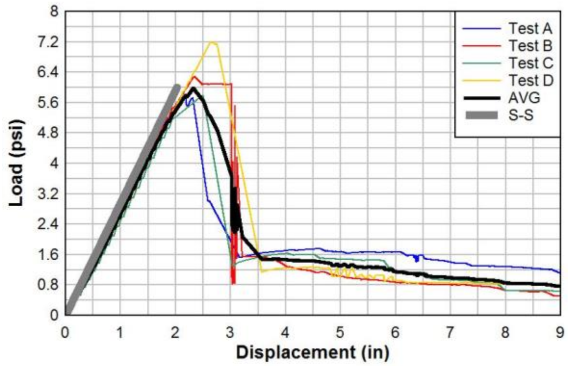

(c) 3-Ply Grade E1.

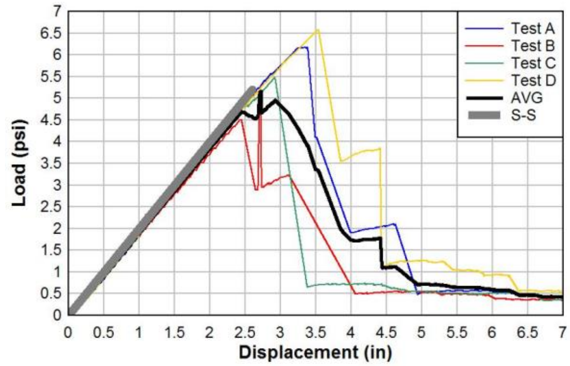

(d) 3-Ply Grade V4.

Figure 2-14. Out-of-Plane Load-Displacement Plots from Phase 1 (No Axial Load).

Table 2-4. Phases 1 & 2 Peak Panel Strength Comparison.[1]

Grade	Ply No.	l_e [in]	r_{u0} [psi]	Axial Load						
				Ph. 1	*Ph. 2*					
				$0\%F_c^{*2}$	$0\%F_c^{*3}$	$5\%F_c^*$	$10\%F_c^*$	$20\%F_c^*$	$30\%F_c^*$	$40\%F_c^*$
V1	3	120	7.43	0.95	-	-	-	-	-	-
		136	5.79	-	1.36	1.42	1.09	1.08	0.90	0.79
		160	4.18	-	-	-	1.10	-	-	-
	5	120	14.72	1.03	-	-	-	-	-	-
		136	11.46	-	1.48	1.37	1.50	1.38	1.23	1.09
E1	3	120	6.73	0.94						
		136	5.24	-	-	-	0.99	-	-	-
V4	3	120	5.70	1.02	-	-	-	-	-	-
		136	4.44	-	-	-	1.18	-	-	-

1 Average measured out-of-plane resistance from either [3] or Table 2-3 (i.e., corrected peak panel strengths) divided by the theoretical expected ultimate resistance assuming pin-roller boundary conditions, r_{u0}, recorded in the fourth column of this table.

2 Augmented out-of-plane resistance due to compression membrane response was not possible in the Phase 1 testing.

3 Augmented out-of-plane resistance due to compression membrane response was possible in the Phase 2 testing.

2.5 PEAK PANEL STRENGTH ANALYSIS

Table 2-5 records the information needed to compute the expected ultimate resistance of an axially-loaded CLT panel according to equation (6). In addition, Table 2-6 compares this expected ultimate resistance with the corrected peak strength data recorded in Table 2-3.

Table 2-5. Computed Ultimate Resistance Using Equation (6).

Panel Description	$\%F_c^*$	P [k]	P_{cE} [k]	C_p	$F_c'A_{parallel}$ [k]	$F_b(S_{eff})'$ [k-in/in]	r_{u0} [psi]	r_u [psi]
12' 3-Ply V1	0	0	204	0.62	297	13.38	5.79	5.79
	5	15						5.35
	10	29						4.92
	20	58						3.99
	30	86						3.07
	40	115						2.15
12' 5-Ply V1	0	0	236	0.89	215	26.49	11.46	11.46
	5	8						11.05
	10	15						10.68
	20	29						9.87
	30	43						9.00
	40	58						8.02
12' 3-Ply E1	10	39	212	0.51	324	12.11	5.24	4.21
12' 3-Ply V4	10	22	142	0.59	210	10.27	4.44	3.71
14' 3-Ply V1	10	29	153	0.49	235	13.38	4.18	3.33

Table 2-6. Test vs. Computed Peak Strengths for Axially-Loaded CLT Panels.

Panel Description	$\%F_c^*$	k [psi/in]	X_E [in]	(1) r_u [psi]	(2) Corrected Peak Strength [psi]	(2) / (1)
12' 3-Ply V1	0	1.79	3.23	5.79	7.90	**1.37**
	5		2.99	5.35	8.23	**1.54**
	10		2.75	4.92	6.30	**1.28**
	20		2.23	3.99	6.23	**1.56**
	30		1.72	3.07	5.22	**1.70**
	40		1.20	2.15	4.59	**2.13**
12' 5-Ply V1	0	6.29	1.82	11.46	16.95	**1.48**
	5		1.76	11.05	15.68	**1.42**
	10		1.70	10.68	17.17	**1.61**
	20		1.57	9.87	15.87	**1.61**
	30		1.43	9.00	14.11	**1.57**
	40		1.27	8.02	12.51	**1.56**
12' 3-Ply E1	10	1.86	2.27	4.21	5.17	**1.23**
12' 3-Ply V4	10	1.24	3.00	3.71	5.23	**1.41**
14' 3-Ply V1	10	0.97	3.44	3.33	4.61	**1.38**

The expected peak strengths computed using equation (6) always exceed, in one case by over 200 percent, the corrected test peak strengths. Generally, the divergence between the two data sets is between 120 and 170 percent.

As there is such a large divergence between the computed and tested peak strengths, there are clearly other structural mechanisms that are contributing strength to the panel than are not accounted for in equation (6) or in the previously-described artificial restraining moment correction. This divergence could be associated with several factors:

(1) Fixed end moment accrual due to applied axial load.

(2) Strengthening of finger joints and other imperfections prone to rupture in bending due to applied axial load.

(3) At higher axial loads, plastic response on the bottom face of panel due to combined axial and flexural compressive stress.

(4) Compression membrane action and/or axial load arching. Although the load platens were fixed in the 0% F_c^* tests (see Appendix B), sizable axial compression forces were measured.

(5) Actual axial compressive stress capacity in excess of the design values recorded in the manufacturer's literature and PRG 320.

All of these phenomena are not artifices of the test setup but rather examples of physical phenomena associated with axially-loaded structural components. To isolate the relative importance and magnitude of the five aforementioned phenomena, additional analysis or testing is necessary.

2.6 RESISTANCE FUNCTION RECOMMENDATIONS

As stated at the outset of this chapter, the purpose of this testing effort was to generate a resistance function that could be used in SDOF dynamic analyses to design axially-loaded CLT panels for blast loads. For CLT panels without axial loads, two idealized resistance functions forms were posited during the Phase 1 effort. One explicitly models the softening response observed in the quasi-static testing; this resistance function form is shown in Figure 2-15a. The other resistance function form is simply an elasto-plastic idealization and uses response limits to limit the amount of accrued plastic strain; this resistance function form is shown in Figure 2-15b.

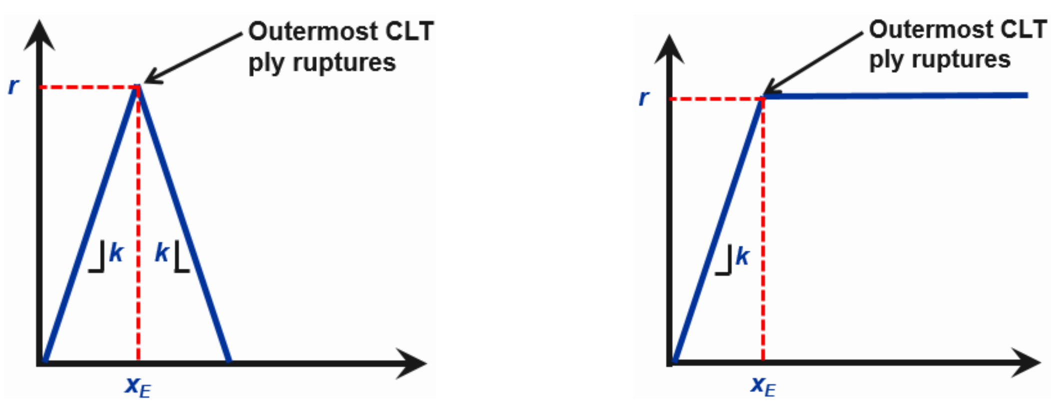

(a) Post-Peak Softening. *(b) Elasto-Plastic.*

Figure 2-15. Idealized Resistance Functions used in SDOF Dynamic Analysis.

While the resistance function with softening better matches the post-peak response of brittle materials, there are several attendant complications:

- While the stability of the response of the analytical degree of freedom is very sensitive to the slope of the softening stiffness, it is very difficult to justify a representative softening stiffness value based on analysis or testing. Indeed, as observed in this testing, the softening stiffness for CLT panels can vary significantly, even for duplicate tests, due to the brittle nature of wood.

- The SDOF response limits currently included in DoD antiterrorism criteria [8] generally assume an elasto-plastic resistance function, even for brittle materials (e.g., cold-formed steel wall studs).

Furthermore, SDOF analyses conducted during the Phase 1 effort indicated that for most problems in which post-peak deformations were computed, the elasto-plastic resistance function yielded comparable or better matching of the test data [9]. Thus, an elasto-plastic resistance function form is assumed in this report.

Figure 2-16a plots the idealized resistance function and normalized (corrected) pressure-displacement data from this testing effort. Where duplicate tests were performed, the data shown is the average curve obtained from the duplicate tests. The x-axis values of the corrected pressure-displacement data are divided by the corresponding elastic limit deflection, X_E, in Table 2-6 and the y-axis values are divided by the corresponding ultimate resistance, r_u, in Table 2-6. Integrating the data shown in Figure 2-16a yields the plot shown in Figure 2-16b. For X/X_E values of less than two, the area under the idealized resistance function is less than that for the average pressure-displacement data generated under this testing effort. Thus, for CLT panels with axial loads less than 40-percent F_c^*, the idealized resistance function will not overpredict the amount of strain energy encapsulated in load bearing CLT wall panels for most cases provided the ductility is kept below two.

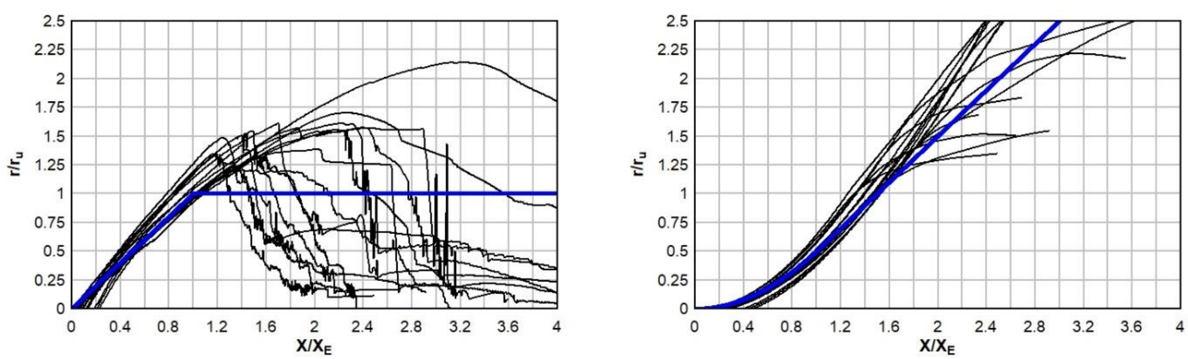

(a) Normalized data. *(b) Integral of normalized data.*

Figure 2-16. Normalized Load-Displacement Data Comparison.

As a final point of comparison, Figure 2-17 groups and averages the normalized curves shown in Figure 2-16a by applied axial load. It is interesting to note that the panels with a lower percentage of axial load demonstrate a pattern of exhibiting more brittle post peak responses when compared to panels with a higher percentage of axial load.

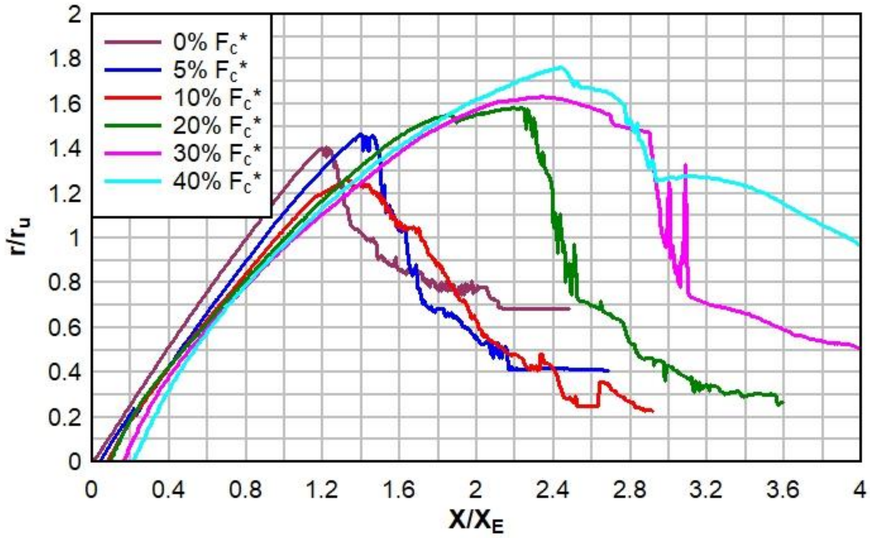

Figure 2-17. Normalized Pressure-Displacement Data Comparison.

In light of the above, the following recommendations and comments are made concerning the generation of a resistance function suitable for axially-loaded CLT panels exposed to blast loads:

- Compute the loading stiffness, *k*, ignoring the effects of axial load.
- Compute the ultimate resistance, r_u, using equation (6). It should be noted that the ultimate resistance should also consider the flatwise shear limit state as mentioned in Section 5.2.

These recommendations assume the axial load is less than 40-percent F_c^* and the displacement ductility is less than 2.0.

It should be noted that while these recommendations may be conservative from a panel response perspective, they will not necessarily be conservative from a connection design perspective. Care should be taken in performing connection design to ensure an adequate factor of safety is employed to account for the potential for augmented ultimate resistance due to material property variability, axial load arching, compression membrane action, etc. As most CLT panels will have axial loads of less than 20% F_c^*, a safety factor of 1.7 (i.e., based on the ratios recorded in Table 2-6) from the *tested* strength of the connection increased for strain rates effects as appropriate is a good place to start. Additional testing and analysis can serve to refine this admittedly conservative safety factor.

It should be noted that applying observations gleaned from a quasi-static test to a dynamic problem may neglect important phenomenology related to duration of load, inertial effects, and damping effects. As wood is especially sensitive to load duration and lightweight and brittle from a material perspective, testing under actual dynamic loads is essential to ensure the assumptions made in the quasi-static space still hold in the dynamic space. The remainder of this report is focused on validation tests in this dynamic space.

CHAPTER 3

ARENA TESTING SETUP

The setup for the four arena blast tests conducted on mass timber structures is described in this chapter. These four arena blast tests are referred to as Tests 4 through 7 to distinguish these tests from the three arena blast tests (i.e., Tests 1 through 3) performed in Phase 1. Section 3.1 describes CLT test structure details such as site layout, panel sizes, connection details, opening details, and construction notes. Section 3.2 then documents details concerning the explosive charges used. Finally, Section 3.3 describes details about the instrumentation employed for each test.

3.1 TEST STRUCTURES

Three single-bay (i.e., 15 feet square), two-story CLT structures originally constructed and tested during Phase 1 were reused for the Phase 2 arena blast tests. Two of the structures had roughly 12-feet story heights and one structure had roughly 10-feet story heights. Other than the story height and material grade, the buildings were identical. One 12-foot story height structure was constructed using Grade V1 CLT panels while the other was constructed using Grade E1 CLT panels. The 10-foot story height structure was constructed using Grade V4 CLT panels. Figure 3-1 shows a plan view of how these tests structures were situated on an existing concrete slab.

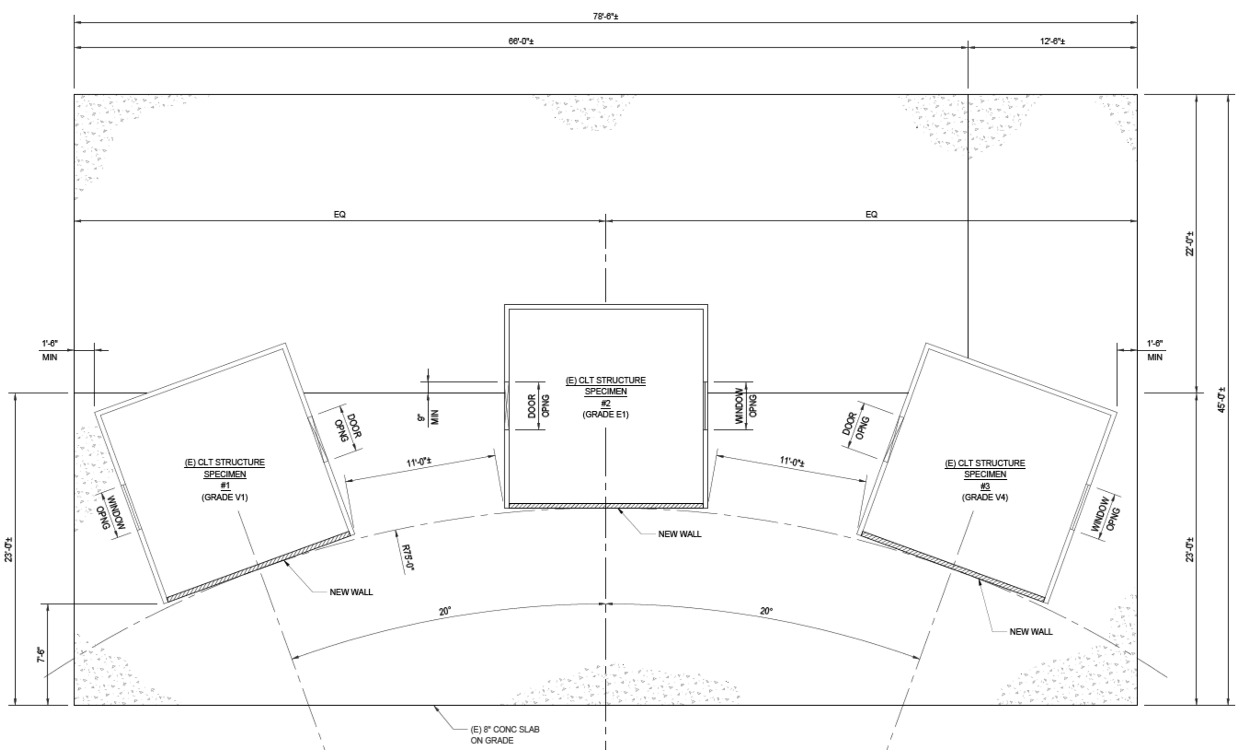

Figure 3-1. Structure Layout Plan.

3.1.1 Existing Condition of Test Structures

The existing condition of the test structures at the conclusion of Phase 1 (i.e., Test 3) is briefly described in this subsection. For more information concerning the test structures, particularly the detailing, the reader is referred to blast testing report from Phase 1 [9].

3.1.1.1 PANELS

Panels were provided by three different CLT manufacturers and all panels and plants were third party certified to ANSI/APA PRG 320 [5] requirements. Grade E1 panels were provided by Nordic Structures, Grade V1 panels were provided by DR Johnson, and Grade V4 panels were provided by SmartLam. Wall and roof panels were 3-ply panels (i.e., $4^1/_8$ inches thick) and the elevated floor panel at the second floor was a 5-ply panel (i.e., $6^7/_8$ inches thick). The width of the individual lamella used to construct the CLT panels varied between grades; 7 inches, $3^1/_4$ inches, and 7 inches wide for the Grade V1, Grade E1, and Grade V4, respectively. The average board lengths and finger jointing used in each lamination also varied by grade. Lamella characteristics of each grade are consistent with requirements of the PRG 320 and those tested at UMaine in Phase 1 [6].

Two different types of CLT construction were included in the buildings. The first floor was constructed using platform framing and the second floor was constructed using balloon framing with a parapet. The utilization of different framing types enabled many of the typical connection configurations found in a CLT building to be tested.

3.1.1.2 CONNECTIONS

Connections were made to emulate typical CLT connection configurations. Five basic types of connections were employed: (1) panel-to-foundation, (2) panel-to-panel splice, (3) wall-to- floor panel (platform framing), (4) wall-to-roof panel (balloon framing), and (5) wall panel at corner.

Most connection configurations utilized $^5/_{16}$-inch diameter SWG ASSY® self-tapping screws (STSs) of various lengths manufactured by MyTiCon to secure adjacent panels to one another. Based on the results of the connection tests performed at UMaine [6], STS length was selected to allow the screw to engage all plies of a given panel where practical. Where screw withdrawal was a potential limit state, the SK (i.e., washer head) screw was utilized (i.e., the bottom screw in Figure 3-2). Otherwise, the ECO (i.e., counter-sunk head) screw was used (i.e., the top two screws in Figure 3-2). Further details concerning the details for the test structures are included in [9].

Figure 3-2. Self-Tapping Screws Used in Test Structure Connections.

3.1.2 Openings

Typical window (i.e., 3'-6" square rough opening) and pedestrian door (i.e., 3'-4$^{1}/_{2}$" wide by 7'-4$^{3}/_{8}$" high rough opening) openings were included in each structure.

The window opening detail and as-installed condition are shown in Figure 3-3. The window opening was cut out of a solid CLT panel and was covered with two $^{3}/_{4}$-inch pieces of plywood to allow blast loads applied at the opening to be transferred to the opening's head, sill, and jambs.

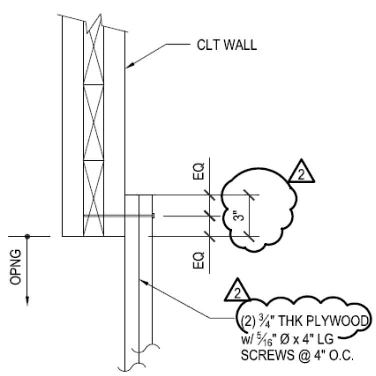

(a) Detail.

(b) As Installed.

Figure 3-3. Window Opening Connection.

Actual 1$^{3}/_{4}$-inch thick by 36-inch wide by 86-inch high pedestrian doors manufactured using 14 gage galvannealed steel were provided by American Direct and manufactured by Ambico. The door shop drawings provided by American Direct are included in Appendix C of [9]. As-installed photographs of the door are included as Figure 3-4a and b. Doors were designed to exhibit a low level of protection (i.e., as defined in UFC 4-010-01) for Explosive Weight II (i.e., as defined in UFC 4-010-02 [10]) with 105-feet of standoff distance.

The door openings were built out using dimensional lumber to accommodate the 5$^{3}/_{4}$-inch wide frame in the 4$^{1}/_{8}$-inch thick 3-ply CLT wall panels. The detail for this door framing detail is shown in Figure 3-4c.

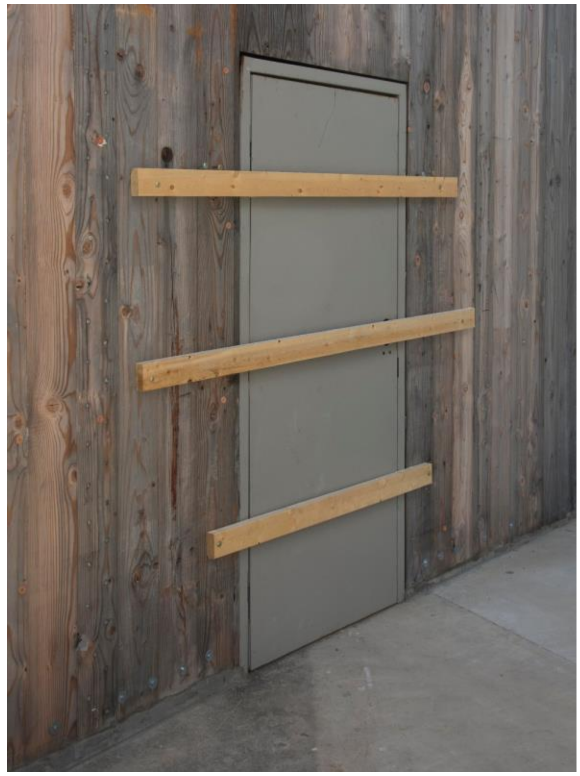

(a) As Installed (Interior). *(b) As Installed (Exterior).*

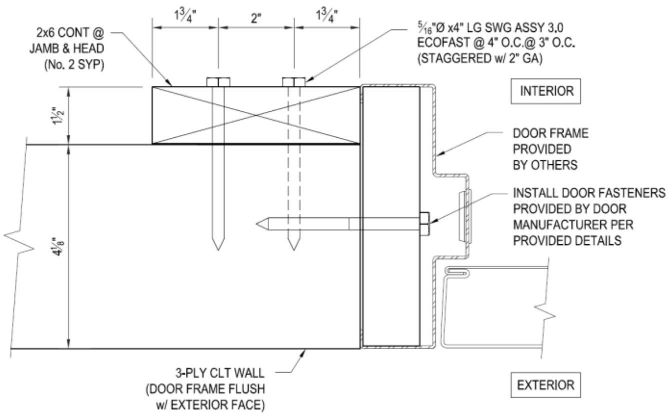

(c) Door Frame Detail.

Figure 3-4. Door Opening Figures.

Two types of fasteners were used to secure the door frame to the CLT test structures: (1) ten $^{1}/_{2}$-inch diameter by 5-inch long lag screws and (used at the Grade E1 and V1 structures) and (2) twenty-eight $^{5}/_{16}$-inch diameter by $5^{1}/_{2}$-inch long SWG ASSY® Kombi STS manufactured by MyTiCon (used at the Grade V4 structure). Fasteners were uniformly spaced along the three supported sides of the door frame as shown in Appendix C of [9].

No locking hardware was employed to lock the door during the blast tests to limit the possibility that the door would jam shut due to the applied blast load. Additionally, no hinges were provided for the Grade V1 or Grade E1 test structures. (Three stainless steel heavy weight bearing hinges (i.e., T4A3386 NRP $4^{1}/_{2}$”x$4^{1}/_{2}$”) manufactured by McKinney were used to secure the door panel to the door frame in the Grade V4 test structure.) Instead, dimensional lumber was used to keep the door closed at the beginning of the test for all test structures as shown in Figure 3-4b.

3.1.3 Modifications to Test Structures for Tests 4 & 5

The purpose of Tests 4 and 5 was to demonstrate the ability of axially-loaded CLT construction to resist blast loads. To prepare the existing test structures for these tests, the following modifications were made:

- The first and second floor front panels, some of which were visibly damaged during the Phase 1 testing, were removed and replaced in kind.
- The roof panels were rotated 90 degrees such that the major strength direction of the roof panels was supported by the front wall panels.
- The structures were loaded with superimposed dead load. Section 3.1.3.1 describes in detail how the superimposed dead load was applied.

These modifications are illustrated in as-built drawings included in Appendix C. A photograph of three test structures following the removal and replacement of the front wall panels is shown in Figure 3-5.

Figure 3-5. Pre-Test 4 Photograph of All Test Structures.

Moisture content readings were taken at both existing and new front panels the day of Test 4 and are recorded in Table 3-1. At least two readings were taken for each location / story combination shown in Table 3-1. All measured moisture content values were greater than 9-percent and less than 15 percent.

Table 3-1. Test Structure Panel Moisture Content Prior to Test 4.

Location	Story	Test Structure CLT Panel Grade		
		V1	*E1*	*V4*
Front Wall	1	12.9	14.4	12.9
	2	12.6	14.3	13.4
Window Side Wall	1	11.9	12.9	11.5
	2	14.3	13.6	12.5
Door Side Wall	1	12.5	11.7	10.8
	2	13.1	13.5	12.7
Back Wall	1	11.0	12.2	12.5
	2	12.6	13.1	13.2
2nd Floor	N/A	12.7	13.0	12.5

3.1.3.1 *TEST STRUCTURE LOADING*

The target *maximum* axial load to be applied to the front wall panels of the test structures was meant to simulate that associated with the a five-story office / residential building. Based on the assumptions shown in Figure 3-6, this axial load was estimated to be approximately 3,000 pounds per linear foot.

PDC-TR 06-08 Load Factor		
Dead	1	
Live	0.35	

Geometry Input Parameters		
Number of Stories	5	
Tributary Width	7.5	[ft]
Wall Height	12	[ft]

Weight Input Parameters		
Exterior Wall Dead Weight	20	[psf]
Floor Dead Weight	40	[psf]
Roof Dead Weight	20	[psf]
Live Load	40	[psf]
Roof Live Load	20	[psf]

Weight Tabulation		
Floor Dead	1200	[plf]
Floor Live	420	[plf]
Roof Dead	150	[plf]
Roof Live	53	[plf]
Wall Dead	1200	[plf]
Total	**3023**	**[plf]**

Figure 3-6. Axial Load Estimate for Exterior Wall of 5-Story Office / Residential Building.

Using this target maximum axial load as a guide, the front walls of the test structures were loaded using precast concrete blocks. The blocks were 2-feet wide by 2-feet tall by 4-feet long and weighed 2,480 pounds each. Each test structure was loaded with a different number of blocks to simulate different levels of axial load. A total of 16 blocks were placed on the Grade V1 structure, 12 blocks were placed on the Grade E1 structure, and 8 blocks were placed on the Grade V4 structure. To ensure the front wall supported as much of the blocks' weight as possible, the blocks were placed within 12 inches of the front wall. A schematic diagram illustrating block placement is included as Figure 3-7. Photographs of block placement on the first-floor in the Grade V1, E1, and V4 structures are included in Figure 3-8 a, b, and c, respectively. Additionally, a photograph of block placement on the roof (identical placement for all three test structures) is included as Figure 3-8d. Finally, Table 3-2 indicates estimated peak front wall axial loads at the bottom of the first-floor front panel and compares this value with their adjusted NDS compression capacities. This estimated axial load includes the tributary weight deriving from both the concrete blocks and the CLT panels.

Table 3-2. Compression Capacity/Demand at First-Floor Front Wall Panels.

Test Structure Grade	P_{max}[1] [plf]	$A_{parallel}$[2] [in^2/ft]	F_c[3] [psi]	C_P[4]	$F_c'A_{parallel}$[5] [plf]	$\frac{P_{max}}{F_c'A_{parallel}}$	% F_c^*[6]
V1	2,600	33.0	1,350	0.49	21,886	11.9%	3.6
E1	2,175	33.0	1,800	0.39	23,413	9.3%	2.3
V4	1,550	33.0	1,000	0.61	20,027	7.7%	2.9

1 Estimated peak axial load at bottom of first-floor front wall panel.

2 Area of front wall panel cross section of CLT layers with fibers parallel to the applied axial load.

3 Reference compression design value from PRG 320 or manufacturer data.

4 Column stability factor as defined in the NDS [3] assuming 12-foot span for Grade V1 and E1 panels and 10-foot span for Grade V4 panels.

5 Adjusted compression capacity of first-floor front wall panel; assumes normal load duration (C_D = 1.0) and C_M = C_t = 1.0.

6 Included for direct comparison with data presented in Chapter 2; assumes ten-minute duration (C_D = 1.6) and C_M = C_t = 1.0.

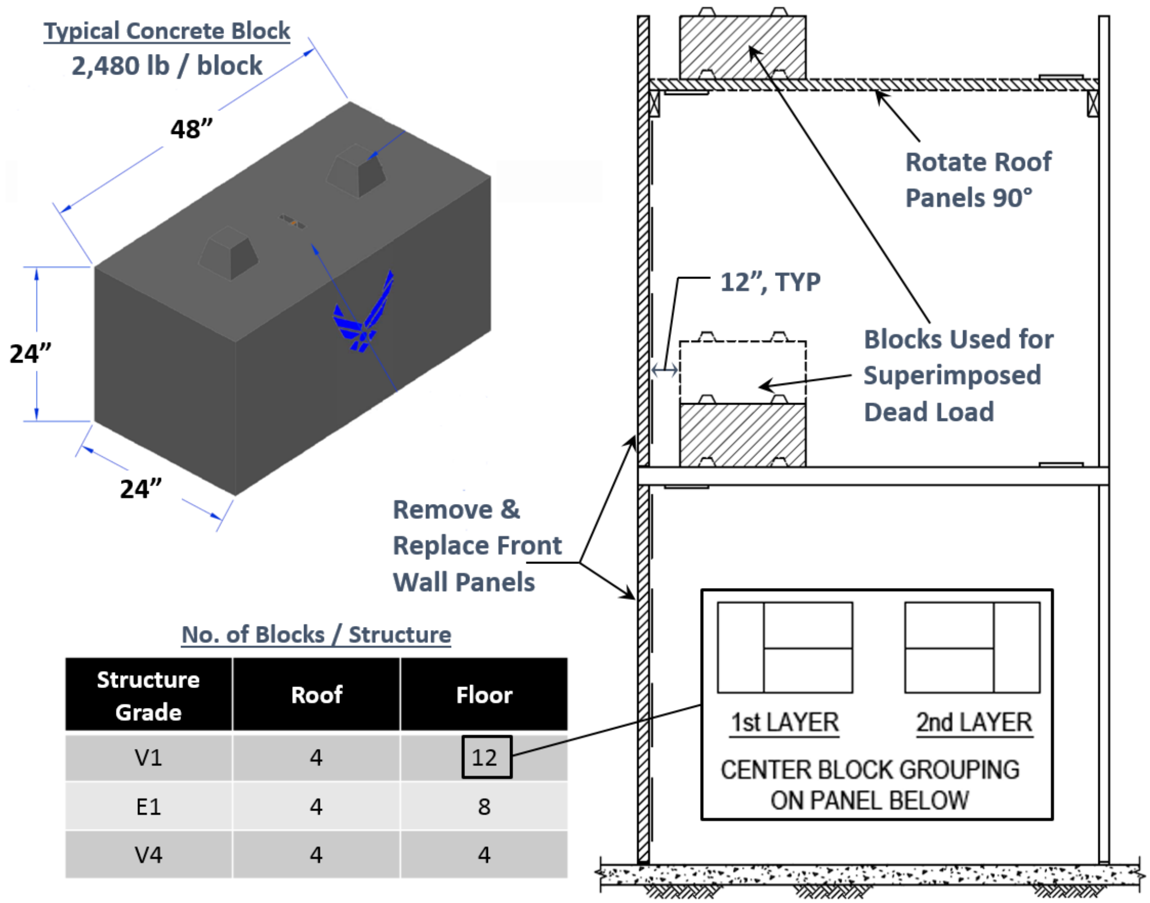

Figure 3-7. Schematic Diagram of Block Placement.

(a) 1st Floor at Grade V1 Structure.

(b) 1st Floor at Grade E1 Structure.

(c) 1st Floor at Grade V4 Structure.

(d) Roof at Grade V4 Structure.

Figure 3-8. Photographs of Block Placement.

3.1.3.2 *CONSTRUCTION*

Lendlease made all the construction modifications to and loaded the test structures prior to Test 4 over the course of five days. As part of the front wall panel removal and replacement, the structures were jacked up to allow for the new front panels to be installed and ensure the front panel would be fully loaded. To jack up the structures, all screws connecting the foundation angle to the CLT wall panels were removed. In side and rear walls where panels were re-used, screws were re-installed in a previously-drilled hole locations and thru-bolts were installed intermittently to accommodate for the reduction in withdrawal capacity of the connection system (i.e., due to loss of thread engagement resulting from screw removal and reinstallation). This modification was calculated to be sufficient to resist the shear forces associated with panel rebound. This connection detail is shown in Figure 3-9.

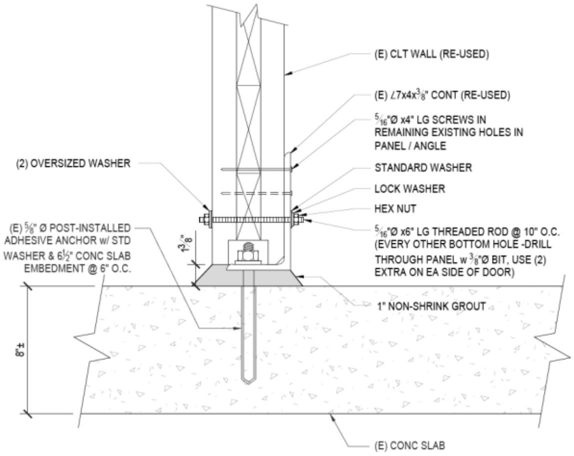

(b) Interior View.

(a) Detail. *(c) Exterior View.*

Figure 3-9. Thru-Bolt Detail at Foundation of Existing Test Structure Wall.

3.1.4 Modifications to Test Structures for Tests 6 & 7

The purpose of Tests 6 and 7 was to demonstrate the ability of alternative mass timber configurations to resist blast loads. The alternative configurations that were tested included: (1) 5-ply CLT wall panels, (2) different connections details that incorporated pre-fabricated brackets, and (3) NLT wall panels. These alternative connection configurations were only installed at the front panels of the test structures. Appendix D includes as-built drawings of the modifications made to each test structure prior to Test 6. The following subsections goes into further detail concerning the modifications that were made to each test structure.

A photograph of three test structures following the removal of the damaged front wall panels from Test 5 and replacement with the alternative mass timber configurations prior to Test 6 is shown in Figure 3-10.

Figure 3-10. Pre-Test 6 Photograph of All Test Structures.

Moisture content readings were taken at both existing and new front panels the day of Test 6 and are recorded in Table 3-3. At least two readings were taken for each location / story combination shown in Table 3-3. While the average of each panel's moisture content based on multiple moisture meter readings were greater than 9-percent and less than 15 percent, a few individual readings were outside of these bounds. These locations are indicated in Table 3-3.

Table 3-3. Test Structure Panel Moisture Content Prior to Test 6.

Location	Story	Test Structure CLT Panel Grade		
		V1	*E1*	*V4*
Front Wall	1	11.3	11.1	10.8[2]
	2	12.3	12.3	11.5[2]
Window Side Wall	1	8.8[1]	10.4	9.8
	2	13.1	11.2	11.7
Door Side Wall	1	10.3	9.3	8.0[1]
	2	13.2	10.2	10.9
Back Wall	1	8.3	9.5	9.4
	2	12.1	11.2	12.0
2nd Floor	N/A	14.4[1]	13.0	12.5

1 At least one reading was less than 9-percent or greater than 15-percent.
2 Moisture content of 2x4 SPF No. 2 NLT.

3.1.4.1 *GRADE V1 BUILDING*

Five-ply Grade V1 CLT wall panels were installed on the front face of the Grade V1 structure. Panel removal and replacement followed the same procedure as used to remove and replace the front wall panels before Test 4 with one exception. To allow for the 5-ply front wall panel to occupy the same maximum footprint area, 2 3/4 inches from the end of the roof panels needed to be removed. This is illustrated in Figure 3-11.

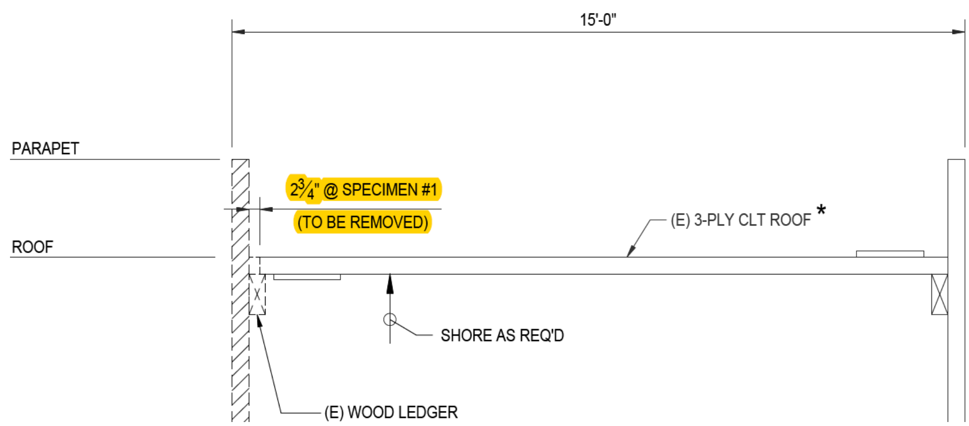

Figure 3-11. Roof Panel Modification in Grade V1 Structure Prior to Test 6.

In general, the connection details utilized in Phase 1 for the 3-ply Grade V1 front wall were used for the 5-ply Grade V1 front wall. Two minor exceptions included:

- Instead of having wall panel splice screws spaced at $2^1/_2$ inches on center, the spacing of these screws was increased to 4 inches on center (Figure 3-12a) to reflect a more typical panel-to-panel condition.

- To reuse the previously-installed anchor bolts, a new steel angle with a longer horizontal leg was installed at the foundation (Figure 3-12b).

Apart from these two minor changes, the details used in the Phase 1 testing were identical to that used in the Phase 2 testing.

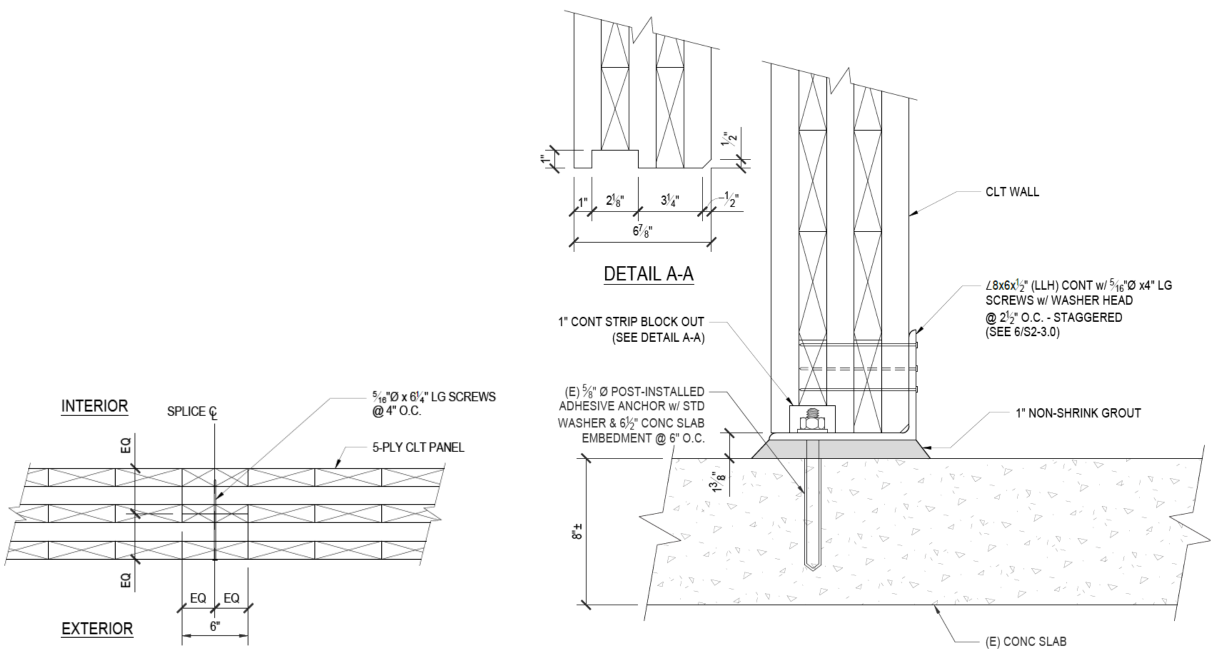

(a) 5-ply wall splice. *(b) Revised foundation detail.*

Figure 3-12. Detail Modifications to Grade V1 Structure Prior to Test 6.

3.1.4.2 *GRADE E1 BUILDING*

Three alternative connection types were installed in the front wall panel of the Grade E1 structure:

- Instead of hot rolled steel angle brackets and self-tapping screws at the underside of the first floor, a connection utilizing only self-tapping screws was installed at this location. The impetus for such a connection was two-fold: (1) to eliminate the material cost associated with a steel angle or prefabricated bracket and (2) to remove the need to hoist a steel bracket overhead and thus ease installation. Screws installed from the top of the floor panel above alternated with screws oriented at a 45-degree angle installed from below. The detail of this connection is shown in Figure 3-13a and a photograph of the installed condition is shown in Figure 3-13b.

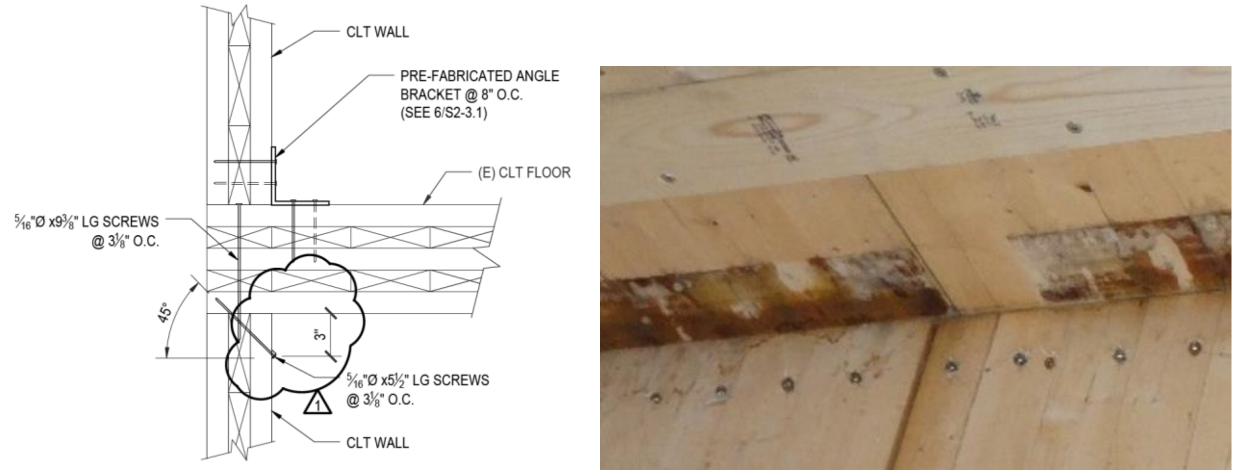

(a) Detail. *(b) Photograph.*

Figure 3-13. Wall Panel to Floor Panel Connection Modification at Underside of 1st Floor in Grade E1 Structure Prior to Test 6.

- At the top of both the first elevated floor panel (Figure 3-14a) and roof panel (Figure 3-14b), pre-fabricated angle brackets were substituted for hot rolled steel angles. The pre-fabricated brackets were spaced at 8 inches on center along the front wall (Figure 3-14c). The brackets were spaced to resist a peak wall dynamic reaction loading of 300 lb/in (i.e., that associated with Test 6) with a safety factor on the ultimate connection capacity of 1.8. Half of the front wall was supported by Simpson Strong Tie (SST) ABR 105 brackets secured with ten Strong-Drive® Connector Screws (i.e., #10 x $2^{1}/_{2}$”) in its vertical leg and fourteen Strong-Drive® Connector Screws in its horizontal leg (Figure 3-14d). The other half of the front wall was supported by MiTek USP HGA10 brackets with four WS15 Wood Screws (i.e., 1/4" x $1^{1}/_{2}$”) in both angle legs (Figure 3-14e). (WS35 Wood Screws (i.e., 1/4” x $3^{1}/_{2}$”) screws were specified to be installed at this location; however, this was missed in construction and only discovered once the screws pulled out of the CLT panel during Test 7.) Both brackets were commercial off-the-shelf brackets and not modified to enhance their blast-resistant capability. The as-tested ultimate capacity assuming a ten-minute duration (i.e., C_D = 1.6) of each bracket in withdrawal (the controlling case) was intended to be approximately the same (i.e., 3,705 lb for the SST bracket and 3,580 lb for the MiTek bracket with $3^{1}/_{2}$” long screws). However, as $1^{1}/_{2}$” long screws were used with the MiTek bracket, the as-tested ultimate capacity of this bracket was actually 2,505 lb.

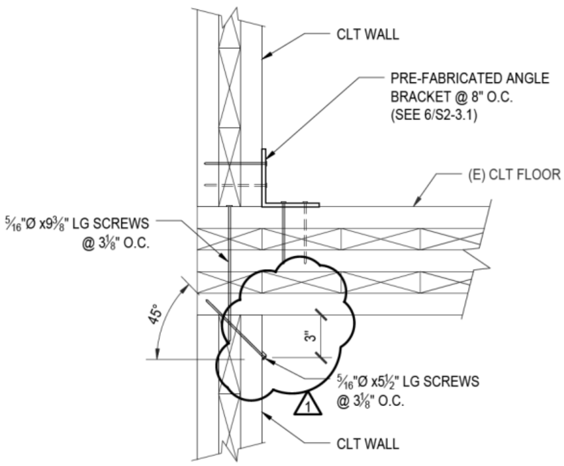

(a) Detail at First Elevated Floor Panel.

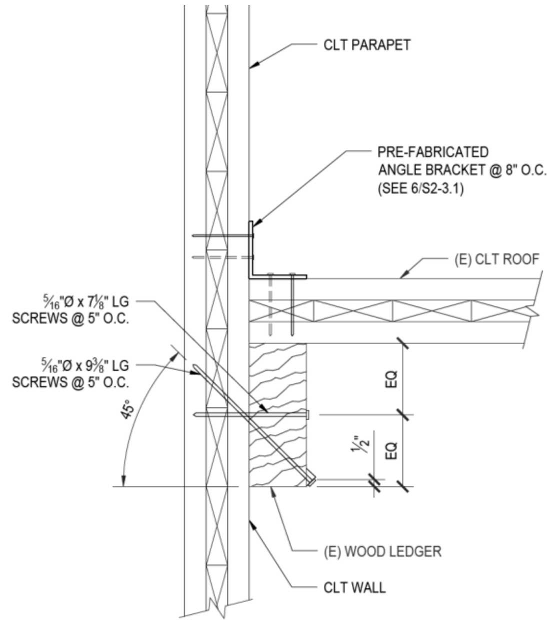

(b) Detail at Roof Panel.

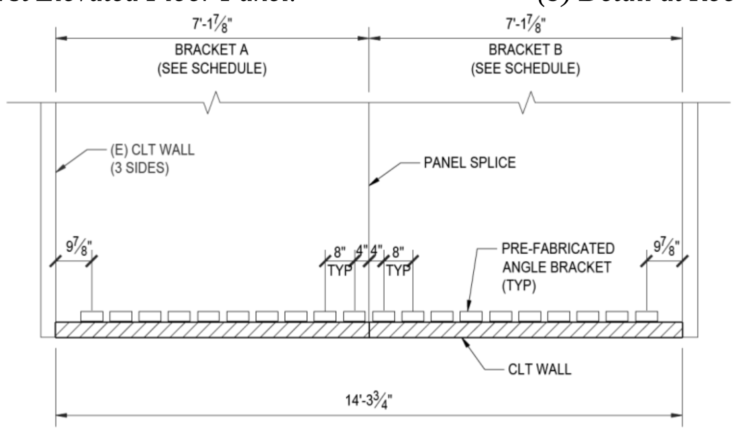

(c) Plan View Showing Bracket Placement Location.

(d) SST ABR105 Bracket.

(e) USP HGA10 Bracket.

Figure 3-14. Wall Panel to Floor Panel Connection Modification at Top Side of Elevated Floor and Roof Panels in Grade E1 Structure Prior to Test 6.

- At the corner wall connections involving the front panel, the hot rolled angle steel was removed and self-tapping screws were spaced at $2^1/_2$ inches on center for the height of the building (Figure 3-15). Screws were intentionally drilled into side grain, rather than end grain, in the narrow edge of the main member panel. The screws were designed to resist blast loads in shear only instead of combined shear and bearing/withdrawal as accomplished in the prior detail. The elimination of heavy steel brackets eases the constructability and cost of these structures.

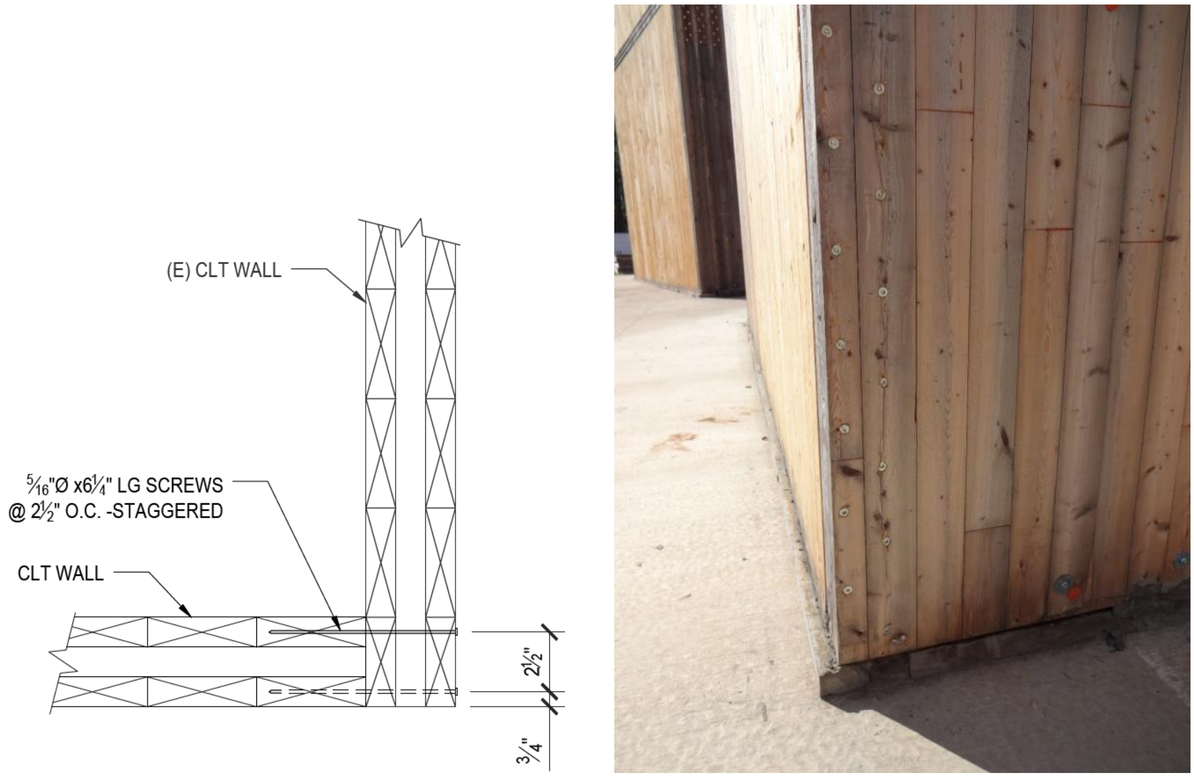

(a) Detail. *(b) Photograph.*

Figure 3-15. Corner Wall Connection Modification in Grade E1 Structure Prior to Test 6.

As in the Grade V1 structure, the spacing of the wall panel half-lap splice at the center of the panel was 4 inches on center (Figure 3-16).

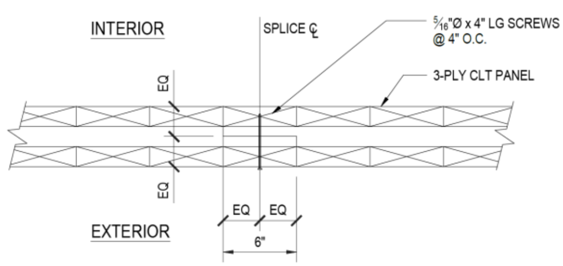

Figure 3-16. Grade E1 Structure Front Wall Panel Splice Detail.

3.1.4.3 *GRADE V4 BUILDING*

Nail-laminated timber (NLT) panels were installed on the front wall of the Grade V4 structure. To construct the NLT panels, 2x4 No. 2 SPF lumber was first stitched together, one lamination to the next, with 0.128" x 3" nails (typical nail unless noted otherwise) at 5 inches on center. In many cases, it was observed that nails were installed at too severe of an angle causing nails to protrude from the back side of the panel (i.e., "shiners") (Figure 3-17a). As panel fabrication continued, installers corrected their nailing angle so this did not persist. Early panels also experienced some bowing in the plane of the wall caused by the ends of the laminations being closer together than at the center of the panel. This was also corrected by the installers. After stitching the laminations and installing the panels onto the building, $^{1}/_{2}$-inch thick plywood was nailed to the exterior side of the NLT panel at 6-inch perimeter / 12-inch in-field spacing with 8d gun nails. Additionally, plywood was installed on the interior face of one half of the first-floor wall panels (Figure 3-17b) but no interior plywood was installed on the second-floor panels (Figure 3-17c). Boundary members were either 2x4, 3x4, or 4x4 pressure-treated Southern pine (i.e., used rather than SPF due to availability). The depth of boundary members was dictated by a desire to limit screw penetration at the discontinuity formed by the boundary member and NLT studs.

With the exception of the wall panel splice, connections were the same as those used in Phase 1 for CLT construction. An effort was made to space screws such that the screw did not land at the discontinuity formed by two adjacent boards (Figure 3-17d). Also, instead of a half-lap connection, the typical wall panel splice detail included in the NLT design handbook [11] was used (Figure 3-17e). Further details concerning plywood orientation and nailing patterns are included in Appendix D. Plywood was not analyzed as part of the load resistance but rather used for load distribution for blast loads. An NLT wall system would most likely need sheathing for lateral resistance anyway so including it on the structure was more representative of actual building installation.

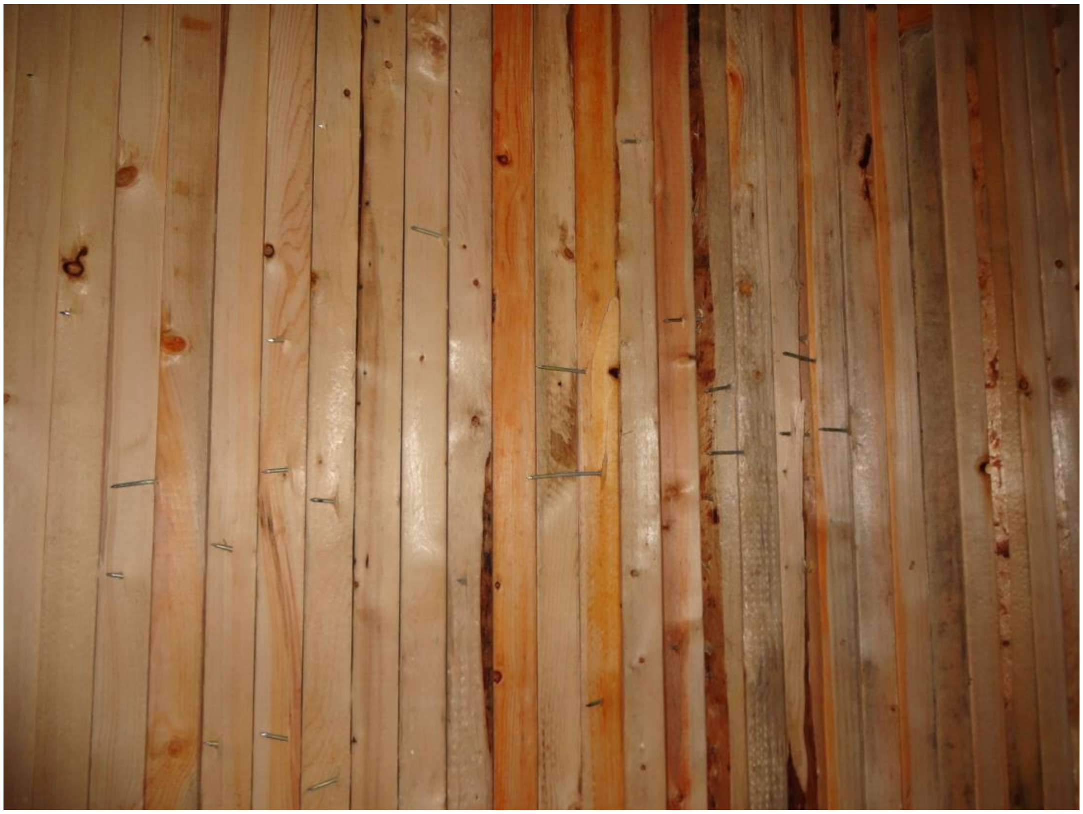
(a) "Shiner" Nails in Exposed Face of NLT Wall Panel.


(b) 1st Floor Interior View.

Figure 3-17. NLT Wall Panel Modifications in Grade V4 Structure Prior to Test 6.

(b) 2nd Floor Interior View.

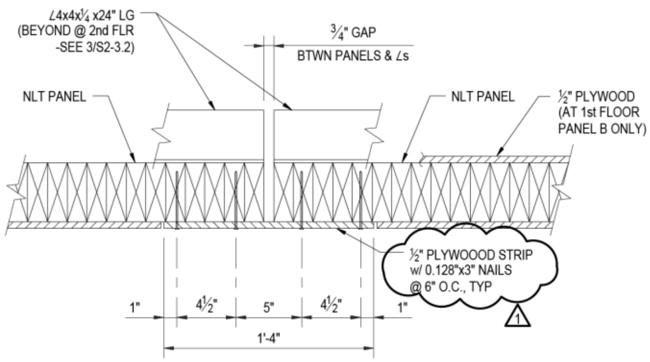

(d) Wall Panel Splice Detail.

(e) Screws into Side Grain.

Figure 3-17. NLT Wall Panel Modifications in Grade V4 Structure Prior to Test 6. (Cont'd)

3.2 EXPLOSIVE CHARGE

3.2.1 Charge Description

Characteristics of the charges utilized for the four arena tests are listed in Table 3-4. Charges were created using flake TNT (ρ = 0.0287 lb/in^3) and formed using Sonotubes® of various diameters and lengths. The method of detonation consisted of replacing 1-pound of flake TNT with a 1-pound cast block of TNT that was tied into a detonator, except for Test 7 where a 5-pound cast block of TNT replaced 5 pounds of flake TNT. The TNT block with its detonator was placed in the top-center of the charge. In all cases, the bottom of the charge was elevated 18 inches off the ground. The ground below the charge was compacted soil.

Table 3-4. Charge Characteristics by Test.

Test	Diameter (D) [in]	Height (H) [in]	H/D	Weight [lb]
4	18	9.17	0.51	67
5	24	15.3	0.64	199
6	18	9.17	0.51	67
7	36	20.7	0.58	610

3.2.2 Standoff Distance

A standoff distance of 75 feet was used for all tests. This standoff distance was measured from the center of the charge to the front face of the CLT test structures.

3.2.3 Charge Weight Selection

Charge weights were selected to build off the testing already performed in Phase 1:

- **Test 4**: Test 4 was identical to Test 2 from Phase 1 except that the structures were loaded with superimposed weight.
- **Test 5**: Test 5 was identical to Test 3 from Phase 1 except that the structures were loaded with superimposed weight.
- **Test 6**: Test 6 was identical to Test 2 from Phase 1 except the alternative mass timber front wall configurations.
- **Test 7**: Test 7 was designed to rupture the 5-ply front walls in the Grade V1 structure. A target response displacement ductility of 1.5 in these panels was used to select the charge size. The process by which displacement ductility was computed is described in Chapter 5.

3.3 INSTRUMENTATION

The instrumentation for each test structure included pressure gages, displacement gages, and video cameras as described below.

3.3.1 Pressure

Table 3-5 provides a summary of the twenty Kulite XT-190 pressure gages that were used for each test:

- Eighteen gages were mounted to the exterior surface of the three test structures (i.e., six per structure) to measure reflected pressure.
- Two gages were mounted to a wood block resting on the ground to measure incident overpressure seventy-five feet away from the explosive charge.

The locations of the reflected pressure gages (i.e., labeled RP1 to RP18) are shown schematically in Figure 3-18 through Figure 3-20. Figure 3-21 shows photographs of the pressure gages used. Self-tapping screws were used to secure the reflected pressure gages to the CLT panel as shown in Figure 3-21a.

Table 3-5. Pressure Gage Summary.

ID	Structure Grade	Measurement	Location	Range
RP1 – RP4	V1	Reflected Pressure	Flush w/ wall (Figure 3-18)	± 35 psi
RP5 – RP6	V1	Reflected Pressure	Flush w/ wall (Figure 3-18)	± 15 psi
RP7 – RP10	E1	Reflected Pressure	Flush w/ wall (Figure 3-19)	± 25 psi
RP11 – RP12	E1	Reflected Pressure	Flush w/ wall (Figure 3-19)	± 10 psi
RP13 – RP19	V4	Reflected Pressure	Flush w/ wall (Figure 3-20)	± 25 psi
RP20 – RP24	V4	Reflected Pressure	Flush w/ wall (Figure 3-20)	± 10 psi
FF1 – FF2	N/A	Incident Overpressure	75 feet from charge	± 15 psi

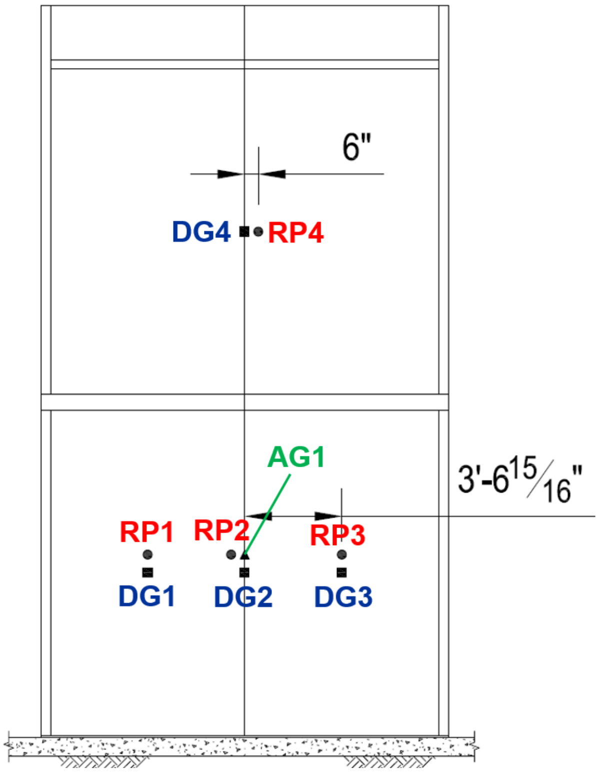

(a) Front Elevation.

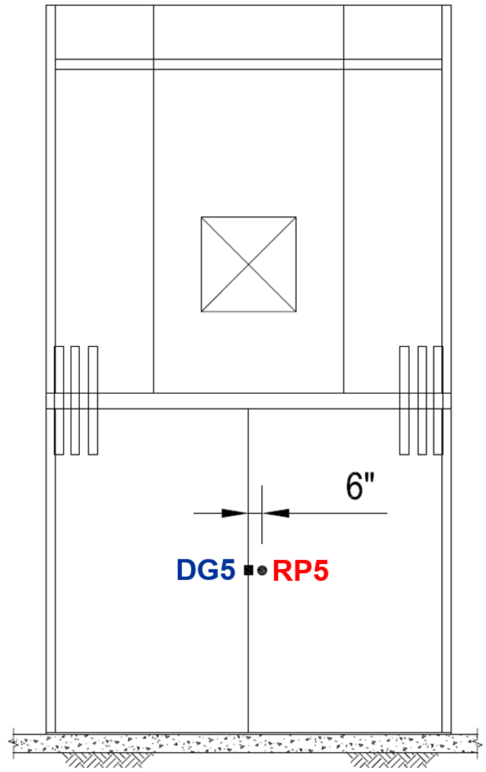

(b) Window (Left) Elevation.

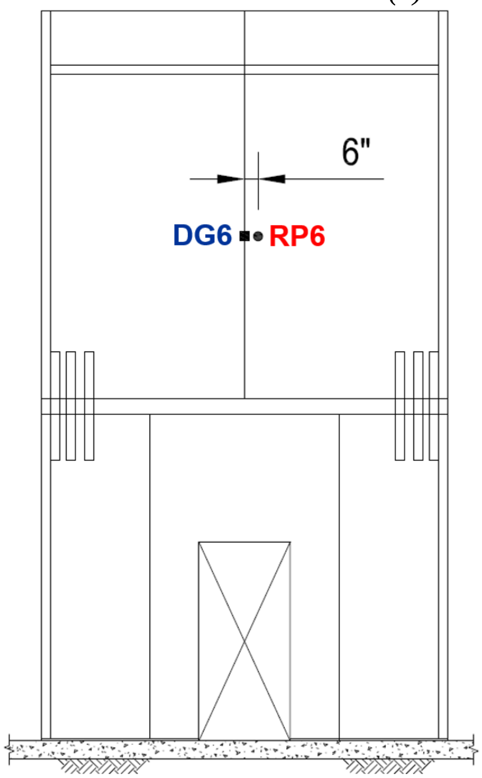

(c) Door (Right) Elevation.

Figure 3-18. Grade V1 Structure Reflected Pressure Gage Key Plan.

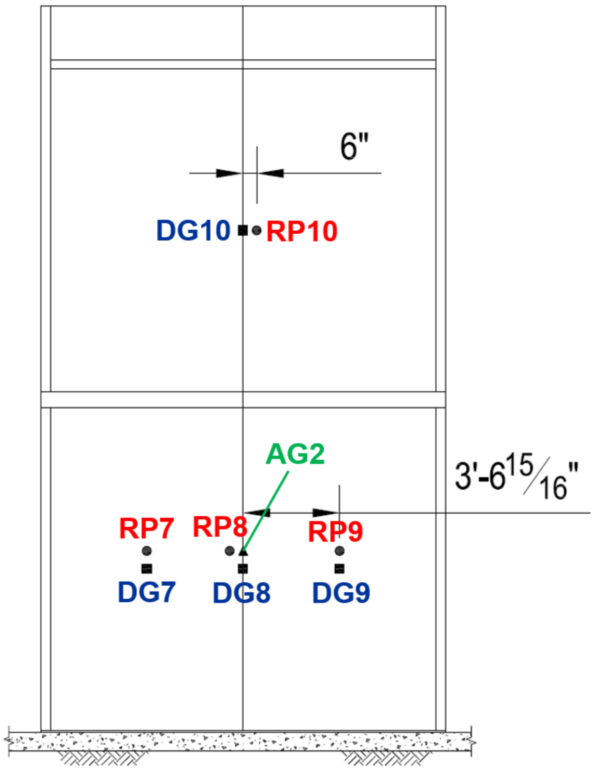

(a) Front Elevation.

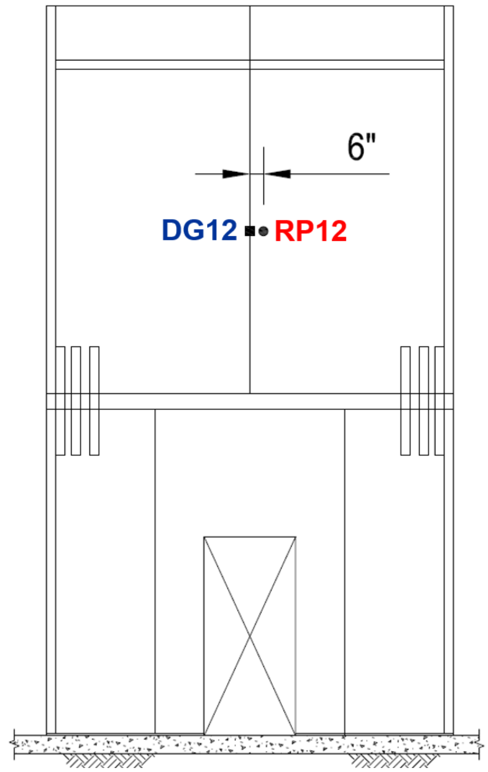

(b) Door (Left) Elevation.

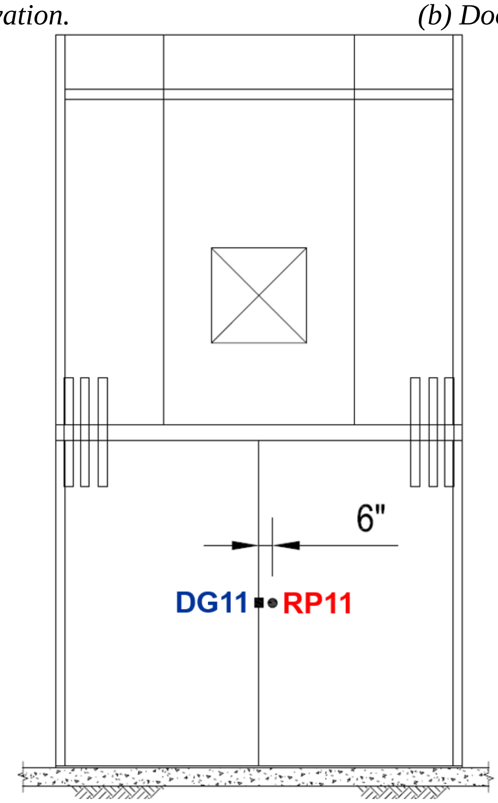

(c) Window (Right) Elevation.

Figure 3-19. Grade E1 Structure Reflected Pressure Gage Key Plan.

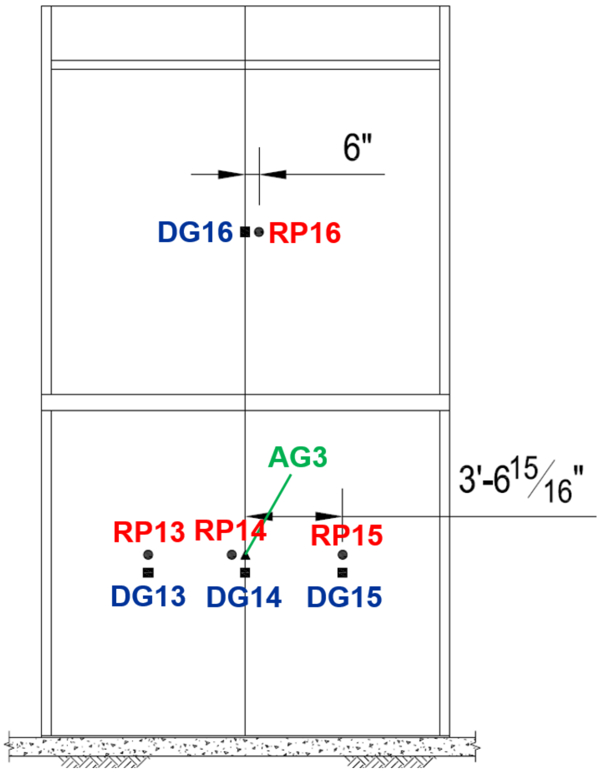

(a) Front Elevation.

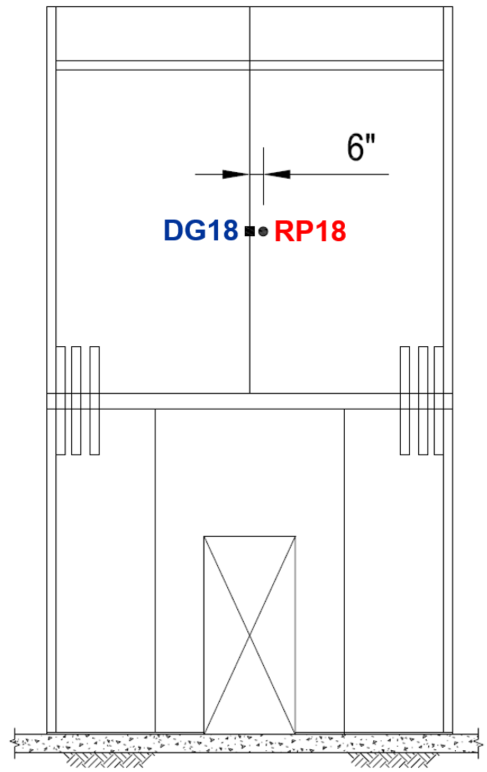

(b) Door (Left) Elevation.

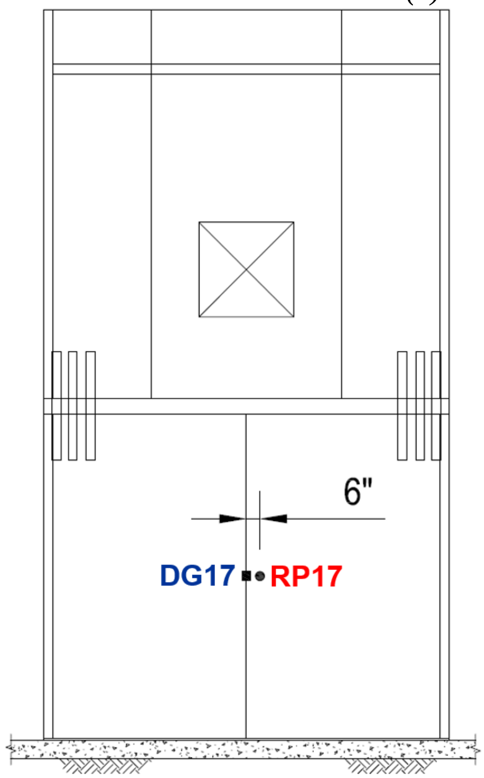

(c) Window (Right) Elevation.

Figure 3-20. Grade V4 Structure Reflected Pressure Gage Key Plan.


(a) Reflected Pressure. *(b) External Incident Overpressure.*

Figure 3-21. Pressure Gages Used in Testing.

3.3.2 Displacement

Table 3-6 provides details concerning the eighteen gages (i.e., six per test structure) used to measure displacement for each test. The displacement gage used was a rack and wheel potentiometer and was supported by stands manufactured out of steel tubes and angles (Figure 3-22). The locations of the displacement gages are shown schematically in Figure 3-18 through Figure 3-20.

Table 3-6. Displacement Gage Summary.

ID	Structure Grade	Measurement	Location	Range
DG1 – DG6	V1	Out-of-Plane Displacement	Flush w/ wall (Figure 3-18)	36” (in) 12” (out)
DG7 – DG12	E1	Out-of-Plane Displacement	Flush w/ wall (Figure 3-19)	36” (in) 12” (out)
DG13 – DG18	V4	Out-of-Plane Displacement	Flush w/ wall (Figure 3-20)	36” (in) 12” (out)

Figure 3-22. Rack and Wheel Displacement Gages with Support Stands.

3.3.3 Acceleration

Table 3-6 provides details concerning the three gages (i.e., one per test structure) used to measure acceleration for each test. The accelerometer used was the 2262A Accelerometer by Endevco (Part No. 2252A-1000). The locations of the accelerometers are shown schematically in Figure 3-18 through Figure 3-20.

Table 3-7. Accelerometer Summary.

ID	Structure Grade	Measurement	Location	Range
AG1	V1	Acceleration	Flush w/ wall (Figure 3-18)	± 0.2 in/ms^2
AG2	E1	Acceleration	Flush w/ wall (Figure 3-19)	± 0.15 in/ms^2
AG3	V4	Acceleration	Flush w/ wall (Figure 3-20)	± 0.15 in/ms^2

3.3.4 Video

Five video cameras were used to record each test from different angles. Details concerning the video cameras are included in Table 3-8. Four of the five cameras were high-speed cameras and were capable of recording at least 3,270 frames per second (fps). Figure 3-23 provides a schematic representation of how the high-speed video cameras were positioned.

Table 3-8. Video Camera Summary.

ID	Camera	View	Resolution / Speed
HS1	Miro 320S Phantom	Side view of Grade V1 structure	1280x720 @ 3270 fps
HS2	Miro 320S Phantom	Between Grades V1 & E1 structures from behind	1280x720 @ 3270 fps
HS3	Miro 320S Phantom	Side view of Grade V4 structure	1280x720 @ 3270 fps
HS4	V12 Phantom	Overall view	1280x720 @ 6960 fps
4K	Sony 4K Ultra-HD	Overall view	32 fps

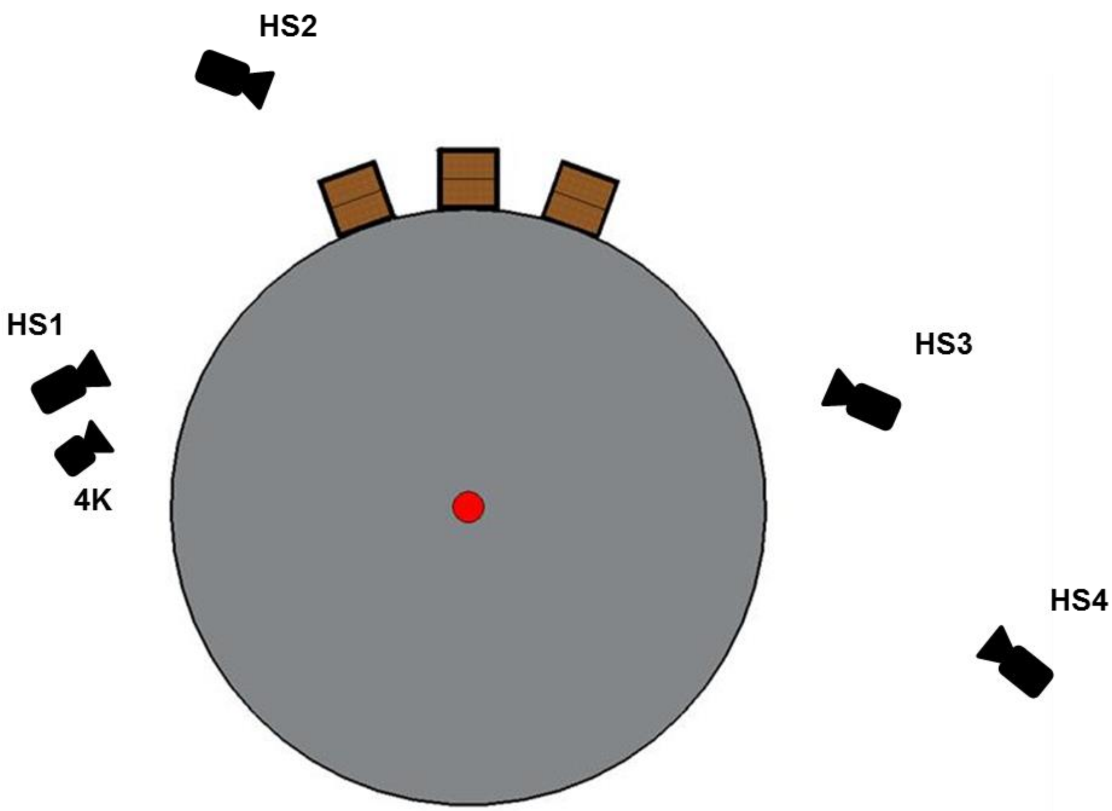

Figure 3-23. Video Camera Key Plan.

CHAPTER 4

ARENA TESTING RESULTS

The results of the Phase 2 arena blast Tests 4 through 7 are described in this chapter. The chapter opens with a description of visual observations made following each test. Then the pressure and displacement data recorded for each test are presented.

4.1 OBSERVATIONS

4.1.1 Test 4

Test 4 was performed on the morning of September 19, 2017. No signs of damage to or permanent deformation in the constituent panels of the test structures were observed following Test 4. While no damage was observed on the CLT panels themselves, the grout placed under the foundation angle cracked and broke up in isolated cases (Figure 4-1).

Photographs of the post-test condition of the first-floor panel directly facing the charge are included as Figure 4-2.

Figure 4-1. Test 4 Post-Test Photograph of Grout Breakup.

(a) Grade V1 – Exterior.

(b) Grade V1 – Interior.

Figure 4-2. Test 4 Post-Test Photographs of First-Floor Front Panel.

(c) Grade E1 – Exterior.

(d) Grade E1 – Interior.

Figure 4-2. Test 4 Post-Test Photographs of First-Floor Front Panel. (Cont'd)

(e) Grade V4 – Exterior.

(f) Grade V4 – Interior.

Figure 4-2. Test 4 Post-Test Photographs of First-Floor Front Panel. (Cont'd)

4.1.2 Test 5

Test 5 was performed in the early afternoon of September 19, 2017. Figure 4-3 show the elevations of the three test structures directly facing the charge following Test 3.

Damage to both interior and exterior faces was observed in all three test structures following Test 5. Observable damage was primarily concentrated in the front panel facing the explosive charge.

Photographs of the post-test condition of the first-floor panel directly facing the charge from the exterior and interior are included as Figure 4-4. For the Grade V1 and Grade E1 test structures, noticeable damage was observed near mid-height and mid-width of the first-floor front panel on both the interior and exterior faces. On the other hand, only minor cracking was observed in the Grade V4 test structure (with shorter plate height) at mid-height / mid-width of the first-floor front panel on the exterior face. No damage on the interior faces of the Grade E1 and Grade V4 test structures were observed. Photographs documenting the localized damage observed in the first-floor front panels of the test structures is included in Figure 4-5 and Figure 4-6.

Figure 4-3. Test 5 Post-Test Photograph of All Test Structures.

(a) Grade V1 – Exterior.

(b) Grade V1 – Interior.

Figure 4-4. Test 5 Post-Test Photographs of First-Floor Front Panel.

(c) Grade E1 – Exterior.

(d) Grade E1 – Interior.

Figure 4-4. Test 5 Post-Test Photographs of First-Floor Front Panel. (Cont'd)

(e) Grade V4 – Exterior.

(f) Grade V4 – Interior.

Figure 4-4. Test 5 Post-Test Photographs of First-Floor Front Panel. (Cont'd)

(a) Grade V1.

(b) Grade V4.

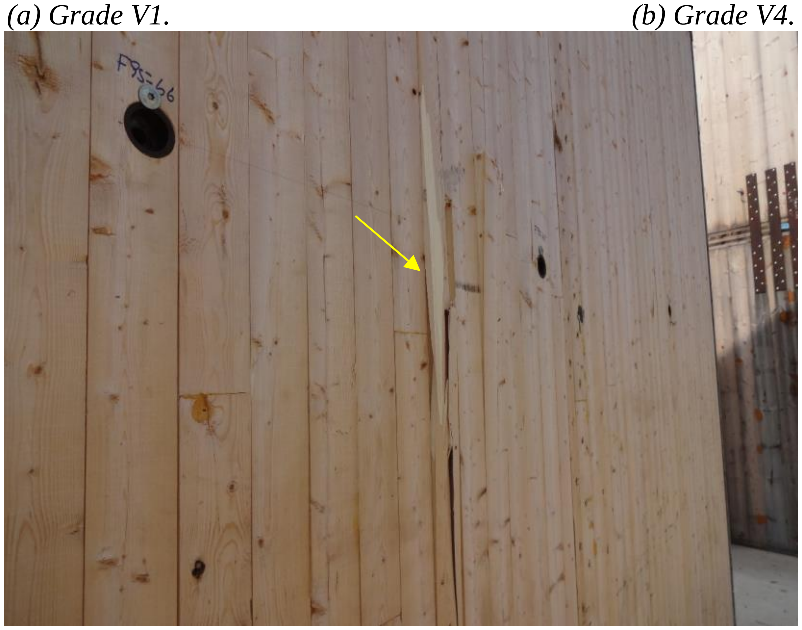

(c) Grade E1.

Figure 4-5. Test 5 Post-Test Photograph of Exterior Face Damage at 1st Floor Front Panel.

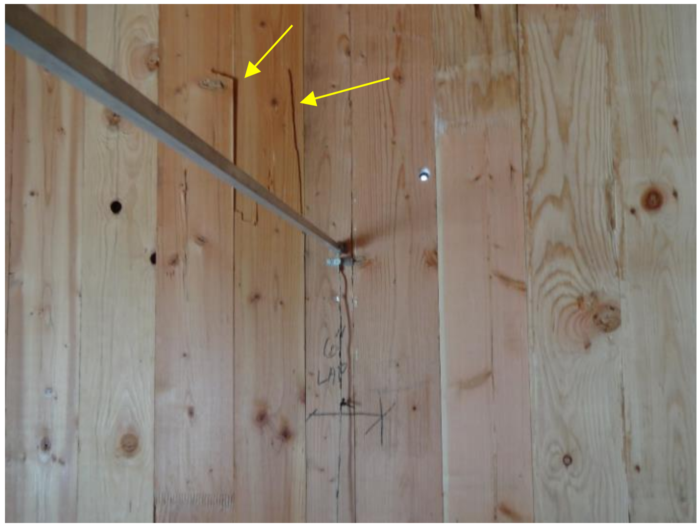

(a) Grade V1.

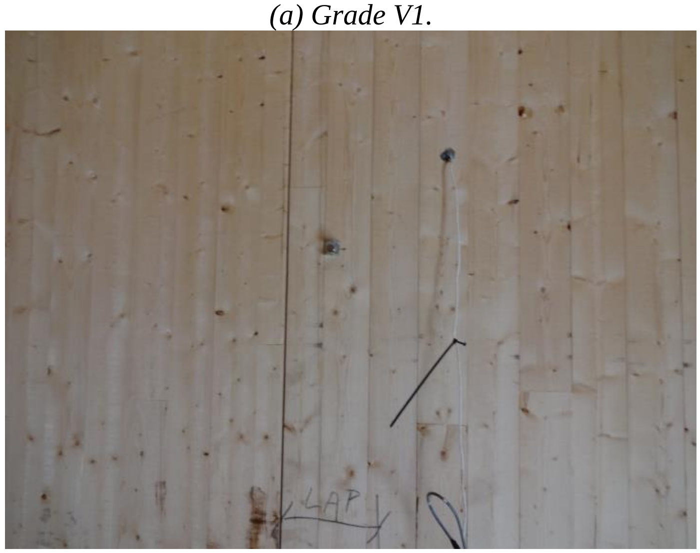

(b) Grade E1.

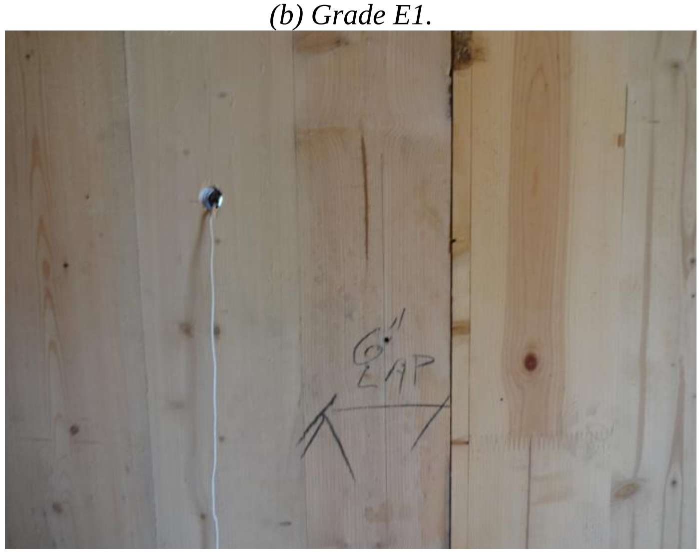

(c) Grade V4.

Figure 4-6. Test 5 Post-Test Photograph of Interior Face Damage at 1st Floor Front Panel.

Unlike following Test 3 in the Phase 1 testing, no CLT panel debris was observed on the floor inside the Grade V4 test structure following Test 5 (Figure 4-7c). Although this result could simply be due to panel variability, it is possible that the presence of axial load in the wall panels served to limit the propensity for CLT panel debris generation. Also, as observed in the Phase 1 testing, no debris was observed on the floor inside the Grade V1 or Grade E1 test structures (Figure 4-7a and b).

(a) Grade V1.

(b) Grade E1.

(c) Grade V4.

Figure 4-7. Test 3 Post-Test Photographs of Floors.

All doors opened (in rebound) during Test 5. Either rupture of the dimensional lumber restraints securing the door or withdrawal of the fasteners securing this dimensional lumber was observed in the test structures (Figure 4-8). It should be noted these lumber restraints were installed to merely keep the door closed at the outset of the test. They were not designed to resist the imposed blast loading, nor would they be installed in an actual building.

(a) 2x rupture (Grade E1).

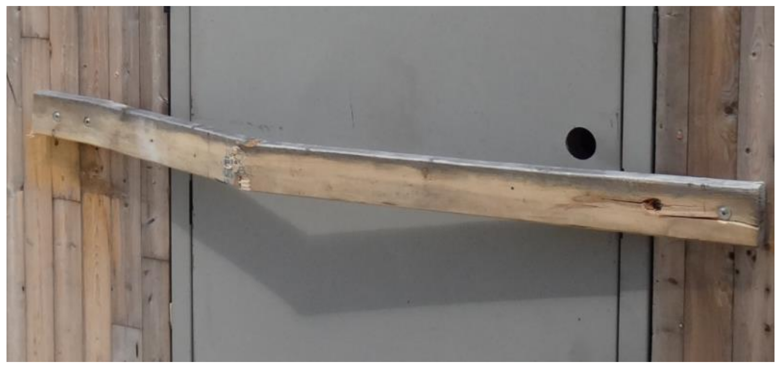

(b) Close-up of 2x rupture (Grade E1).

(c) Fastener pull-through and 2x splitting (Grade V4).

(d) Close-up of fastener pull-through and 2x splitting (Grade V4).

Figure 4-8. Test 5 Post-Test Photograph of Damage at Door Restraints.

4.1.3 Test 6

Test 6 was performed on the morning of October 26, 2017. No signs of damage to or permanent deformation in the constituent panels of the test structures with the CLT front walls were observed following Test 6. However, partial nail pullout was observed for the test structure with the NLT front walls at both the first and second floors (Figure 4-9). However, no nails pulled entirely out of the panel and full structural integrity remained intact (as plywood was not intended to contribute to bending capacity) at both test structure stories. No damage to the alternate connection configurations included in the Grade E1 CLT test structure was observed (Figure 4-10).

Photographs of the post-test condition of the first-floor panel directly facing the charge are included as Figure 4-11.

(a) Typical nail pullout observed.

(b) Panel disengagement due to nail pullout at top of structure.

Figure 4-9. Test 6 Post-Test Photograph of Nail Pullout.

(a) Front wall panel connection at underside of elevated floor in Grade E1 test structure.

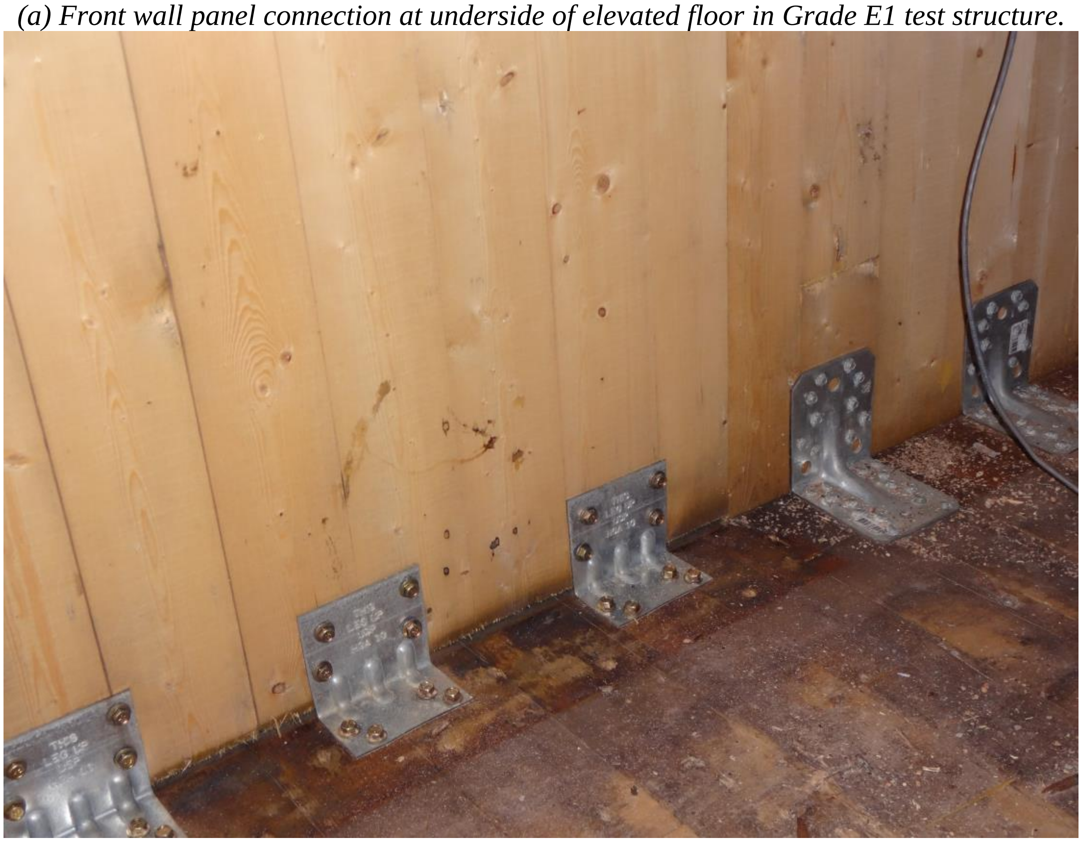

(b) Front wall panel connection at top side of elevated floor in Grade E1 test structure.

Figure 4-10. Test 6 Post-Test Photograph of Alternate Connections.

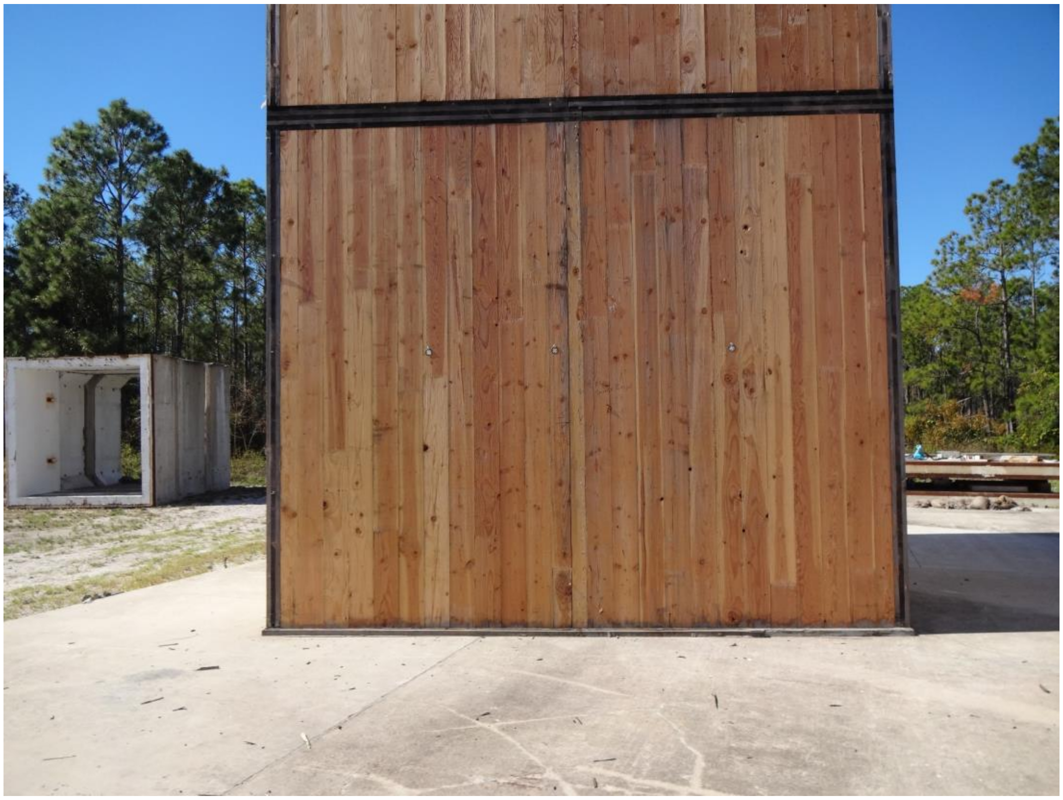

(a) Grade V1 – Exterior.

(b) Grade V1 – Interior.

Figure 4-11. Test 6 Post-Test Photographs of First-Floor Front Panel.

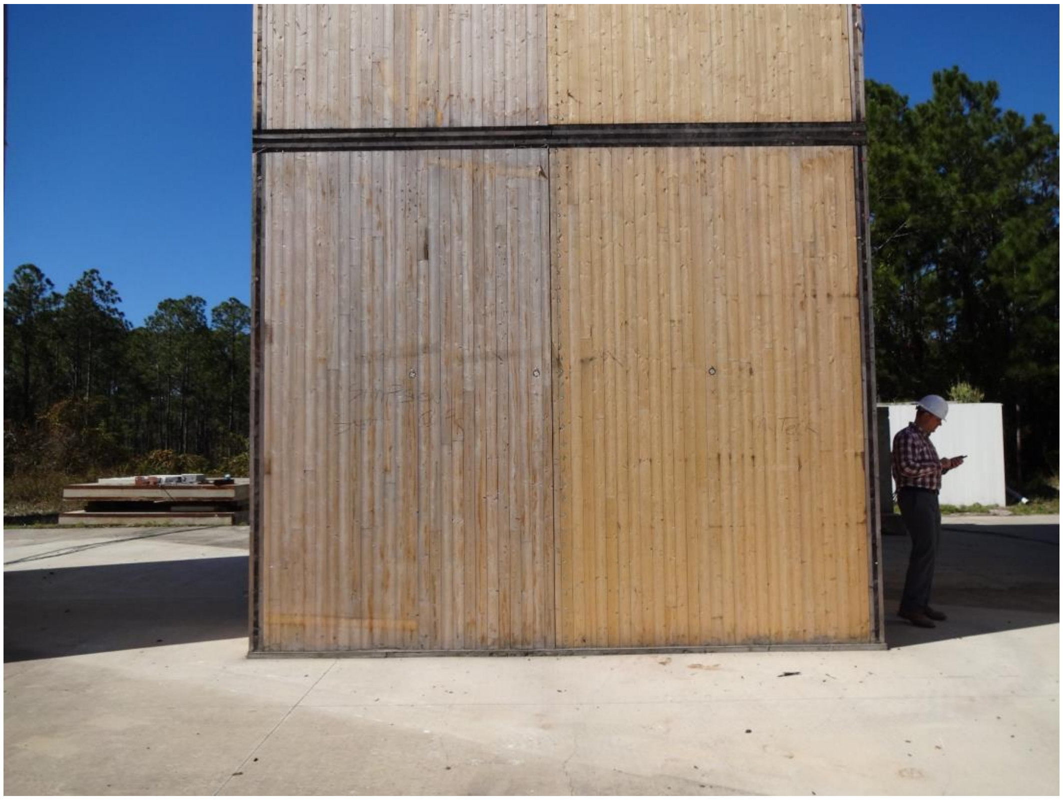

(c) Grade E1 – Exterior.

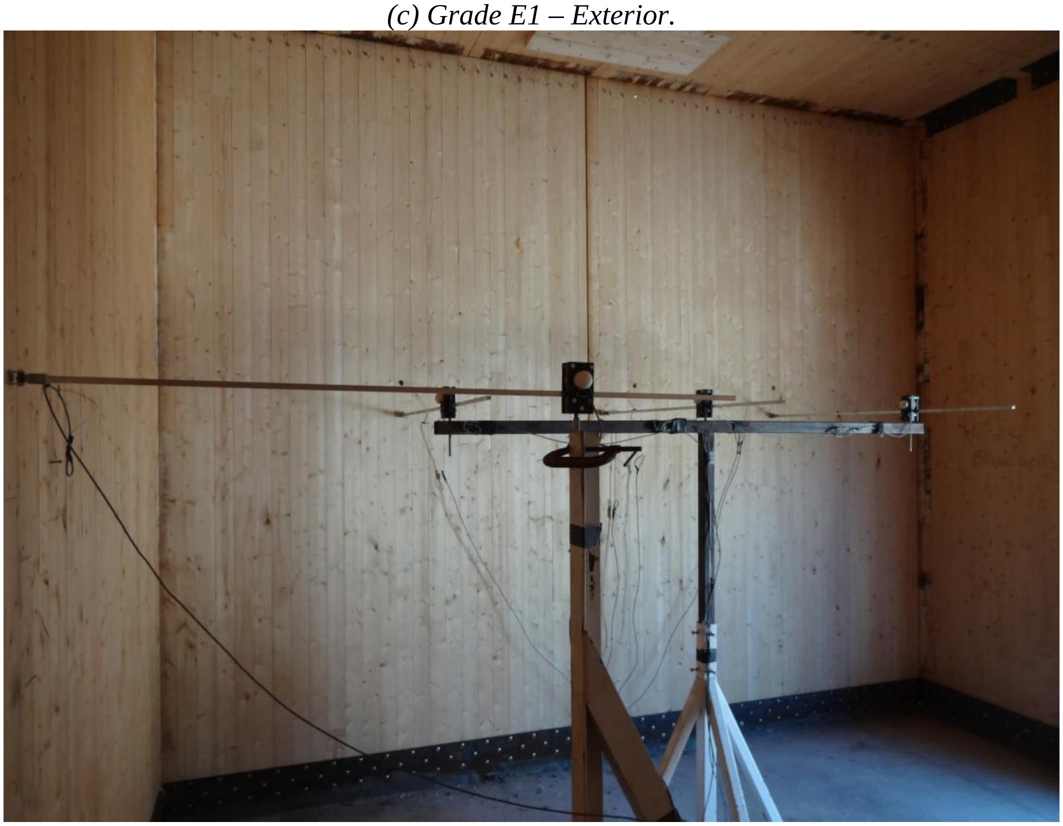

(d) Grade E1 – Interior.

Figure 4-11. Test 6 Post-Test Photographs of First-Floor Front Panel. (Cont'd)

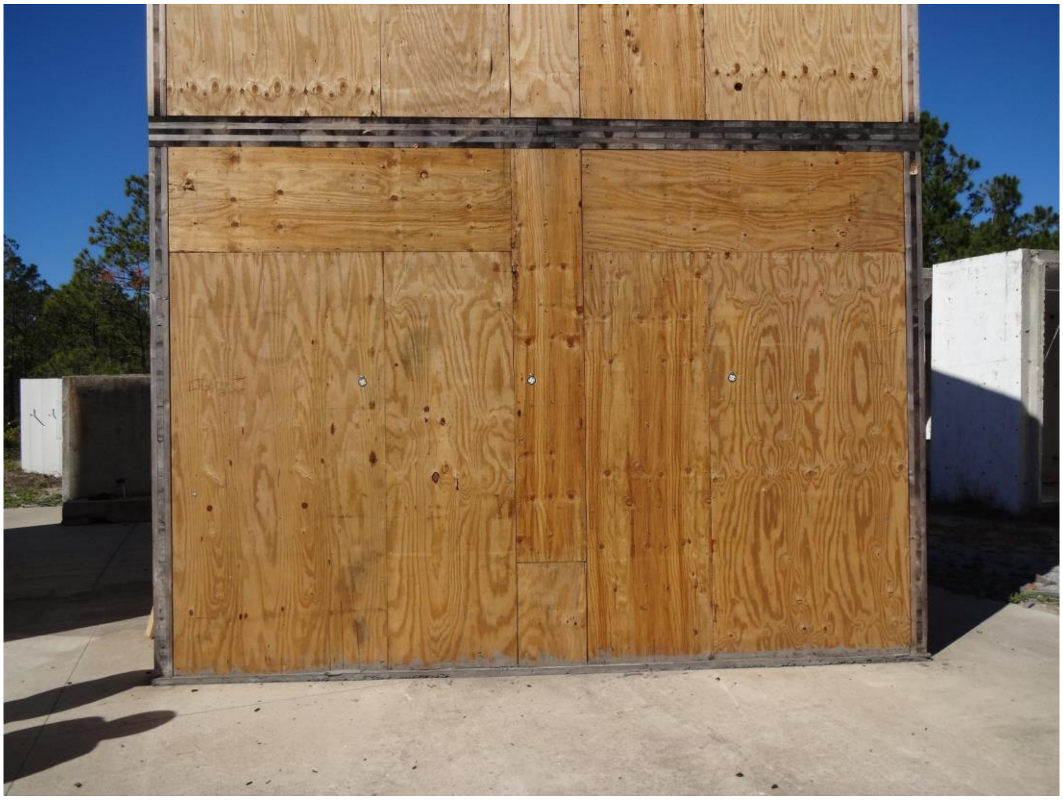

(e) NLT – Exterior.

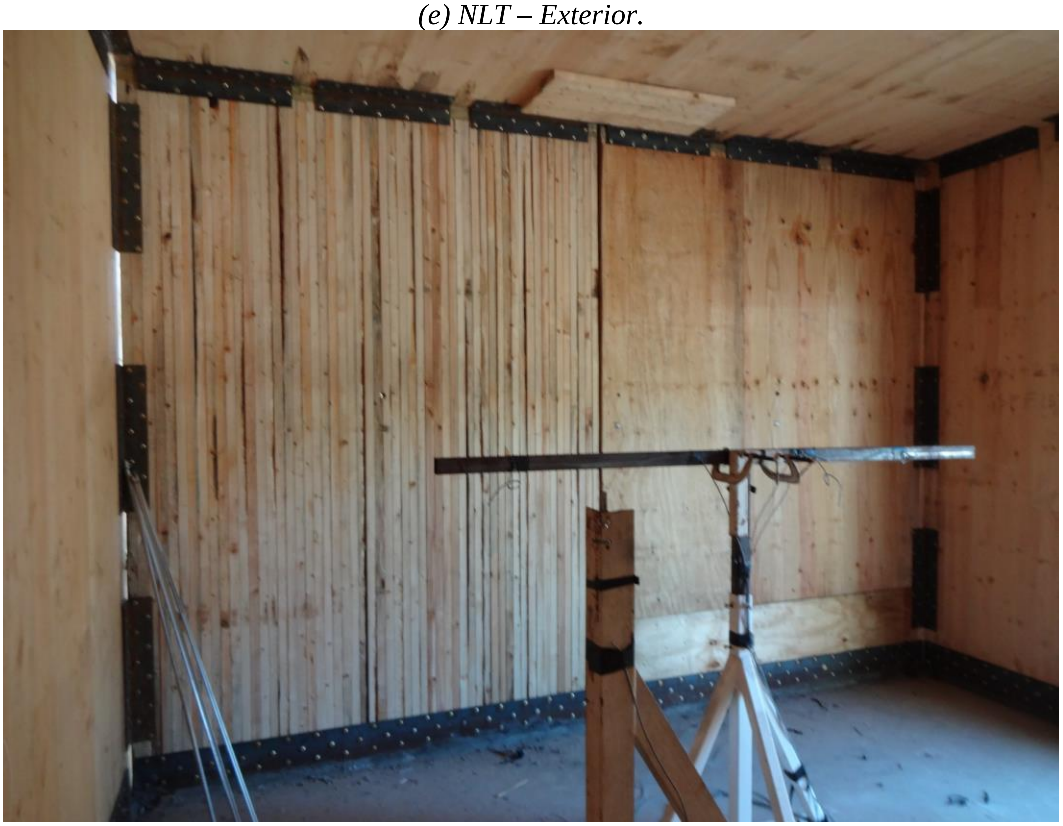

(f) NLT – Interior.

Figure 4-11. Test 6 Post-Test Photographs of First-Floor Front Panel. (Cont'd)

4.1.4 Test 7

Test 7 was performed in the early afternoon of October 26, 2017. Figure 4-12 shows the front elevations of the three test structures directly facing the charge following Test 7. Extensive damage was observed in each test structure; however structures were structurally stable and intact. The following subsections will document the damage exhibited by each test structure.

Figure 4-12. Test 7 Post-Test Photograph of All Test Structures.

4.1.4.1 *GRADE V1 STRUCTURE (5-PLY FRONT WALL)*

Localized damage was observed on the 5-ply front and 3-ply side wall panels of the Grade V1 structure. No damage was observed on the 3-ply wall panels at the back side of the structure.

- **Front Wall**: Photographs documenting the damage to the 5-ply Grade V1 front wall panels are included in Figure 4-13. No damage was observed post-test at the exterior face of the front wall panels (Figure 4-13a). However, panel rupture over a significant portion of the wall at midspan was observed from the interior (Figure 4-13b and c). In addition, a few small pieces of debris were generated from the front wall panel rupturing (Figure 4-13b).

(a) Exterior Face.

Figure 4-13. Test 7 Post-Test Photographs of Front Panels in Grade V1 Structure.

(b) Interior Face.

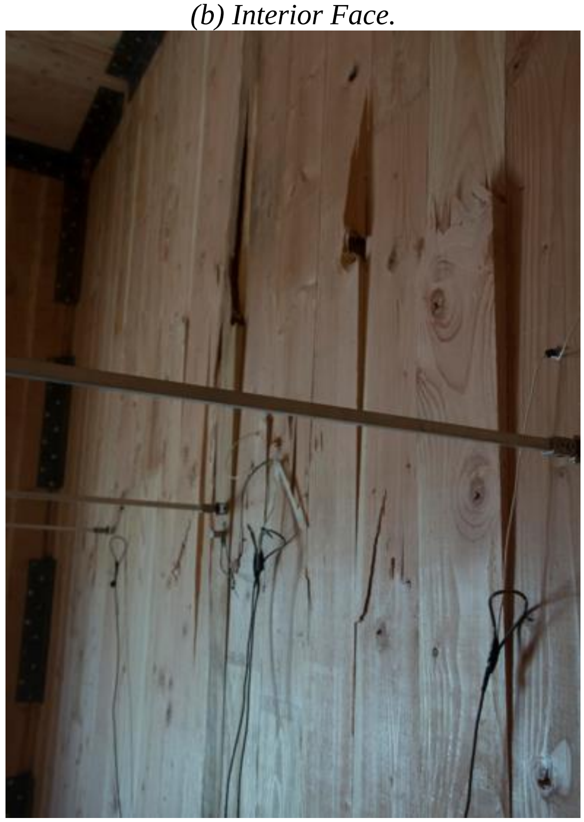

(c) Close-Up of Interior Face Damage.

Figure 4-13. Test 7 Post-Test Photographs of Front Panels in Grade V1 Structure. (Cont'd)

- **Side Wall with Window**: Photographs documenting the damage to the 3-ply Grade V1 window-side wall panels are included in Figure 4-14. Very localized damage was observed on the exterior and interior faces of the first-floor side wall (Figure 4-14a and Figure 4-14b). Additionally, very localized damage was observed in CLT panel acting as the jamb for the window at the second floor (Figure 4-14c).

(a) 1st Floor Exterior.

Figure 4-14. Test 7 Post-Test Photographs of Window-Side Panels in Grade V1 Structure.

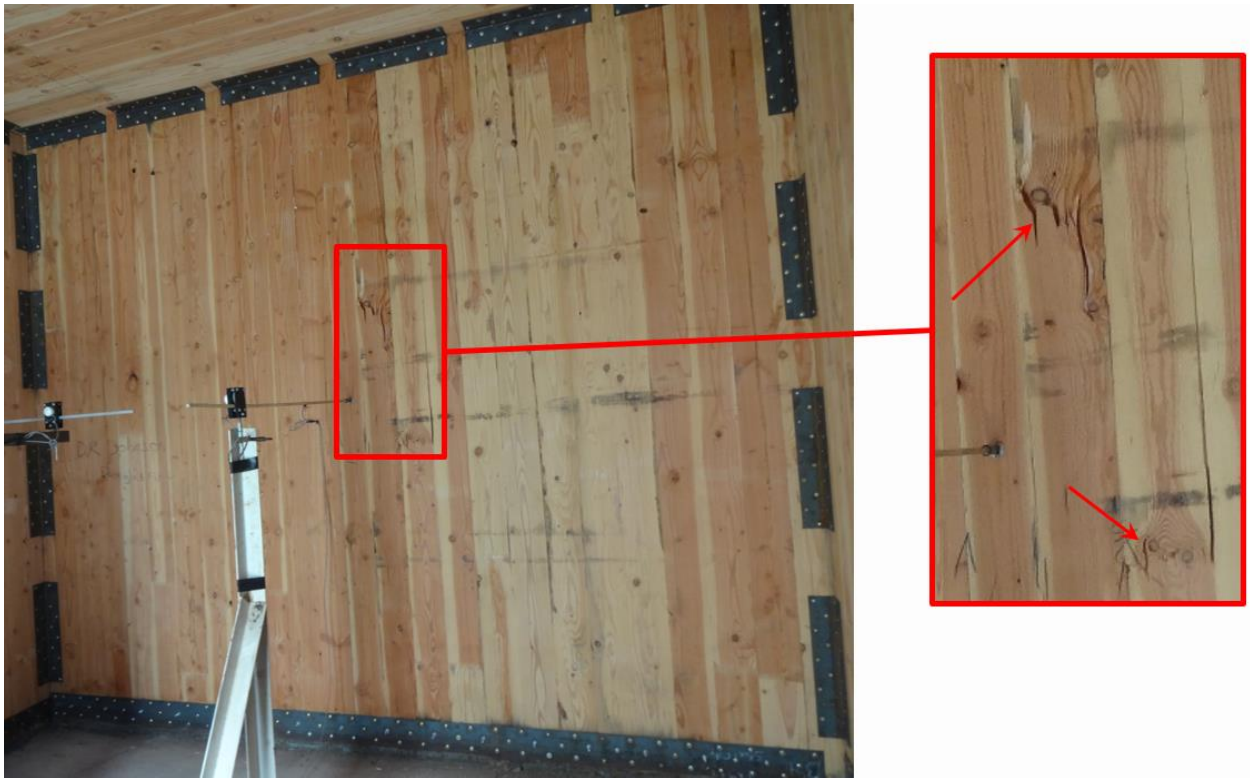

(b) 1st Floor Interior.

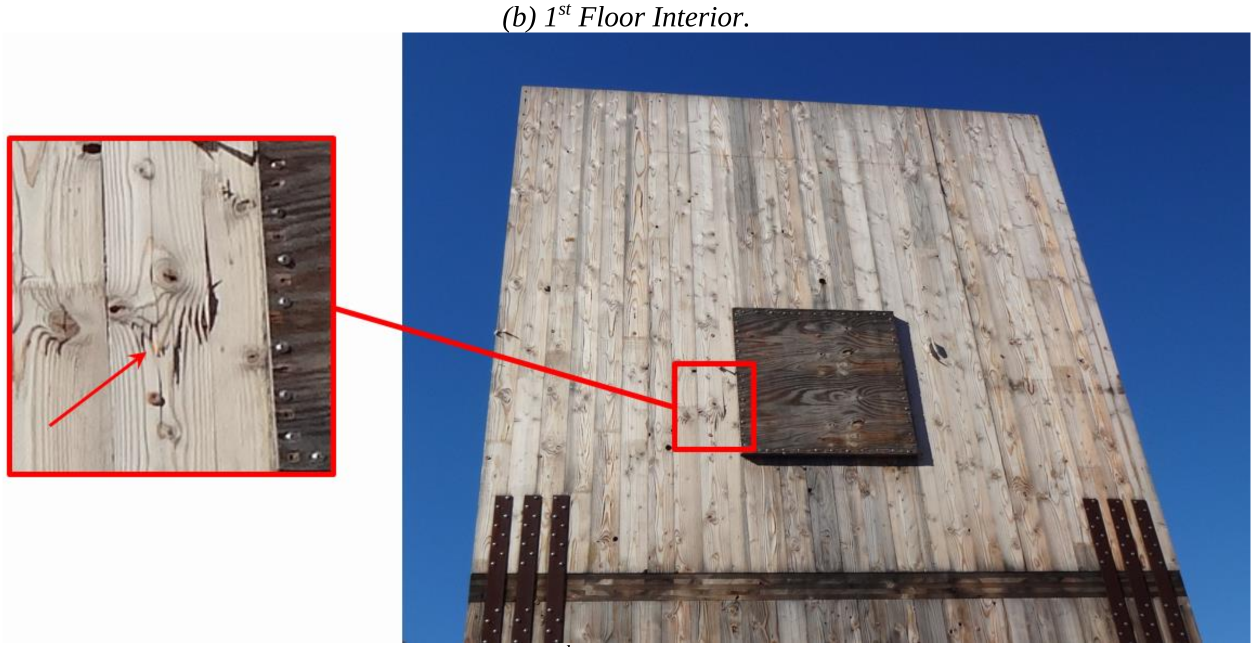

(c) 2nd Floor Exterior.

Figure 4-14. Test 7 Post-Test Photographs of Window-Side Panels in Grade V1 Structure. (Cont'd)

- **Side Wall with Door**: Photographs documenting the damage to the 3-ply Grade V1 door-side wall panels are included in Figure 4-14. During the test, the door rebounded out of its frame and broke the 2x member intended to restrain the door in rebound (Figure 4-15a). It should be noted that the door was only designed to resist the blast loads associated with Test 6. Very localized damage was observed in the CLT panel acting as the jamb for the door (Figure 4-15b). While no damage was observed on the interior face of the first-floor side wall panel, partial self-tapping screw withdrawal was observed in several instances (Figure 4-15c). Additionally, inelastic deformation of the door frame was observed at its top corners (Figure 4-15c).

(a) Door Rebounds Out of Frame.

Figure 4-15. Test 7 Post-Test Photographs of Door-Side Panels in Grade V1 Structure.

(b) Localized Damage at Door Jamb.

(c) Localized Damage Near Top of Door Frame.

Figure 4-15. Test 7 Post-Test Photographs of Door-Side Panels in Grade V1 Structure. (Cont'd)

4.1.4.2 *GRADE E1 STRUCTURE (ALTERNATIVE FRONT WALL CONNECTIONS)*

As expected, significant damage was observed in the 3-ply Grade E1 front wall panels, both in the CLT panels themselves and at the connections, and minimal localized damage was observed in the 3-ply Grade E1 side wall panels. No damage was observed on the 3-ply wall panels at the back side of the structure.

- **Front Wall at First-Floor**: Photographs documenting the damage to the 3-ply Grade E1 first-floor front wall panels are included in Figure 4-16. Significant damage was observed at the wall panel's exterior (Figure 4-16a) and interior (Figure 4-16b) faces at mid-span. Entire lamella separated on the interior face and were thrown into the interior space as debris (Figure 4-16c). Additionally, the screws connecting the first-floor wall panels to the first elevated floor pulled out of their respective "main member" panel (Figure 4-16d). One exception to this observation is indicated in Figure 4-16d. However, it should be noted that this screw was installed within 4D of an adjacent screw as shown in a pre-test photograph (Figure 4-16e). No damage was observed at the base angle connection (Figure 4-16f).

(a) Exterior Face.

Figure 4-16. Test 7 Post-Test Photographs of 1st Floor Front Wall Panels in Grade E1 Structure.

(b) Interior Face.

(c) Ground Inside Structure.

Figure 4-16. Test 7 Post-Test Photographs of 1st Floor Front Wall Panels in Grade E1 Structure. (Cont'd)

(d) Wall Panel at Top.

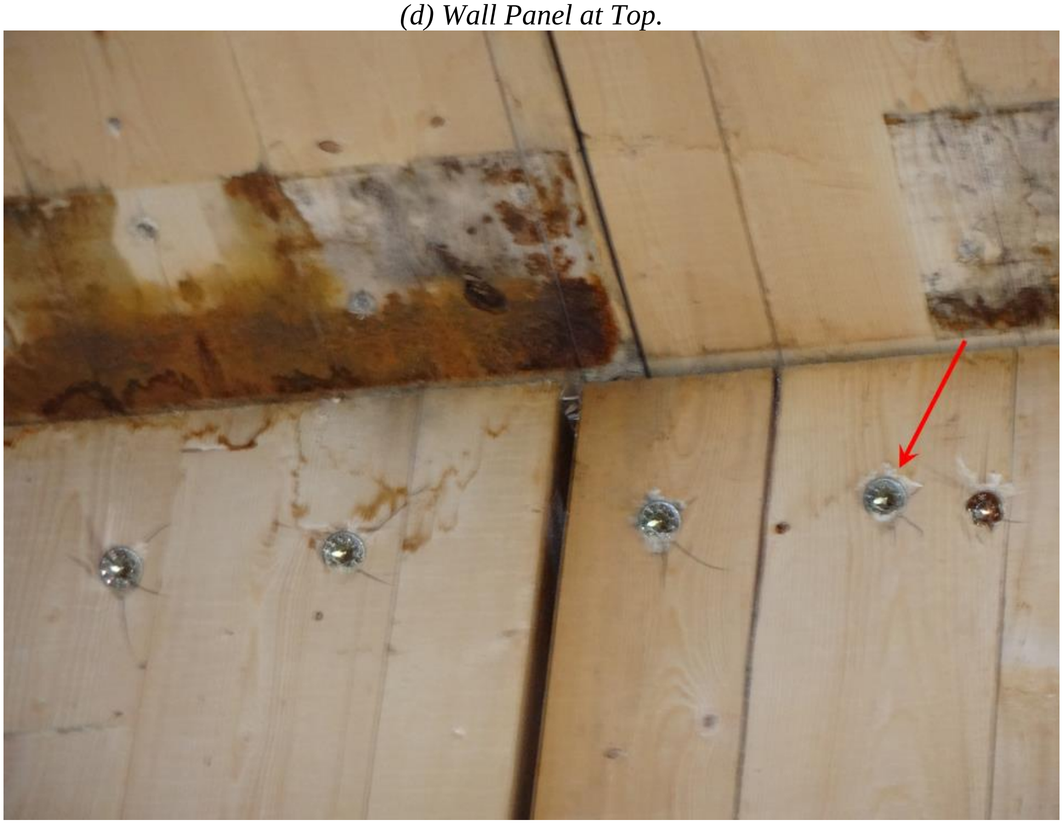

(e) Pre-Test Condition at Top of Wall Panel.

Figure 4-16. Test 7 Post-Test Photographs of 1st Floor Front Wall Panels in Grade E1 Structure. (Cont'd)

(f) Base Angle Connection.

Figure 4-16. Test 7 Post-Test Photographs of 1st Floor Front Wall Panels in Grade E1 Structure. (Cont'd)

- **Front Wall at Second-Floor**: Photographs documenting the damage to the 3-ply Grade E1 second-floor front wall panels are included in Figure 4-17. While no damage was observed on the exterior face at the second-floor front wall panel (Figure 4-17a), several boards near mid-span of the wall separated at the glue line from the rest of the wall panel and fell straight down (Figure 4-17b and Figure 4-17c). No damage at the wall panel's connection was observed for the SST connection brackets (Figure 4-17d); however, significant angle yielding and fastener pullout were observed at the MiTek brackets. (It should be noted that due to a miscommunication, $1^1/_2$-inch long screws rather than the specified $3^1/_2$-inch long screws were installed with the MiTek angle. It is expected that the post-test result at this connection would be different in the event the longer screw was installed.)

(a) Exterior Face.

Figure 4-17. Test 7 Post-Test Photographs of 2nd Floor Front Wall Panels in Grade E1 Structure.

(b) Interior Face.

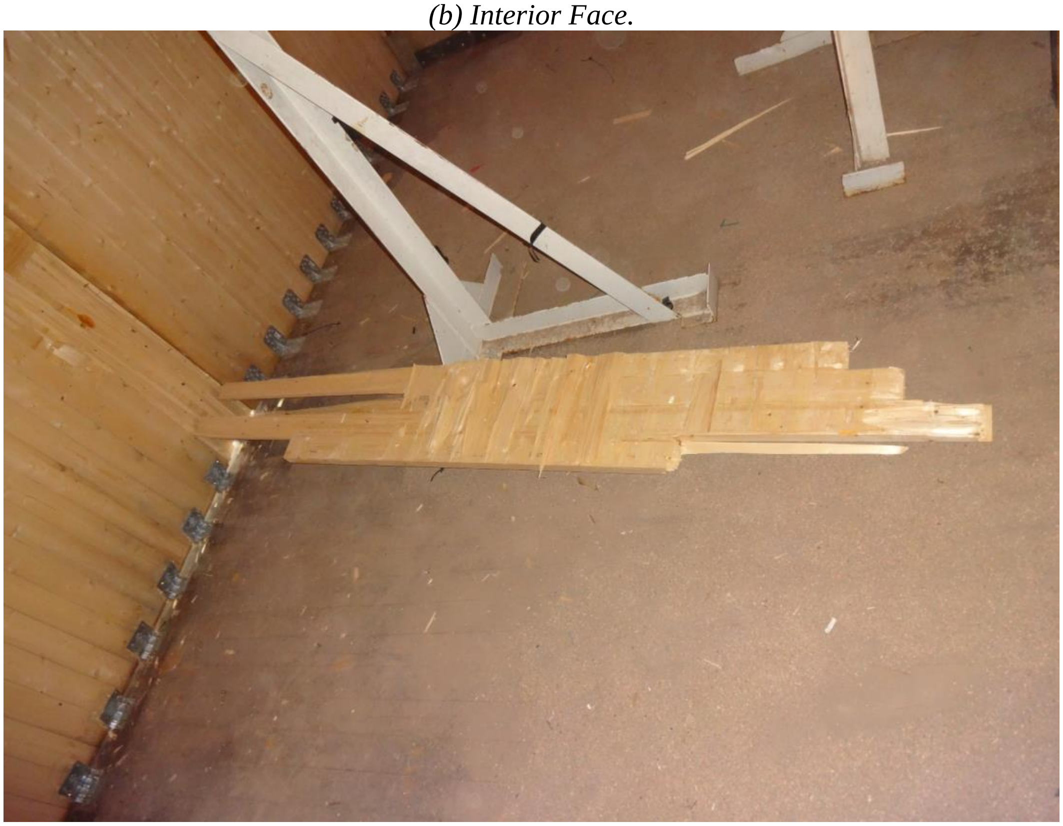

(c) Delaminated Boards on Interior Face.

Figure 4-17. Test 7 Post-Test Photographs of 2nd Floor Front Wall Panels in Grade E1 Structure. (Cont'd)

(d) SST Brackets.

(e) MiTek Brackets.

Figure 4-17. Test 7 Post-Test Photographs of 2nd Floor Front Wall Panels in Grade E1 Structure. (Cont'd)

- **Side Wall with Window**: Photographs documenting the damage to the 3-ply Grade E1 window-side wall panels are included in Figure 4-18. Localized damage was observed on the exterior face of the first-floor side wall on the window side (Figure 4-18a). No corresponding damage was observed on the interior face at the first-floor. Additionally, no damage was observed at either the exterior or interior faces at the second floor (Figure 4-18b and c).

(a) 1st Floor Exterior Face.

Figure 4-18. Test 7 Post-Test Photographs of Window-Side Panels in Grade E1 Structure.

(b) 2nd Floor Exterior Face.

(c) 2nd Floor Interior Face.

Figure 4-18. Test 7 Post-Test Photographs of Window-Side Panels in Grade E1 Structure. (Cont'd)

- **Side Wall with Door**: Photographs documenting the damage to the 3-ply Grade V1 door-side wall panels are included in Figure 4-19. Very localized damage in the CLT wall panel was observed on the exterior face near the top of the door frame (Figure 4-19a); however, no corresponding damage was observed on the interior face. Similarly, minimal damage was observed on the second-floor wall panel (Figure 4-19b) but no corresponding damage was observed on the interior face.

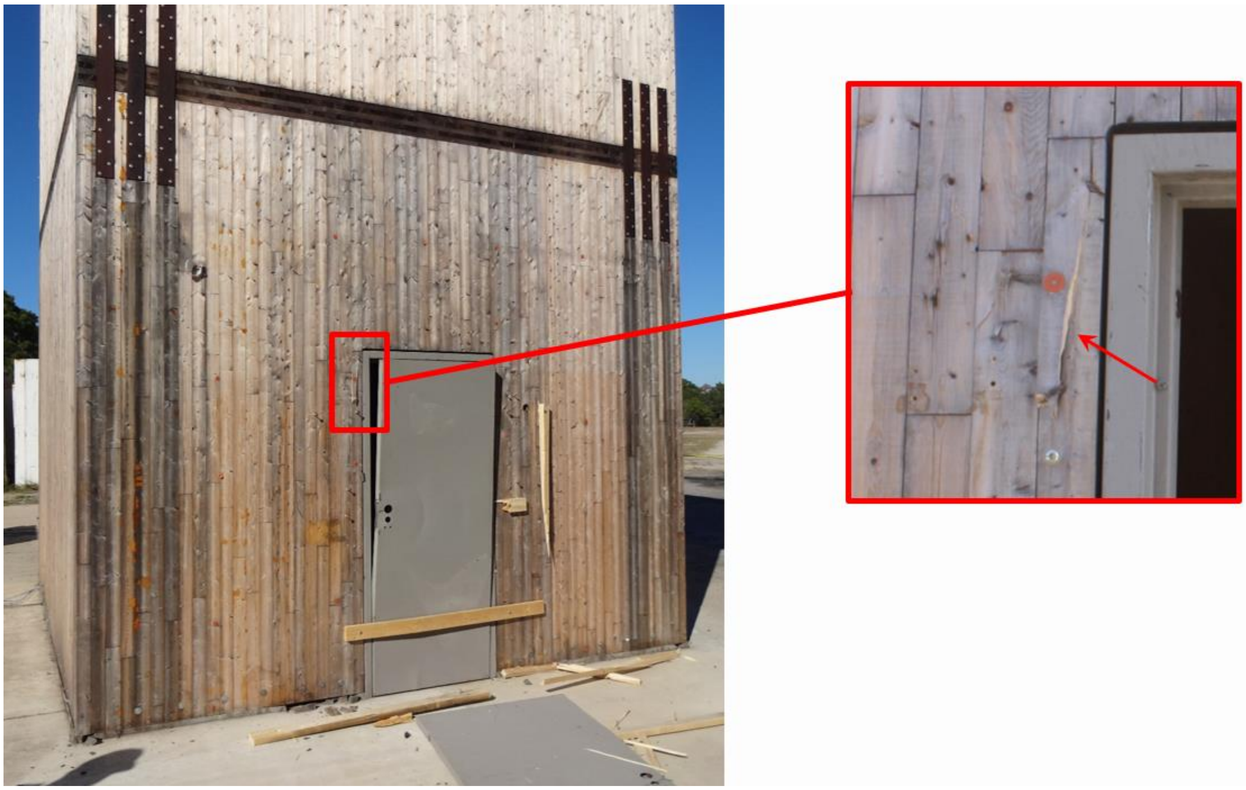

(a) 1st Floor Exterior Face.

Figure 4-19. Test 7 Post-Test Photographs of Door-Side Panels in Grade E1 Structure.

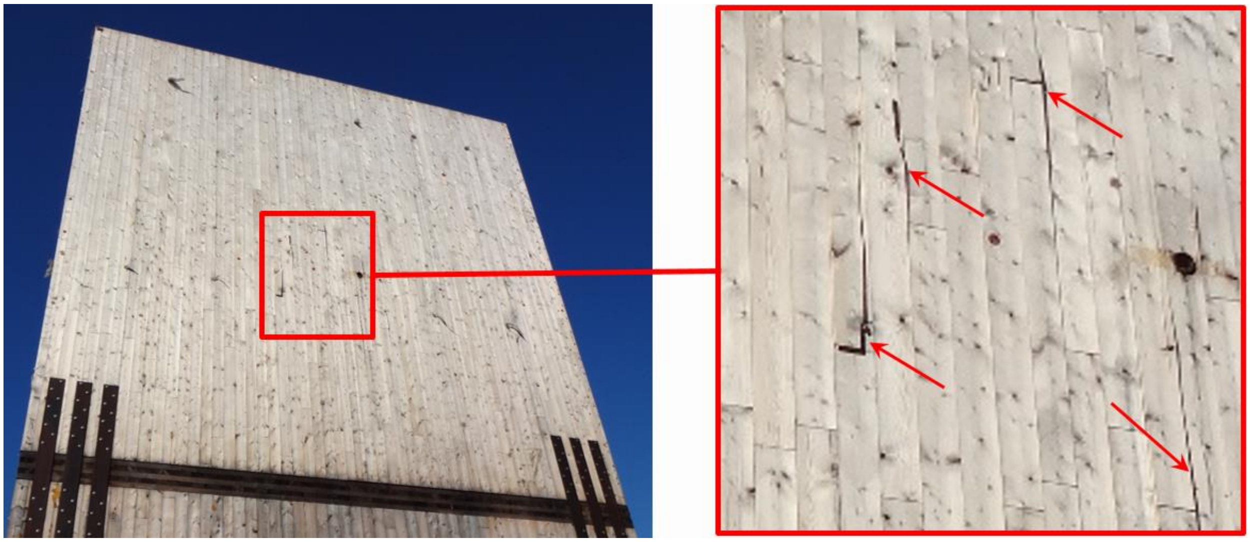

(b) 2nd Floor Exterior Face.

Figure 4-19. Test 7 Post-Test Photographs of Door-Side Panels in Grade E1 Structure. (Cont'd)

4.1.4.3 *GRADE V1 STRUCTURE (NLT FRONT WALL)*

As expected, significant damage was observed in the 2x4 NLT front wall panels. However, no damage was observed on either the side or back walls to the Grade V4 panels.

- **Front Wall**: Photographs documenting the damage to the 2x4 NLT first-floor front wall panels are included in Figure 4-20. For the half of the first-floor wall panel that did not have plywood sheathing on its interior face, significant damage was observed at panel mid-span (Figure 4-20a). Most of the 2x4 studs comprising the NLT panel were completely ruptured through (Figure 4-20b). Conversely, the portion of the NLT panel that had plywood sheathing did not appear to have ruptured studs (Figure 4-20c). At both the exterior and interior faces, plywood sheathing disengaged from the 2x members (Figure 4-20d, Figure 4-20e, and Figure 4-20f). Apart from the disengaged plywood, a small amount of timber debris, presumably from the ruptured 2x4 studs, was observed on the ground inside the test structure (Figure 4-20g). Minimal damage was observed at the connections at the top and bottom of the wall, although several of the screws were slightly pulled out of the 2x laminations at the base angle (Figure 4-20h).

(a) Interior Face w/o Sheathing.

(b) Close-up of Stud Rupture (From Below).

Figure 4-20. Test 7 Post-Test Photographs of Front Panels in Grade V4 Structure.

(c) Interior Face of Portion of NLT Wall with Plywood Sheathing.

(d) Plywood Disengagement at Exterior Face – 1st Floor.

Figure 4-20. Test 7 Post-Test Photographs of Front Panels in Grade V4 Structure. (Cont'd)

(e) Plywood Disengagement at Exterior Face – 2^{nd} Floor.

(f) Plywood Disengagement at Interior Face.

Figure 4-20. Test 7 Post-Test Photographs of Front Panels in Grade V4 Structure. (Cont'd)

(g) Ground Inside Structure.

(h) Base Angle Connection.

Figure 4-20. Test 7 Post-Test Photographs of Front Panels in Grade V4 Structure. (Cont'd)

- **Side Walls**: Photographs documenting the condition of the 3-ply Grade V4 CLT side wall panels are included in Figure 4-21. Figure 4-21a and Figure 4-21b show the first-floor wall panel at the exterior and interior faces, respectively. Similarly, Figure 4-21c and Figure 4-21d show the first-floor wall panel at the exterior and interior faces, respectively. No damage to the side walls, either on the first or second floor, was observed at the conclusion of Test 7.

(a) 1st Floor Exterior Face – Window Side.

(b) 1st Floor Interior Face – Window Side.

Figure 4-21. Test 7 Post-Test Photographs of Side Wall Panels in Grade V4 Structure.

(c) 1st Floor Exterior Face – Door Side.

(d) 1st Floor Interior Face – Door Side.

Figure 4-21. Test 7 Post-Test Photographs of Side Wall Panels in Grade V4 Structure. (Cont'd)

4.2 RECORDED DATA

Pressure and panel displacement data was recorded using the instrumentation described in Chapter 3. All raw unfiltered pressure and displacement data recorded during the three tests is included in a Quick Look Report in Appendix E.

4.2.1 Pressure Data

Figure 4-22 plots the recorded incident overpressure data (i.e., by gages FF1 and FF2) and the average of these two gages for each of the four tests.

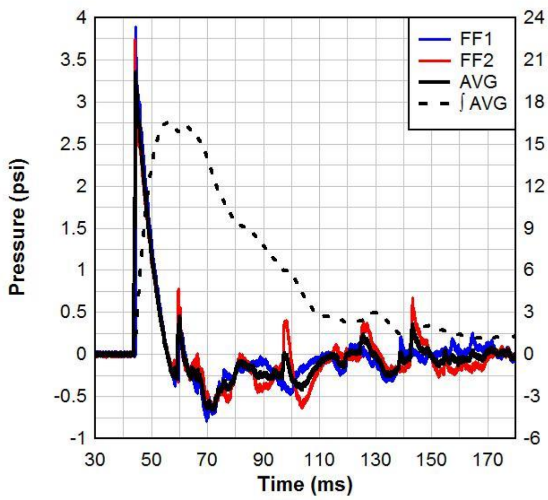

(a) Test 4.

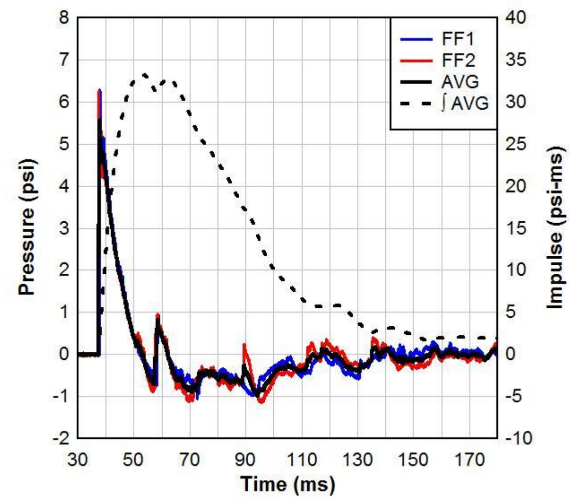

(b) Test 5.

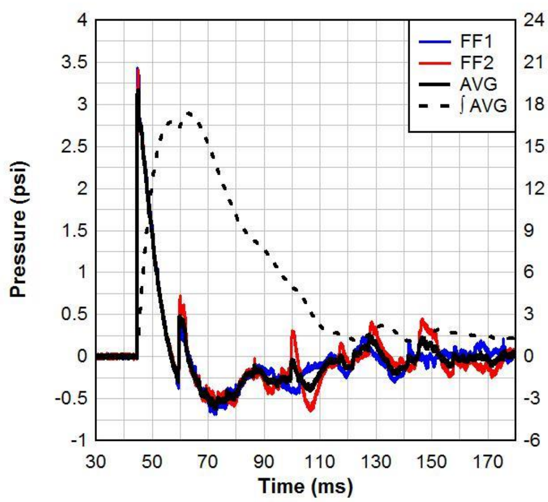

(c) Test 6.

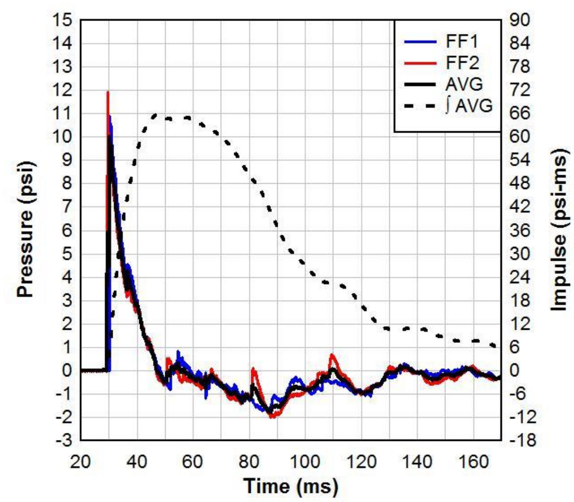

(d) Test 7.

Figure 4-22. Incident Overpressure Data.

Similarly, Figure 4-23 plots the reflected pressure data recorded at the mid-structure gage located on the first-floor front panels (i.e., by gages RP2, RP8, and RP14) and the average of these three gages for Tests 4, 5, and 6. Reflective pressure gages were only used on the Grade V1 structure for Test 7 and thus, Figure 4-23 only shows data recorded by RP2. Plots of the remaining pressure histories are included in Appendix E.

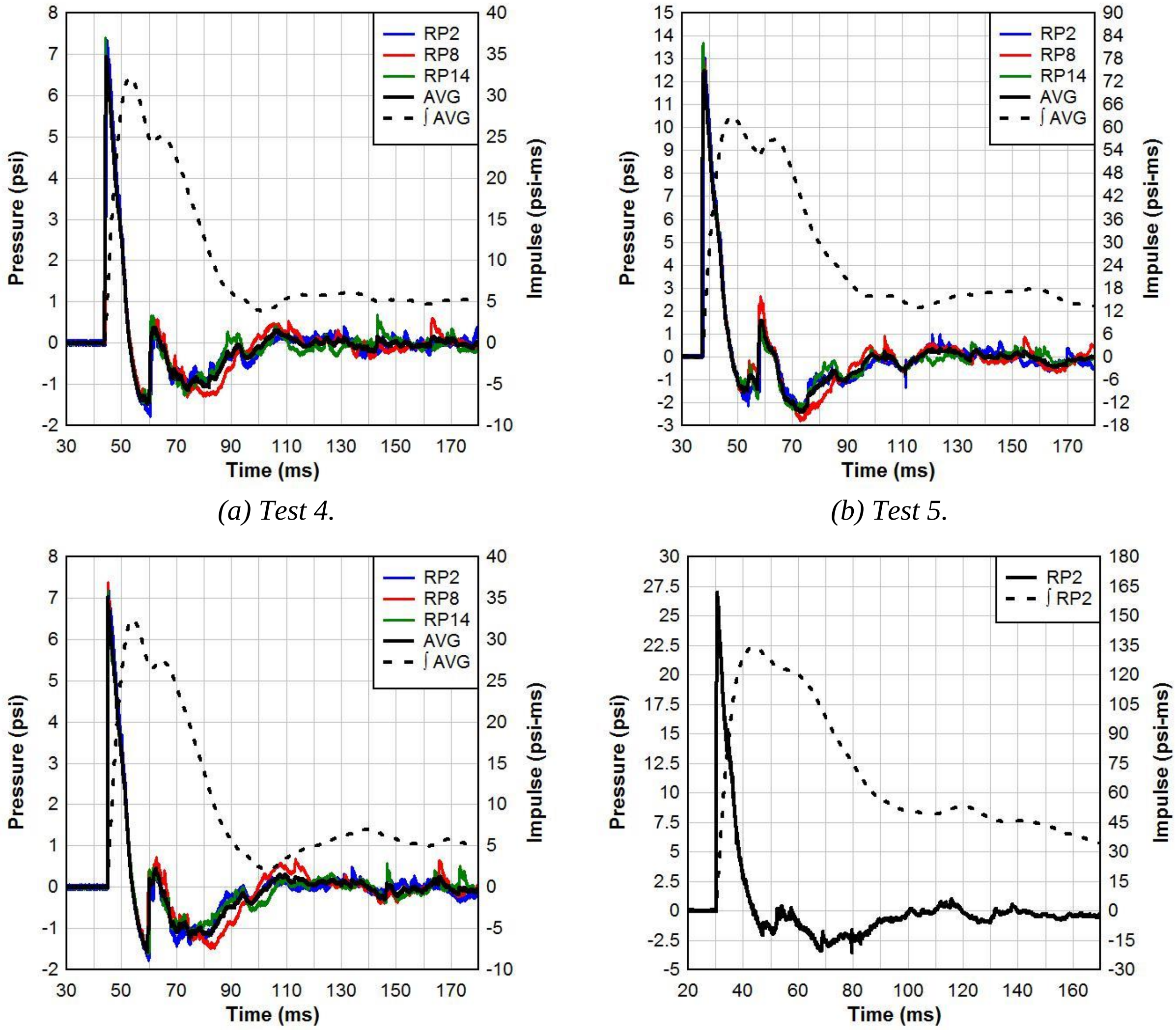

(a) Test 4. *(b) Test 5.*

(c) Test 6. *(d) Test 7.*

Figure 4-23. Reflected Pressure Data at First-Floor Front Panels.

Table 4-1 provides a summary of the incident and peak reflected pressure positive phase data for all three shots. The values shown in Table 4-1 are generated based on the average curves shown in Figure 4-22 and Figure 4-23.

Table 4-1. Pressure Data Summary.

Test	Time of Arrival [ms]	Incident Overpressure [psi]	Incident Impulse [psi-ms]	Peak Reflected Pressure [psi]	Peak Reflected Impulse [psi-ms]
4	43.8	3.82	16.5	7.22	32.1
5	37.2	6.27	33.2	13.4	62.8
6	44.6	3.43	17.3	7.25	32.3
7	29.4	11.4	65.8	27.0	134

4.2.2 Displacement Data

4.2.2.1 TESTS 4 & 5

Figure 4-24, Figure 4-25, and Figure 4-26 plot the peak recorded panel displacements at the 3-ply CLT front panel of the Grade V1, Grade E1, and Grade V4 test structures, respectively, for Tests 4 and 5. Plots of the remaining displacement histories from Tests 4 and 5 are included in Appendix E.

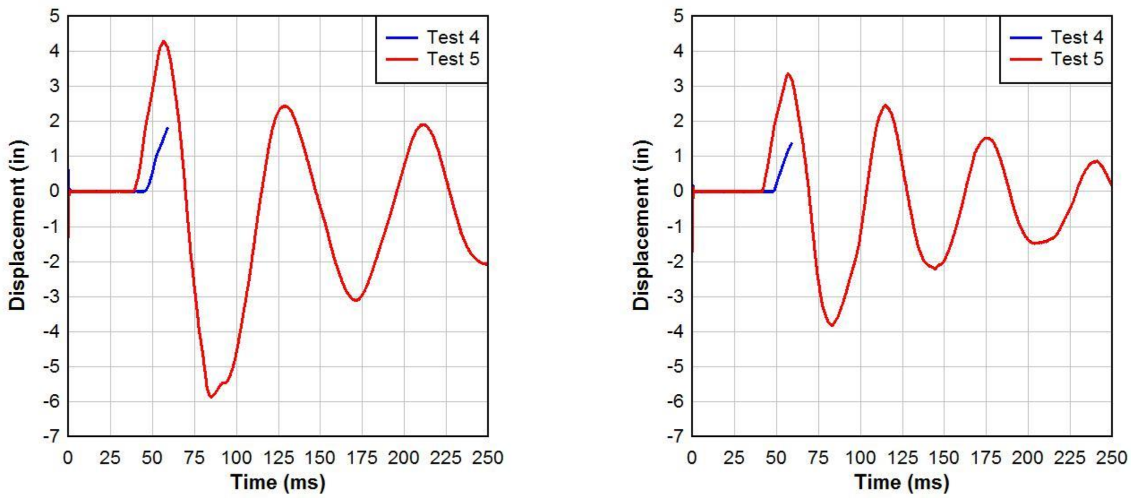

(a) 1st Floor Center (DG2). *(b) 2nd Floor Center (DG4).*

Figure 4-24. Displacement Data for Grade V1 Structure for Tests 4 & 5.

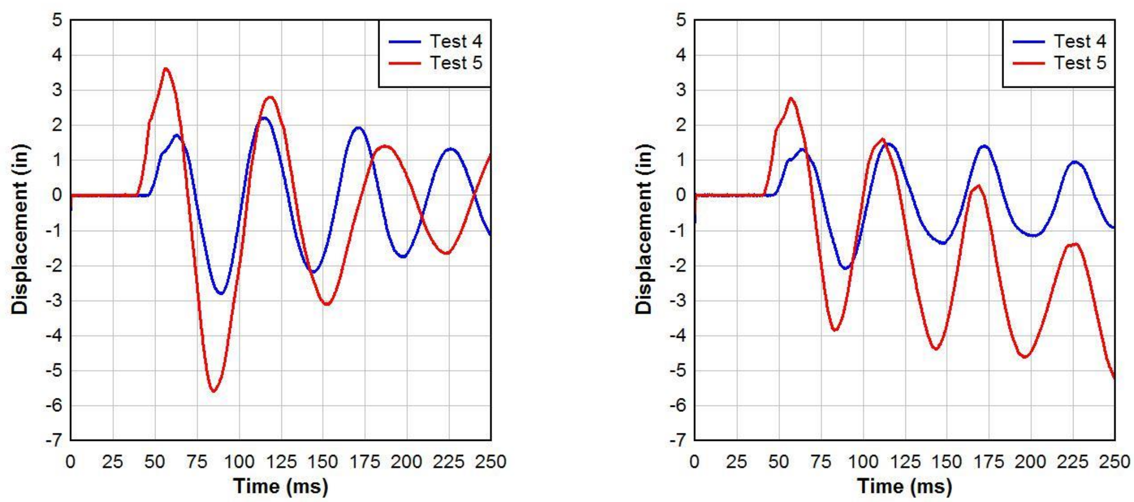

(a) 1st Floor Center (DG8). *(b) 2nd Floor Center (DG10).*

Figure 4-25. Displacement Data for Grade E1 Structure for Tests 4 & 5.

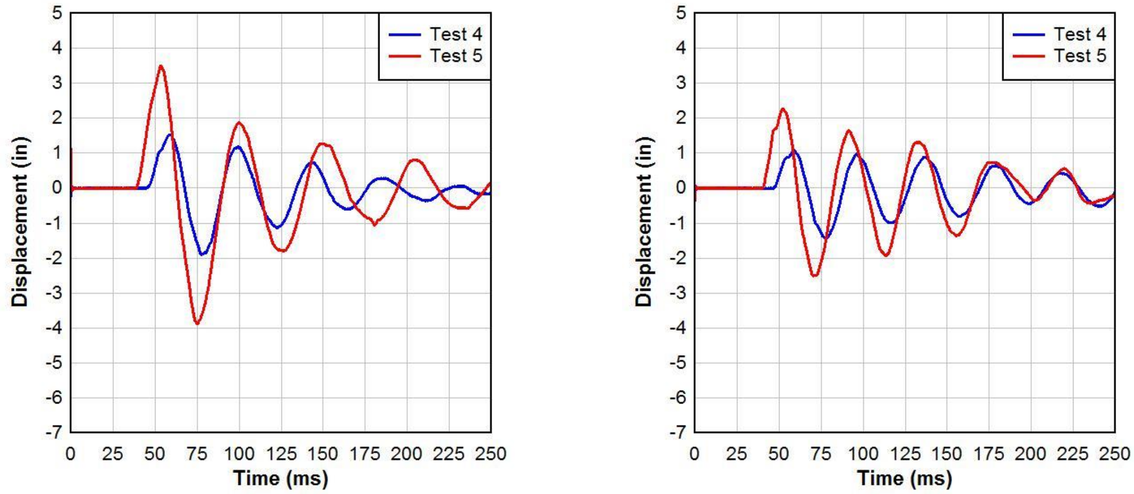

(a) 1st Floor Center (DG14). *(b) 2nd Floor Center (DG16).*

Figure 4-26. Displacement Data for Grade V4 Structure for Tests 4 & 5.

Table 4-2 provides a summary of the inbound and rebound displacements for six locations on each test structure for Tests 4 and 5. The values shown in Table 4-2 are peak displacements for the first displacement cycle.

Table 4-2. Peak Displacement Data Summary for Tests 4 & 5.

Location	Test	CLT Panel Grade					
		V1		E1		V4	
		Inbound [in]	*Rebound [in]*	*Inbound [in]*	*Rebound [in]*	*Inbound [in]*	*Rebound [in]*
1st Floor Front Left (DG1, DG7, DG13)	4	1.34	N/A[1]	1.36	-1.38	1.12	-0.95
	5	2.66	-2.24	2.66	-2.88	2.25	-1.59
1st Floor Front Center (DG2, DG8, DG14)	4	N/A[1]	N/A[1]	1.72	-2.81	1.53	-1.92
	5	4.29	-5.87	3.63	-5.59	3.50	-3.87
1st Floor Front Right (DG3, DG9, DG15)	4	1.40	N/A[1]	1.36	-1.33	1.14	-0.97
	5	2.79	-3.58	2.67	-2.37	2.29	-1.42
2nd Floor Front (DG4, DG10, DG16)	4	N/A[1]	N/A[1]	1.33	-2.09	1.08	-1.44
	5	3.36	-3.82	2.78	-3.85	2.27	-2.51
1st Floor Side (DG5, DG11, DG17)	4	0.92	-1.11	0.97	-1.52	0.69	-0.72
	5	1.71	-1.81	1.87	-2.64	1.30	-1.24
2nd Floor Side (DG6, DG12, DG18)	4	0.91	-1.31	0.93	-1.36	0.66	-0.84
	5	1.74	-2.36	1.61	-2.38	1.19	-1.62

1 Gage malfunction – no displacement recorded.

4.2.2.2 *TESTS 6 & 7*

Figure 4-27, Figure 4-28, and Figure 4-29 plot the peak recorded panel displacements at the 5-ply CLT front panels of the Grade V1 structure, 3-ply CLT front panels of the Grade E1 structure, and 2x4 NLT front panels of the Grade V4 test structure, respectively, for Test 6. Displacement data is also plotted for the Grade V1 structure for Test 7. (Instrumentation was removed from the Grade E1 and V4 structures prior to Test 7 as both front panels were expected to catastrophically fail.) Plots of the remaining displacement histories from Tests 6 and 7 are included in Appendix E.

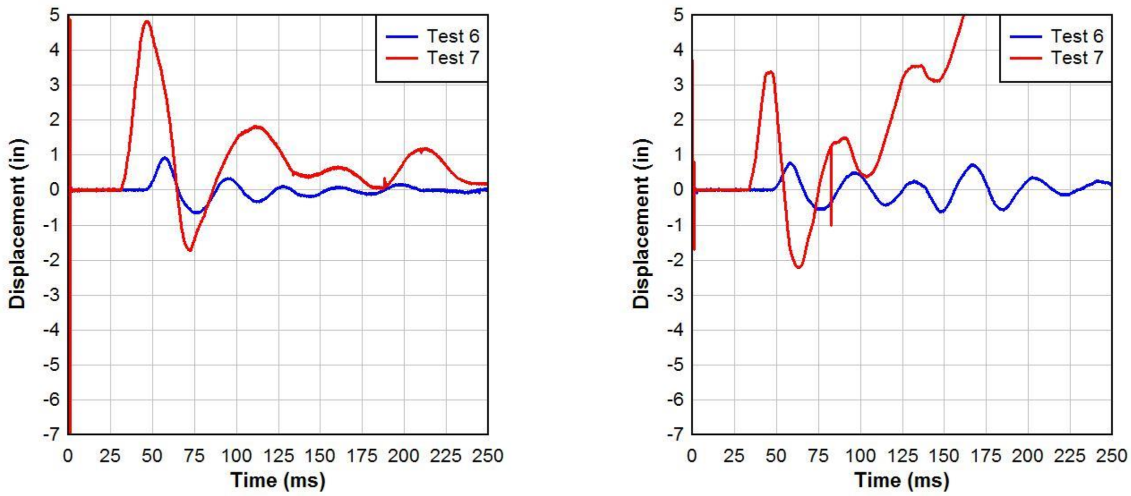

(a) 1st Floor Center (DG2). *(b) 2nd Floor Center (DG4).*

Figure 4-27. Displacement Data for 5-Ply CLT Front Panel on Grade V1 Structure for Tests 6 & 7.

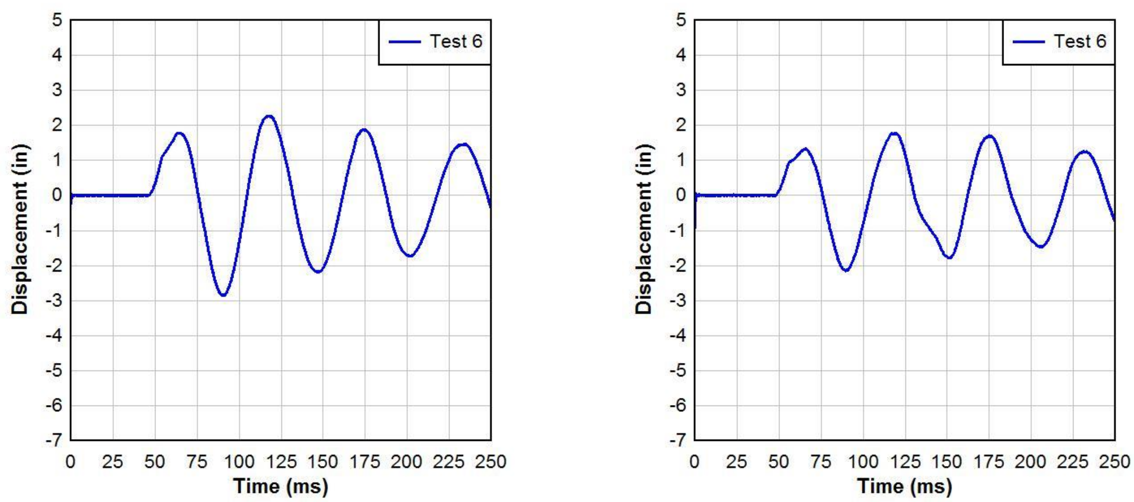

(a) 1st Floor Center (DG8). *(b) 2nd Floor Center (DG10).*

Figure 4-28. Displacement Data for 3-Ply CLT Front Panel on Grade E1 Structure for Test 6.

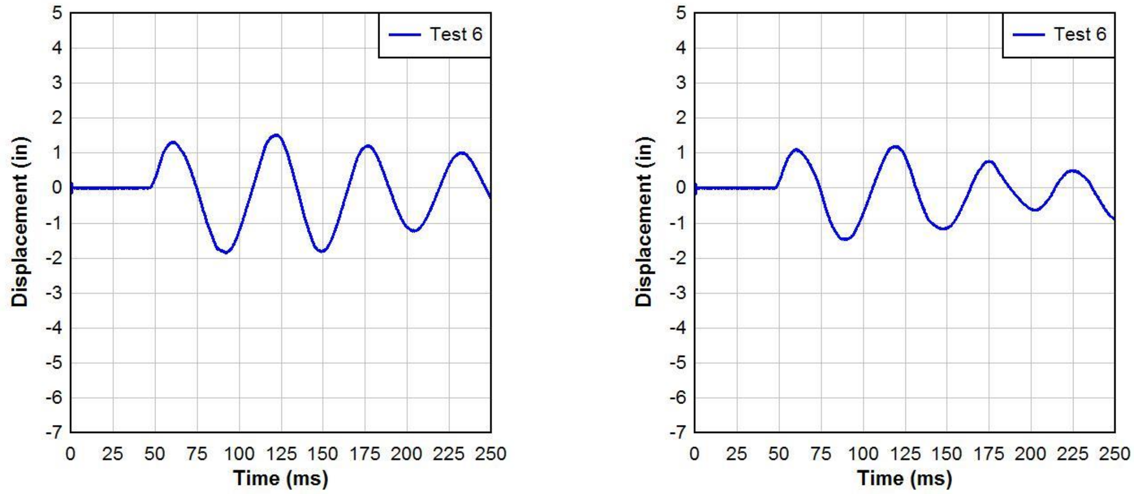

(a) 1st Floor Center (DG14). *(b) 2nd Floor Center (DG16).*

Figure 4-29. Displacement Data for 2x4 NLT Front Panel on Grade V4 Structure for Test 6.

Table 4-3 and Table 4-4 provide a summary of the inbound and rebound displacements for the front and side wall panels, respectively, on each test structure for Tests 6 and 7. The values shown in Table 4-3 and Table 4-4 are peak displacements for the first displacement cycle.

Table 4-3. Peak Displacement Data Summary for Front Wall Panels in Tests 6 & 7.

Location	Test	PANEL DESCRIPTION					
		5-Ply Grade V1 CLT		3-Ply Grade E1 CLT		2x4 NLT	
		Inbound [in]	*Rebound [in]*	*Inbound [in]*	*Rebound [in]*	*Inbound [in]*	*Rebound [in]*
1st Floor Front Left (DG1, DG7, DG13)	6	0.48	-0.36	1.34	-1.31	1.44	-1.93
	7	2.10	-0.99	N/A[1]	N/A[1]	N/A[1]	N/A[1]
1st Floor Front Center (DG2, DG8, DG14)	6	0.93	-0.66	1.79	-2.86	1.32	-1.85
	7	4.83	-1.73	N/A[1]	N/A[1]	N/A[1]	N/A[1]
1st Floor Front Right (DG3, DG9, DG15)	6	0.47	-0.35	1.36	-1.42	1.45	-1.85
	7	1.99	-0.72	N/A[1]	N/A[1]	N/A[1]	N/A[1]
2nd Floor Front (DG4, DG10, DG16)	6	0.79	-0.56	1.35	-2.15	1.11	-1.47
	7	3.40	-2.22	N/A[1]	N/A[1]	N/A[1]	N/A[1]

1 Instrumentation removed – no displacement recorded.

Table 4-4. Peak Displacement Data Summary for Side Wall Panels in Tests 6 & 7.

Location	Test	CLT PANEL GRADE					
		V1		E1		V4	
		Inbound [in]	*Rebound [in]*	*Inbound [in]*	*Rebound [in]*	*Inbound [in]*	*Rebound [in]*
1st Floor Side (DG5, DG11, DG17)	6	0.96	-1.30	0.98	-1.63	0.67	-0.85
	7	3.29	-3.19	N/A[1]	N/A[1]	N/A[1]	N/A[1]
2nd Floor Side (DG6, DG12, DG18)	6	0.91	-1.46	0.83	-1.57	0.65	-0.97
	7	3.55	-3.74	N/A[1]	N/A[1]	N/A[1]	N/A[1]

1 Instrumentation removed – no displacement recorded.

4.2.3 Acceleration Data

4.2.3.1 TESTS 4 & 5

Figure 4-30a, Figure 4-31a, and Figure 4-32a plot the accelerations at the 3-ply CLT first-floor front panels of the Grade V1, Grade E1, and Grade V4 test structures, respectively, for Tests 4 and 5. In addition, this acceleration data was integrated to obtain the corresponding first-floor front panel velocities shown in Figure 4-30b, Figure 4-31b, and Figure 4-32b.

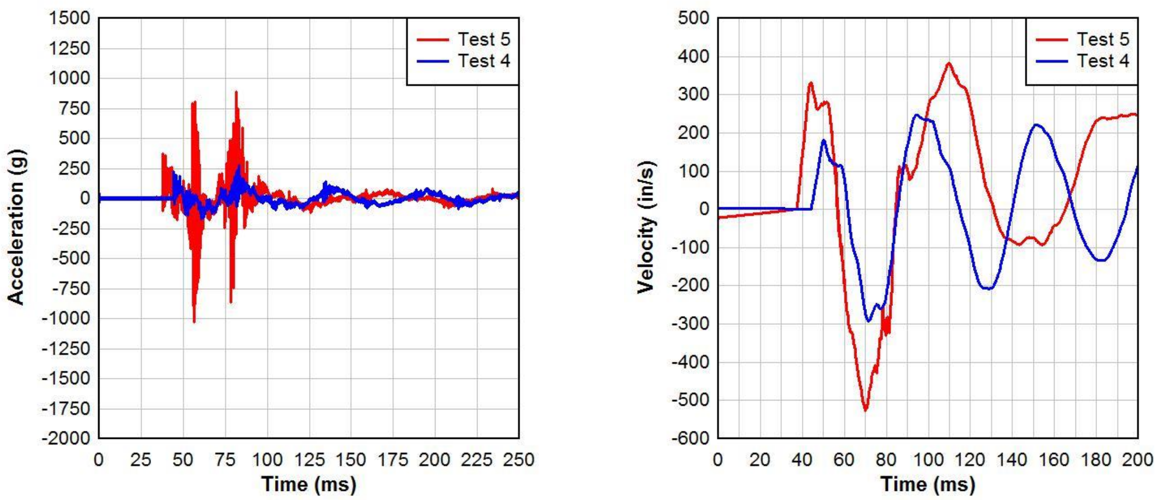

(a) Acceleration (AG1). *(b) Velocity (AG1).*

Figure 4-30. Accelerometer Data for Grade V1 Structure for Tests 4 & 5.

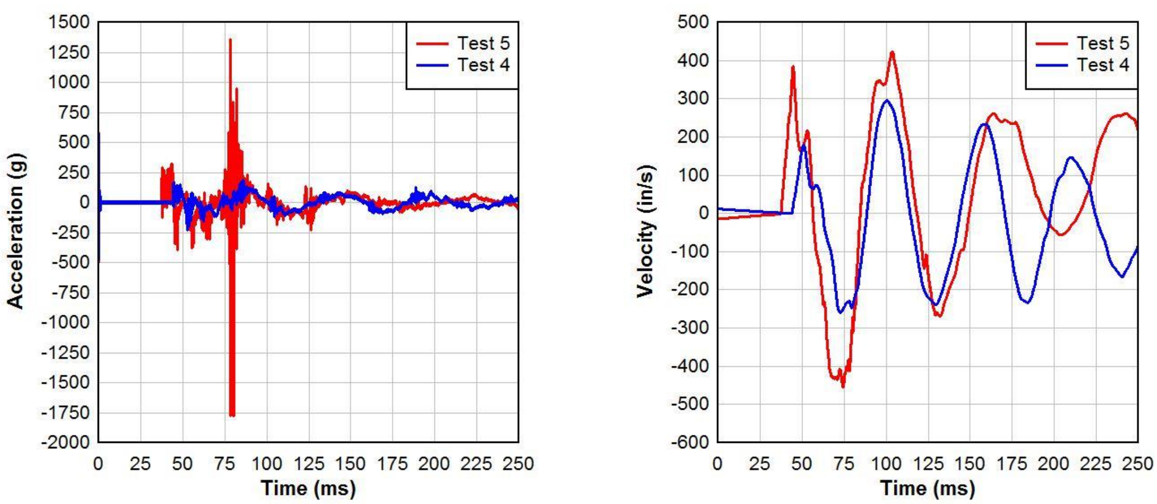

(a) Acceleration (AG2). *(b) Velocity (AG2).*

Figure 4-31. Accelerometer Data for Grade E1 Structure for Tests 4 & 5.

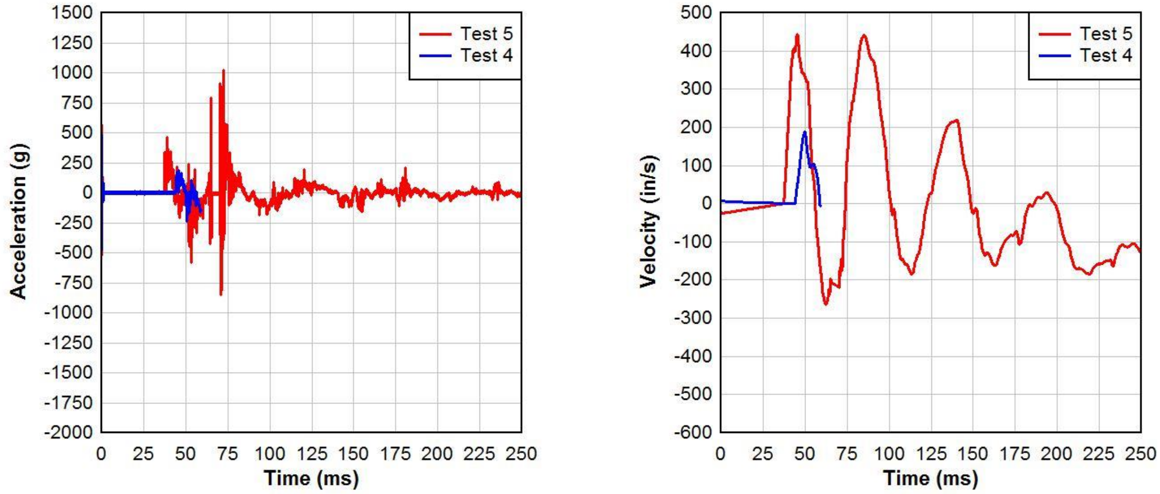

(a) Acceleration (AG3). *(b) Velocity (AG3).*

Figure 4-32. Accelerometer Data for Grade V4 Structure for Tests 4 & 5.

4.2.3.2 *TESTS 6 & 7*

Figure 4-33a and Figure 4-34a plot the peak recorded panel accelerations at the 5-ply CLT first-floor front panels of the Grade V1 structure and the 3-ply CLT first-floor front panels of the Grade E1 structure, respectively, for Test 6. Acceleration data is also plotted for the Grade V1 structure for Test 7. (Instrumentation was removed from the Grade E1 structures prior to Test 7 as its front panels were expected to catastrophically fail.) In addition, this acceleration data was integrated to obtain the corresponding first-floor front panel velocities shown in Figure 4-33b and Figure 4-34b. No acceleration data was captured at the 2x4 NLT panels of the Grade V4 structure.

Upon reviewing the accelerometer data, it is apparent that the range for the AG1 accelerometer during Test 7 was insufficient to capture peak accelerations. As such, both this acceleration trace and the corresponding velocity trace shown in Figure 4-33 underrepresent the actual acceleration and velocity of the 5-ply CLT first-floor front panels of the Grade V1 structure.

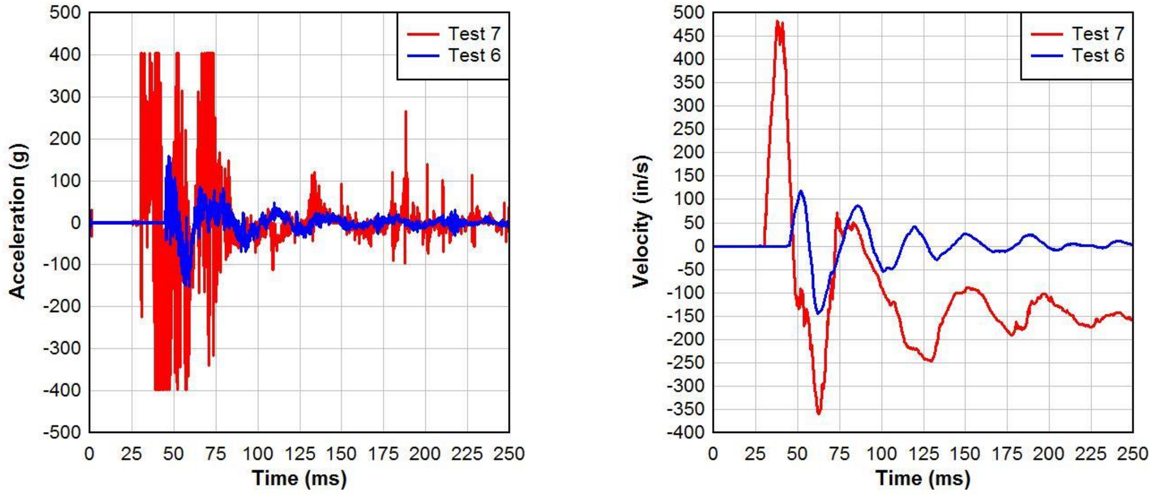

(a) Acceleration (AG1). *(b) Velocity (AG1).*

Figure 4-33. Accelerometer Data for 5-Ply CLT Front Panel on Grade V1 Structure for Tests 6 & 7.

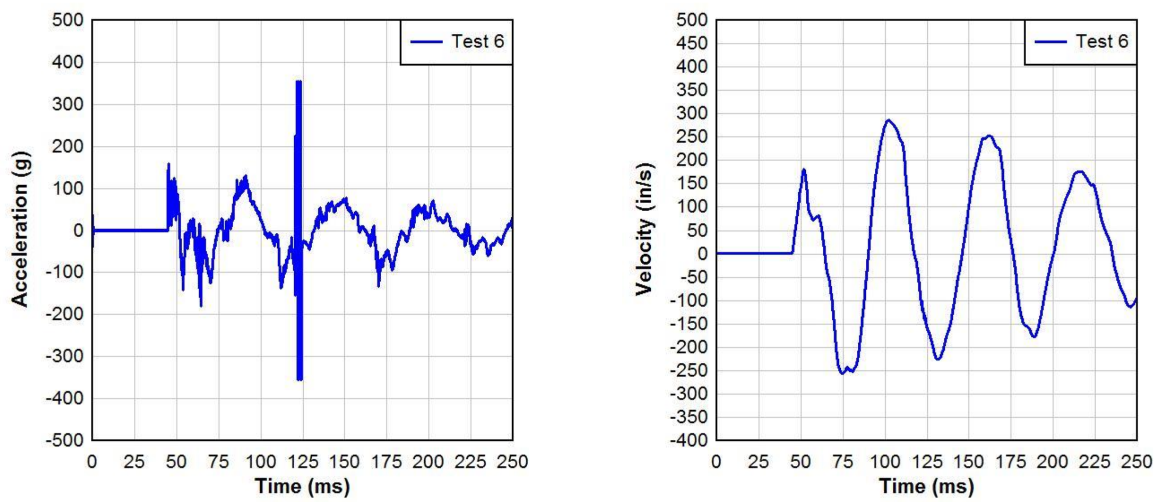

(a) Acceleration (AG2). *(b) Velocity (AG2).*

Figure 4-34. Accelerometer Data for 3-Ply CLT Front Panel on Grade E1 Structure for Test 6.

CHAPTER 5

ARENA TESTING DATA COMPARISONS

This test data obtained from the four blast tests described herein is compared with analytical methods commonly used to design blast-resistant structures for airblast loading. The chapter opens with comparing the recorded airblast pressures with the Kingery-Bulmash equations [12]. Next, the recorded displacement response of the constituent panels of the CLT test structures is compared with idealized SDOF dynamic analysis calculations. The chapter is concluded by drawing conclusions concerning the use of these analytical models to design CLT structures for airblast loading.

5.1 AIRBLAST LOADING

Figure 5-1 compares the average curve shown in Figure 4-22 with that generated using the Kingery-Bulmash (K-B) equations assuming a hemispherical surface burst. In general, the measured and computed data compare well in terms of peak pressure, positive phase impulse, and time of arrival.

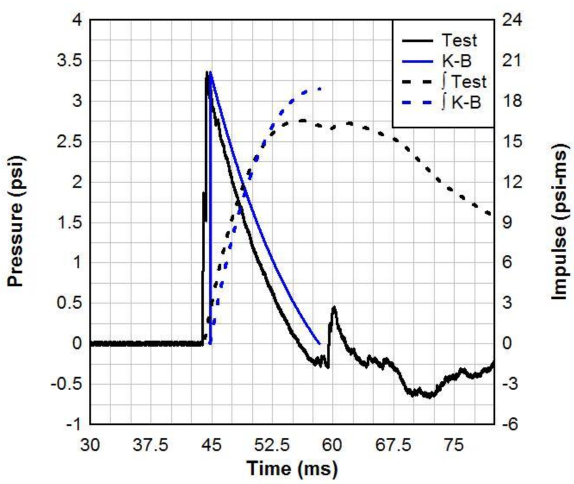

(a) Test 4.

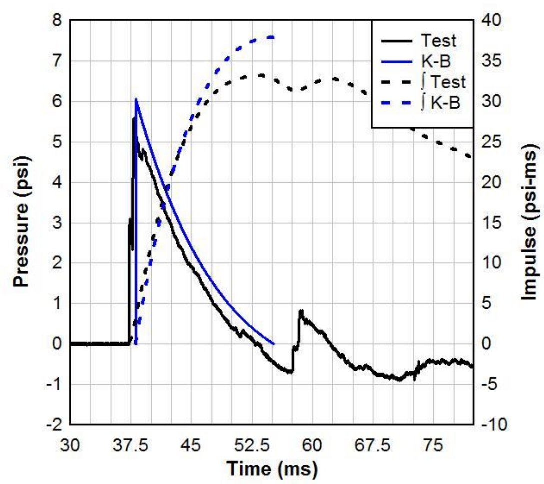

(b) Test 5.

Figure 5-1. Incident Overpressure Data Comparisons.

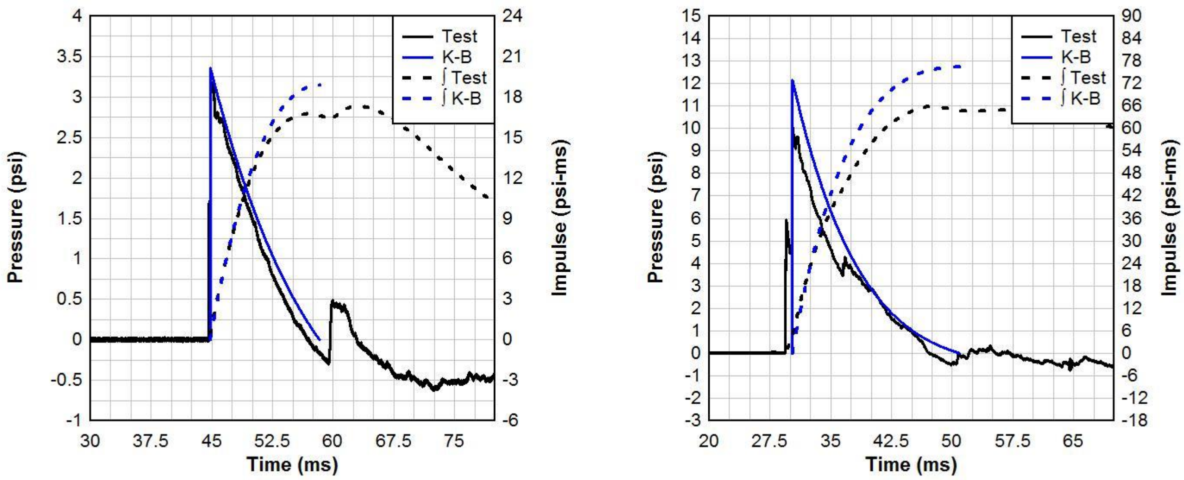

(c) Test 6. *(d) Test 7.*

Figure 5-1. Incident Overpressure Data Comparisons. (Cont'd)

Figure 5-2 compares the average curve shown in Figure 4-23 with that computed using the K-B equations. In general, the measured and computed data compare well in terms of peak pressure and time of arrival for all shots. However, it is apparent that the positive phase impulses diverge by a noticeable margin. This divergence is likely due to clearing effects not being accounted for in the K-B-generated curve.

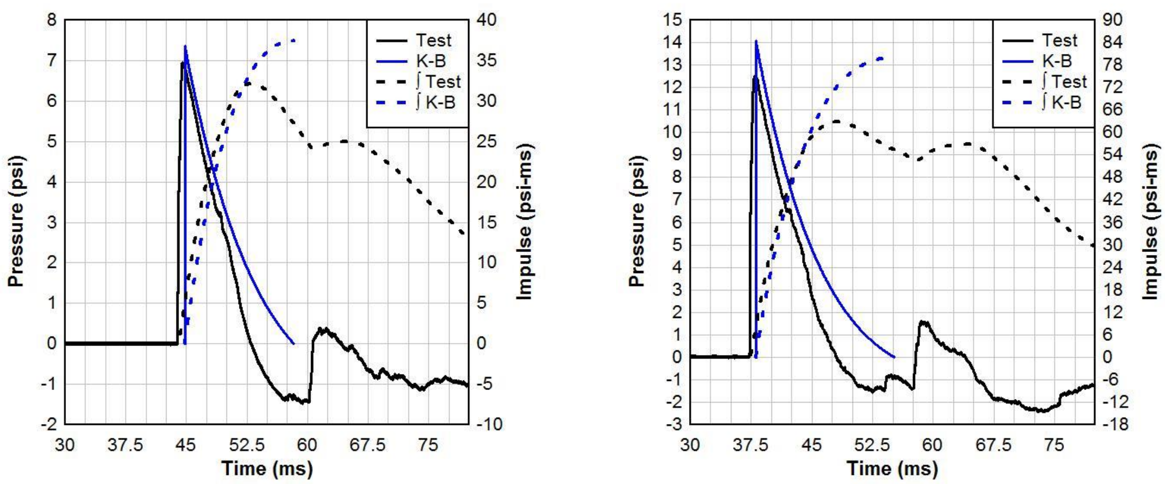

(a) Test 4. *(b) Test 5.*

Figure 5-2. Reflected Pressure Data Comparisons at First-Floor Front Panels.

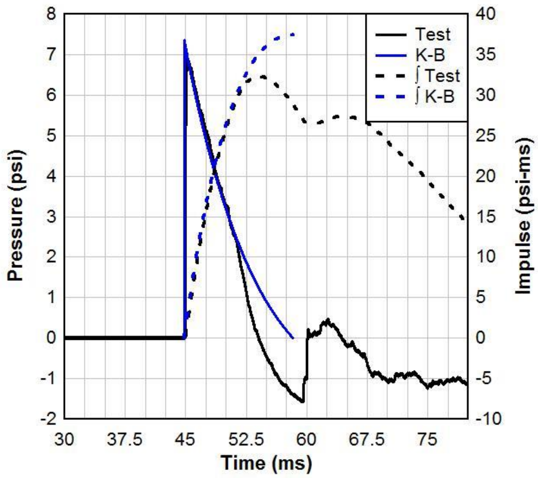

(c) Test 6.

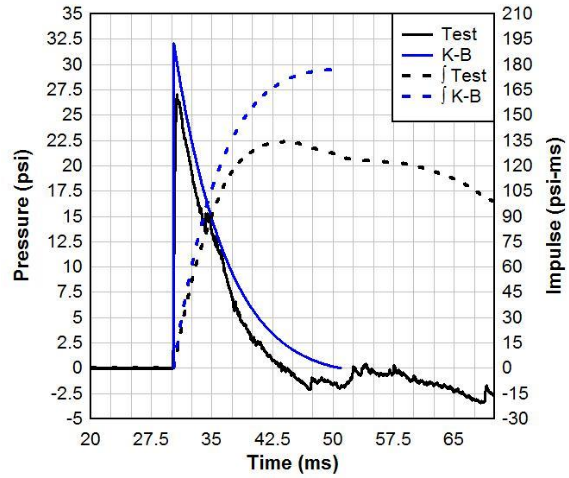

(d) Test 7.

Figure 5-2. Reflected Pressure Data Comparisons at First-Floor Front Panels. (Cont'd)

Table 5-1 provides a summary of the peak incident and reflected pressure positive phase data for all three shots.

Table 5-1. Pressure Data Comparison with Kingery-Bulmash Equations.

Test	Time of Arrival [ms]		Incident Overpressure [psi]		Incident Impulse [psi-ms]		Peak Reflected Pressure [psi]		Peak Reflected Impulse [psi-ms]	
	Test[1]	*K-B*[2]	*Test*[1]	*K-B*[2]	*Test*[1]	*K-B*[2]	*Test*[1]	*K-B*[2]	*Test*[1]	*K-B*[2]
4	43.8	44.8	3.82	3.37	16.5	18.9	7.22	7.36	32.1	37.5
5	37.2	38.1	6.27	6.06	33.2	37.9	13.4	14.1	62.8	80.0
6	44.6	44.8	3.43	3.37	17.3	18.9	7.25	7.36	32.3	37.5
7	29.4	30.3	11.4	12.2	65.8	76.4	27.0	32.1	134	177

1 Average of test data shown in Figure 4-22 and Figure 4-23.
2 As computed by the Kingery-Bulmash equations assuming hemispherical surface burst.

5.2 STRUCTURAL RESPONSE

A series of SDOF dynamic analyses were performed using the pressure histories recorded for each test and compared to the recorded test data. The resistance function utilized for these SDOF calculations consisted of linear elastic response characterized by a stiffness, k, to an ultimate resistance, r_u, followed by a perfectly plastic post-peak response. The idealized resistance function is shown in Figure 5-3.

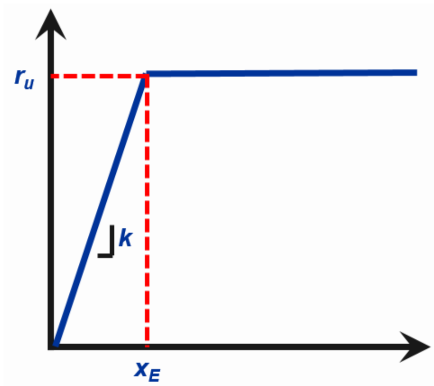

Figure 5-3. Idealized Resistance Function used in SDOF Dynamic Analysis.

The following assumptions were employed for all SDOF analyses performed:

- The boundary conditions were idealized pin-roller.
- The mass used in the SDOF calculation, m, was assumed to be uniformly distributed over the blast-load-applied-area (i.e., the product of length, L, and tributary width, b_{trib}). The following CLT panel densities were assumed to compute m:
    - Grade V1 CLT: 35 pcf
    - Grade E1 CLT: 32.5 pcf
    - Grade V4 CLT: 30 pcf
    - 2x4 No. 2 S-P-F NLT: 32.5 pcf
- Viscous damping was applied. The fraction of critical damping was assumed to be 2-percent.

The parameters used to construct the CLT panel resistance function (i.e., k, r_u) for each grade of CLT were computed based on the major strength direction allowable stress design (ASD) reference design values reported in [5][7]:

- The stiffness, k, was computed based on an apparent bending stiffness, EI_{app}; which was generated by combining the effective bending stiffness, EI_{eff}, with the effective shear stiffness, GA_{eff}, values via Equation 10.4-1 of the NDS.

- The ultimate resistance, r_u, was based on the lower of the bending, F_bS_{eff}, and flatwise shear, V_s, reference design values. (It should be noted that the 0.85 conservatism factor applied to the bending reference design value mentioned in Annex A was not removed.) These strengths were multiplied by static and dynamic increase factors.

  - The static increase factor (SIF) transformed the ASD reference design value into an average expected value assuming a load duration of 10 minutes. This increase factor consisted of three subfactors: one, K_{char}, to transform the ASD value to the characteristic (i.e., 5-percent exclusion) value, another, K_{avg}, to transform the characteristic value to the average expected value, and a third, K_{size}, to account for the size effect inherent in brittle materials [13]. These subfactors were a function of the species/grade combination of the major strength direction ply, panel ply number, and applied stress type. The final subfactors used, as well as the resulting SIF, are shown in Table 5-2. More information concerning the derivation of these factors is included in Ref. [14].

Table 5-2. Subfactors & Resulting SIFs Used in CLT SDOF Analyses.

CLT Grade	Ply No.	Stress Type	K_{char}	K_{size}	K_{avg}	*SIF*
V1	3	Bending	1.30	1.34	2.30	4.00
E1				0.95	1.35	1.67
V4				1.34	2.05	3.56
V1	5			1.15	2.30	3.45
All		Flatwise Shear	2.00	1.00	1.30	2.60

  - The dynamic increase factor (DIF) accounted for the duration of the applied (blast) load and was set equal to 2.0 (i.e., the NDS load duration factor, C_D, for an "impact" duration).

  - The 0.9 reduction factor recommended in Section C-2.1 of Ref. [14] was applied to the ultimate resistance.

The NLT panel resistance function employed, including the SIF and DIF, was that generated by the "Wood Beam" module of SBEDS 4.1 [15]. The 0.5-inch thick plywood sheathing on the front face of the NLT panel only contributed supported weight (i.e., the sheathing was not assumed to be composite with the 2x4 studs and therefore did not augment the analytical ultimate resistance of the NLT panel).

The resulting SDOF dynamic analysis parameters for all cases considered based on the above assumptions are shown in Table 5-3 for Tests 4 and 5 and Table 5-4 for Tests 6 and 7.

Table 5-3. Dynamic Analysis Parameters for Tests 4 & 5 SDOF Analyses.

Panel Description	DG	Blast Load	Description	L [ft]	b_{trib} [ft]	m [psi-ms^2/in]	k [psi/in]	r [psi]	x_E [in]
3-Ply Grade V1 CLT	2	RP2	1st floor front	12	1	216.2	1.44	5.80	4.02
	4	RP4	2nd floor front						
	5	RP5	1st floor left						
	6	RP6	2nd floor right						
3-Ply Grade E1 CLT	8	RP8	1st floor front	12	1	200.8	1.50	5.21	3.47
	10	RP10	2nd floor front						
	11	RP11	1st floor right						
	12	RP12	2nd floor left						
3-Ply Grade V4 CLT	14	RP14	1st floor front	10	1	185.3	2.00	6.50	3.25
	16	RP16	2nd floor front						
	17	RP17	1st floor right						
	18	RP18	2nd floor left						

Table 5-4. Dynamic Analysis Parameters for Tests 6 & 7 SDOF Analyses.

Panel Description	DG	Blast Load	Description	L [ft]	b_{trib} [ft]	m [psi-ms^2/in]	k [psi/in]	r [psi]	x_E [in]
5-Ply Grade V1 CLT	2	RP2	1st floor front	12	1	360.4	5.11	11.50	2.25
	4	RP4	2nd floor front						
3-Ply Grade V1 CLT	5	RP5	1st floor left	12	1	216.2	1.44	5.80	4.02
	6	RP6	2nd floor right						
3-Ply Grade E1 CLT	8	RP8	1st floor front	12	1	200.8	1.50	5.21	3.47
	10	RP10	2nd floor front						
	11	RP11	1st floor right						
	12	RP12	2nd floor left						
2x4 No.2 SPF NLT	14	RP14	1st floor front	10	1	206.3	1.85	4.96	2.68
	16	RP16	2nd floor front						
3-Ply Grade V4 CLT	17	RP17	1st floor right	10	1	185.3	2.00	6.50	3.25
	18	RP18	2nd floor left						

Figure 5-4 and Figure 5-5 show comparisons of how the SDOF dynamic analysis results obtained using these resistance functions compared with the test data for the front panels of each test structure for Tests 4 and 5 and Tests 6 and 7, respectively.

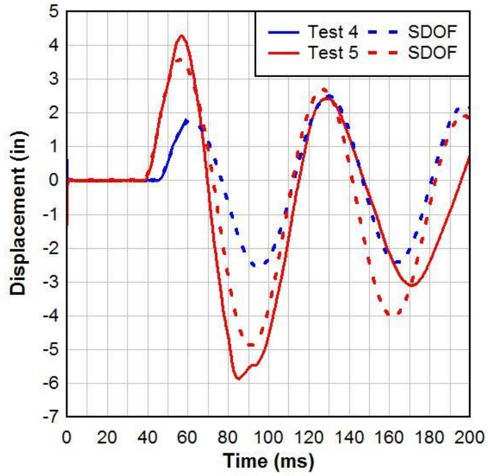

(a) 3-Ply Grade V1 CLT (1st Floor).

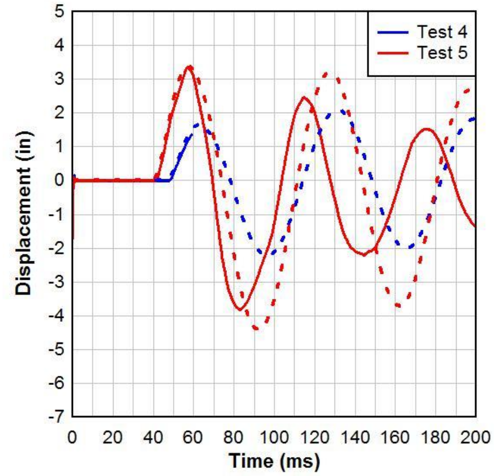

(b) 3-Ply Grade V1 CLT (2nd Floor).

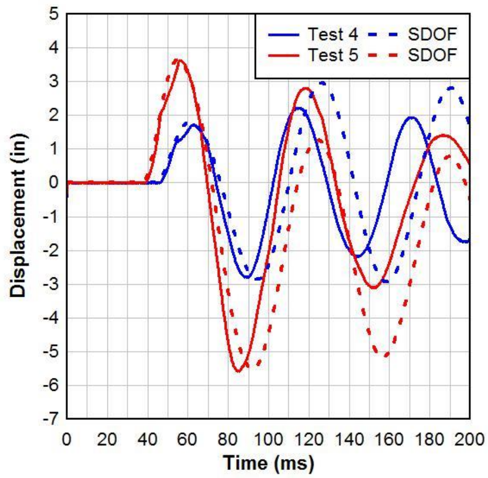

(c) 3-Ply Grade E1 CLT (1st Floor).

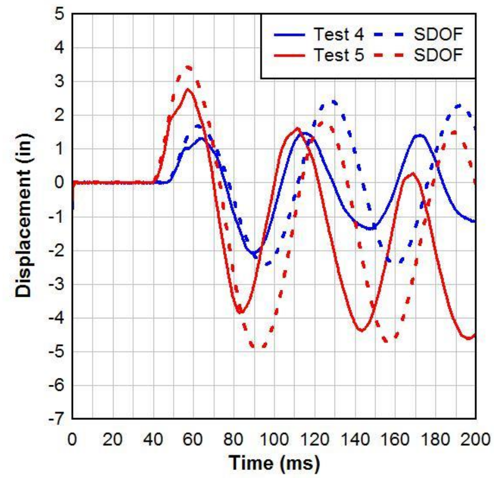

(d) 3-Ply Grade E1 CLT (2nd Floor).

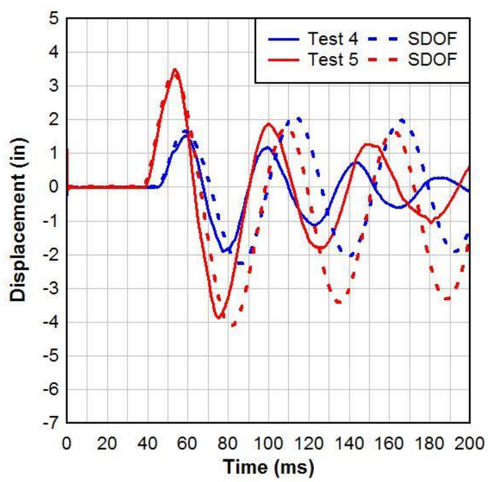

(e) 3-Ply Grade V4 CLT (1st Floor).

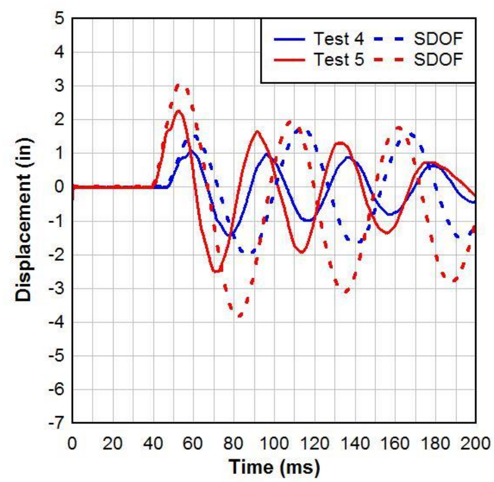

(f) 3-Ply Grade V4 CLT (2nd Floor).

Figure 5-4. Tests 4 & 5 Front Panel Displacement Comparisons.

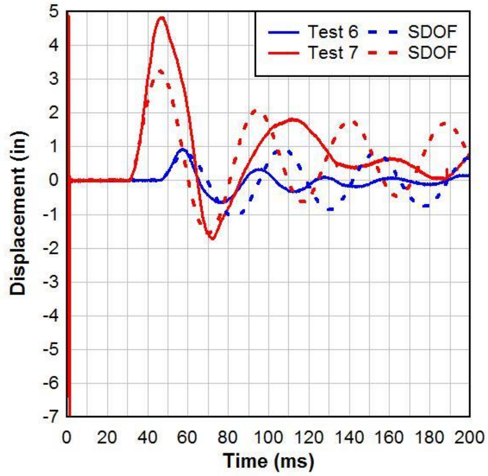

(a) 5-Ply Grade V1 CLT (1st Floor).

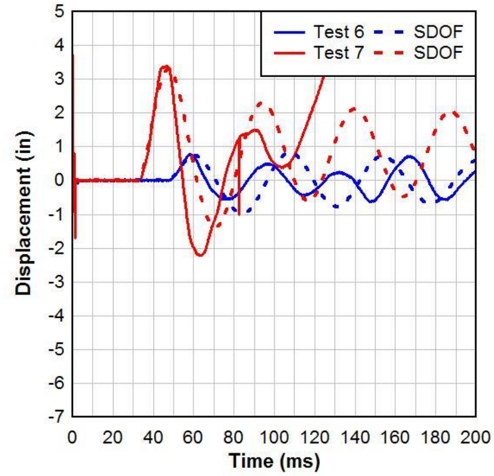

(b) 5-Ply Grade V1 CLT (2nd Floor).

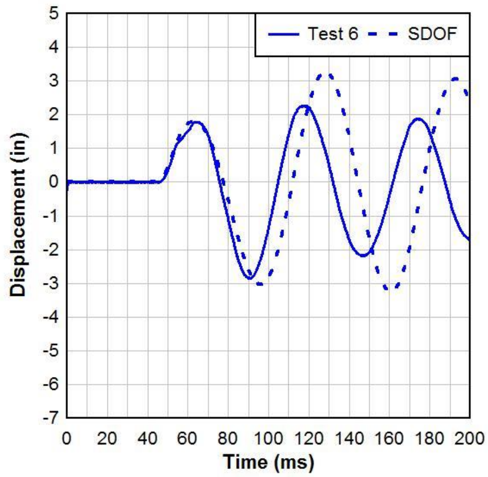

(c) 3-Ply Grade E1 CLT (1st Floor).

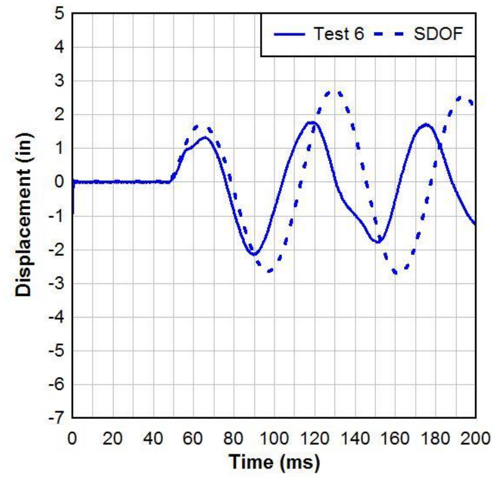

(d) 3-Ply Grade E1 CLT (2nd Floor).

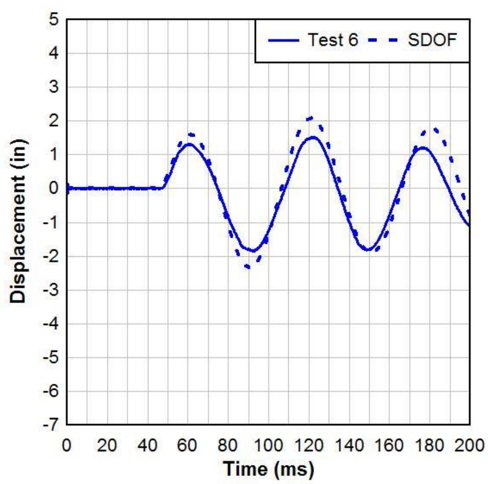

(e) 2x4 No. 2 S-P-F NLT (1st Floor).

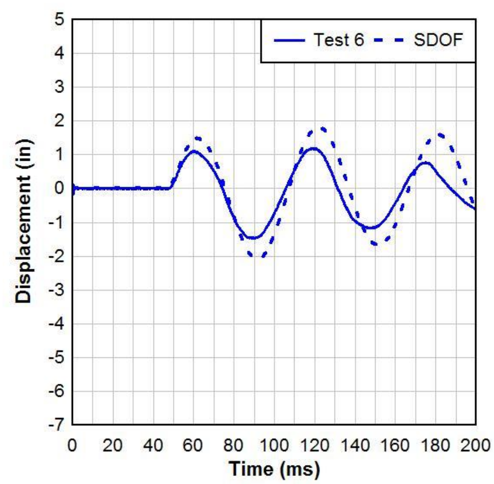

(f) 2x4 No. 2 S-P-F NLT (2nd Floor).

Figure 5-5. Tests 6 & 7 Front Panel Displacement Comparisons.

Table 5-5 through Table 5-9 record the results of these SDOF dynamic analyses by mass timber panel type and compare the computed values with those recorded in the tests. Where the difference between the test and computed displacement exceeded 20 percent of the test value, the difference percentage is highlighted in blue (i.e., the SDOF was at least 20 percent greater than the test value) or red (i.e., the SDOF was at least 20 percent less than the test value).

Table 5-5. 3-Ply Grade V1 CLT Panel Displacement Summary.

DG	Blast Load	Test	1st Inbound Displacement				1st Rebound Displacement				μ[2]
			Test [in]	*SDOF [in]*	*% Diff.*	μ_{in}[1]	*Test [in]*	*SDOF [in]*	*% Diff.*	μ_{rb}[1]	
2	RP2	4	N/A[3]	1.76	N/A[3]	0.44	N/A[3]	-2.55	N/A[3]	0.63	**0.63**
		5	4.29	3.57	-16.7%	0.89	-5.87	-4.88	-16.8%	1.22	**1.22**
4	RP4	4	N/A[3]	1.64	N/A[3]	0.41	N/A[3]	-2.21	N/A[3]	0.55	**0.55**
		5	3.36	3.37	0.4%	0.84	-3.82	-4.40	15.3%	1.10	**1.10**
5	RP5	4	0.92	0.96	4.5%	0.24	-1.11	-1.31	18.1%	0.33	**0.33**
		5	1.71	1.81	5.8%	0.45	-1.81	-2.39	31.9%	0.59	**0.59**
		6	0.96	0.99	2.9%	0.25	-1.30	-1.45	11.8%	0.36	**0.36**
		7	3.29	3.49	6.0%	0.87	-3.19	-4.21	31.8%	1.05	**1.05**
6	RP6	4	0.91	1.05	15.2%	0.26	-1.31	-1.44	10.0%	0.36	**0.36**
		5	1.74	2.01	15.3%	0.50	-2.36	-2.67	13.0%	0.66	**0.66**
		6	0.91	1.08	18.6%	0.27	-1.46	-1.61	10.2%	0.40	**0.40**
		7	3.55	3.95	11.2%	0.98	-3.74	-4.78	27.7%	1.19	**1.19**

1 Equal to the SDOF displacement divided by the corresponding x_E value in Table 5-4.
2 Maximum of μ_{in} and μ_{rb}.
3 Gage malfunction – no displacement recorded.

Table 5-6. 5-Ply Grade V1 CLT Panel Displacement Summary.

DG	Blast Load	Test	1st Inbound Displacement				1st Rebound Displacement				μ[2]
			Test [in]	*SDOF [in]*	*% Diff.*	μ_{in}[1]	*Test [in]*	*SDOF [in]*	*% Diff.*	μ_{rb}[1]	
2	RP2	6	0.93	0.79	-15.1%	0.35	-0.66	-1.07	61.9%	0.47	**0.47**
		7	4.83	3.23	-33.2%	1.43	-1.73	-1.56	-10.1%	0.69	**1.43**
4	RP4	6	0.79	0.74	-5.9%	0.33	-0.56	-0.97	73.8%	0.43	**0.43**
		7	3.40	3.30	-3.0%	1.47	-2.22	-1.38	-37.7%	0.62	**1.47**

1 Equal to the SDOF displacement divided by the corresponding x_E value in Table 5-4.
2 Maximum of μ_{in} and μ_{rb}.

Table 5-7. 3-Ply Grade E1 CLT Panel Displacement Summary.

DG	Blast Load	Test	1st Inbound Displacement				1st Rebound Displacement				μ^2
			Test [in]	*SDOF [in]*	*% Diff.*	$\mu_{in}{}^1$	*Test [in]*	*SDOF [in]*	*% Diff.*	$\mu_{rb}{}^1$	
8	RP8	4	1.72	1.79	4.0%	0.52	-2.81	-2.86	1.9%	0.83	**0.83**
		5	3.63	3.65	0.5%	1.05	-5.59	-5.50	-1.6%	1.59	**1.59**
		6	1.79	1.80	0.3%	0.52	-2.86	-3.04	6.3%	0.88	**0.88**
10	RP10	4	1.33	1.67	25.7%	0.48	-2.09	-2.42	15.7%	0.70	**0.70**
		5	2.78	3.43	23.3%	0.99	-3.85	-4.95	28.7%	1.43	**1.43**
		6	1.35	1.69	24.9%	0.49	-2.15	-2.64	22.9%	0.76	**0.76**
11	RP11	4	0.97	1.11	14.6%	0.32	-1.52	-1.69	11.2%	0.49	**0.49**
		5	1.87	2.12	13.4%	0.61	-2.64	-3.02	14.3%	0.87	**0.87**
		6	0.98	1.07	9.7%	0.31	-1.63	-1.80	10.3%	0.52	**0.52**
12	RP12	4	0.93	0.98	5.3%	0.28	-1.36	-1.38	1.6%	0.40	**0.40**
		5	1.61	1.85	14.7%	0.53	-2.38	-2.49	4.6%	0.72	**0.72**
		6	0.83	1.02	22.5%	0.29	-1.57	-1.56	-0.9%	0.45	**0.45**

1 Equal to the SDOF displacement divided by the corresponding x_E value in Table 5-4.
2 Maximum of μ_{in} and μ_{rb}.

Table 5-8. 3-Ply Grade V4 CLT Panel Displacement Summary.

DG	Blast Load	Test	1st Inbound Displacement				1st Rebound Displacement				μ^2
			Test [in]	*SDOF [in]*	*% Diff.*	$\mu_{in}{}^1$	*Test [in]*	*SDOF [in]*	*% Diff.*	$\mu_{rb}{}^1$	
14	RP14	4	1.53	1.65	7.6%	0.51	-1.92	-2.27	18.4%	0.70	**0.70**
		5	3.50	3.35	-4.4%	1.03	-3.87	-4.11	6.3%	1.27	**1.27**
16	RP16	4	1.08	1.54	42.4%	0.47	-1.44	-2.01	39.5%	0.62	**0.62**
		5	2.27	3.09	36.1%	0.95	-2.51	-3.85	53.2%	1.18	**1.18**
17	RP17	4	0.69	0.87	25.7%	0.27	-0.72	-1.08	50.0%	0.33	**0.33**
		5	1.30	1.68	29.5%	0.52	-1.24	-1.87	50.9%	0.58	**0.58**
		6	0.67	0.87	30.5%	0.27	-0.85	-1.15	35.0%	0.35	**0.35**
18	RP18	4	0.66	0.97	46.4%	0.30	-0.84	-1.41	68.4%	0.44	**0.44**
		5	1.19	1.85	55.1%	0.57	-1.62	-2.44	50.5%	0.75	**0.75**
		6	0.65	0.95	45.5%	0.29	-0.97	-1.48	52.5%	0.46	**0.46**

1 Equal to the SDOF displacement divided by the corresponding x_E value in Table 5-4.
2 Maximum of μ_{in} and μ_{rb}.

Table 5-9. 2x4 No. 2 SPF NLT Panel Displacement Summary.

DG	Blast Load	Test	1st Inbound Displacement				1st Rebound Displacement				μ^2
			Test [in]	*SDOF [in]*	*% Diff.*	$\mu_{in}{}^1$	*Test [in]*	*SDOF [in]*	*% Diff.*	$\mu_{rb}{}^1$	
14	RP14	6	1.32	1.59	20.3%	0.59	-1.85	-2.34	26.3%	0.87	**0.87**
16	RP16	6	1.11	1.48	33.5%	0.55	-1.47	-2.09	42.1%	0.78	**0.78**

[1] Equal to the SDOF displacement divided by the corresponding x_E value in Table 5-4.
[2] Maximum of μ_{in} and μ_{rb}.

5.3 DATA INTERPRETATION

5.3.1 Tests 4 & 5

Tests 4 and 5 essentially repeated Tests 2 and 3 of Phase 1 but with CLT test structures with axially-loaded front wall panels. Thus, to draw appropriate and complete conclusions from Tests 4 and 5, it is helpful to compare the input blast loads and output structural response from the two sets of tests.

Table 5-10 compares the blast loading measured during the two sets of tests. It can be seen that the Phase 2 reflected pressures and impulses are within 10 percent of the Phase 1 values.

Table 5-10. Tests 2 & 3 (Phase 1) and Tests 4 & 5 (Phase 2) Pressure Data.

Test	Time of Arrival [ms]		Incident Overpressure [psi]		Incident Impulse [psi-ms]		Peak Reflected Pressure [psi]		Peak Reflected Impulse [psi-ms]	
	Ph.1	*Ph.2*	*Ph.1*	*Ph.2*	*Ph.1*	*Ph.2*	*Ph.1*	*Ph.2*	*Ph.1*	*Ph.2*
2 / 4	44.8	43.8	3.37	3.82	18.0	16.5	7.94	7.22	32.9	32.1
3 / 5	38.1	37.2	6.06	6.27	33.3	33.2	13.2	13.4	65.2	62.8

Similarly, Table 5-11 compares the displacement gage data collected at identical points on the test structures during the two sets of tests. Where the Phase 2 data deviates more than 20 percent from the Phase 1 data, the values are listed in red. A quick survey of the table indicates that, in general, the displacements recorded are consistent between the two sets of tests. One notable exception is the first-floor front wall panel in the Grade V4 structure during Tests 3 and 5. As can be seen in Figure 5-6a, the SDOF calculation predicts the initial inbound and rebound displacements recorded during Test 5 well but fails to capture Test 3's inbound displacement. However, examining the location of the gage (Figure 5-6b) indicates that the displacement gage was attached to a board that ruptured and potentially disengaged from the rest of the panel during Test 3. It is conceivable considering the gage's location and the post-test wall damage adjacent to the gage that the board to which the gage was attached potentially disengaged from the rest of the wall panel during Test 3, thus explaining the marked difference between the two recorded displacements.

Table 5-11. Tests 2 & 3 (Phase 1) and Tests 4 & 5 (Phase 2) Displacement Data.

DG [1]	Test	STRUCTURE GRADE											
		V1				E1				V4			
		Inbound [in]		*Rebound [in]*		*Inbound [in]*		*Rebound [in]*		*Inbound [in]*		*Rebound [in]*	
		Ph.1	*Ph.2*	*Ph.1*	*Ph.2*	*Ph.1*	*Ph.2*	*Ph.1*	*Ph.2*	*Ph.1*	*Ph.2*	*Ph.1*	*Ph.2*
1 / 7 / 13	2 / 4	1.41	1.34	-1.37	N/A[2]	1.30	1.36	-1.20	-1.38	1.28	1.12	-1.02	-0.95
	3 / 5	2.80	2.66	-2.57	-2.24	2.67	2.66	-2.62	-2.88	2.67	2.25	-1.64	-1.59
2 / 8 / 14	2 / 4	2.04	N/A[2]	-2.64	N/A[2]	1.96	1.72	-2.75	-2.81	1.83	1.53	-2.04	-1.92
	3 / 5	4.28	4.29	-6.15	-5.87	3.90	3.63	-6.12	-5.59	**4.57**	**3.50**	-4.05	-3.87
3 / 9 / 15	2 / 4	1.33	1.40	-1.49	N/A[2]	1.41	1.36	-1.28	-1.33	1.23	1.14	-1.17	-0.97
	3 / 5	2.69	2.79	**-2.73**	**-3.58**	2.79	2.67	-2.20	-2.37	2.52	2.29	**-2.67**	**-1.42**
4 / 10 / 16	2 / 4	1.71	N/A[2]	-2.13	N/A[2]	1.47	1.33	-2.15	-2.09	1.26	1.08	-1.42	-1.44
	3 / 5	3.30	3.36	-3.91	-3.82	3.07	2.78	-3.84	-3.85	2.47	2.27	-2.98	-2.51
5 / 11 / 17	2 / 4	0.92	0.92	-1.18	-1.11	1.01	0.97	-1.66	-1.52	0.73	0.69	-0.86	-0.72
	3 / 5	1.67	1.71	-1.94	-1.81	1.97	1.87	-2.78	-2.64	1.36	1.30	-1.45	-1.24
6 / 12 / 18	2 / 4	**1.33**	**0.91**	-1.57	-1.31	0.81	0.93	-1.52	-1.36	0.65	0.66	-1.06	-0.84
	3 / 5	1.46	1.74	-2.57	-2.36	1.51	1.61	-2.79	-2.38	1.09	1.19	-1.79	-1.62

[1] Displacement gage (DG) numbers are based on the key plans included in Figure __ through Figure __ of this report.

[2] Gage malfunction – no displacement recorded.

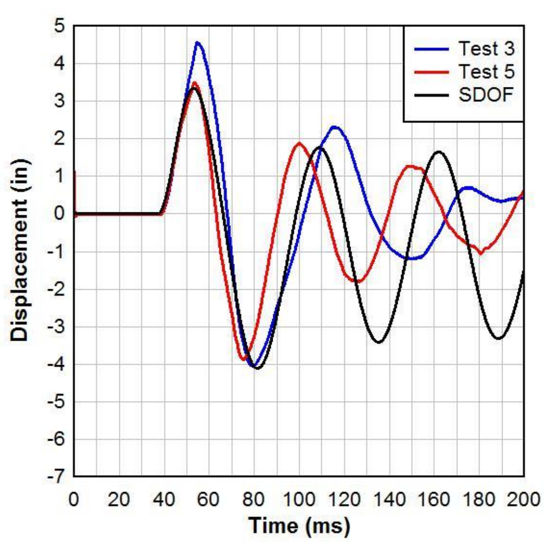

(a) Displacement History.

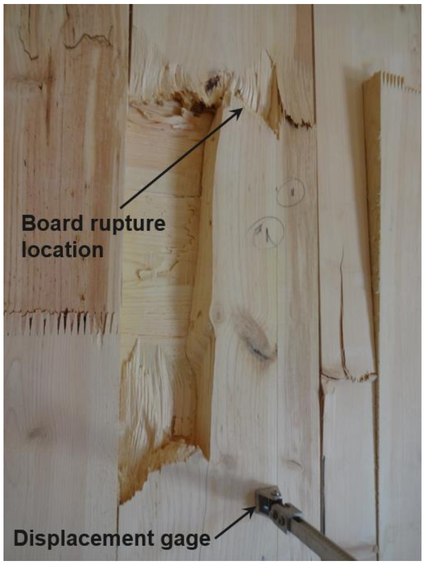

(b) Test 3 Gage Location.

Figure 5-6. First-Floor Front Panel Comparison in Grade V4 Structure for Tests 3 & 5.

Figure 5-7 compares the first-floor front wall displacement histories obtained from the Phase 1 and 2 testing. As indicated by reviewing the displacements in Table 5-11, the recorded displacement histories align well for all test structures given the Grade V4 structure caveat discussed above.

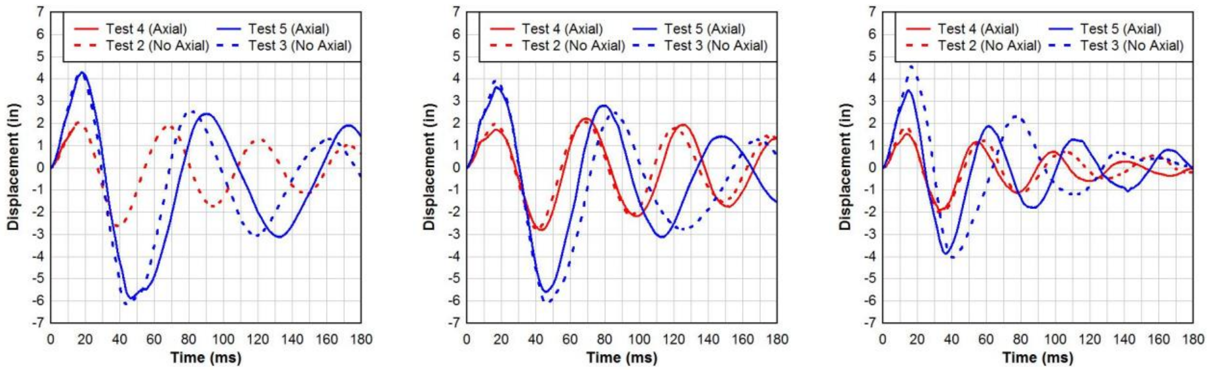

(a) Grade V1. *(b) Grade E1.* *(c) Grade V4.*

Figure 5-7. First-Floor Front Panel Displacement Comparisons.

Given roughly the same applied blast load and resulting displacement response of the front wall panels, it might be presumed that the wall panel damage observed following Tests 3 and 5 would be similar. However, comparing the observed damage on the interior face of the first-floor front wall panels between the Tests 3 and 5 (Figure 5-8) indicates greater board rupture and disengagement occurred in the test structures without axial load. This finding was consistently observed across the three CLT grades considered and is consistent with the quasi-static testing documented in Chapter 2.

(a) Grade V1 (Axial). *(b) Grade E1 (Axial).* *(c) Grade V4 (Axial).*

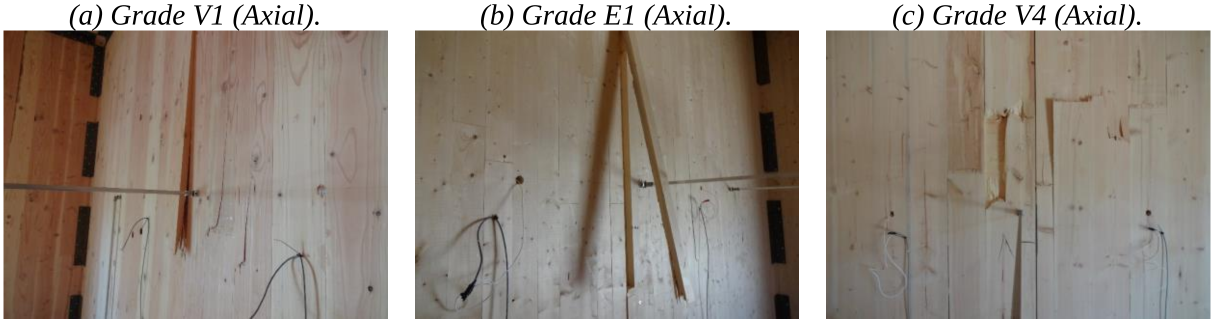

(d) Grade V1 (No Axial). *(e) Grade E1 (No Axial).* *(f) Grade V4 (No Axial).*

Figure 5-8. Test 3/5 Damage to the Interior Face of First-Floor Front Panels.

With the above in mind, the following findings are noted concerning the response of axially-loaded CLT wall panels to blast loads:

(1) An elasto-plastic resistance function that does not consider the presence of axial load and was constructed using the SIF/DIF factors identified in this chapter well approximated, or was conservatively higher than, the initial inbound and rebound displacement responses of the CLT wall panels for the blast loads associated with Tests 4 and 5 (Table 5-5, Table 5-7, and Table 5-8).

(2) CLT panels were capable of resisting tributary superimposed dead load when exposed to blast loads that caused localized panel rupture. For the Grade V1 structure (i.e., the structure with the largest superimposed dead load), rupture was observed on both the exterior and interior faces of the first-floor front wall panel following Test 5. For the Grade E1 and V4 structures, panel rupture was only observed on the exterior face, with only minor cracking being observed in the Grade V4 wall panels, following Test 5. Peak computed displacement ductility for the front walls using the blast loads measured during Test 5 ranged from 1.22 (Grade V4) to 1.59 (Grade E1) (Table 5-5, Table 5-7, and Table 5-8).

(3) For the same applied blast loads and resulting panel displacements, load bearing CLT panels exhibited less observable damage than those without axial load. Thus, the presence of axial load can serve to augment the strength of the panel (see Chapter 2 conclusions) and limit the propensity for lamella disengagement when compared to the same panel without axial load.

(4) As with the unloaded structures tested in Phase 1, the rebound response often exceeded the inbound response, indicating the need to consider the negative phase of blast loads when designing load bearing CLT wall panels.

5.3.2 Tests 6 & 7

For Tests 1 through 3 of Phase 1 and Tests 4 and 5 of Phase 2, the testing focus was 3-ply CLT panels of different grades (i.e., V1, E1, and V4), span lengths (i.e., 10 and 12 feet), and axial stresses (i.e., between 0 and 12-percent F_c'). Connections involving hot rolled steel angle brackets and self-tapping screws were kept constant between each of these five tests. During Tests 6 and 7, alternative mass timber configurations were exposed to blast loads including 5-ply CLT panels, alternative connection configurations involving prefabricated angle brackets and self-tapping screws only, and NLT wall panels. Based on the results of these final two tests, the following additional findings were realized:

(1) In general, the elasto-plastic resistance function constructed using the SIF/DIF factors identified in this chapter well approximated, or was conservatively higher than, the initial inbound and rebound displacement responses of the 5-ply CLT wall panels for the blast loads associated with Tests 6 and 7 (Table 5-6). One notable exception is the first-floor front panel response at DG2 in Test 7. It is clear upon reviewing the displacement history in Figure 5-5a that the SDOF calculation fails to approximate this initial inbound displacement. However, as for the first-floor front panel gage in Test 3, the DG2 gage is located on a board that ruptured during Test 7 (Figure 5-9) and it is possible that the board locally deflected more than the wall as a result. More testing on 5-ply CLT panels that are brought to failure should be conducted to further assess the robustness of the SDOF model for 5-ply panels in the post-peak realm.

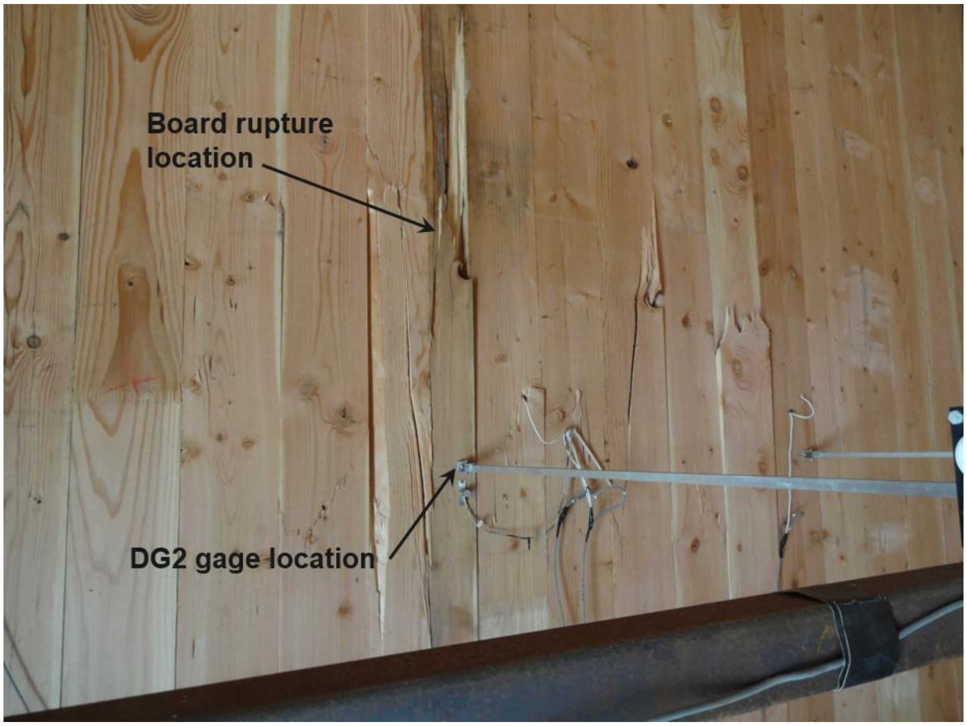

Figure 5-9. Location DG2 in 5-Ply Grade V1 First-Floor Front Wall Panel.

(2) The elasto-plastic resistance function constructed using the SIF/DIF factors identified in this chapter well approximated, or was conservatively higher than, the initial inbound and rebound displacement responses of the 3-ply CLT wall panels for the blast loads associated with Tests 6 and 7 (Table 5-5, Table 5-7, and Table 5-8). It is also interesting to note that the where the panels exhibited observable damage during testing, the computed displacement ductility was always greater than one, lending support to the SIF and DIF factors used to construct the resistance function.

(3) The resistance function employed and SIF/DIF factors included in the "Wood Beam" module of SBEDS 4.1 conservatively approximated the elastic response of the NLT panels in Test 6 (Table 5-9). The 0.5-inch thick plywood sheathing on the front face of the NLT panel only contributed supported weight (i.e., the sheathing was not assumed to be composite with the 2x4 studs and therefore did not augment the analytical ultimate resistance of the NLT panel).

(4) The presence of plywood on the back face of NLT panels can increase the strength of the panel and prevent rupture of the panel's constituent studs but can also become a debris hazard depending on how the plywood is attached. Care should be exercised when attaching anything to the back side of a wall that is loaded at high strain rates.

(5) Although not intentional (i.e., the shorter screws were substituted in error), the failure of the prefabricated bracket due to self-tapping screw withdrawal in Test 7 (see Section 4.1.4.2) provided a helpful data point from which to assess connection design in CLT structures exposed to blast loads. The ultimate dynamic capacity of this connection bracket is approximately 3,100 pounds (i.e., computed by multiplying the reported ASD capacity

of 835 pounds by a test-to-ASD value safety factor of 3 [16] and a 1.25 DIF). Since the brackets were spaced at 8 inches on center, if the connection was designed to resist the ultimate resistance of the panel (i.e., 5.21 psi Table 5-4), the theoretical shear demand would have been approximately 3,000 pounds. Even though the demand is less than the capacity, Test 7 showed that the screws completely withdrew from the panel, which underlies the importance of utilizing an appropriate safety factor when designing CLT connections for blast loads.

(6) Care should be utilized when specifying toe-screw connections to resist blast loads. Test data has indicated screws in the diagonal orientation, while strong, have limited post-peak deformation capability [17]. Additionally, Test 7 indicated that when this connection is overloaded, it is prone to fail catastrophically.

(7) In light of the scenarios raised in points (6) and (7), it is important to select a factor of safety when designing CLT connections for blast loads that considers the factors that would serve to augment the connection demand. Examples of such factors include the:

a. variation in the modulus of rupture of the CLT panel's constituent lumber;

b. CLT panel's axial load (see Chapter 2);

c. rotational restraint associated with end condition details;

d. post-peak deformation response of the relevant connection limit states; and

e. relative importance, redundancy, and reliability of the connection.

(8) Door and window openings, while not designed explicitly for the blast loads associated with Test 7, responded well and only exhibited minor damage in the test's wake. However, using an SDOF dynamic analysis model to approximate the panel's minor strength direction response above or below the opening would indicate significant damage had occurred during Test 7 (i.e., see Grade E1 SDOF computed responses at openings for the much smaller applied blast load associated with Test 3 [9] as an example). A more refined analysis method (e.g., MDOF analytical model or a two-way spanning panel) and/or a better approximation of minor strength direction ultimate resistance is necessary to design CLT opening boundary members more in keeping with observed test response.

CHAPTER 6

SUMMARY AND CONCLUSIONS

6.1 SUMMARY

As part of a Forest Products Laboratory Coalition for Advanced Wood Structures Grant, WoodWorks, Karagozian and Case, Inc., and the Air Force Civil Engineer Center (AFCEC) partnered via a Cooperative Research and Development Agreement to extend the work documented in [1] (i.e., Phase 1) as part of a follow-on Phase 2 effort. The overarching objectives of this Phase 2 effort were to investigate:

- the response of axially-loaded cross-laminated timber (CLT) construction exposed to blast loads; and
- the response of alternative mass timber panel and connection configurations exposed to blast loads.

Towards this end, two distinct series of tests were performed as part of the Phase 2 effort:

- A total of twenty-four quasi-static laboratory tests were used to investigate the out-of-plane bending response of axially-loaded CLT panels in their major strength direction under a uniformly-applied transverse quasi-static load. These tests varied the applied axial load, CLT grade, number of panel plies, and panel length and were performed using AFCEC's load tree testing apparatus.
- A total of four arena blast tests were performed on three existing full-scale CLT structures constructed at Tyndall AFB. The first two tests were used to demonstrate the ability of axially-loaded CLT to resist blast loads while the second two tests were used to demonstrate the ability of alternative mass timber configurations to resist blast loads. In both test series, the first shot was intended to keep the panels elastic and the second shot was intended to rupture panels. Ruptured panels were removed and replaced prior to performing the first test in each series.

6.2 CONCLUSIONS

Based on the results of this testing effort, the following general conclusions are made:

- When compared to a CLT panel without axial load, the presence of axial load serves to increase the ultimate resistance of the CLT panel.
- Provided the displacement of the panel is kept within a displacement ductility of two, an axially-loaded CLT panel response can be safely designed ignoring the effect of axial load.
- CLT panels were capable of resisting tributary superimposed dead load when exposed to blast loads that caused localized panel rupture.

- The static and dynamic increase factors used to approximate the expected ultimate resistance showed good correlation with arena blast test results.

- An SDOF dynamic analysis can be used to approximate peak displacements in 3-ply and 5-ply CLT panels without openings.

- As identified in Phase 1, the rebound response of CLT often controls over its inbound response, thus underlying the importance of considering the negative phase of the blast loading when designing CLT components and systems for blast loading.

- As identified in Phase 1, visually graded CLT panels demonstrate significantly greater out-of-plane bending strength than that associated with the characteristic values defined in PRG 320.

6.3 RESPONSE LIMITS

Based on the post-test photographs included in this report and in the Phase 1 blast testing report, the observed damage at the first-floor wall panels can be correlated with the component damage level definitions included in Table 2-4 of PDC-TR 06-08. This information is included in Table 6-1.

Table 6-1. First-Floor Wall Panel Damage from Tests 1-7 Correlated to PDC-TR 06-08 Component Damage Levels.

Component Damage Level[1]	Description of Component Damage	Examples from Tests 1 Through 7
Blowout	Component is overwhelmed by the blast load causing debris with significant velocities	• 3-ply E1 front wall following Test 7
Hazardous Failure	Component has failed, and debris velocities range from insignificant to very significant	N/A
Heavy Damage	Component has not failed, but it has significant permanent deflections causing is to be unrepairable	N/A
Moderate Damage	Component has some permanent deflection. It is generally repairable, if necessary, although replacement may be more economical and aesthetic	• All front walls following Tests 3 & 5 • 5-ply V1 front wall following Test 7 • All 3-ply side walls following Test 7
Superficial Damage	Component has no visible permanent damage	• All walls following Tests 1, 2, 4, & 6

1 From PDC-TR 06-08 [8].

Using the pressure histories recorded during Tests 1 through 7 as the input blast loads and the resistance function generation process, SIFs, and DIFs documented in Section 5.2, a bar chart can be constructed that plots computed displacement ductility of the first-floor front and side wall panels across a spectrum of blast loads. In addition, this plot designates where the PDC-TR 06-08 component damage levels fall.

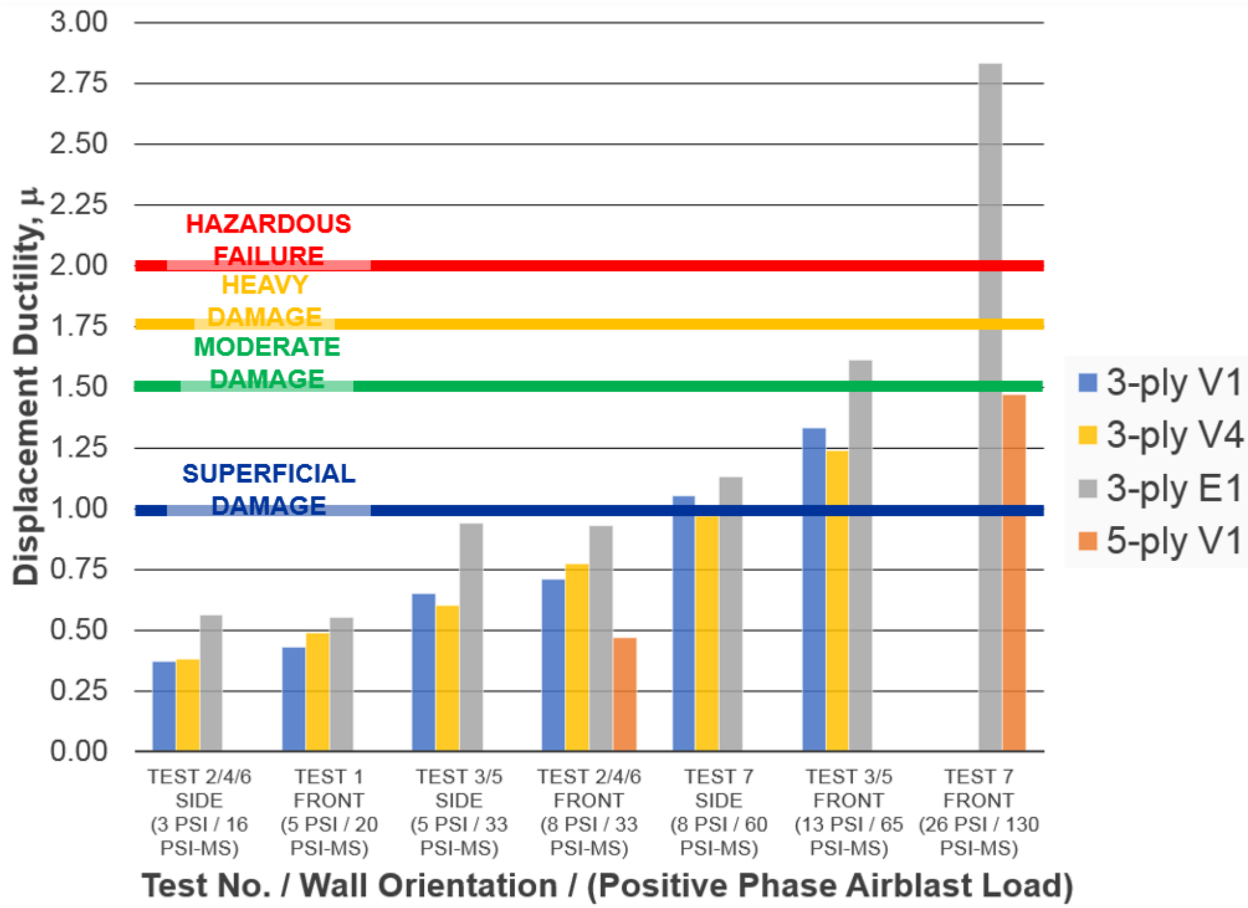

Figure 6-1. Applied Blast Load vs. Computed Displacement Ductility with PDC-TR 06-08 Component Damage Levels Indicated.

Commentary concerning the displacement ductility value assigned to each component damage level is shown in

- **Superficial Damage (μ < 1.0)**: When the computed displacement ductility is less than one, no visual signs of damage were observed in the CLT wall panels.

- **Moderate Damage (1 ≤ μ < 1.5)**: The extent of the damage observed in most of the front wall panels following Tests 3, 5, and 7 was limited and localized near midspan. It is thought that such wall panel could be repaired relatively easily with additional lumber boards and/or thin gauge steel plates.

- **Heavy Damage (1 ≤ μ < 1.75)**: No examples matching the “heavy damage” description appear in the testing performed. This response limit is simply placed halfway between the “moderate damage” and “hazardous failure” component damage levels.

- **Hazardous Failure (1.75 ≤ μ < 2)**: The displacement ductility value of 2 is based on the reasoning included in Section 2.6 of this report.

- **Blowout ($\mu \geq 2$)**: The front wall panel in the Grade E1 structure following Test 7 was completely overwhelmed by the blast load and exhibited a displacement ductility well over two.

6.4 FUTURE AREAS OF RESEARCH

While the research conducted to this point provides a solid foundation upon which to base protective design guidance for CLT structures, the following areas of additional research would serve to curtail conservatism in the analysis and design approaches for such structures:

- The minor strength direction bending strength values for CLT panels in Annex A of PRG 320 appears to be too conservative from an ultimate response perspective. Further testing to justify more representative peak bending strengths in the minor strength direction may allow for openings in blast-loaded structures to be designed more economically. Additionally, better quantification of the minor strength direction strength and stiffness will enable more explicit consideration of the two-way action inherent in CLT construction.

- Dynamic characterization of different timber species and dowel-type connections at blast-relevant strain rates will assist refining the DIFs used in design.

- Additional testing on 5-ply panels will assist in assessing the robustness of the SDOF resistance function defined herein.

APPENDIX A

REFERENCES

[1] Podesto, L. and M. K. Weaver, "Blast-Resistant Testing for Mass Timber Exterior Walls: Final Accomplishment Report," Karagozian & Case, Inc., Glendale, CA, Report No. TR-17-08.1, 9 October 2016.

[2] "DoD Minimum Antiterrorism Standards for Buildings, with Change 1", U.S. Army Corps of Engineers, UFC 4-010-01, 2013.

[3] "National Design Specification for Wood Construction, 2018 Edition", American Wood Council, 16 November 2017.

[4] Karacabeyli, E. and B. Douglas, "CLT Handbook, US Edition," FPInnovations, Pointe-Claire, Quebec, Canada, 2013.

[5] "Standard for Performance-Rated Cross-Laminated Timber", The Engineered Wood Association, ANSI/APA PRG 320, 2018.

[6] Nagy, E. and M.K. Weaver, "Quasi-Static Out-of-Plane Testing of CLT and NLT Panels," Karagozian & Case, Inc., Glendale, CA, TR-16-42.1, 2016.

[7] "APA Product Report: SmartLam Cross-Laminated Timber," The Engineered Wood Association, PR-L319, 15 August 2017.

[8] "Single Degree of Freedom Structural Response Limits for Antiterrorism Design" U.S. Army Corps of Engineers, PDC-TR 06-08, 7 January 2008.

[9] Weaver, M.K, Newberry, C., O'Laughlin, C., and L. Podesto, "Results from Blast Tests of Full-Scale Cross-Laminated Timber Structures," Karagozian & Case, Inc., Glendale, CA, Report No. TR-17-17.1, 27 September 2017.

[10] "DoD Minimum Antiterrorism Standoff Distances for Buildings," U.S. Army Corps of Engineers, UFC 4-010-02, 2012. *(Limited Distribution)*

[11] "Nail-Laminated Timber: U.S. Design & Construction Guide v1.0," Binational Softwood Lumber Council, 2017.

[12] Kingery, N.C. and G. Bulmash, "Airblast Parameters from TNT Spherical Air Burst and Hemispherical Surface Burst", U.S. Army Ballistic Research Laboratory, Aberdeen Proving Ground, MD, ARBRL-TR-02555, 1984. *(Limited Distribution)*

[13] Bohannan, B., "Effect of Size on Bending Strength of Wood Members," Forest Products Laboratory, FPL 56, May 1966.

[14] "Cross-Laminated Timber Analysis Guidance for Airblast Loading," U.S. Army Corps of Engineers, PDC-TR 18-02, September 2018.

[15] "Single degree of freedom Blast Effects Design Spreadsheet, Version 4.1," U.S. Army Corps of Engineers, 10 March 2009.

[16] Ray Yu (personal communication) 16 January 2017.

[17] Hossain, A., Lakshman, R., and T. Tannert, "Shear Connections with Self-Tapping Screws for Cross-Laminated Timber Panels," *Proceedings of 2015 Structures Congress*, Portland, OR, 23-25 April 2015.

APPENDIX B

LABORATORY TESTING RESULTS

LIST OF FIGURES

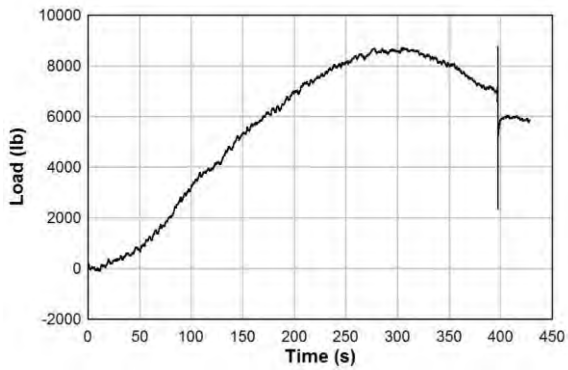

(a) Axial Load vs. Time.

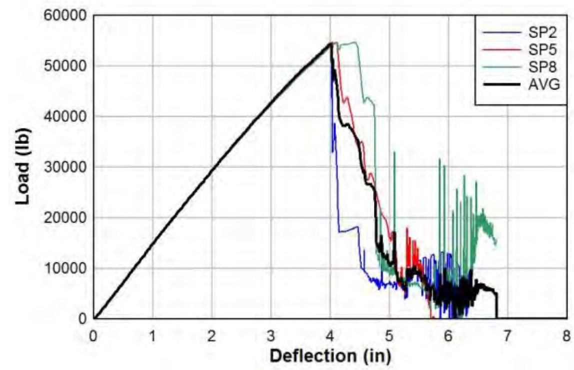

(b) Out-of-Plane Load vs. Displacement.

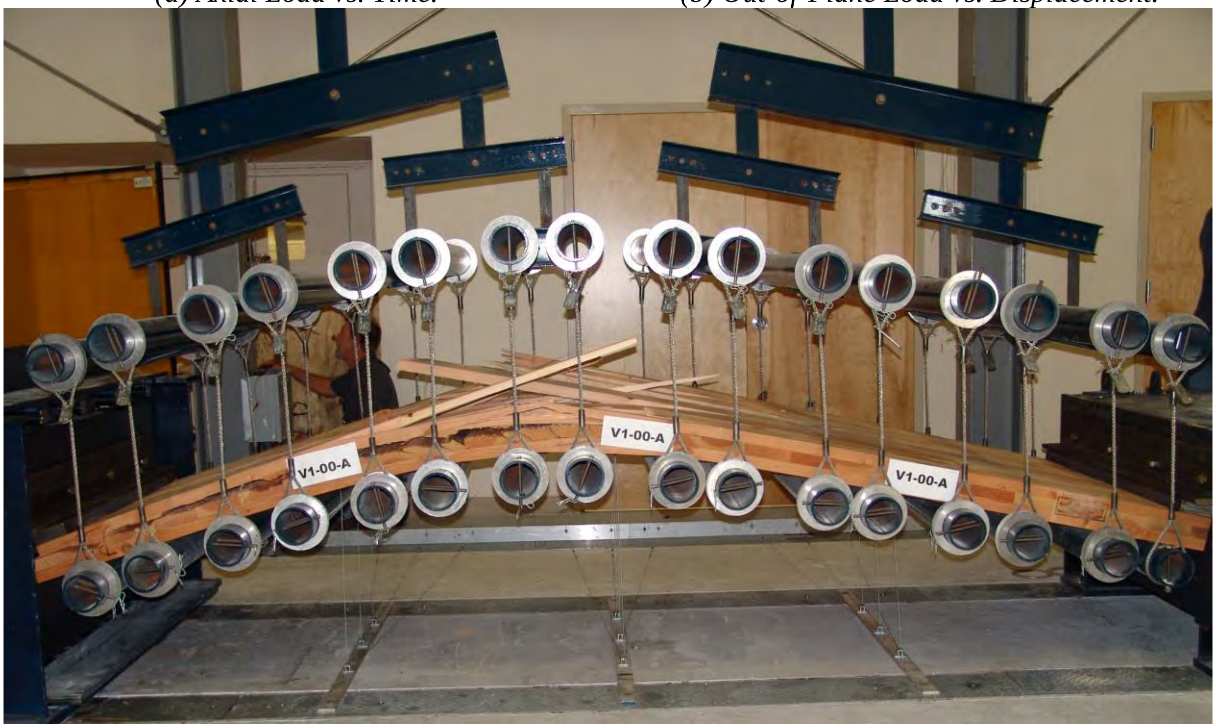

(c) Elevation.

(d) Left Support.

(e) Right Support.

Figure B-1. 12' Long, 3-Ply Grade V1 CLT Panel w/ 0%F_c^* Axial Load (Test V1-00-A).

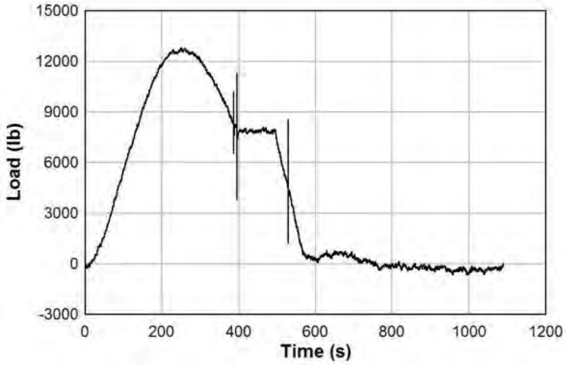

(a) Axial Load vs. Time.

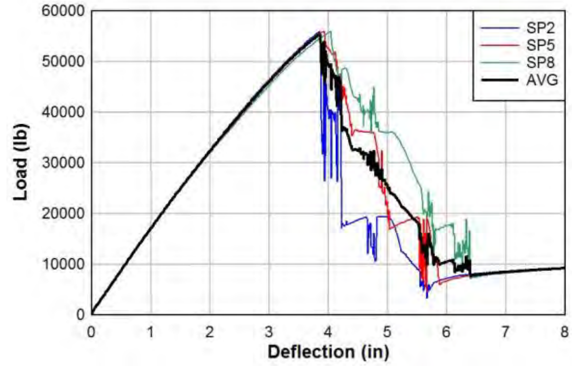

(b) Out-of-Plane Load vs. Displacement.

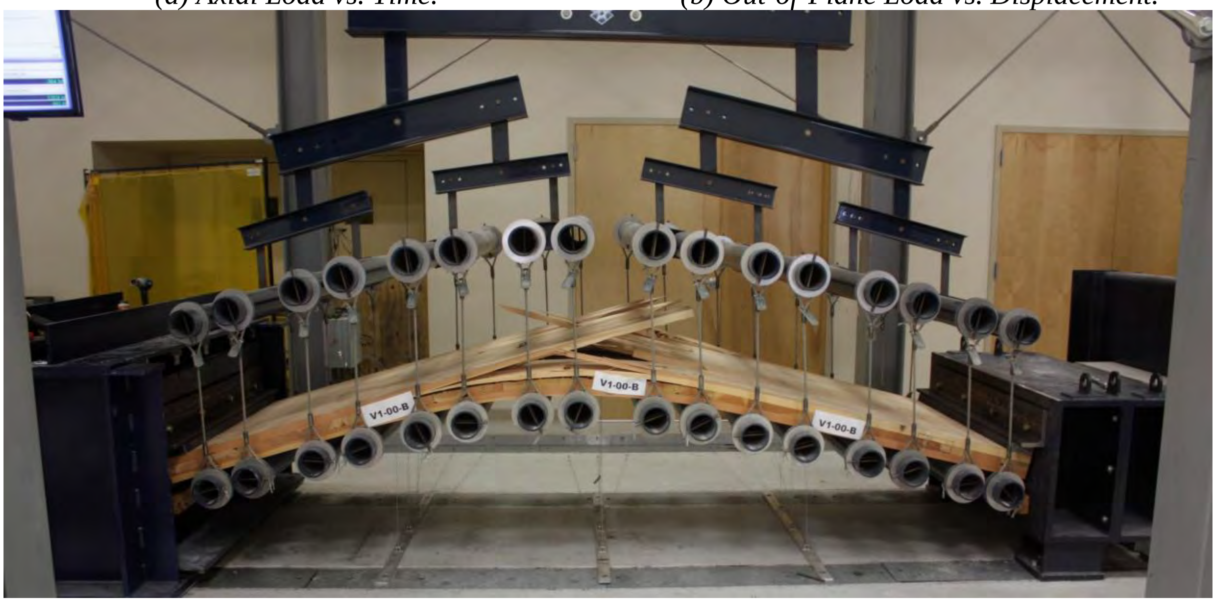

(c) Elevation.

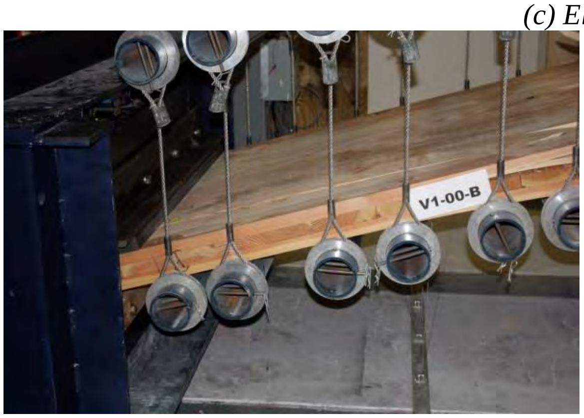

(d) Left Support.

(e) Right Support.

Figure B-2. 12' Long, 3-Ply Grade V1 CLT Panel w/ 0%F_c^* Axial Load (Test V1-00-B).

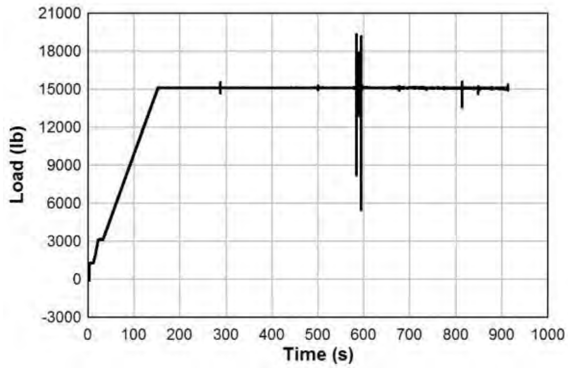

(a) Axial Load vs. Time.

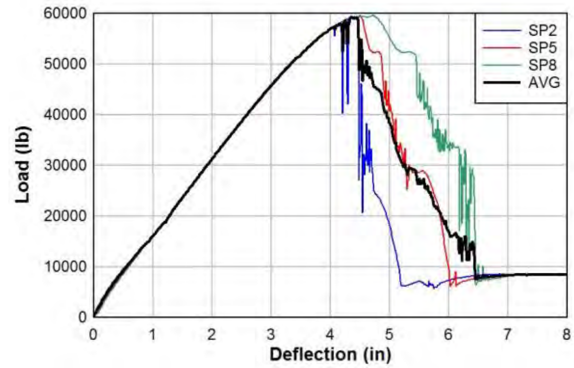

(b) Out-of-Plane Load vs. Displacement.

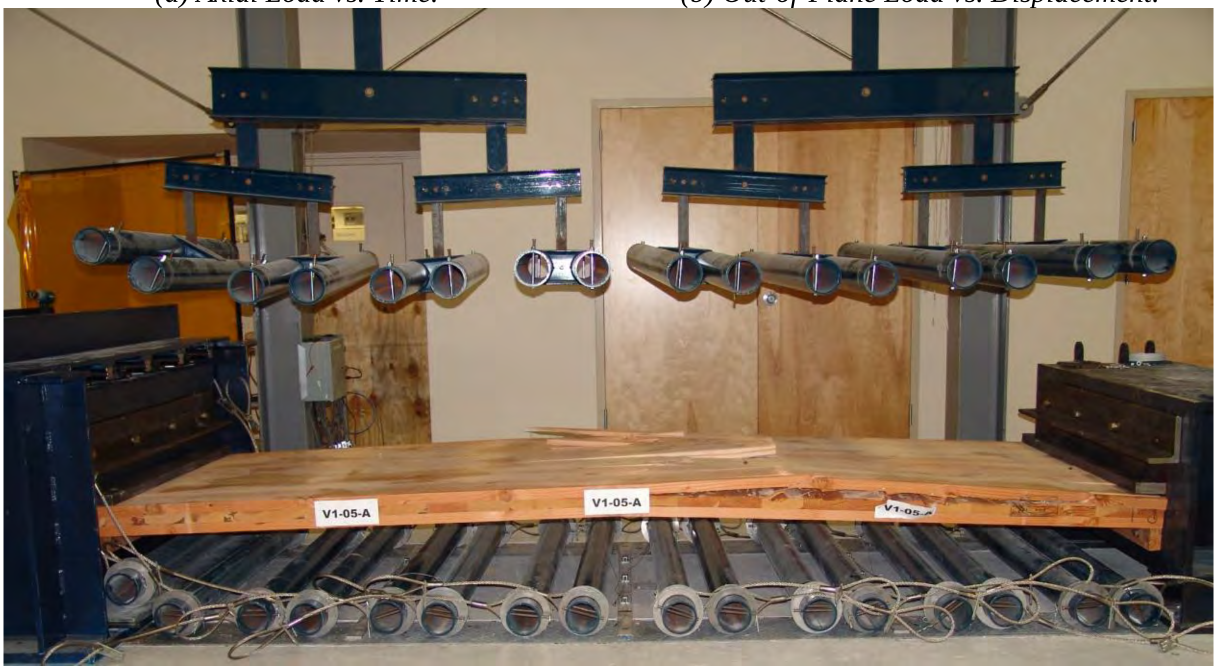

(c) Elevation.

(d) Left Support.

(e) Right Support.

Figure B-3. 12' Long, 3-Ply Grade V1 CLT Panel w/ 5%F_c^* Axial Load (Test V1-05-A).

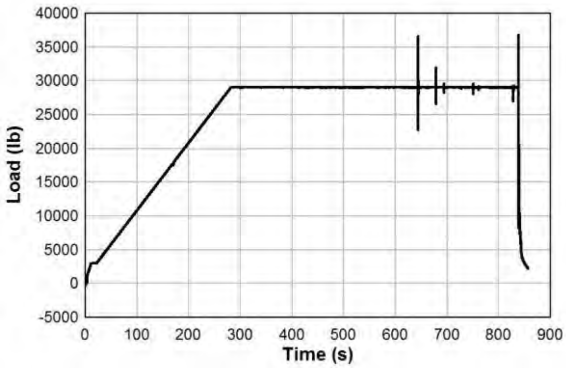

(a) Axial Load vs. Time.

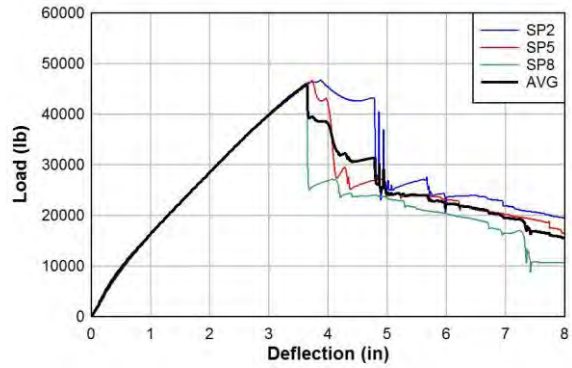

(b) Out-of-Plane Load vs. Displacement.

(c) Elevation.

(d) Left Support.

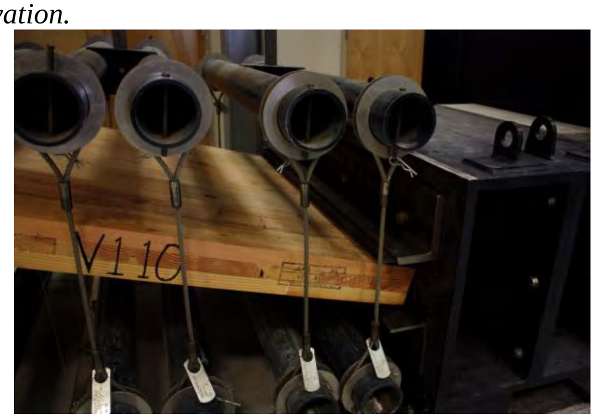

(e) Right Support.

Figure B-4. 12' Long, 3-Ply Grade V1 CLT Panel w/ 10%F_c^* Axial Load (Test V1-10-A).

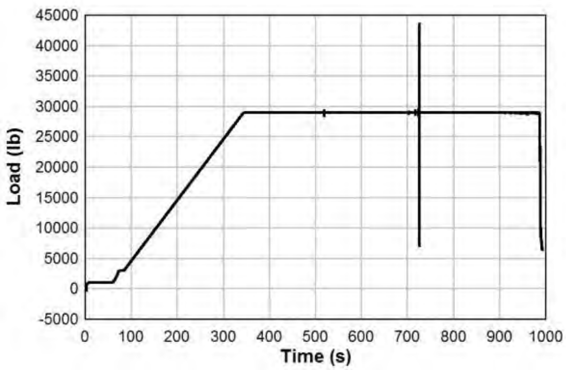

(a) *Axial Load vs. Time.*

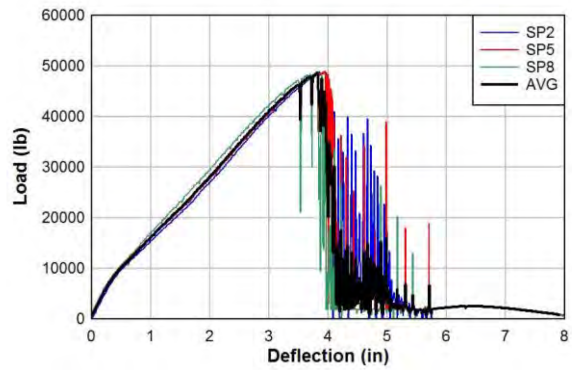

(b) *Out-of-Plane Load vs. Displacement.*

(c) Elevation.

(d) Left Support. *(e) Right Support.*

Figure B-5. 12' Long, 3-Ply Grade V1 CLT Panel w/ 10%F_c^* Axial Load (Test V1-10-B).

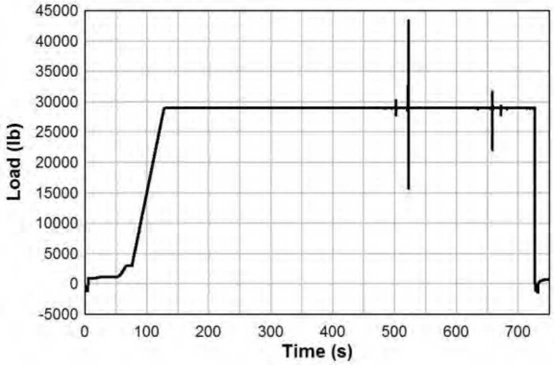

(a) Axial Load vs. Time.

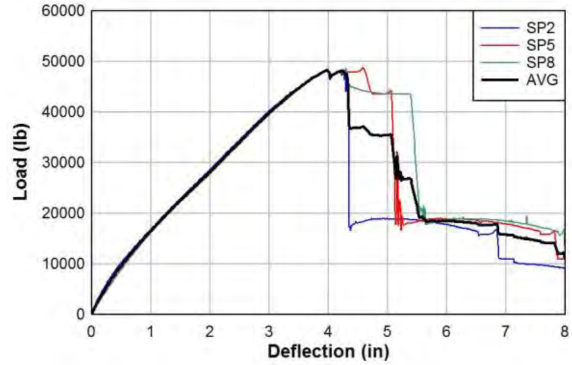

(b) Out-of-Plane Load vs. Displacement.

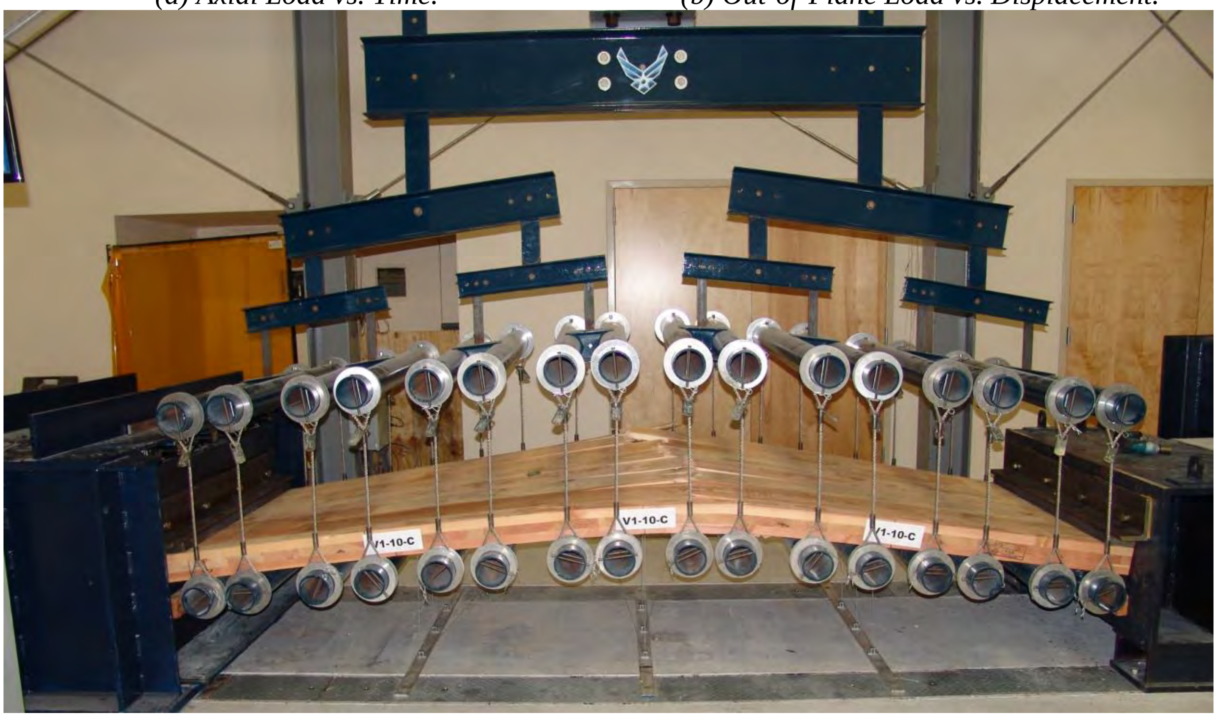

(c) Elevation.

(d) Left Support.

(e) Right Support.

Figure B-6. 12' Long, 3-Ply Grade V1 CLT Panel w/ 10%F_c^* Axial Load (Test V1-10-C).

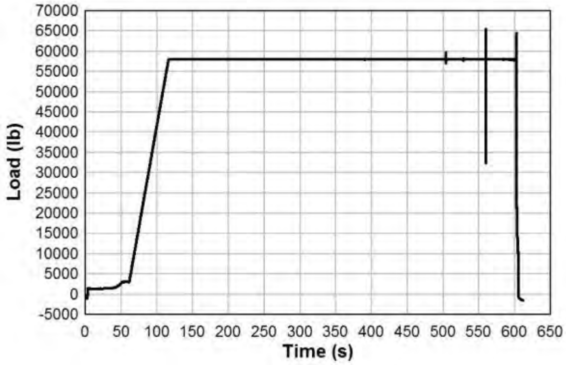

(a) Axial Load vs. Time.

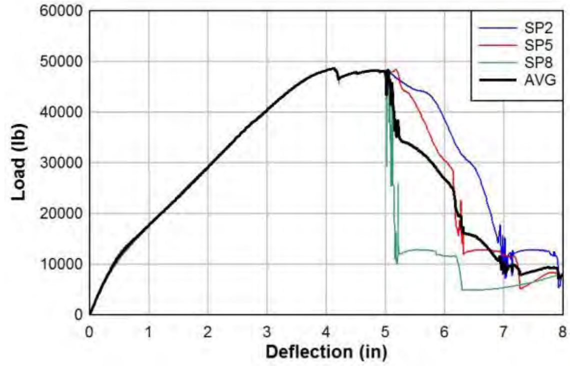

(b) Out-of-Plane Load vs. Displacement.

(c) Elevation.

(d) Left Support.

(e) Right Support.

Figure B-7. 12' Long, 3-Ply Grade V1 CLT Panel w/ 20%F_c^* Axial Load (Test V1-20-A).

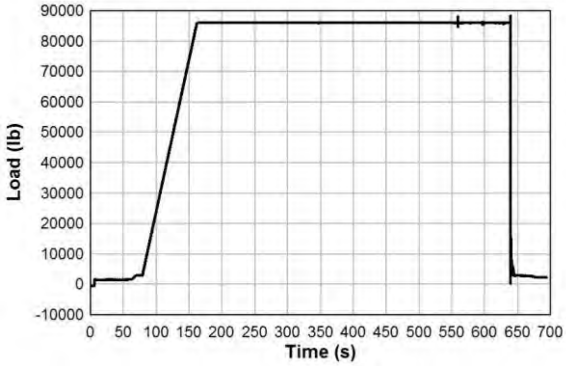

(a) Axial Load vs. Time.

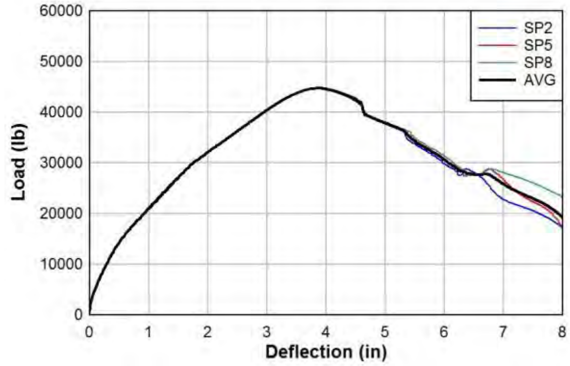

(b) Out-of-Plane Load vs. Displacement.

(c) Elevation.

(d) Left Support.

(e) Right Support.

Figure B-8. 12' Long, 3-Ply Grade V1 CLT Panel w/ 30%F_c^* Axial Load (Test V1-30-A).

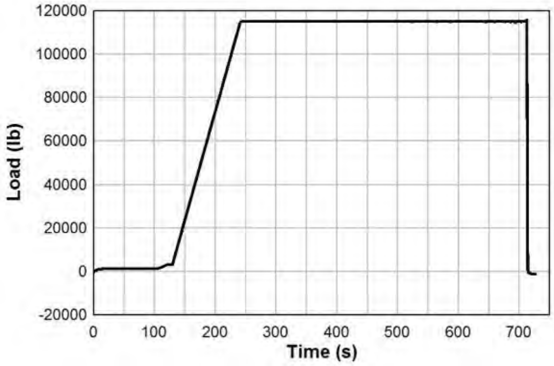

(a) Axial Load vs. Time.

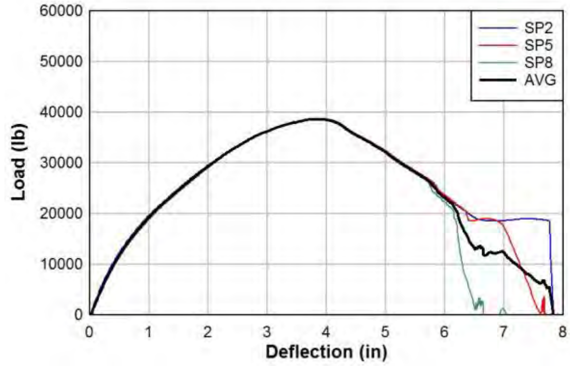

(b) Out-of-Plane Load vs. Displacement.

(c) Elevation.

(d) Left Support.

(e) Right Support.

Figure B-9. 12' Long, 3-Ply Grade V1 CLT Panel w/ 40%F_c^* Axial Load (Test V1-40-A).

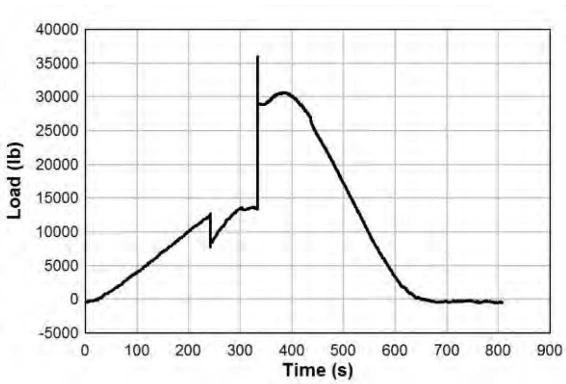

(a) *Axial Load vs. Time.*

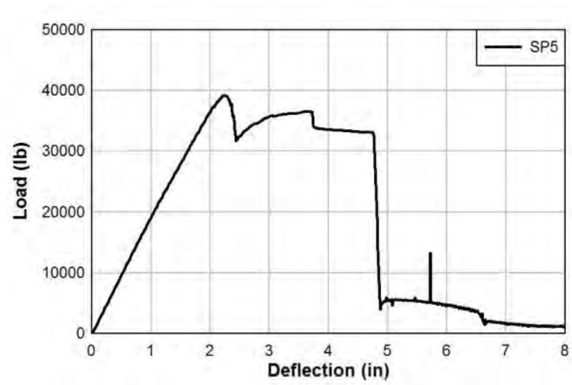

(b) *Out-of-Plane Load vs. Displacement.*

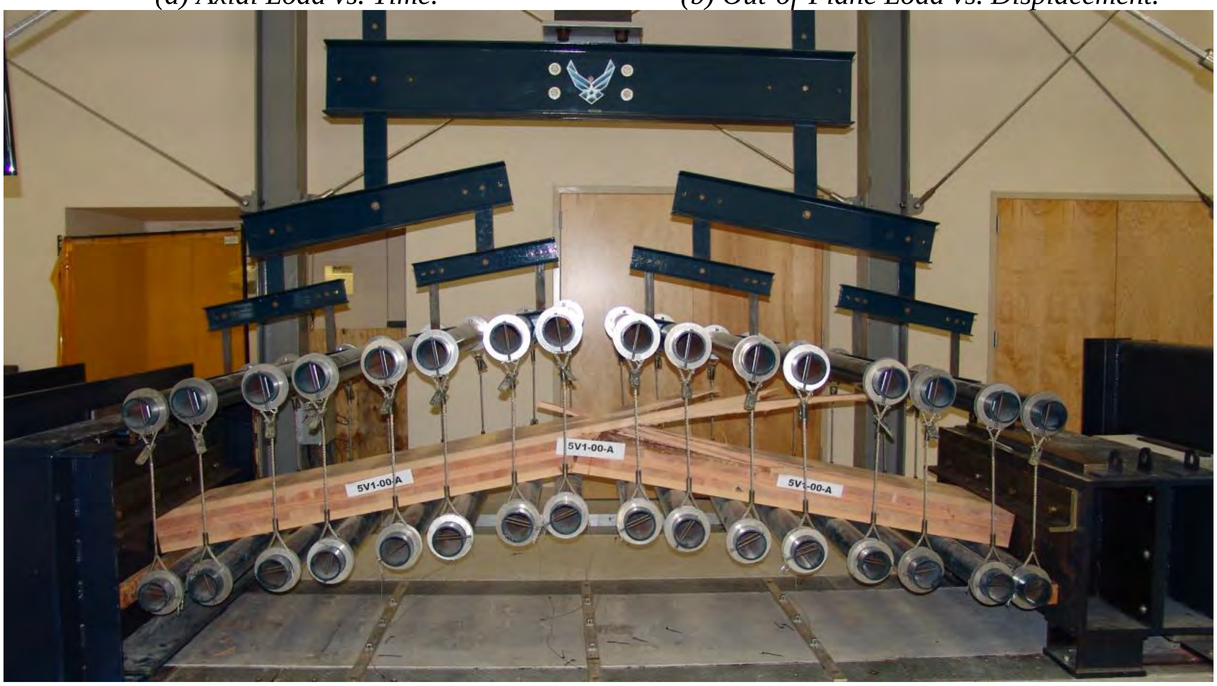

(c) Elevation.

(d) Left Support.

(e) Right Support.

Figure B-10. 12' Long, 5-Ply Grade V1 CLT Panel w/ 0%F_c^* Axial Load (Test 5V1-00-A).

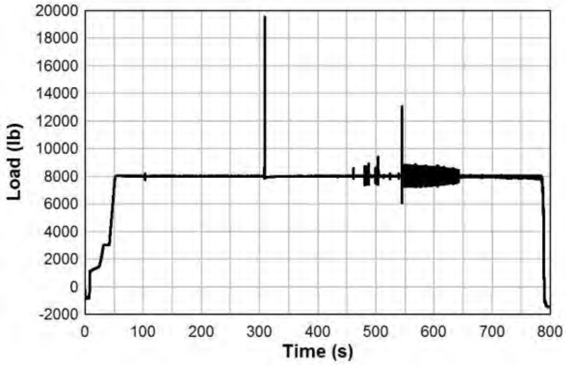

(a) Axial Load vs. Time.

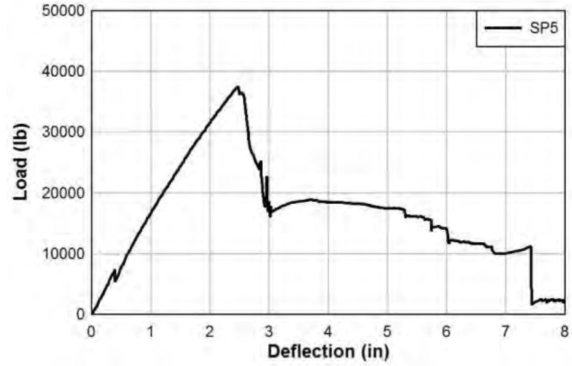

(b) Out-of-Plane Load vs. Displacement.

(c) Elevation.

(d) Left Support.

(e) Right Support.

Figure B-11. 12' Long, 5-Ply Grade V1 CLT Panel w/ 5%F_c^* Axial Load (Test 5V1-05-A).

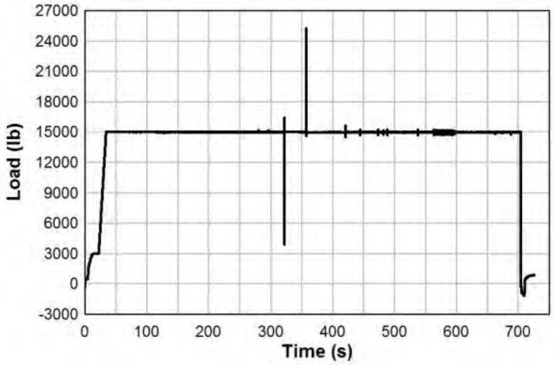

(a) Axial Load vs. Time.

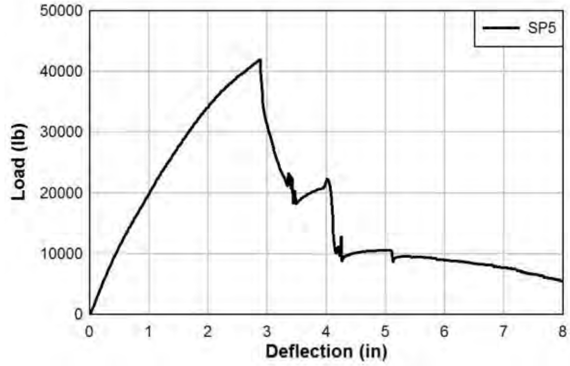

(b) Out-of-Plane Load vs. Displacement.

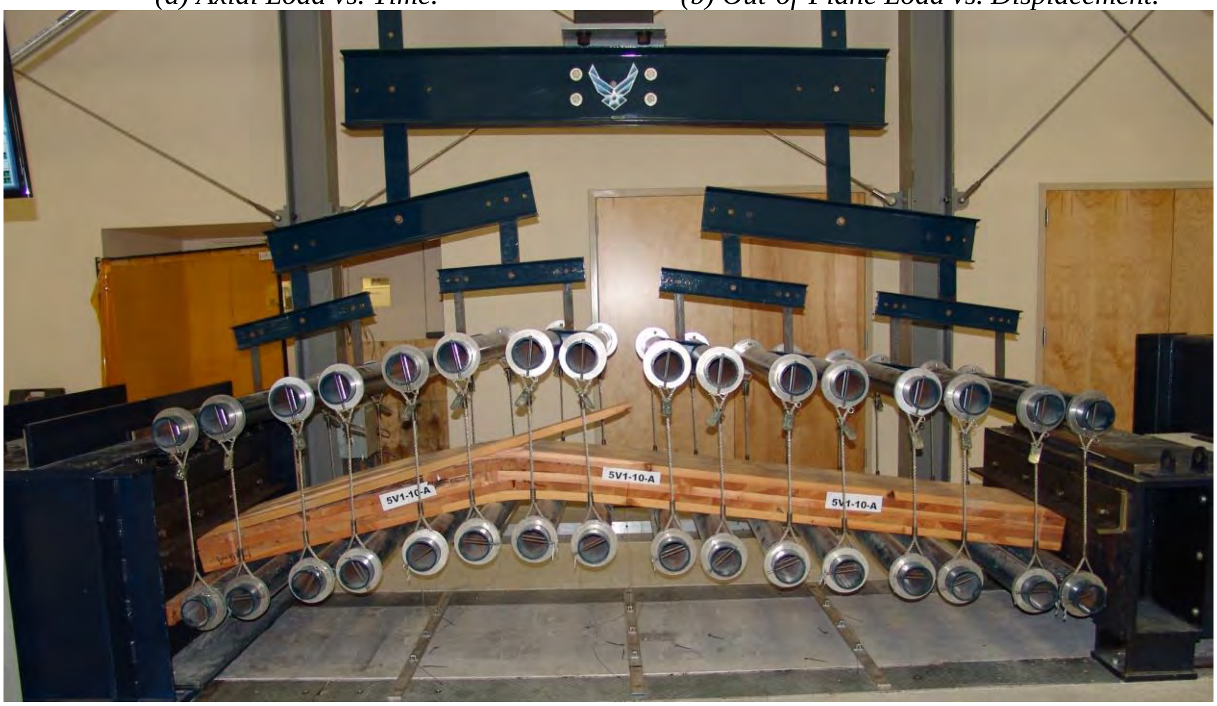

(c) Elevation.

(d) Left Support.

(e) Right Support.

Figure B-12. 12' Long, 5-Ply Grade V1 CLT Panel w/ 10%F_c^* Axial Load (Test 5V1-10-A).

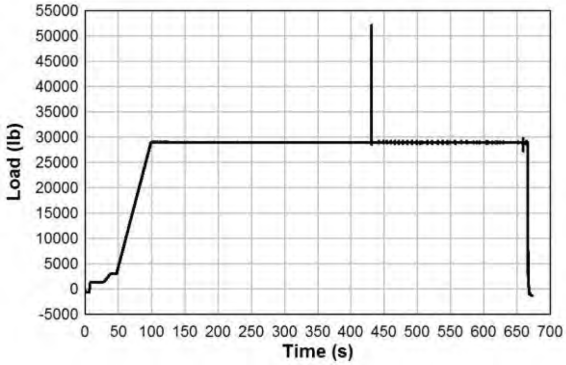

(a) Axial Load vs. Time.

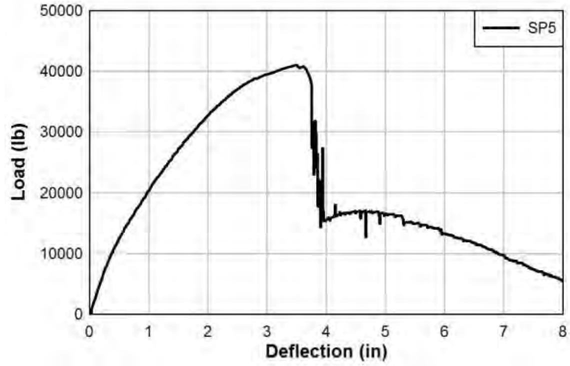

(b) Out-of-Plane Load vs. Displacement.

(c) Elevation.

(d) Left Support.

(e) Right Support.

Figure B-13. 12' Long, 5-Ply Grade V1 CLT Panel w/ 20%F_c^* Axial Load (Test 5V1-20-A).

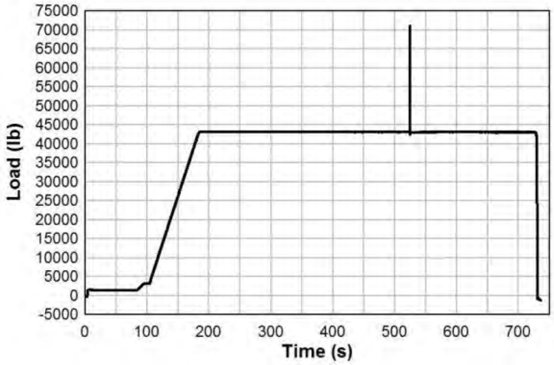

(a) Axial Load vs. Time.

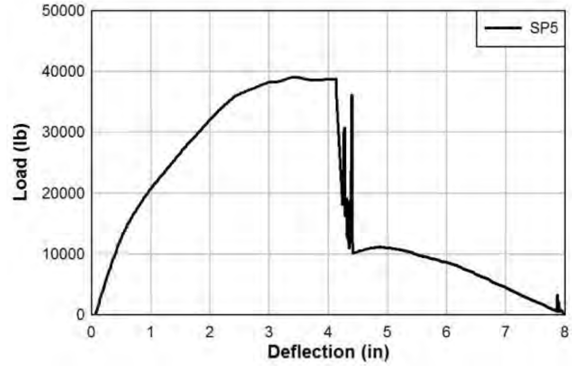

(b) Out-of-Plane Load vs. Displacement.

(c) Elevation.

(d) Left Support.

(e) Right Support.

Figure B-14. 12' Long, 5-Ply Grade V1 CLT Panel w/ 30%F_c^* Axial Load (Test 5V1-30-A).

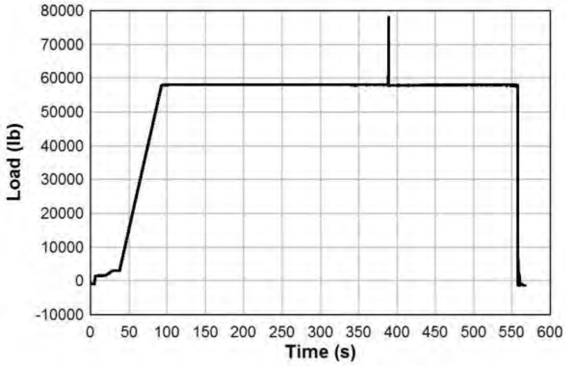

(a) Axial Load vs. Time.

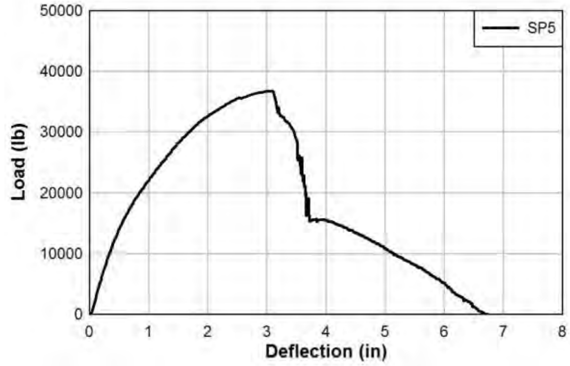

(b) Out-of-Plane Load vs. Displacement.

(c) Elevation.

(d) Left Support.

(e) Right Support.

Figure B-15. 12' Long, 5-Ply Grade V1 CLT Panel w/ 40%F_c^* Axial Load (Test 5V1-40-A).

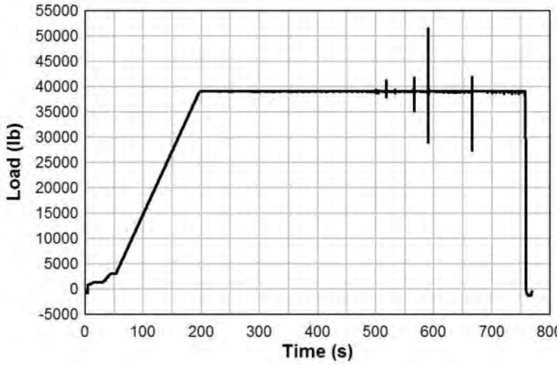

(a) Axial Load vs. Time.

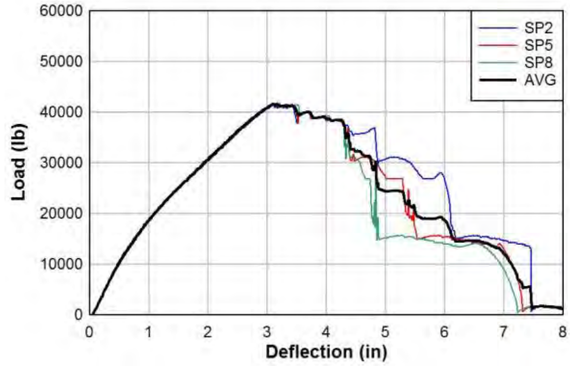

(b) Out-of-Plane Load vs. Displacement.

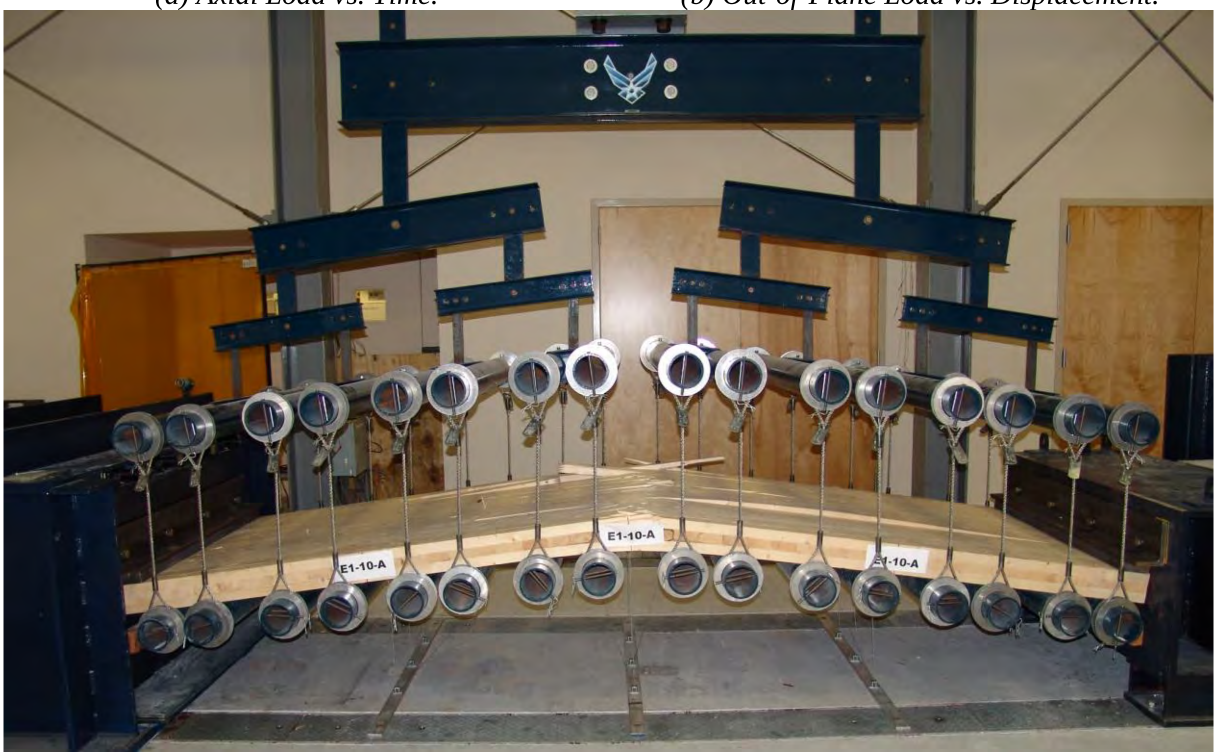

(c) Elevation.

(d) Left Support.

(e) Right Support.

Figure B-16. 12' Long, 3-Ply Grade E1 CLT Panel w/ 10%F_c^* Axial Load (Test E1-10-A).

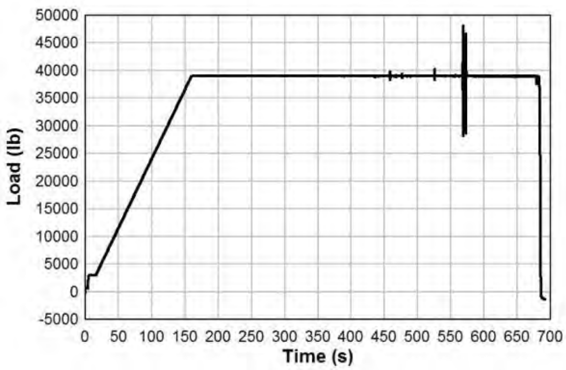

(a) Axial Load vs. Time.

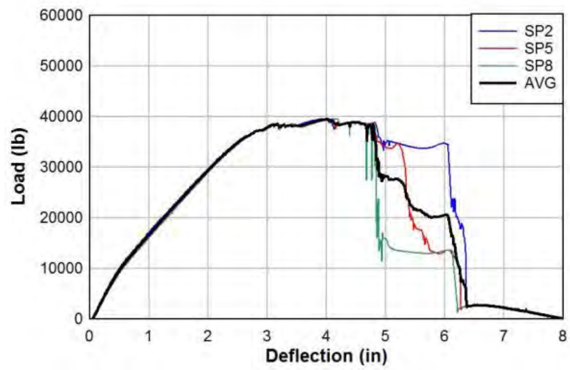

(b) Out-of-Plane Load vs. Displacement.

(c) Elevation.

(d) Left Support.

(e) Right Support.

Figure B-17. 12' Long, 3-Ply Grade E1 CLT Panel w/ 10%F_c^* Axial Load (Test E1-10-B).

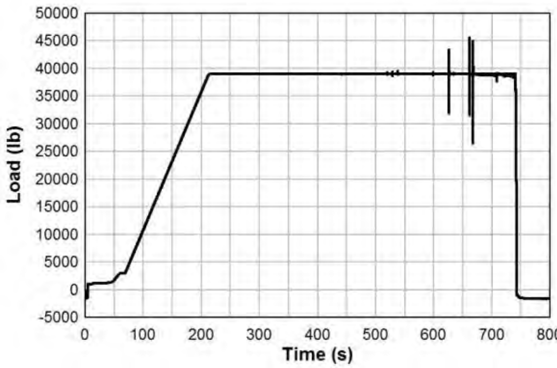

(a) Axial Load vs. Time.

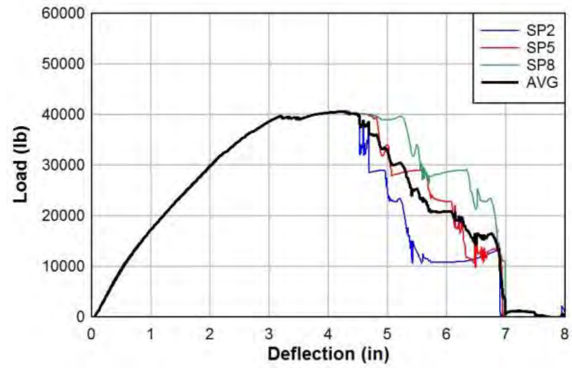

(b) Out-of-Plane Load vs. Displacement.

(c) Elevation.

(d) Left Support.

(e) Right Support.

Figure B-18. 12' Long, 3-Ply Grade E1 CLT Panel w/ 10%F_c^* Axial Load (Test E1-10-C).

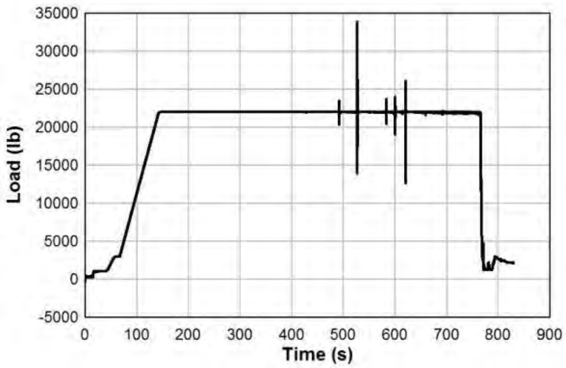

(a) Axial Load vs. Time.

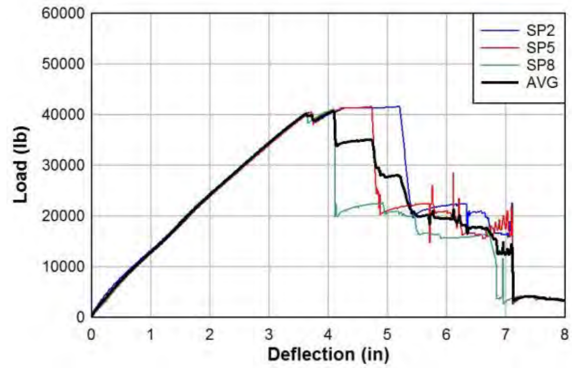

(b) Out-of-Plane Load vs. Displacement.

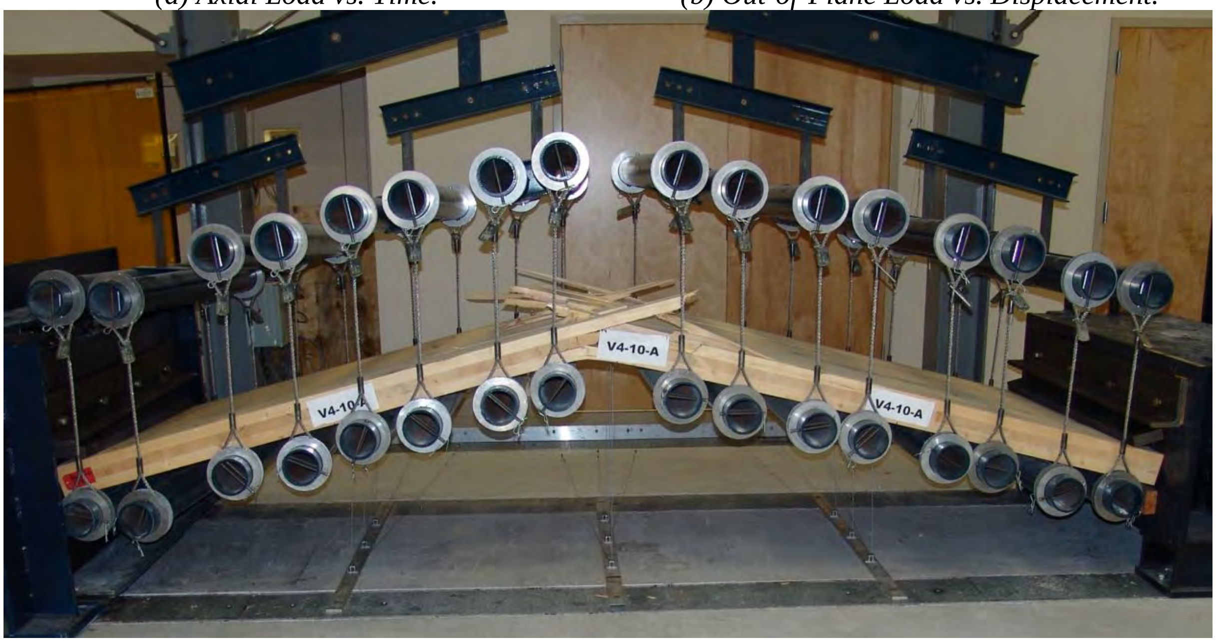

(c) Elevation.

(d) Left Support.

(e) Right Support.

Figure B-19. 12' Long, 3-Ply Grade V4 CLT Panel w/ 10%F_c^* Axial Load (Test V4-10-A).

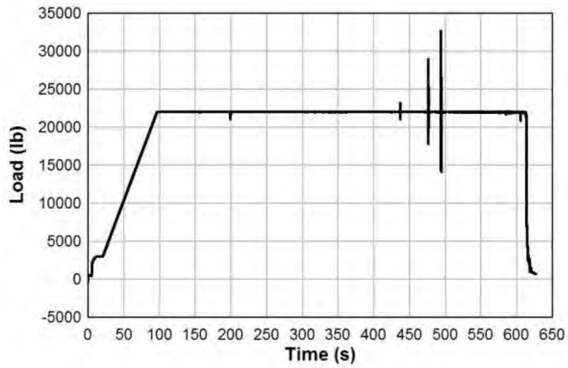

(a) Axial Load vs. Time.

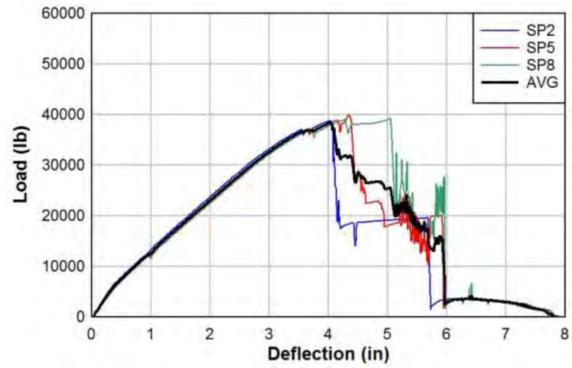

(b) Out-of-Plane Load vs. Displacement.

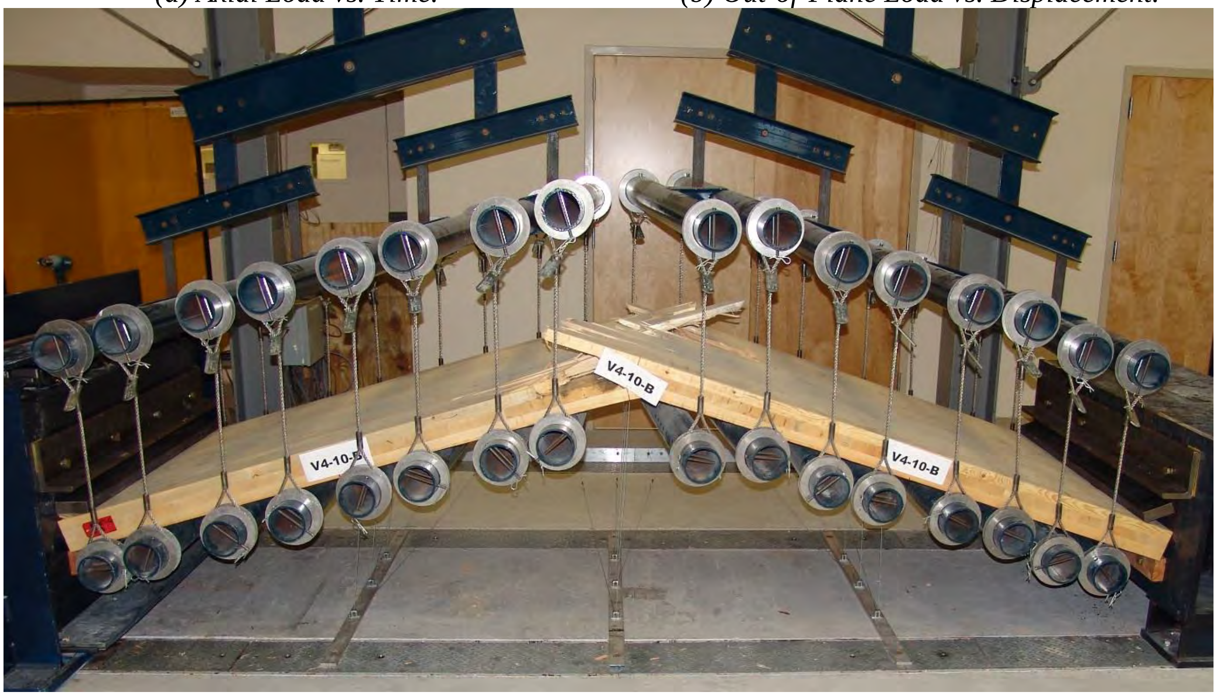

(c) Elevation.

(d) Top of Panel.

(e) Bottom of Panel.

Figure B-20. 12' Long, 3-Ply Grade V4 CLT Panel w/ 10%F_c^* Axial Load (Test V4-10-B).

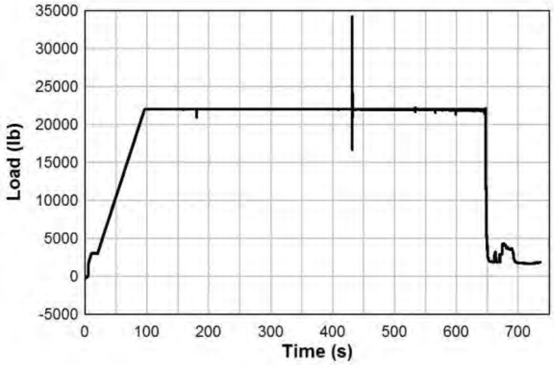

(a) Axial Load vs. Time.

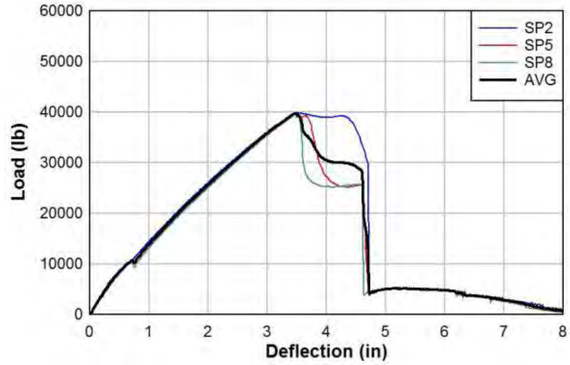

(b) Out-of-Plane Load vs. Displacement.

(c) Elevation.

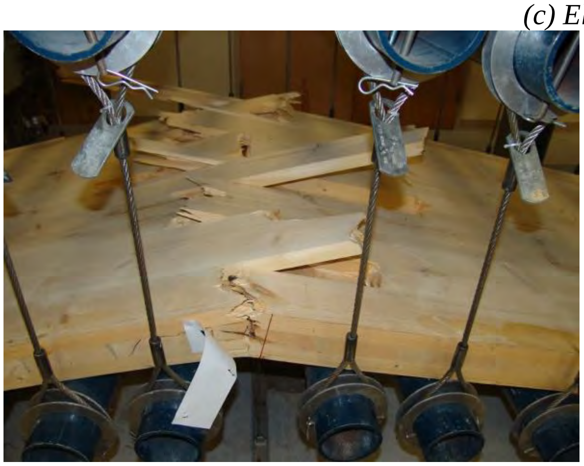

(d) Top of Panel.

(e) Bottom of Panel.

Figure B-21. 12' Long, 3-Ply Grade V4 CLT Panel w/ 10%F_c^* Axial Load (Test V4-10-C).

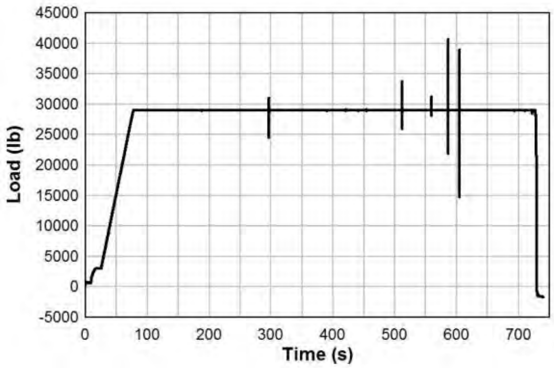

(a) Axial Load vs. Time.

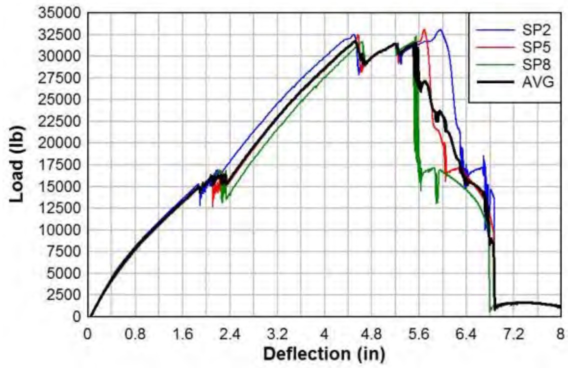

(b) Out-of-Plane Load vs. Displacement.

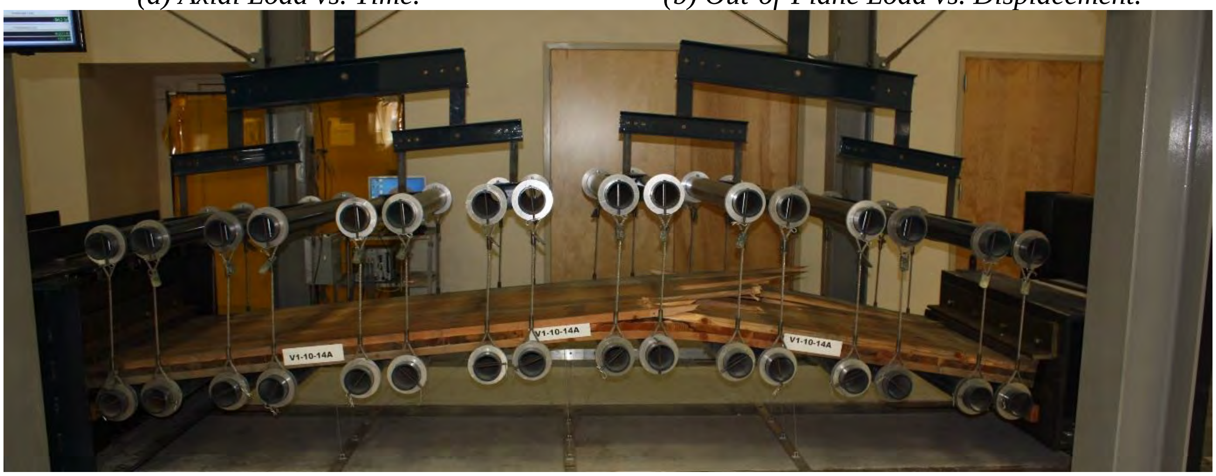

(c) Elevation.

(d) Top of Panel.

(e) Close-In.

Figure B-22. 14' Long, 3-Ply Grade V1 CLT Panel w/ 10%F_c^* Axial Load (Test V1-10-14A).

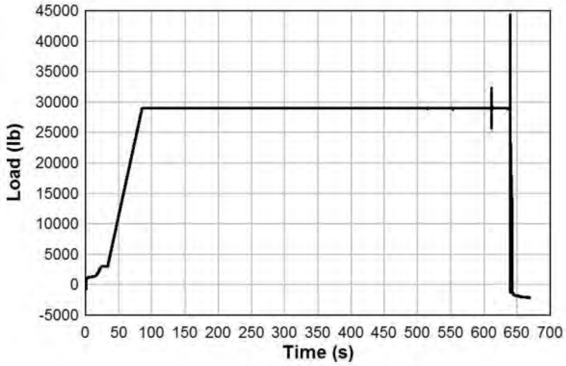

(a) Axial Load vs. Time.

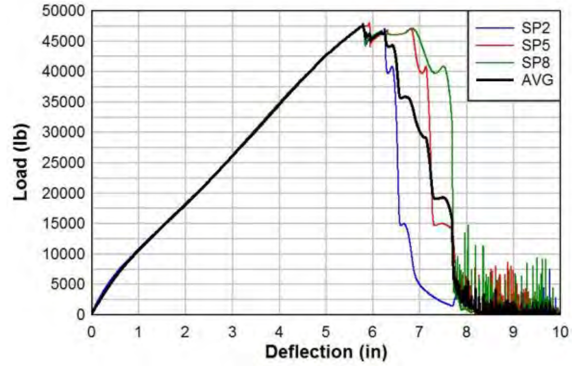

(b) Out-of-Plane Load vs. Displacement.

(c) Elevation.

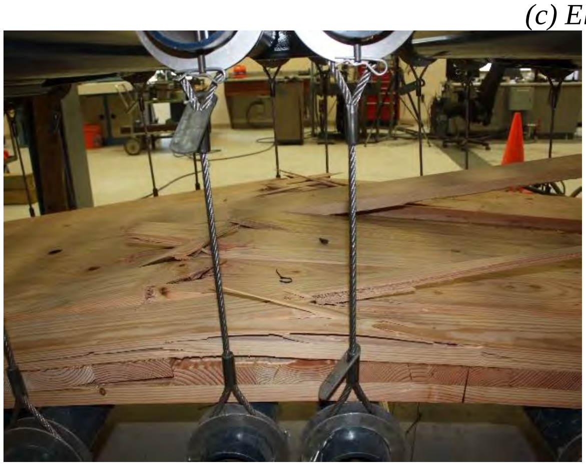

(d) Top of Panel.

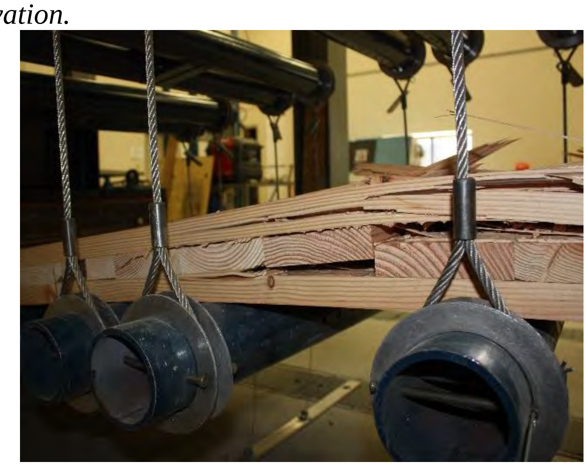

(e) Side of Panel.

Figure B-23. 14' Long, 3-Ply Grade V1 CLT Panel w/ 10%F_c^* Axial Load (Test V1-10-14B).

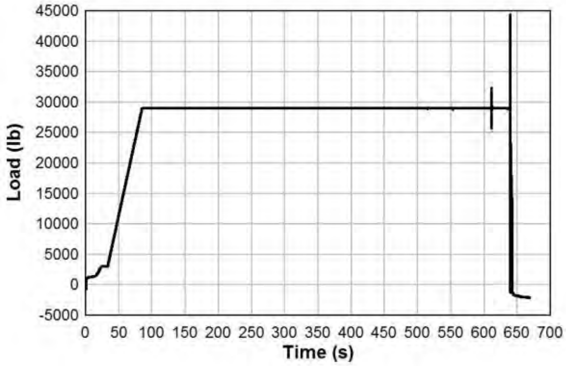

(a) Axial Load vs. Time.

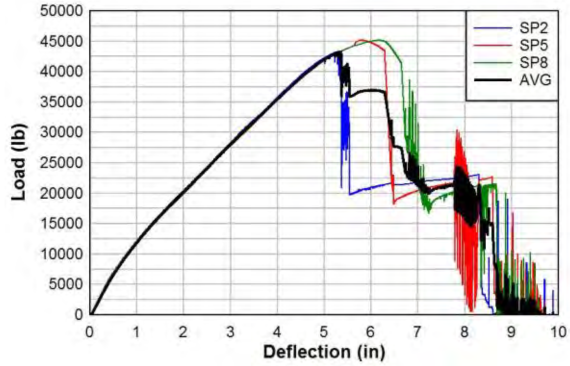

(b) Out-of-Plane Load vs. Displacement.

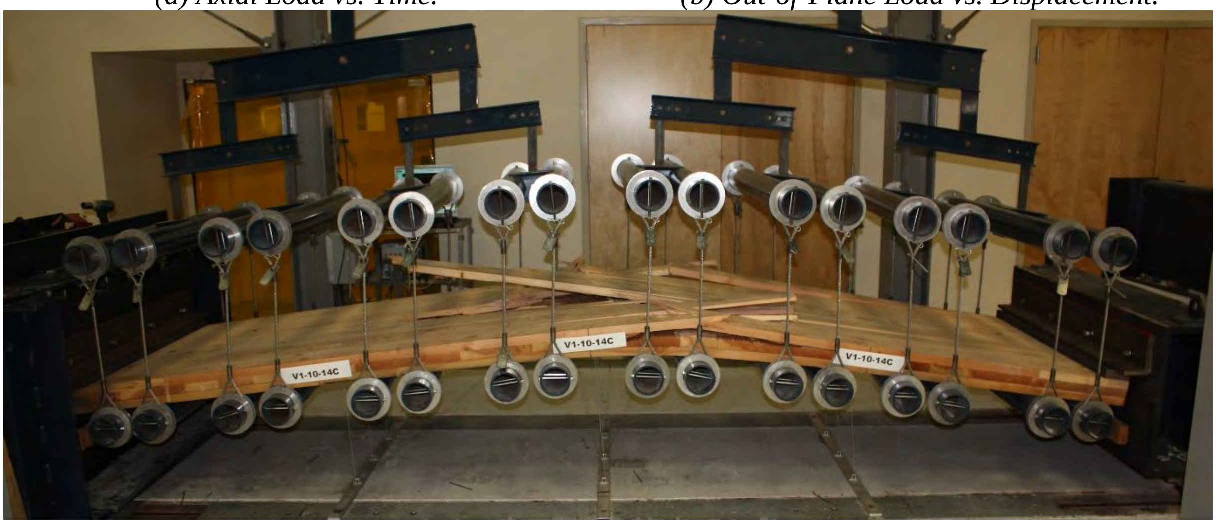

(c) Elevation.

(d) Top of Panel.

(e) Bottom of Panel.

Figure B-24. 14' Long, 3-Ply Grade V1 CLT Panel w/ 10%F_c^* Axial Load (Test V1-10-14C).

APPENDIX C

CONSTRUCTION DRAWINGS FOR ARENA BLAST TESTS 4 & 5

GENERAL NOTES

GENERAL

1. THE CONTRACTOR SHALL VERIFY ALL EXISTING CONDITIONS AND DIMENSIONS AT THE SITE BEFORE STARTING WORK.
2. TYPICAL DETAILS AND GENERAL NOTES ARE APPLICABLE UNLESS OTHERWISE DETAILED OR NOTED ON THE DRAWINGS.
3. EXISTING CONDITIONS AS SHOWN ON THE DRAWINGS ARE FOR REFERENCE ONLY. CONTRACTOR IS REQUIRED TO VERIFY ALL EXISTING CONDITIONS AND DIMENSION DURING FIELD SURVEYS.
4. THE CONTRACTOR IS RESPONSIBLE FOR ALL TEMPORARY SHORING AND BRACING.
5. PROVIDE NON-SHRINK GROUT IN ACCORDANCE WITH ASTM C1107.

STRUCTURAL STEEL:

1. STRUCTURAL STEEL SHALL CONFORM TO ASTM A36.
2. MATERIALS AND WORKMANSHIP SHALL CONFORM TO THE SPECIFICATIONS OF THE AMERICAN INSTITUTE OF STEEL CONSTRUCTION.
3. USE HILTI HY-200R ADHESIVE BY HILTI WITH ASTM A36 THREADED ROD WHERE "POST-INSTALLED ADHESIVE ANCHOR" IS INDICATED ON THE DRAWINGS. INSTALL IN ACCORDANCE WITH MANUFACTURER'S RECOMMENDATIONS. NUTS SHALL BE IN ACCORDANCE WITH ASTM A563, GRADE A, HEAVY HEX, AND WASHERS SHALL BE IN ACCORDANCE WITH ASTM F436.

WOOD FRAMING:

1. CLT STRUCTURE SPECIMENS SHALL BE CONSTRUCTED WITH THE ANSI/APA PRG 320-2012 GRADE INDICATED BELOW:
   - A. #1: GRADE VI BY DR JOHNSON.
   - B. #2: GRADE E1 BY NORDIC.
   - C. #3: GRADE V4 BY SMARTLAM.
2. FRAMING LUMBER SHALL BE SPRUCE-PINE-FIR, GRADE MARKED No. 2 OR BETTER UNLESS NOTED OTHERWISE.
3. PLYWOOD SHALL BE GRADE MARKED STRUCTURAL I. ORIENTED STRAND BOARD (OSB) MAY BE SUBSTITUTED FOR PLYWOOD. OSB SHALL HAVE THE SAME PANEL SPAN RATING AND SHALL BE OF THE SAME THICKNESS AS THE SPECIFIED PLYWOOD. ALL PLYWOOD/OSB SHALL BE BONDED WITH EXTERIOR GLUE.
4. UNLESS NOTED OTHERWISE, USE ASSY SK SCREWS BY MYTICON FOR STEEL-TO-WOOD CONNECTIONS AND ASSY ECO FOR WOOD-TO-WOOD CONNECTIONS WITH THE DIAMETER & LENGTH AS INDICATED.
5. SCREWS & NAILS SHALL BE INSTALLED AT LEAST ONE INCH FROM CENTER OF SCREW OR NAIL TO CRACKS, CHECKS, OR GAPS IN OUTER PLY OF CLT. INSTALLER SHALL CONSULT WITH DESIGNER WHERE THIS IS NOT POSSIBLE.

K&C
Karagozian & Case
700 North Brand Blvd., Suite 700
Glendale, CA 91203-3215
Tel: 818-240-1919 Fax: 818-240-4966
www.kcse.com

Mark	Date	Appr.	Description
1	09-01-2017	MW	MISC REVISIONS
0	08-10-2017	MW	FINAL TEST ARTICLE

Revisions

PROJECT

BLAST TESTING OF LOADED MASS TIMBER STRUCTURES

SHEET TITLE

GENERAL NOTES

DRAWN	CHECKED	APPROVED	DATE ISSUED
CJ	MW	LT	08/10/2017

JOB NO. 2396_2017

FILE NAME: S001_2396.DWG

SHEET NUMBER

S-0.1

1

September 1, 2017

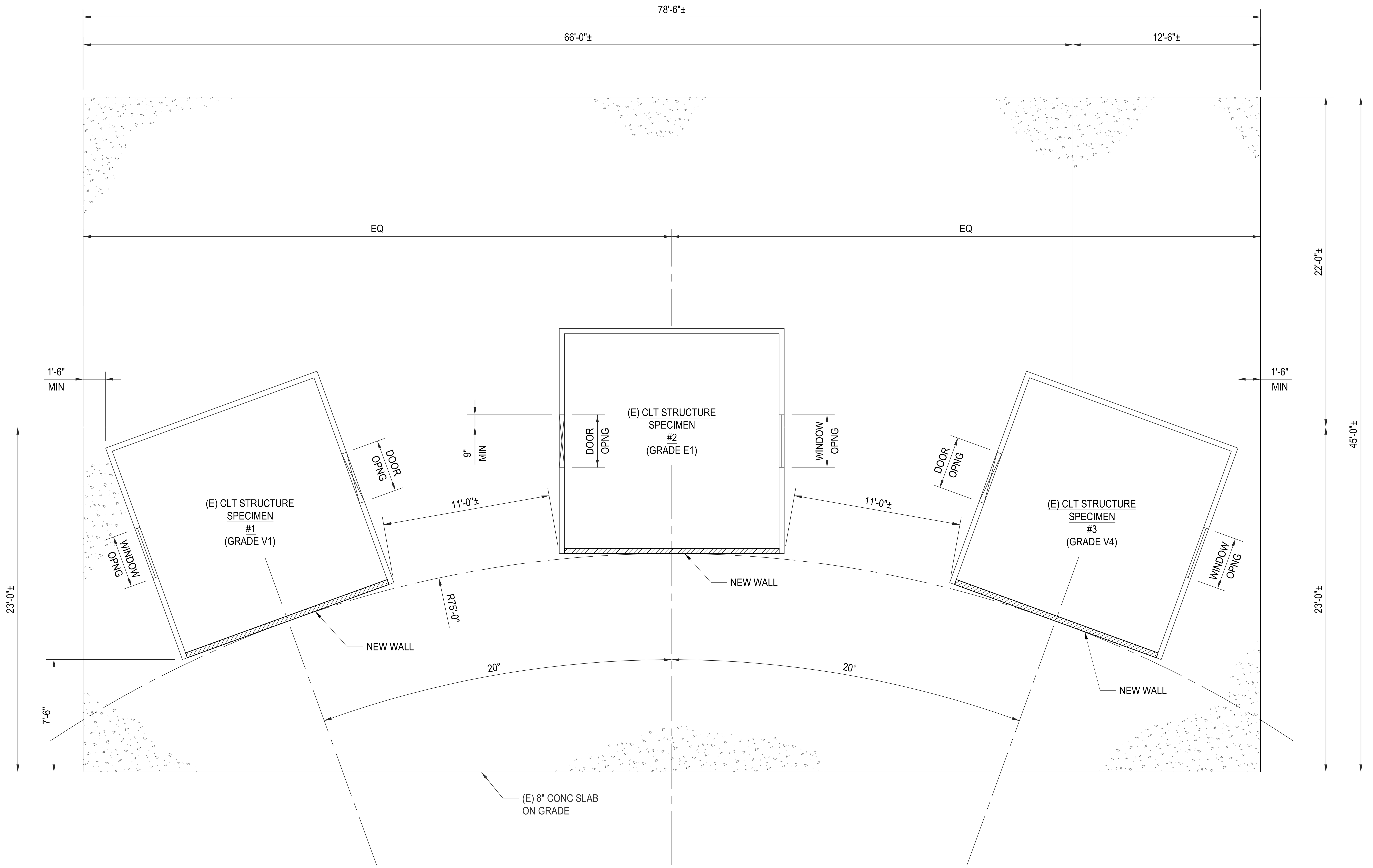

A S-0.2 **SITE PLAN**

SCALE: 1/4"=1'-0"

4' 0 3' 6' 9' 12'

1/4" = 1'-0"

K&C
Karagozian & Case

700 North Brand Blvd., Suite 700
Glendale, CA 91203-3215
Tel: 818-240-1919 Fax: 818-240-4966

www.kcse.com

Mark	Date	Appr.	Description
1	09-01-2017	MW	MISC REVISIONS
0	08-10-2017	MW	FINAL TEST ARTICLE

Revisions

PROJECT

BLAST TESTING OF LOADED MASS TIMBER STRUCTURES

SHEET TITLE

SITE PLAN

DRAWN	CHECKED	APPROVED	DATE ISSUED
CJ	MW	LT	08/10/2017

JOB NO. 2396_2017

FILE NAME: S002_2396.DWG

SHEET NUMBER

S-0.2

1

September 1, 2017

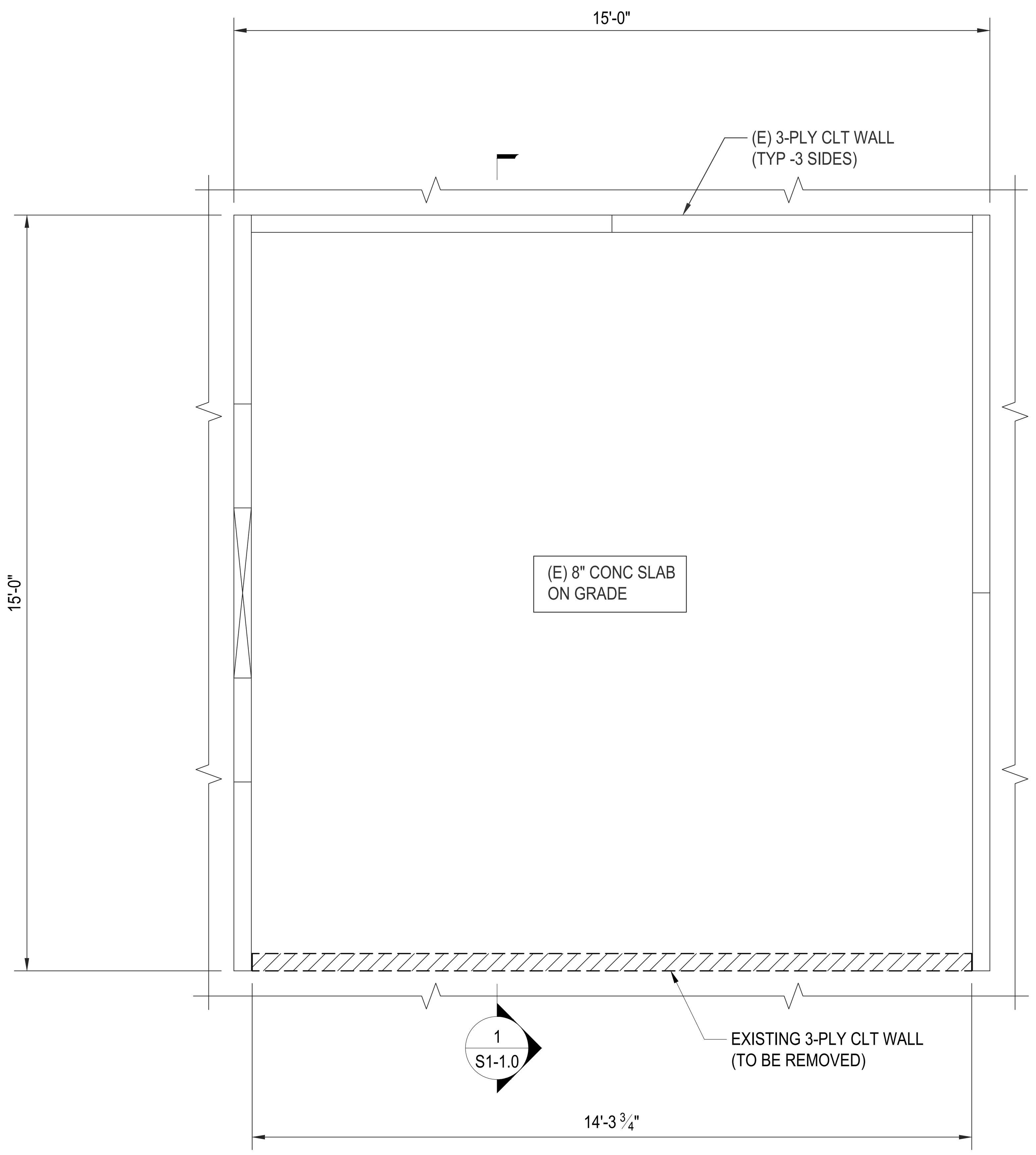

A DEMOLITION PLAN
S1-1.0 SCALE: 1/2"=1'-0"

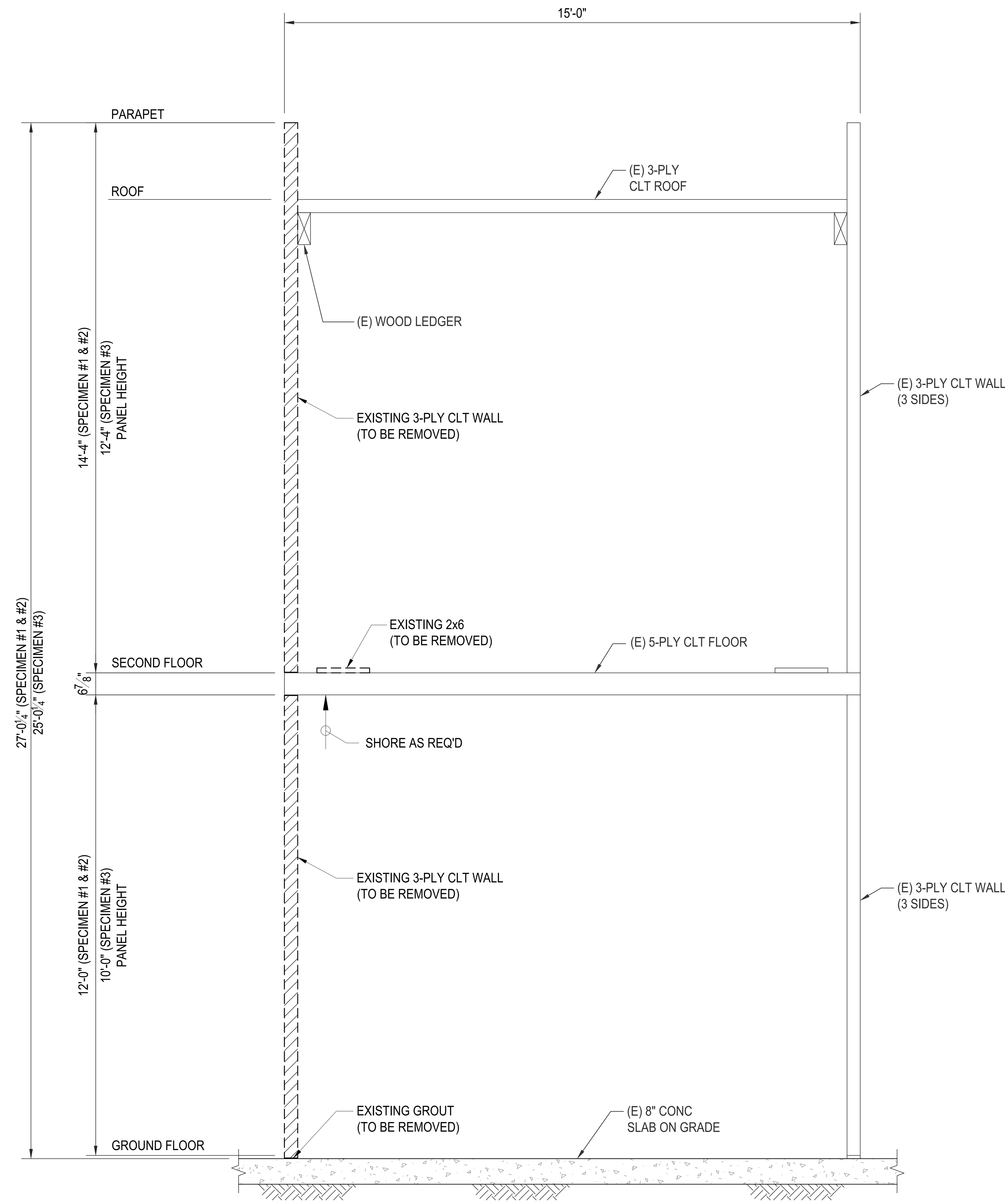

1 DEMOLITION SECTION
S1-1.0 SCALE: 1/2"=1'-0"

2' 0 2' 4' 8'
1/2" = 1'-0"

K&C
Karagozian & Case

700 North Brand Blvd., Suite 700
Glendale, CA 91203-3215
Tel: 818-240-1919 Fax: 818-240-4966
www.kcse.com

Mark	Date	Appr.	Description
1	09-01-2017	MW	MISC REVISIONS
0	08-10-2017	MW	FINAL TEST ARTICLE

Revisions

PROJECT

BLAST TESTING OF LOADED MASS TIMBER STRUCTURES

SHEET TITLE

TESTS 4 & 5
DEMOLITION PLAN
& SECTION

DRAWN	CHECKED	APPROVED	DATE ISSUED
CJ	MW	LT	08/10/2017

JOB NO.	FILE NAME:
2396_2017	S1_100_2396.DWG

SHEET NUMBER
S1-1.0
1

September 1, 2017

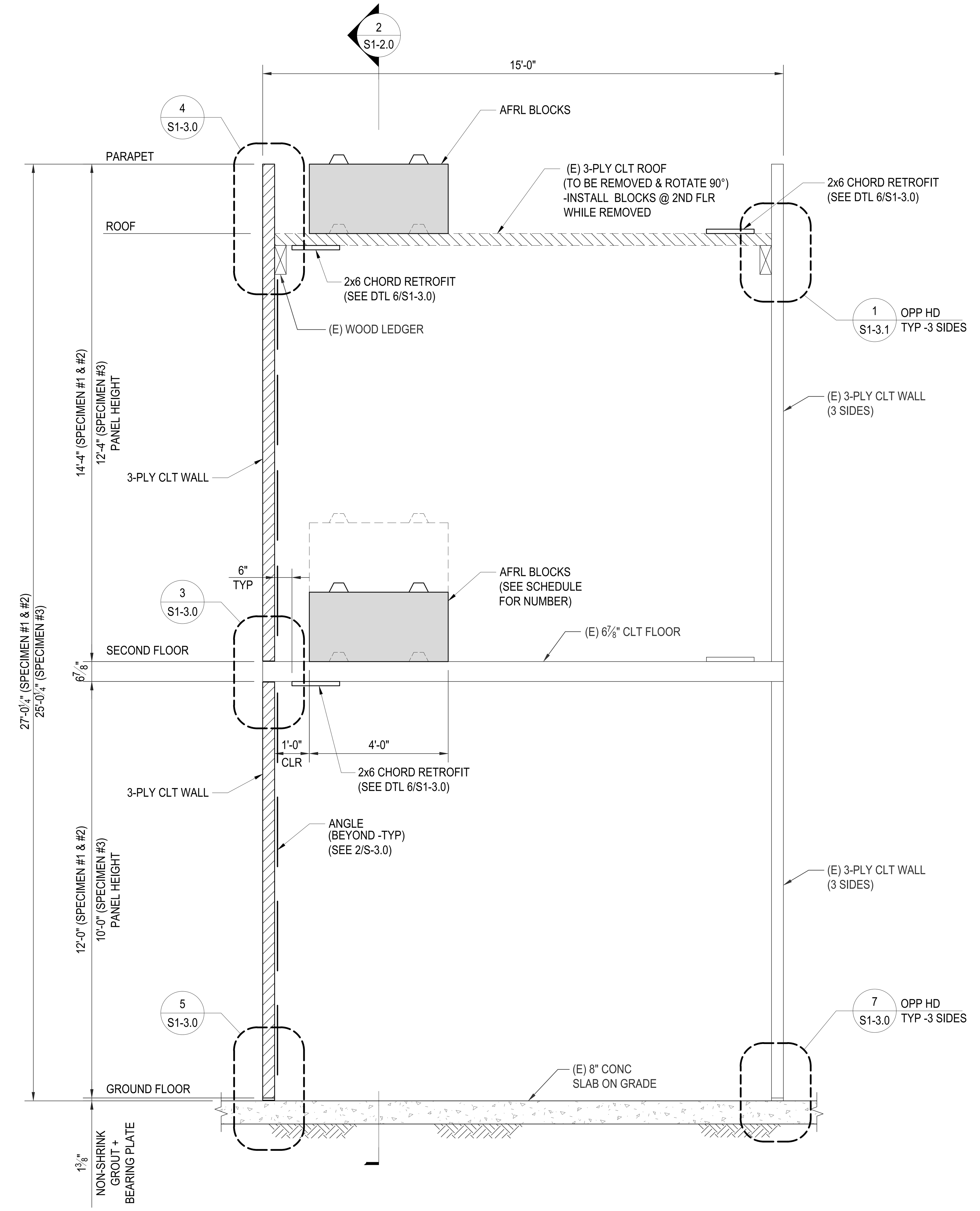

1
S1-2.0
SECTION
SCALE: 1/2"=1'-0"

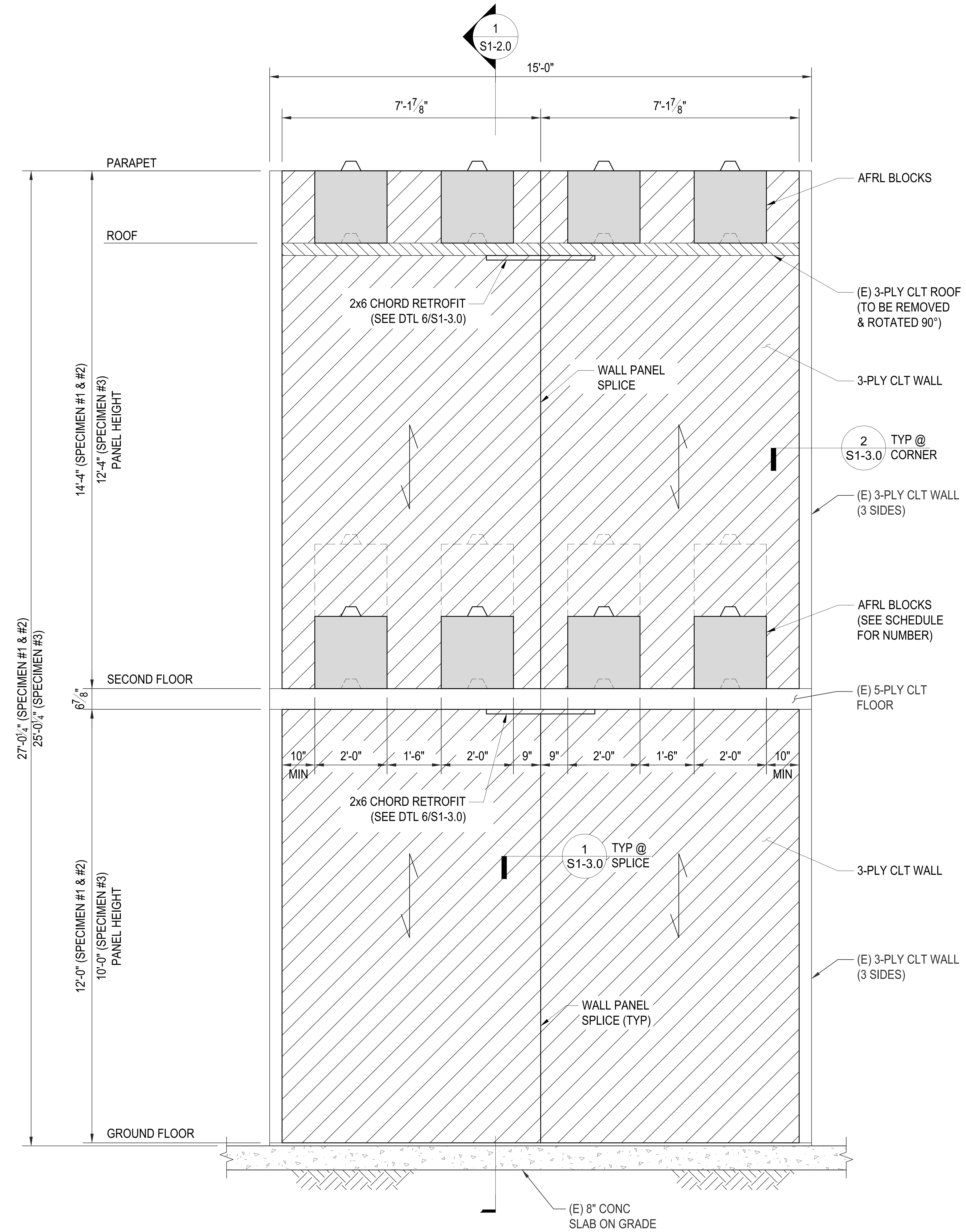

2
S1-2.0
SECTION
SCALE: 1/2"=1'-0"

NOTE: FOR 12 BLOCKS
ORIENT AS FOLLOWS

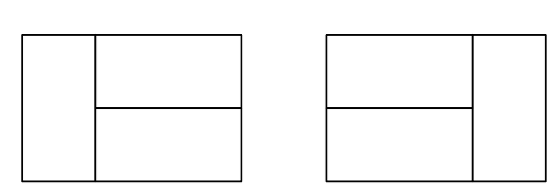

1st LAYER   2nd LAYER

CENTER BLOCK GROUPING
ON PANEL BELOW

LOADING BLOCK SCHEDULE		
SPECIMEN	No. OF BLOCKS	
	ROOF	FLOOR
#1	4	12
#2	4	8
#3	4	4

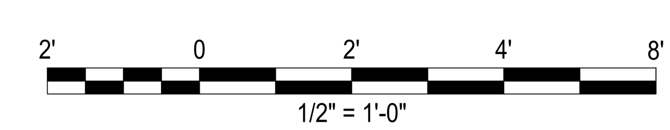

Karagozian & Case
700 North Brand Blvd., Suite 700
Glendale, CA 91203-3215
Tel: 818-240-1919 Fax: 818-240-4966
www.kcse.com

Mark	Date	Appr.	Description
1	09-01-2017	MW	MISC REVISIONS
0	08-10-2017	MW	FINAL TEST ARTICLE

Revisions

PROJECT

BLAST TESTING OF LOADED MASS TIMBER STRUCTURES

SHEET TITLE

TESTS 4 & 5
SECTIONS

DRAWN	CHECKED	APPROVED	DATE ISSUED
CJ	MW	LT	08/10/2017

JOB NO.: 2396_2017
FILE NAME: S1_200_2396.DWG

SHEET NUMBER

S1-2.0

September 1, 2017

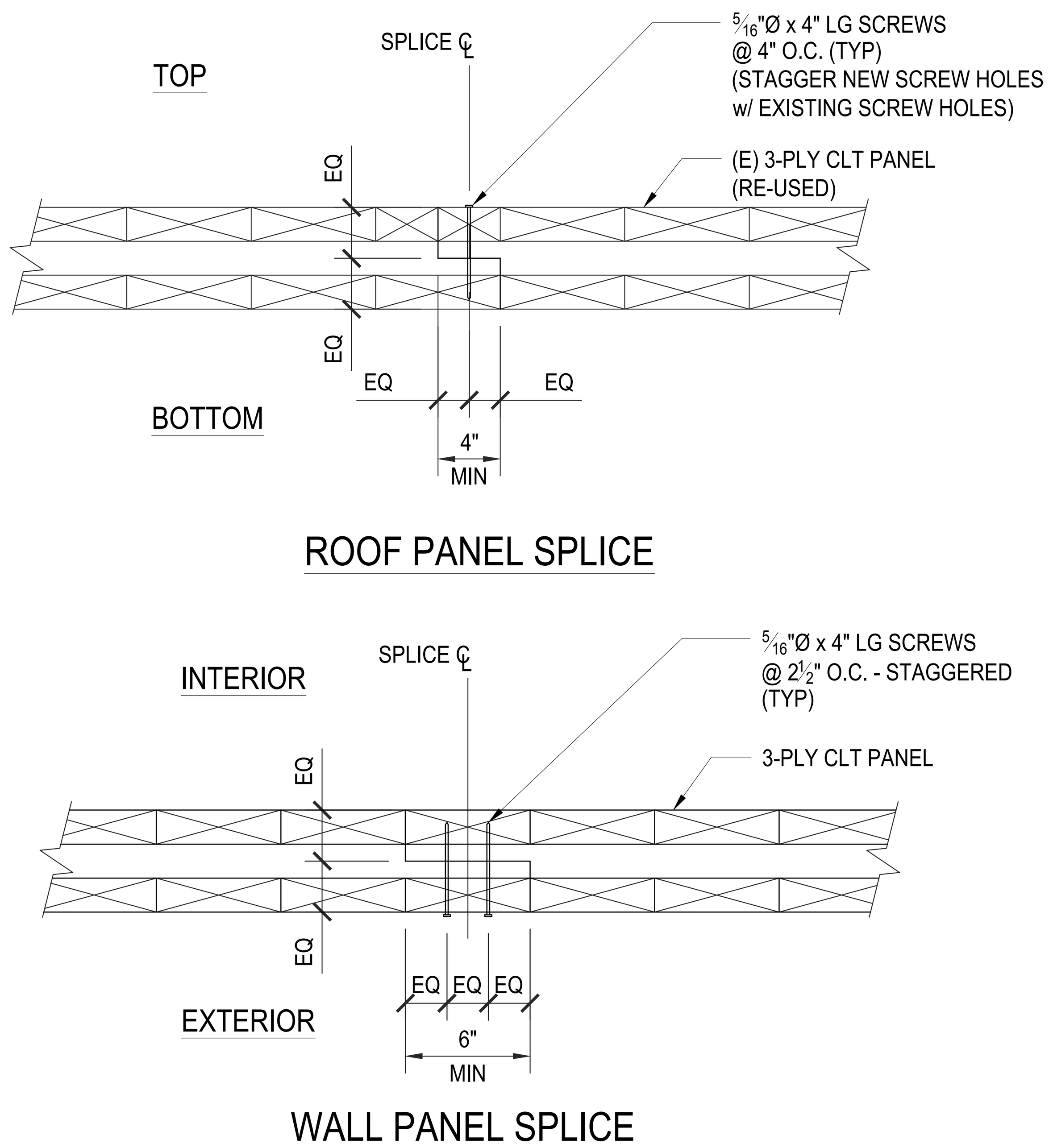

1 PANEL SPLICE DETAIL
S1-3.0 SCALE: 2"=1'-0"

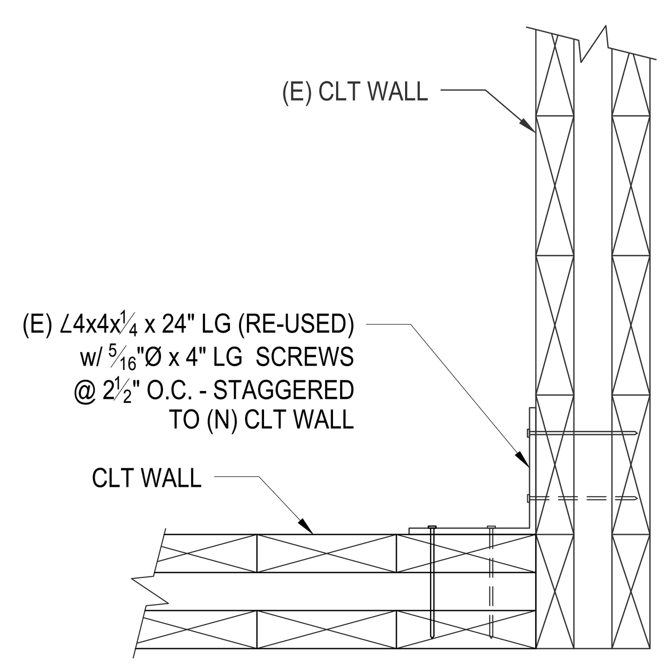

2 PLAN DETAIL (TYP @ WALL CORNER)
S1-3.0 SCALE: 2"=1'-0"

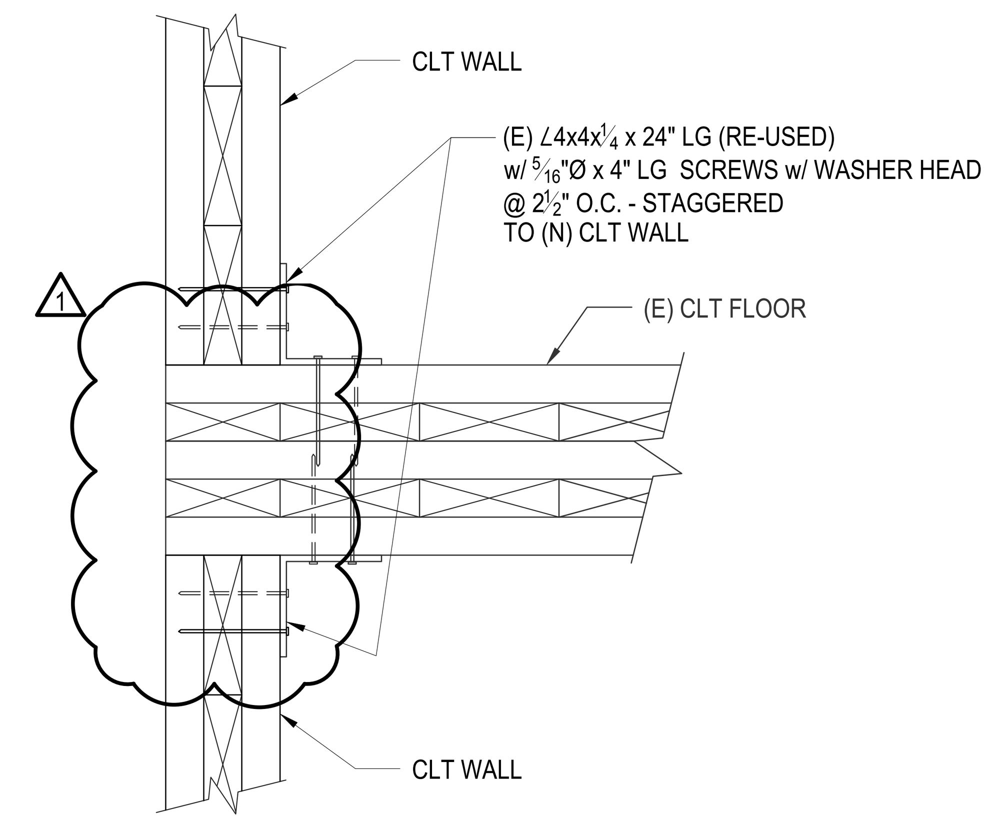

3 SECTION (TYP @ 2ND FLOOR)
S1-3.0 SCALE: 2"=1'-0"

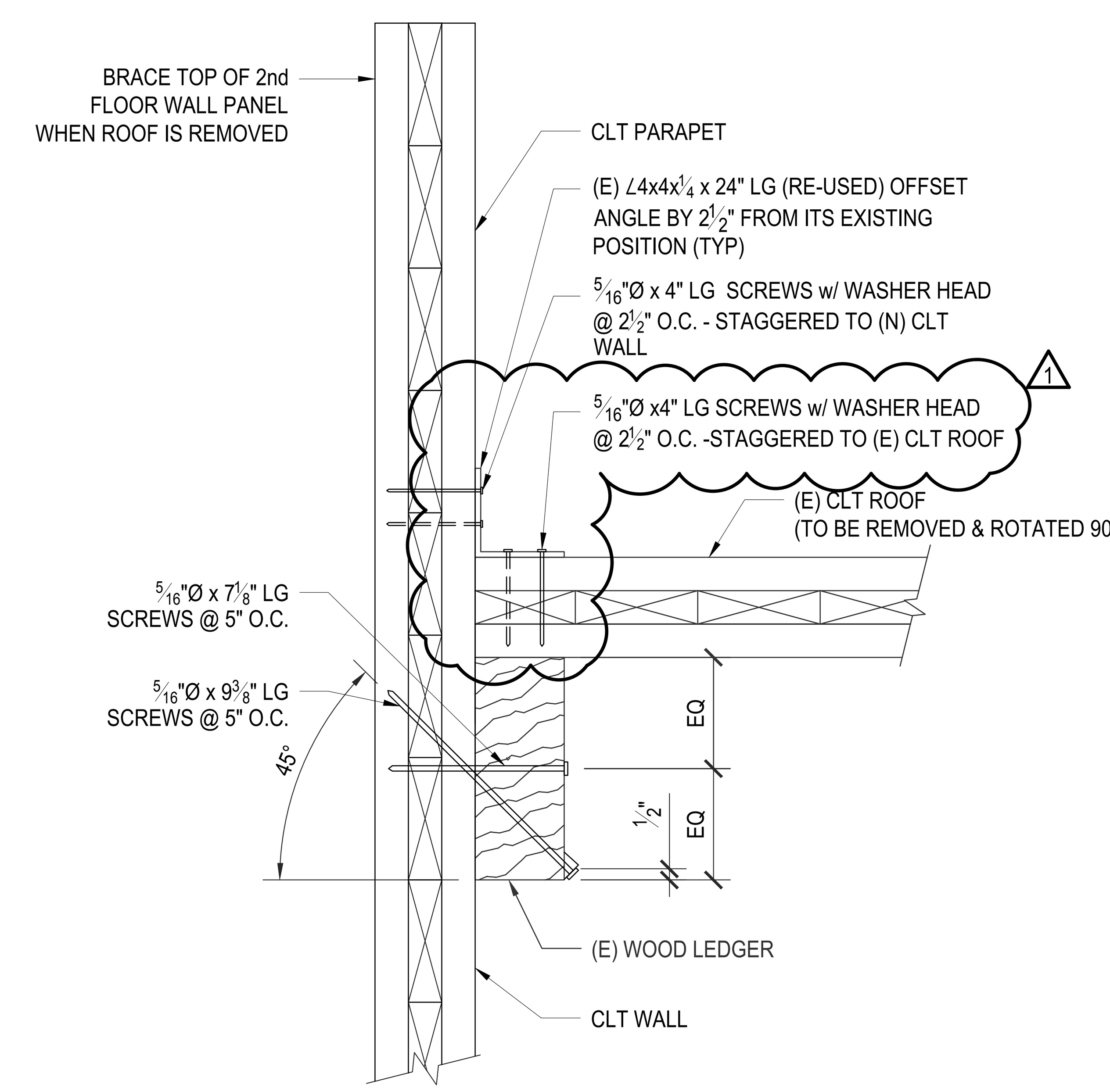

4 SECTION (TYP @ ROOF)
S1-3.0 SCALE: 2"=1'-0"

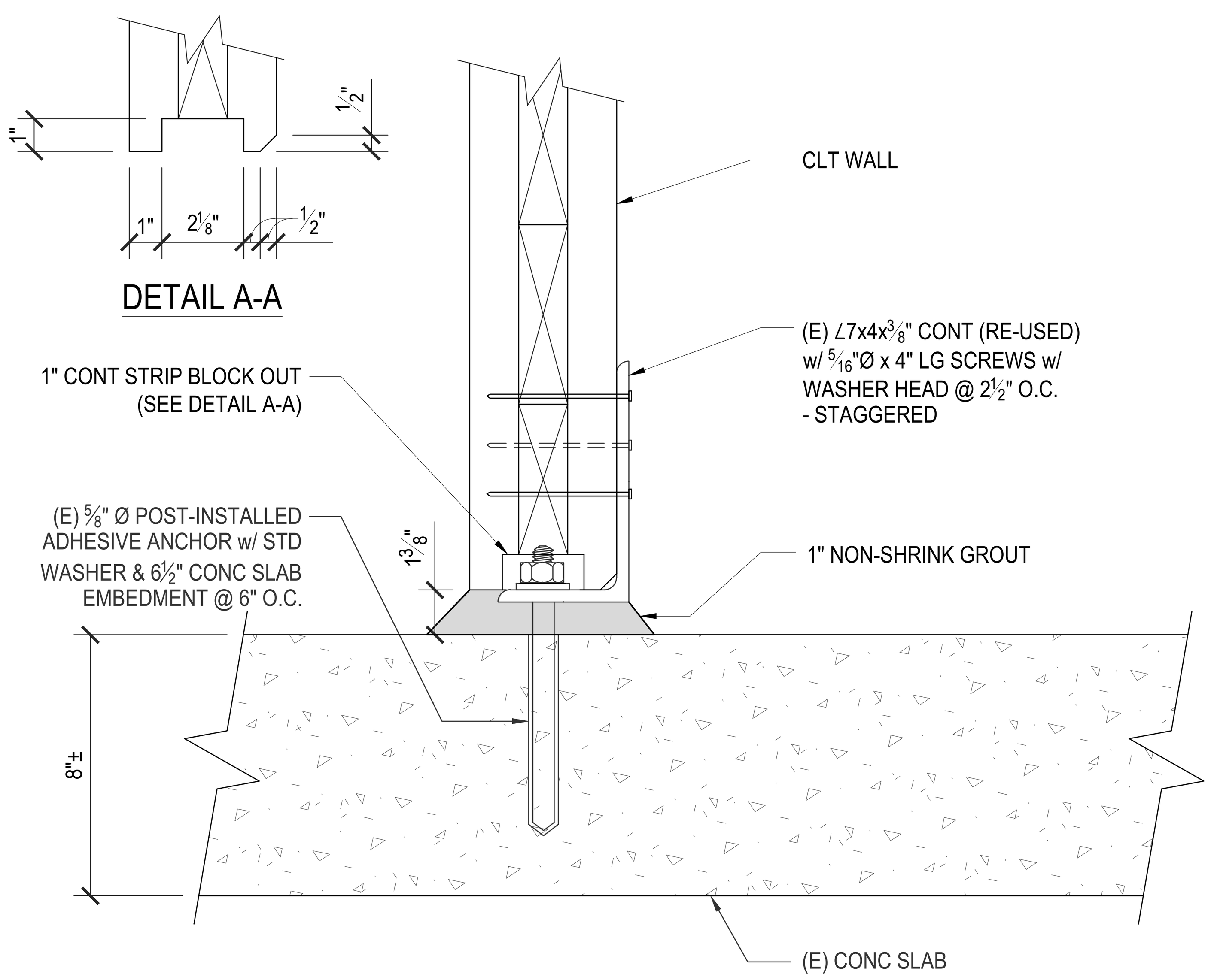

5 SECTION (TYP @ FLOOR)
S1-3.0 SCALE: 3"=1'-0"

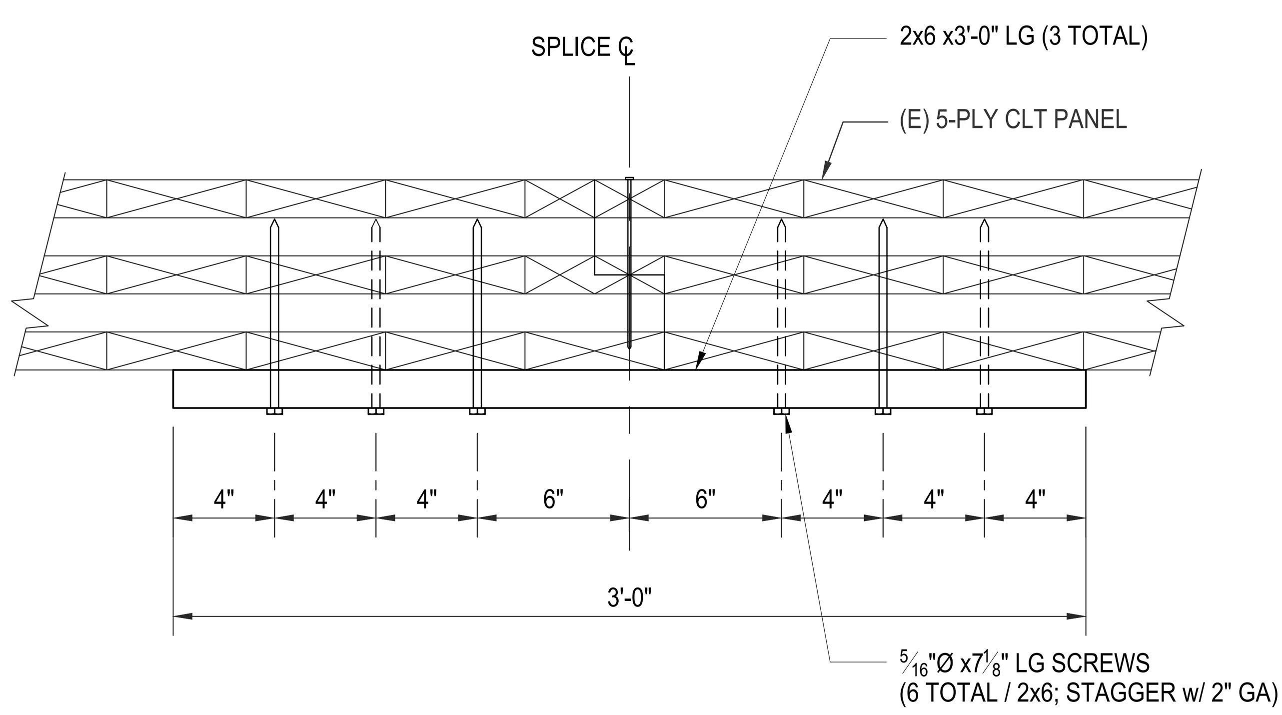

6 SECTION @ CHORD RETROFIT
S1-3.0 SCALE: 2"=1'-0"

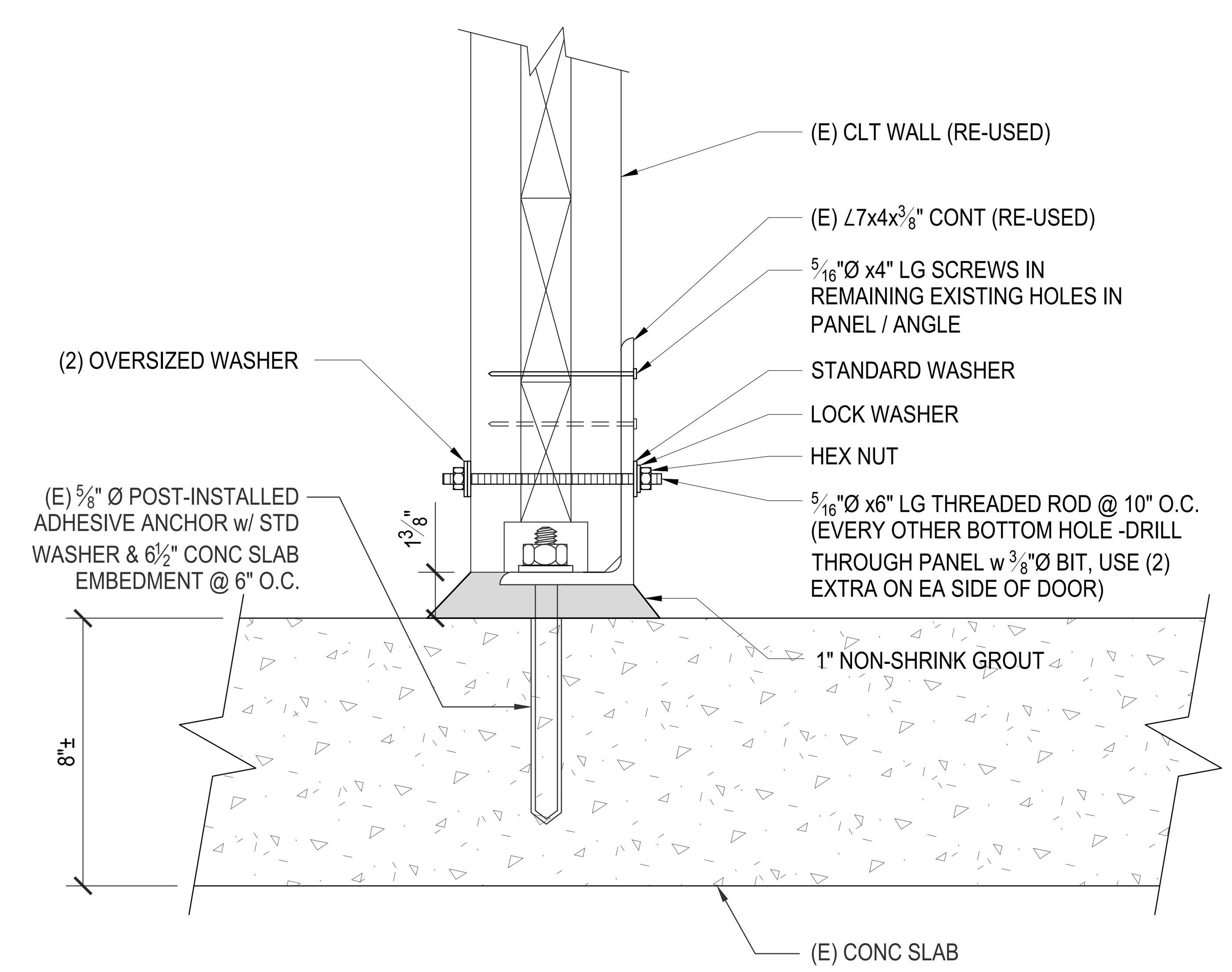

7 SECTION (TYP @ FLOOR)
S1-3.0 SCALE: 3"=1'-0"

NOTE:

1. IT IS PERMISSIBLE TO RE-USE FASTENERS THAT ARE REMOVED PROVIDED THE FASTENER SHOWS NO SIGNS OF DAMAGE OR DEFORMATION FROM ITS ORIGINAL STATE.

6" 0 6" 1' 1'-6"
2" = 1'-0"

3" 0 3" 6" 1'-0"
3" = 1'-0"

K&C
Karagozian & Case
700 North Brand Blvd., Suite 700
Glendale, CA 91203-3215
Tel: 818-240-1919 Fax: 818-240-4966
www.kcse.com

Mark	Date	Appr.	Description
1	09-01-2017	MW	MISC REVISIONS
0	08-10-2017	MW	FINAL TEST ARTICLE

Revisions

PROJECT

BLAST TESTING OF LOADED MASS TIMBER STRUCTURES

SHEET TITLE

TESTS 4 & 5 DETAILS

DRAWN	CHECKED	APPROVED	DATE ISSUED
CJ	MW	LT	08/10/2017

JOB NO.	FILE NAME:
2396_2017	S1_300_2396.DWG

SHEET NUMBER

S1-3.0

1

September 1, 2017

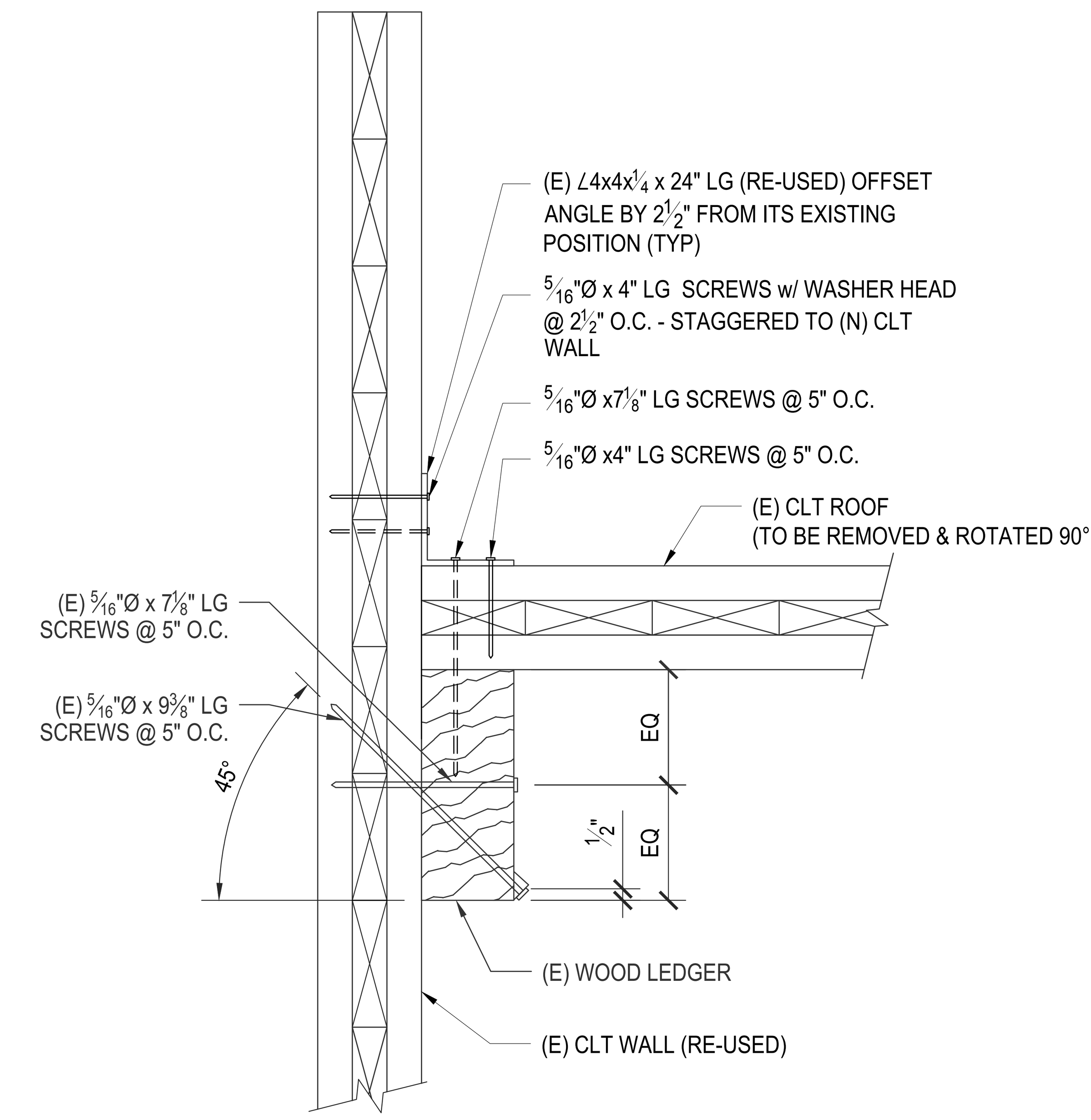

1
S1-3.1

SECTION (TYP @ ROOF)

SCALE: 2"=1'-0"

NOTE:

1. IT IS PERMISSIBLE TO RE-USE FASTENERS THAT ARE REMOVED PROVIDED THE FASTENER SHOWS NO SIGNS OF DAMAGE OR DEFORMATION FROM ITS ORIGINAL STATE.

6" 0 6" 1' 1'-6"

2" = 1'-0"

K&C
Karagozian & Case

700 North Brand Blvd., Suite 700
Glendale, CA 91203-3215
Tel: 818-240-1919 Fax: 818-240-4966
—
www.kcse.com

Mark	Date	Appr.	Description
1	09-01-2017	MW	MISC REVISIONS
0	08-10-2017	MW	FINAL TEST ARTICLE

Revisions

PROJECT

BLAST TESTING OF LOADED MASS TIMBER STRUCTURES

SHEET TITLE

TESTS 4 & 5
DETAILS

DRAWN	CHECKED	APPROVED	DATE ISSUED
CJ	MW	LT	08/10/2017

JOB NO. 2396_2017
FILE NAME: S1_301_2396.DWG

SHEET NUMBER
S1-3.1
1

September 1, 2017

APPENDIX D

CONSTRUCTION DRAWINGS FOR ARENA BLAST TESTS 6 & 7

GENERAL NOTES

GENERAL

1. THE CONTRACTOR SHALL VERIFY ALL EXISTING CONDITIONS AND DIMENSIONS AT THE SITE BEFORE STARTING WORK.

2. TYPICAL DETAILS AND GENERAL NOTES ARE APPLICABLE UNLESS OTHERWISE DETAILED OR NOTED ON THE DRAWINGS.

3. EXISTING CONDITIONS AS SHOWN ON THE DRAWINGS ARE FOR REFERENCE ONLY. CONTRACTOR IS REQUIRED TO VERIFY ALL EXISTING CONDITIONS AND DIMENSION DURING FIELD SURVEYS.

4. THE CONTRACTOR IS RESPONSIBLE FOR ALL TEMPORARY SHORING AND BRACING.

5. PROVIDE NON-SHRINK GROUT IN ACCORDANCE WITH ASTM C1107.

STRUCTURAL STEEL:

1. STRUCTURAL STEEL SHALL CONFORM TO ASTM A36.

2. MATERIALS AND WORKMANSHIP SHALL CONFORM TO THE SPECIFICATIONS OF THE AMERICAN INSTITUTE OF STEEL CONSTRUCTION.

3. USE HILTI HY-200R ADHESIVE BY HILTI WITH ASTM A36 THREADED ROD WHERE "POST-INSTALLED ADHESIVE ANCHOR" IS INDICATED ON THE DRAWINGS. INSTALL IN ACCORDANCE WITH MANUFACTURER'S RECOMMENDATIONS. NUTS SHALL BE IN ACCORDANCE WITH ASTM A563, GRADE A, HEAVY HEX, AND WASHERS SHALL BE IN ACCORDANCE WITH ASTM F436.

WOOD FRAMING:

1. CLT STRUCTURE SPECIMENS SHALL BE CONSTRUCTED WITH THE ANSI/APA PRG 320-2012 GRADE INDICATED BELOW:
   A. #1: GRADE VI BY DR JOHNSON.
   B. #2: GRADE E1 BY NORDIC.
   C. #3: GRADE V4 BY SMARTLAM.

2. FRAMING LUMBER SHALL BE SPRUCE-PINE-FIR, GRADE MARKED No. 2 OR BETTER UNLESS NOTED OTHERWISE.

3. PLYWOOD SHALL BE GRADE MARKED STRUCTURAL I. ORIENTED STRAND BOARD (OSB) MAY BE SUBSTITUTED FOR PLYWOOD. OSB SHALL HAVE THE SAME PANEL SPAN RATING AND SHALL BE OF THE SAME THICKNESS AS THE SPECIFIED PLYWOOD. ALL PLYWOOD/OSB SHALL BE BONDED WITH EXTERIOR GLUE.

4. UNLESS NOTED OTHERWISE, USE ASSY SK SCREWS BY MYTICON FOR STEEL-TO-WOOD CONNECTIONS AND ASSY ECO FOR WOOD-TO-WOOD CONNECTIONS WITH THE DIAMETER & LENGTH AS INDICATED.

5. SCREWS & NAILS SHALL BE INSTALLED AT LEAST ONE INCH FROM CENTER OF SCREW OR NAIL TO CRACKS, CHECKS, OR GAPS IN OUTER PLY OF CLT. INSTALLER SHALL CONSULT WITH DESIGNER WHERE THIS IS NOT POSSIBLE.

K&C
Karagozian & Case

700 North Brand Blvd., Suite 700
Glendale, CA 91203-3215
Tel: 818-240-1919 Fax: 818-240-4966
—
www.kcse.com

Mark	Date	Appr.	Description
1	09-01-2017	MW	MISC REVISIONS
0	08-10-2017	MW	FINAL TEST ARTICLE

Revisions

PROJECT

BLAST TESTING OF LOADED MASS TIMBER STRUCTURES

SHEET TITLE

GENERAL NOTES

DRAWN	CHECKED	APPROVED	DATE ISSUED
CJ	MW	LT	08/10/2017

JOB NO.: 2396_2017

FILE NAME: S001_2396.DWG

SHEET NUMBER

S-0.1 1

September 1, 2017

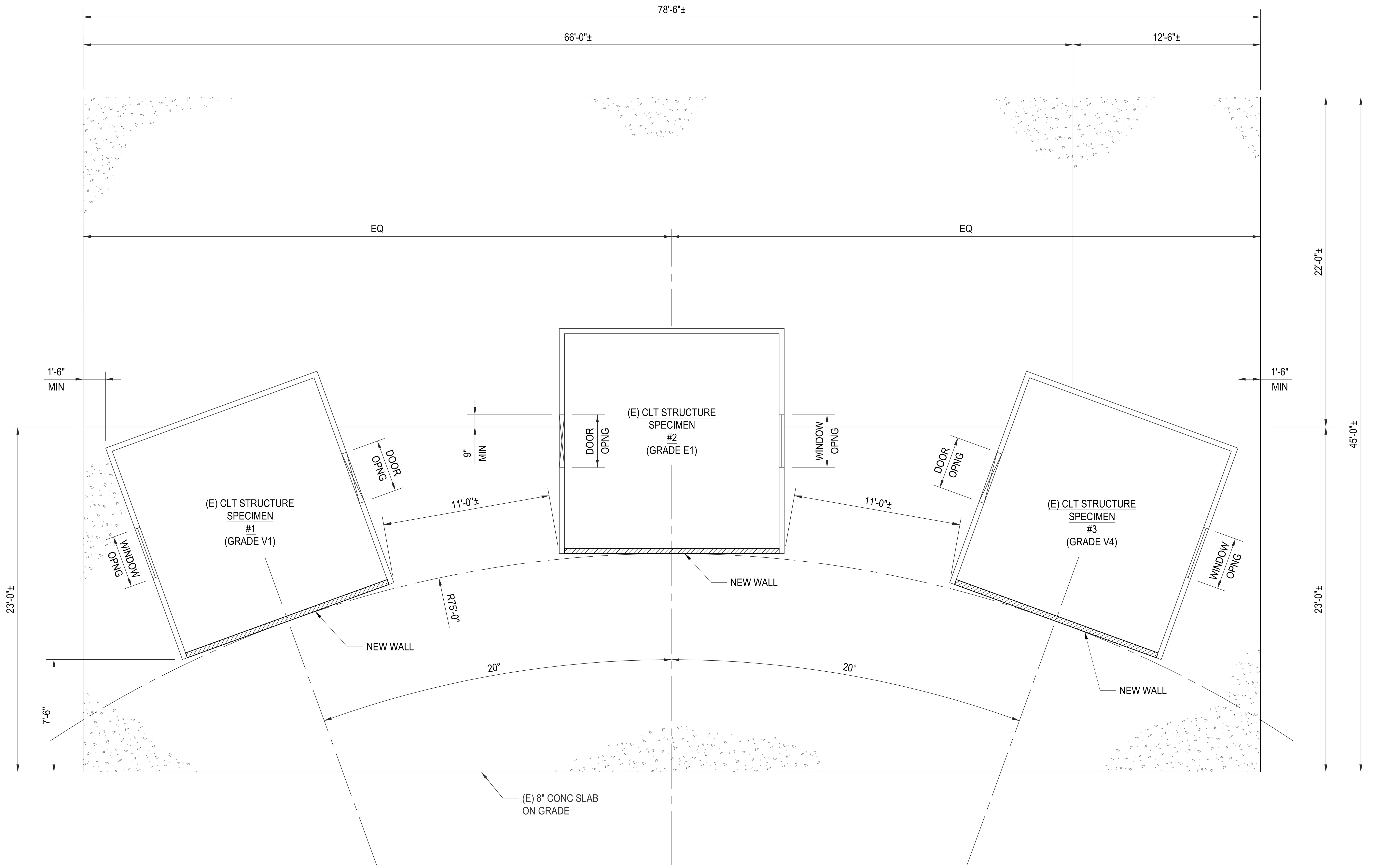

A / S-0.2 **SITE PLAN**

SCALE: 1/4"=1'-0"

4' 0 3' 6' 9' 12'

1/4" = 1'-0"

Karagozian & Case

700 North Brand Blvd., Suite 700
Glendale, CA 91203-3215
Tel: 818-240-1919 Fax: 818-240-4966

www.kcse.com

Mark	Date	Appr.	Description
1	09-01-2017	MW	MISC REVISIONS
0	08-10-2017	MW	FINAL TEST ARTICLE

Revisions

PROJECT

BLAST TESTING OF LOADED MASS TIMBER STRUCTURES

SHEET TITLE

SITE PLAN

DRAWN	CHECKED	APPROVED	DATE ISSUED
CJ	MW	LT	08/10/2017

JOB NO. 2396_2017

FILE NAME: S002_2396.DWG

SHEET NUMBER

S-0.2 1

September 1, 2017

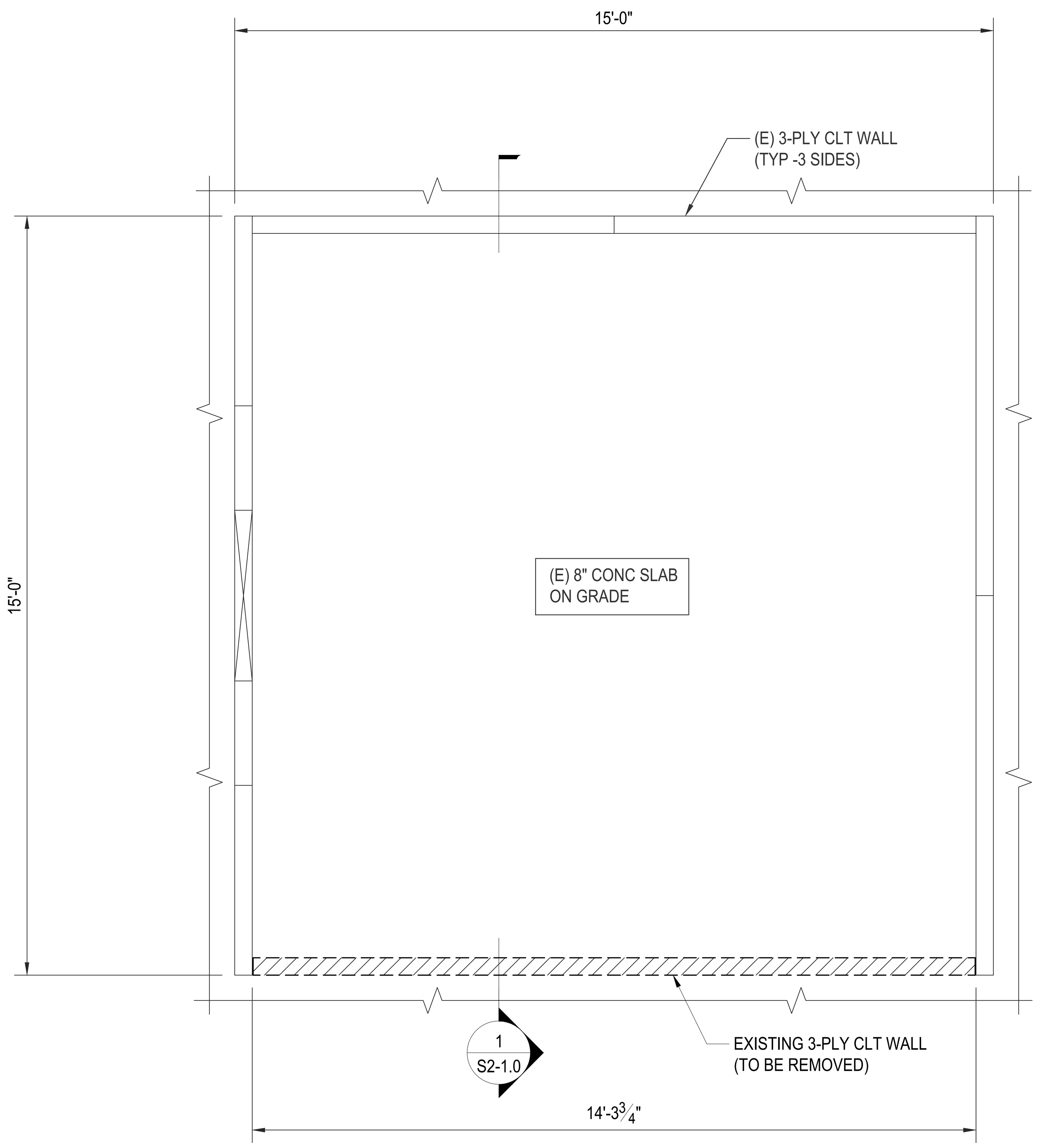

A DEMOLITION PLAN
S2-1.0 SCALE: 1/2"=1'-0"

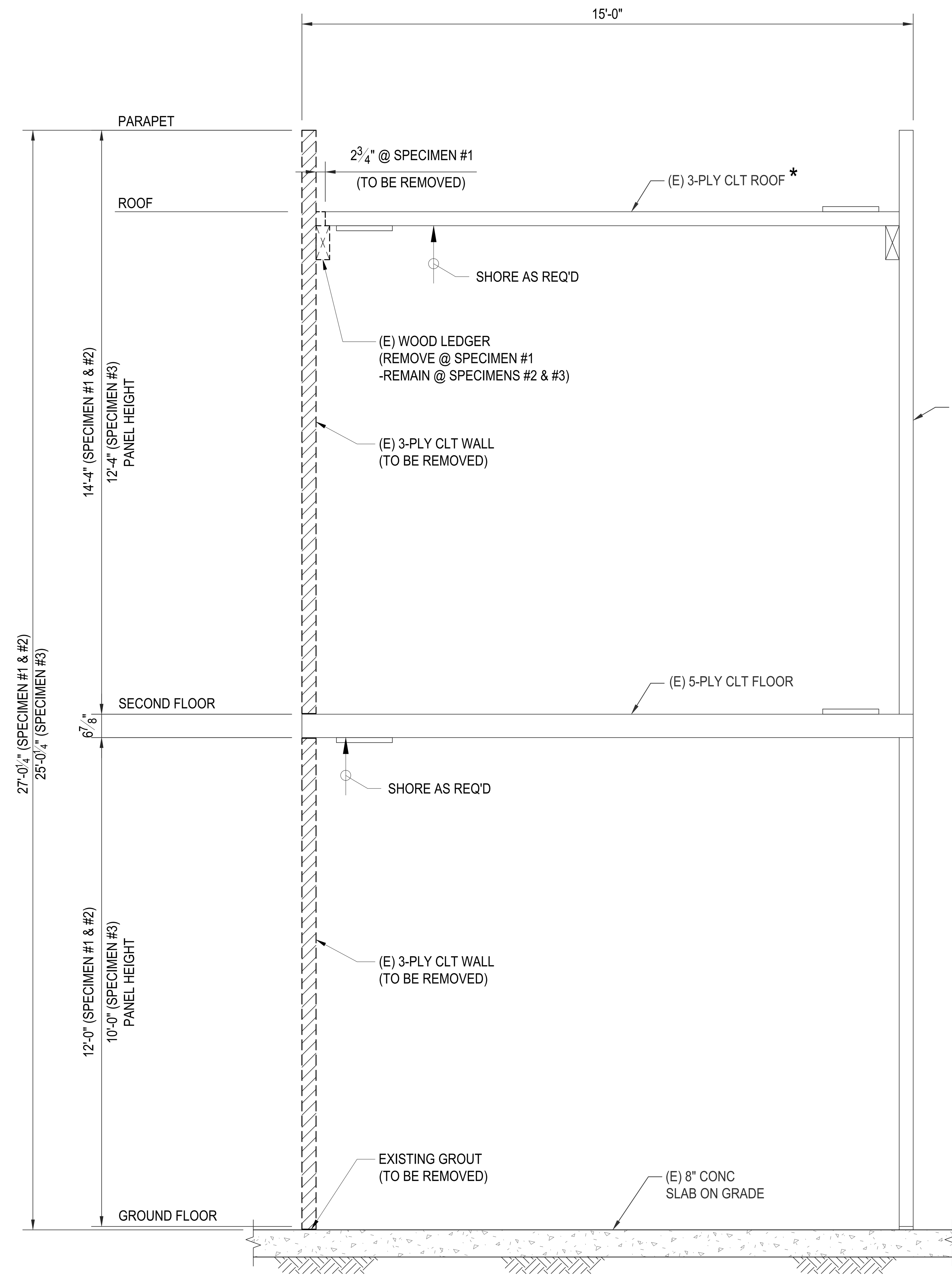

* NOTE: (E) ROOF PANELS WILL NEED TO BE REMOVED TO REMOVE AFRL BLOCKS FROM 2nd FLOOR;
REPLACE ROOF PANELS PER DETAILS 1/S1-3.0, 6/S1-3.0 & 1/S1-3.1;
ENSURE MIN DISTANCE OF 1" FROM EXISTING HOLE FOR NEW SCREW PENETRATIONS

1 DEMOLITION SECTION
S2-1.0 SCALE: 1/2"=1'-0"

2' 0 2' 4' 8'
1/2" = 1'-0"

K&C
Karagozian & Case
700 North Brand Blvd., Suite 700
Glendale, CA 91203-3215
Tel: 818-240-1919 Fax: 818-240-4966
www.kcse.com

Mark	Date	Appr.	Description
1	09-01-2017	MW	MISC REVISIONS
0	08-10-2017	MW	FINAL TEST ARTICLE

Revisions

PROJECT

BLAST TESTING OF LOADED MASS TIMBER STRUCTURES

SHEET TITLE

TESTS 6 & 7
DEMOLITION PLAN
& SECTION

DRAWN	CHECKED	APPROVED	DATE ISSUED
CJ	MW	LT	08/10/2017

JOB NO. 2396_2017 FILE NAME: S2_100_2396.DWG

SHEET NUMBER
S2-1.0

1

September 1, 2017

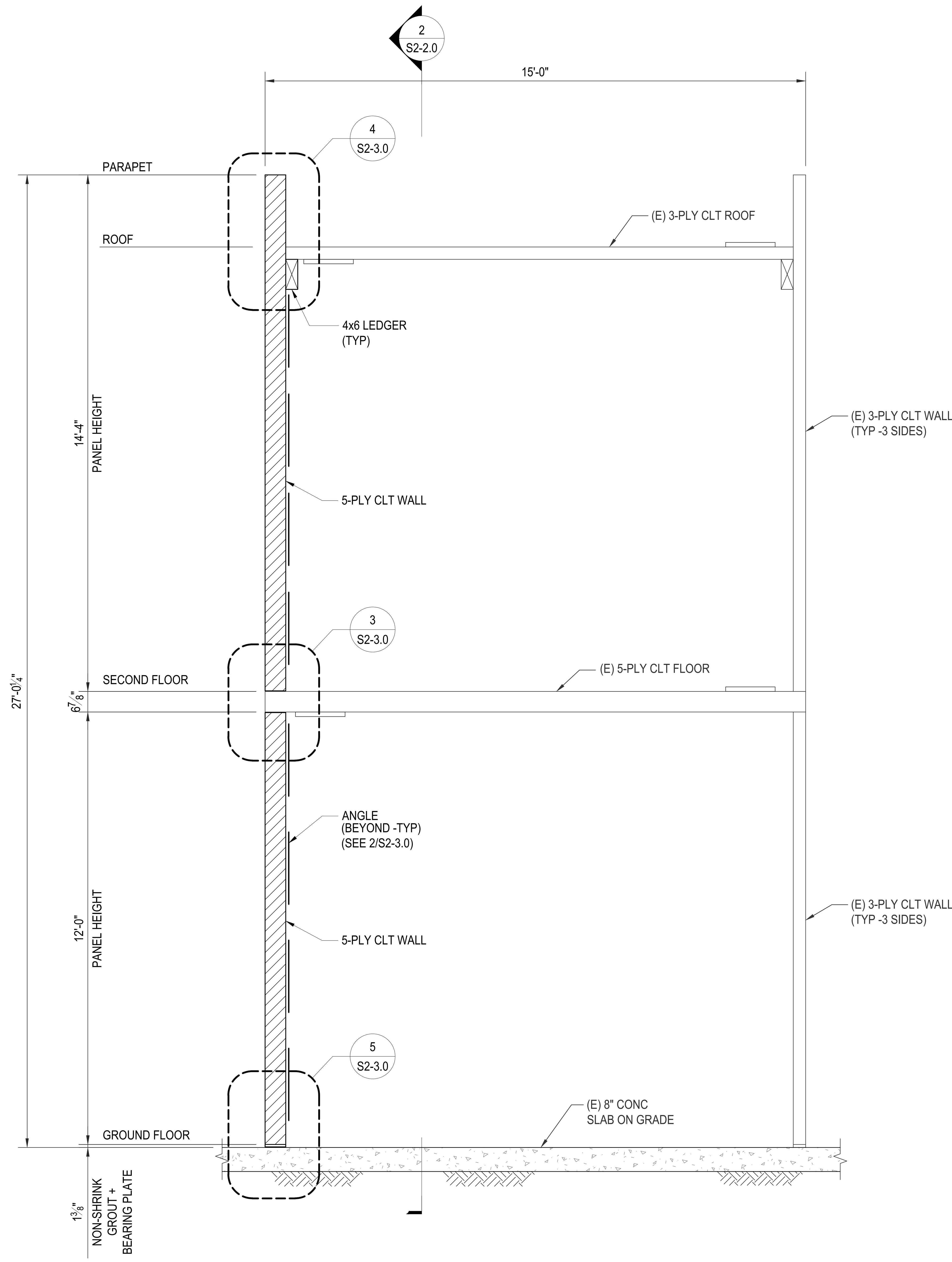

1 S2-2.0 SECTION

SCALE: 1/2"=1'-0"

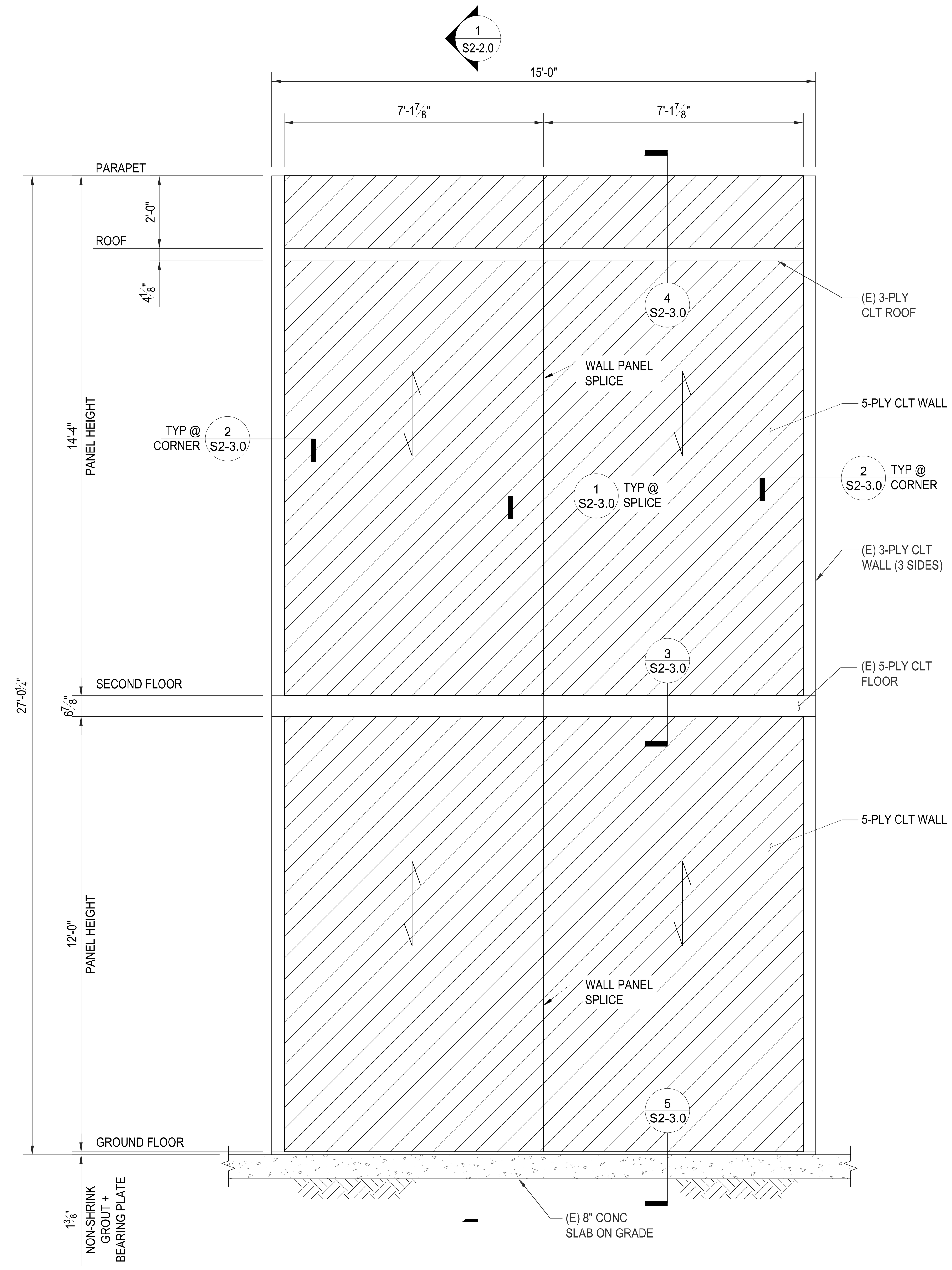

2 S2-2.0 SECTION

SCALE: 1/2"=1'-0"

2' 0 2' 4' 8'

1/2" = 1'-0"

K&C
Karagozian & Case
700 North Brand Blvd., Suite 700
Glendale, CA 91203-3215
Tel: 818-240-1919 Fax: 818-240-4966
—
www.kcse.com

Mark	Date	Appr.	Description
1	09-01-2017	MW	MISC REVISIONS
0	08-10-2017	MW	FINAL TEST ARTICLE

Revisions

PROJECT

BLAST TESTING OF LOADED MASS TIMBER STRUCTURES

SHEET TITLE

TESTS 6 & 7
SECTIONS
SPECIMEN #1

DRAWN	CHECKED	APPROVED	DATE ISSUED
CJ	MW	LT	08/10/2017

JOB NO. 2396_2017

FILE NAME: S2_200_2396.DWG

SHEET NUMBER

S2-2.0 1

September 1, 2017

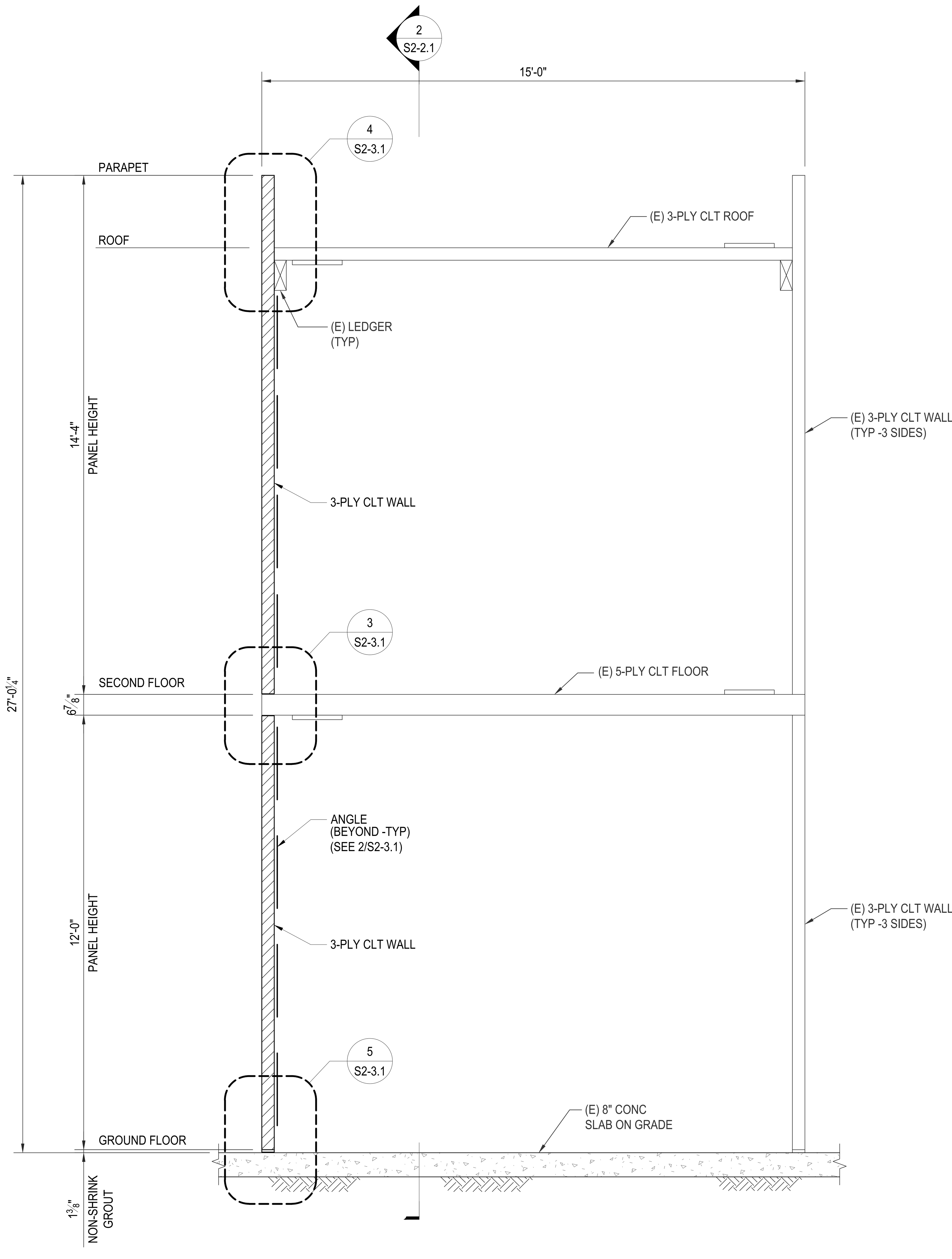

1
S2-2.1

SECTION

SCALE: 1/2"=1'-0"

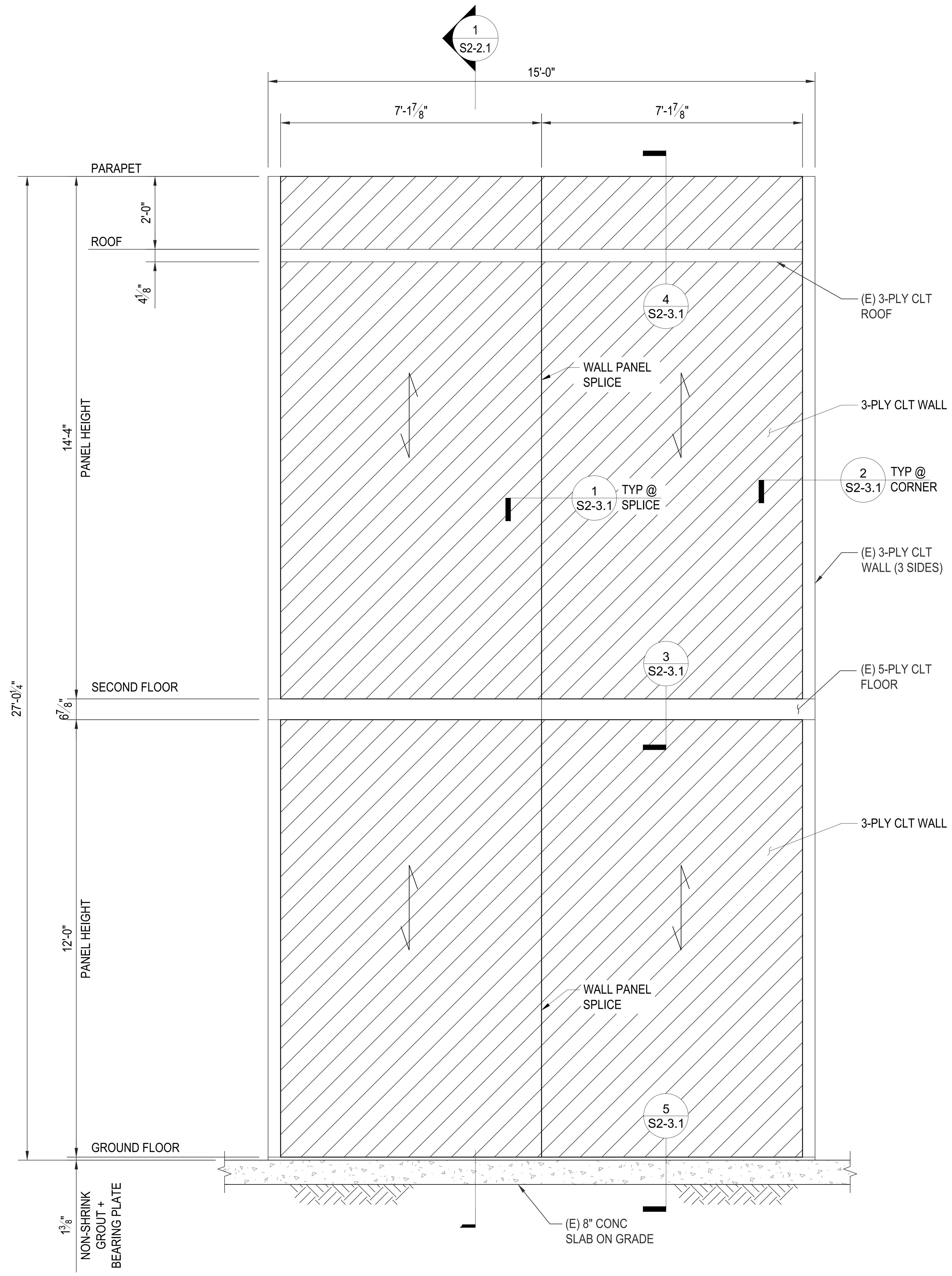

2
S2-2.1

SECTION

SCALE: 1/2"=1'-0"

2' 0 2' 4' 8'
1/2" = 1'-0"

K&C
Karagozian & Case

700 North Brand Blvd., Suite 700
Glendale, CA 91203-3215
Tel: 818-240-1919 Fax: 818-240-4966
www.kcse.com

Mark	Date	Appr.	Description
1	09-01-2017	MW	MISC REVISIONS
0	08-10-2017	MW	FINAL TEST ARTICLE

Revisions

PROJECT

BLAST TESTING OF LOADED MASS TIMBER STRUCTURES

SHEET TITLE

TESTS 6 & 7
SECTIONS
SPECIMEN #2

DRAWN	CHECKED	APPROVED	DATE ISSUED
CJ	MW	LT	08/10/2017

JOB NO.	FILE NAME:
2396_2017	S2_201_2396.DWG

SHEET NUMBER

S2-2.1

1

September 1, 2017

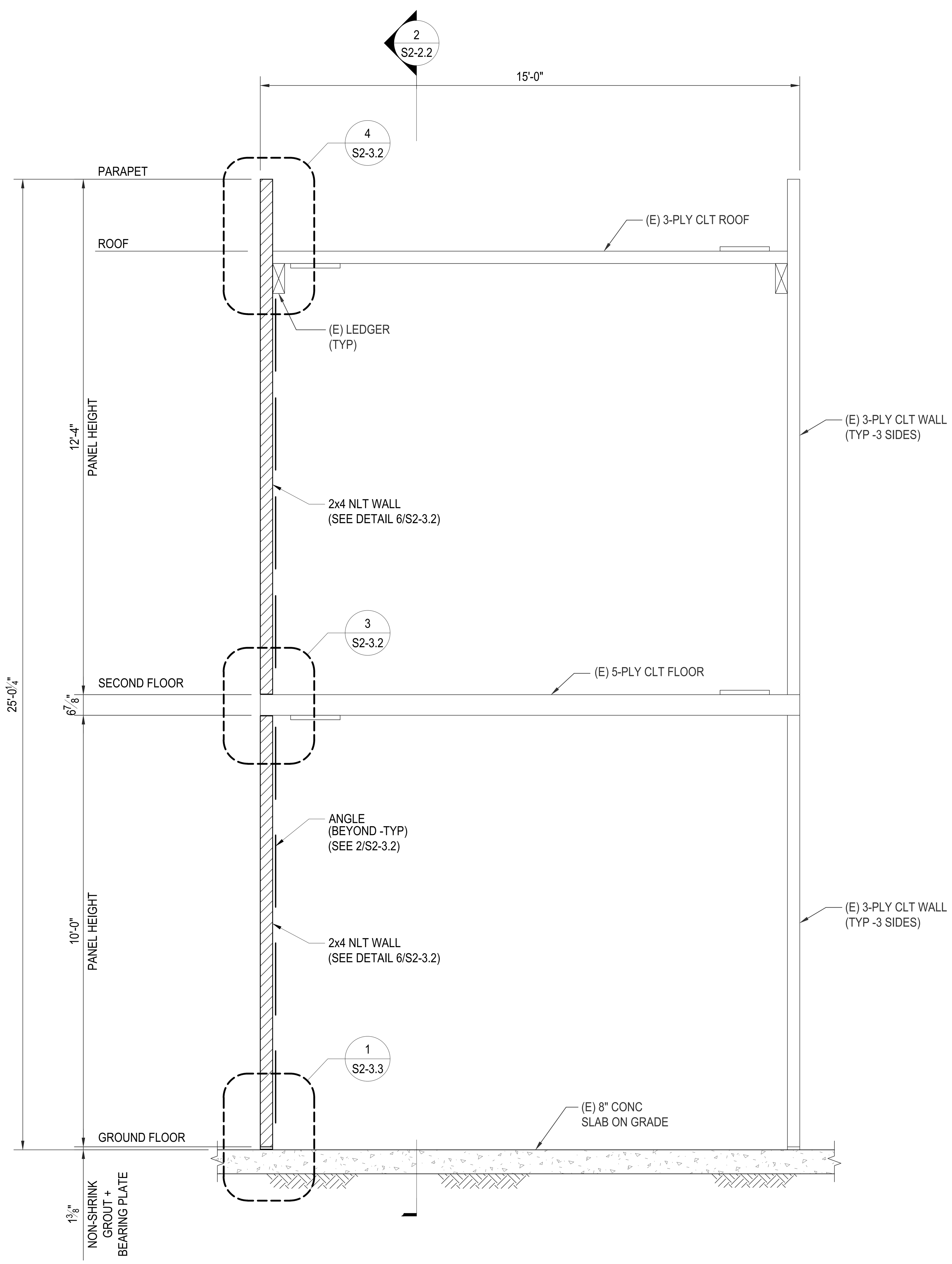

1 S2-2.2 SECTION

SCALE: 1/2"=1'-0"

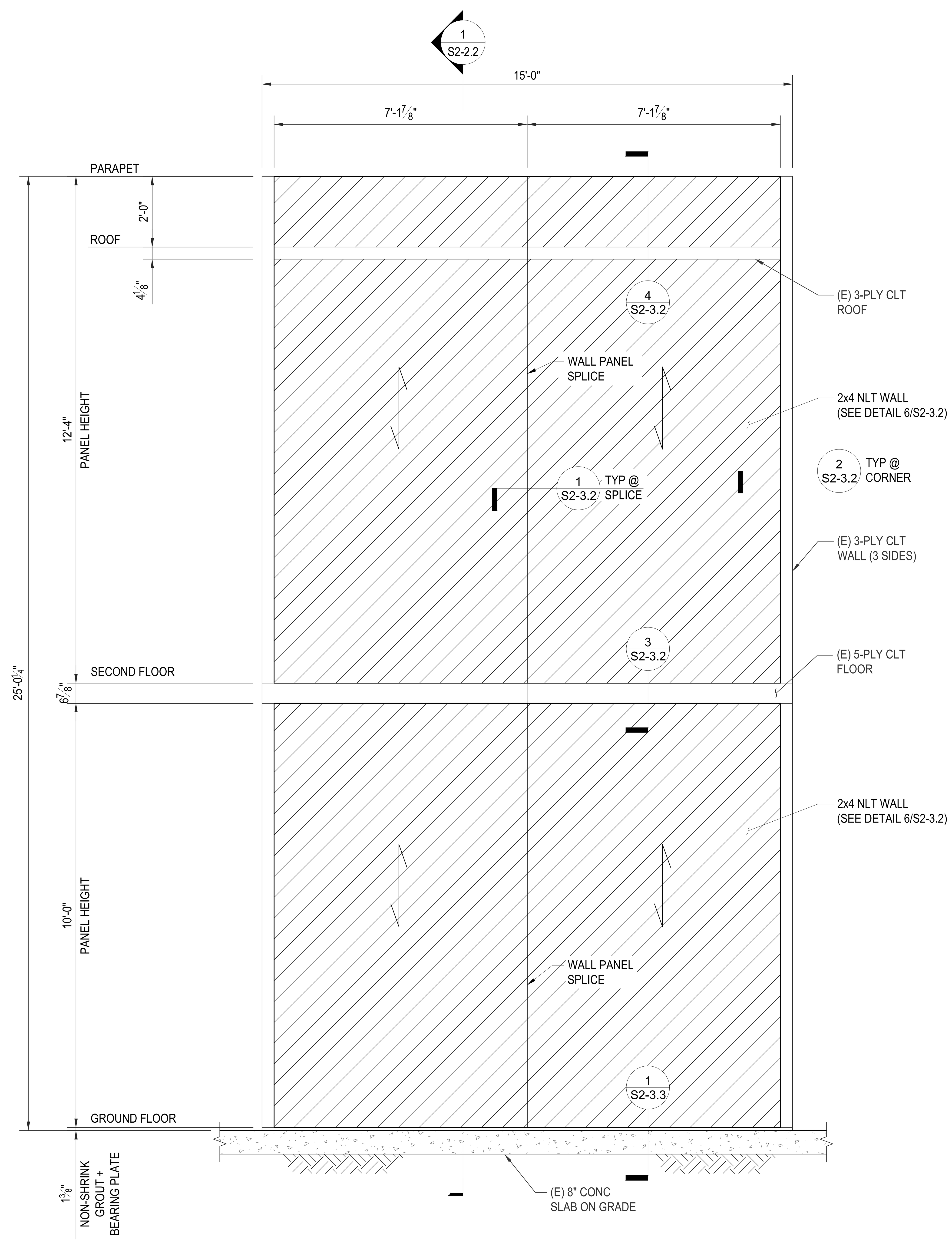

2 S2-2.2 SECTION

SCALE: 1/2"=1'-0"

2' 0 2' 4' 8'

1/2" = 1'-0"

K&C
Karagozian & Case

700 North Brand Blvd., Suite 700
Glendale, CA 91203-3215
Tel: 818-240-1919 Fax: 818-240-4966

www.kcse.com

Mark	Date	Appr.	Description
1	09-01-2017	MW	MISC REVISIONS
0	08-10-2017	MW	FINAL TEST ARTICLE

Revisions

PROJECT

BLAST TESTING OF LOADED MASS TIMBER STRUCTURES

SHEET TITLE

TESTS 6 & 7
SECTIONS
SPECIMEN #3

DRAWN	CHECKED	APPROVED	DATE ISSUED
CJ	MW	LT	08/10/2017

JOB NO.	FILE NAME:
2396_2017	S2_202_2396.DWG

SHEET NUMBER

S2-2.2

1

September 1, 2017

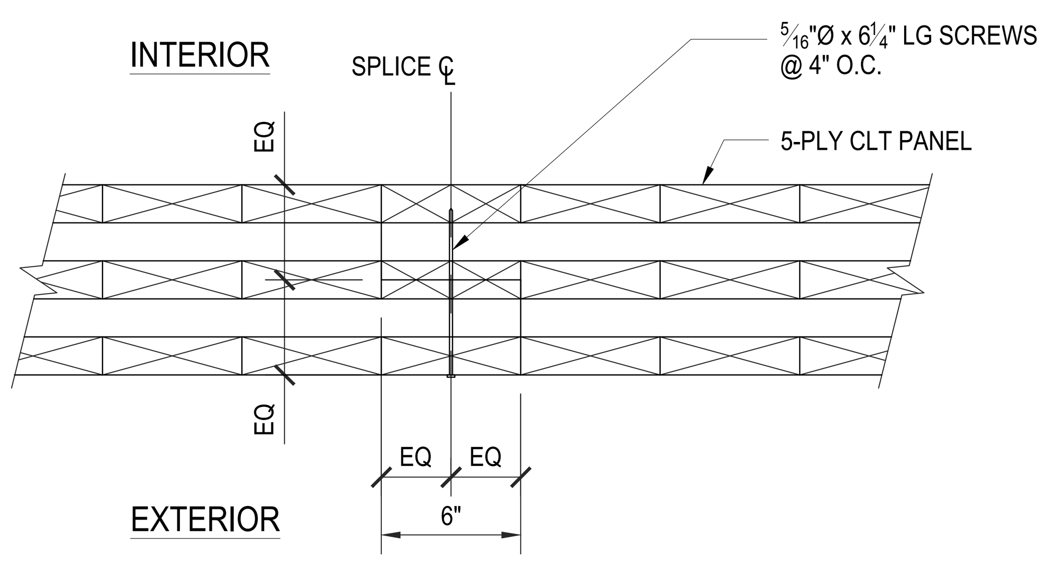

1 S2-3.0 WALL PANEL SPLICE DETAIL
SCALE: 2"=1'-0"

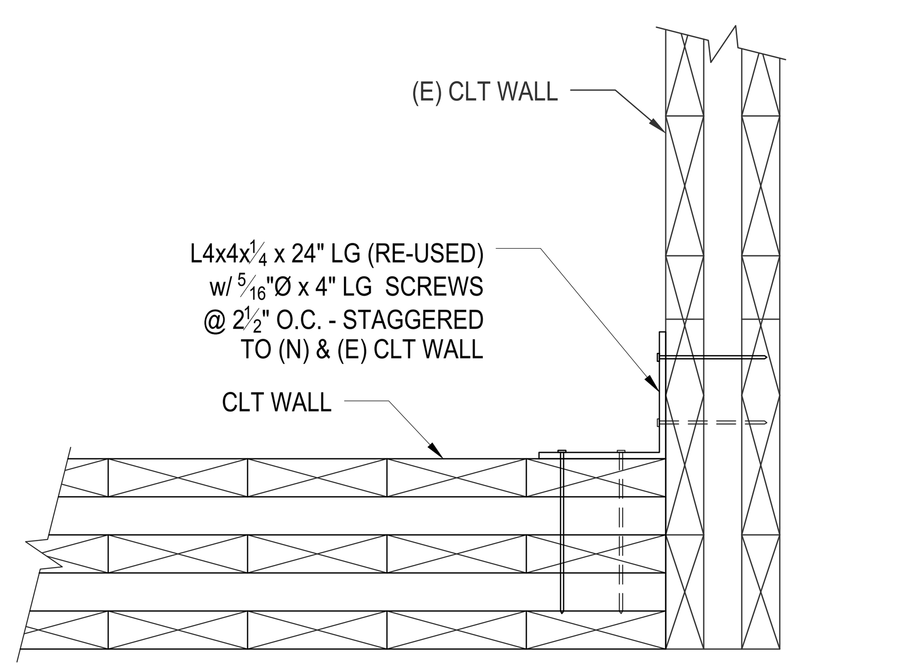

2 S2-3.0 PLAN DETAIL (TYP @ WALL CORNER)
SCALE: 2"=1'-0"

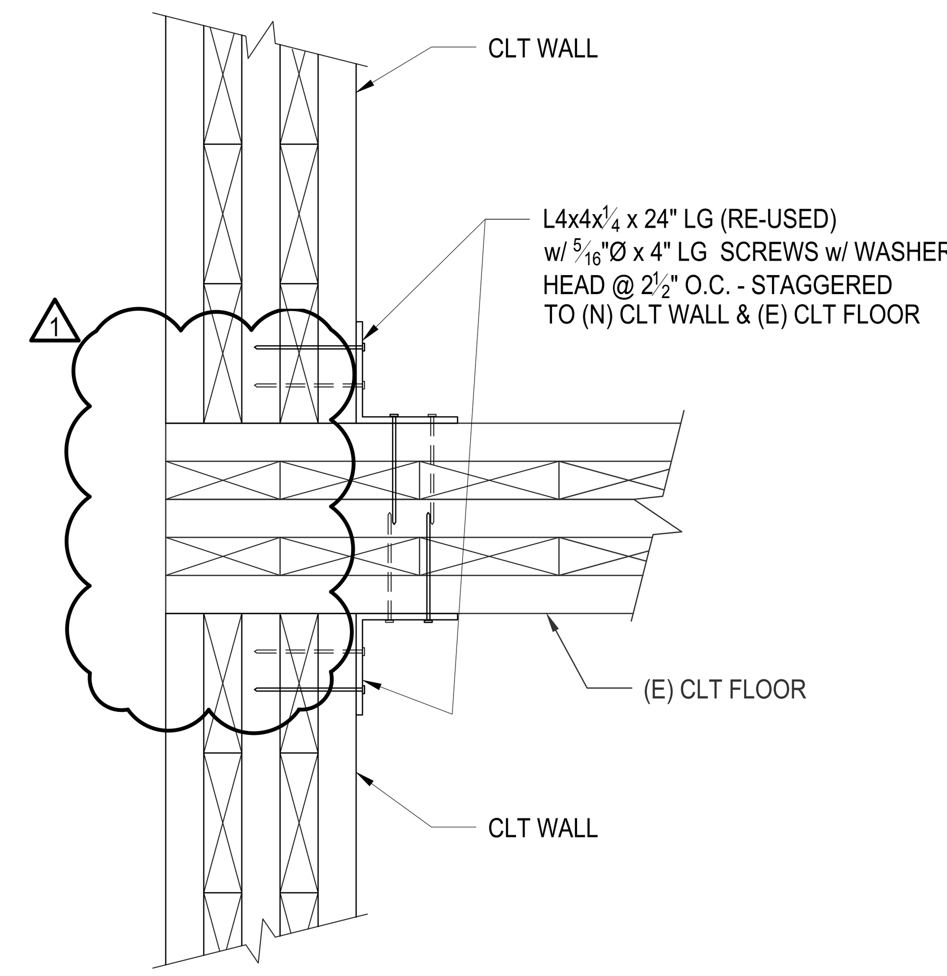

3 S2-3.0 SECTION (TYP @ 2ND FLOOR)
SCALE: 2"=1'-0"

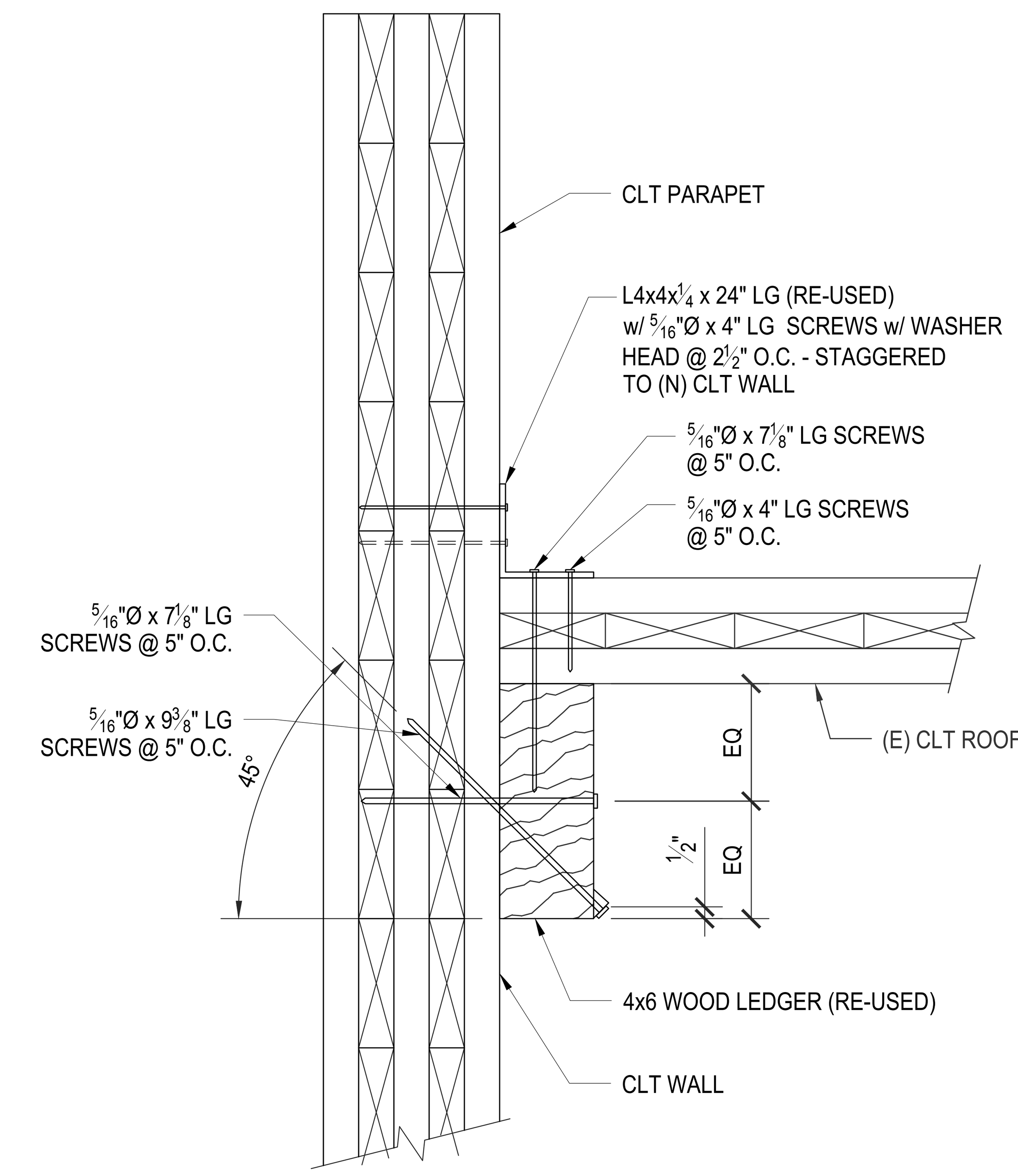

4 S2-3.0 SECTION (TYP @ ROOF)
SCALE: 2"=1'-0"

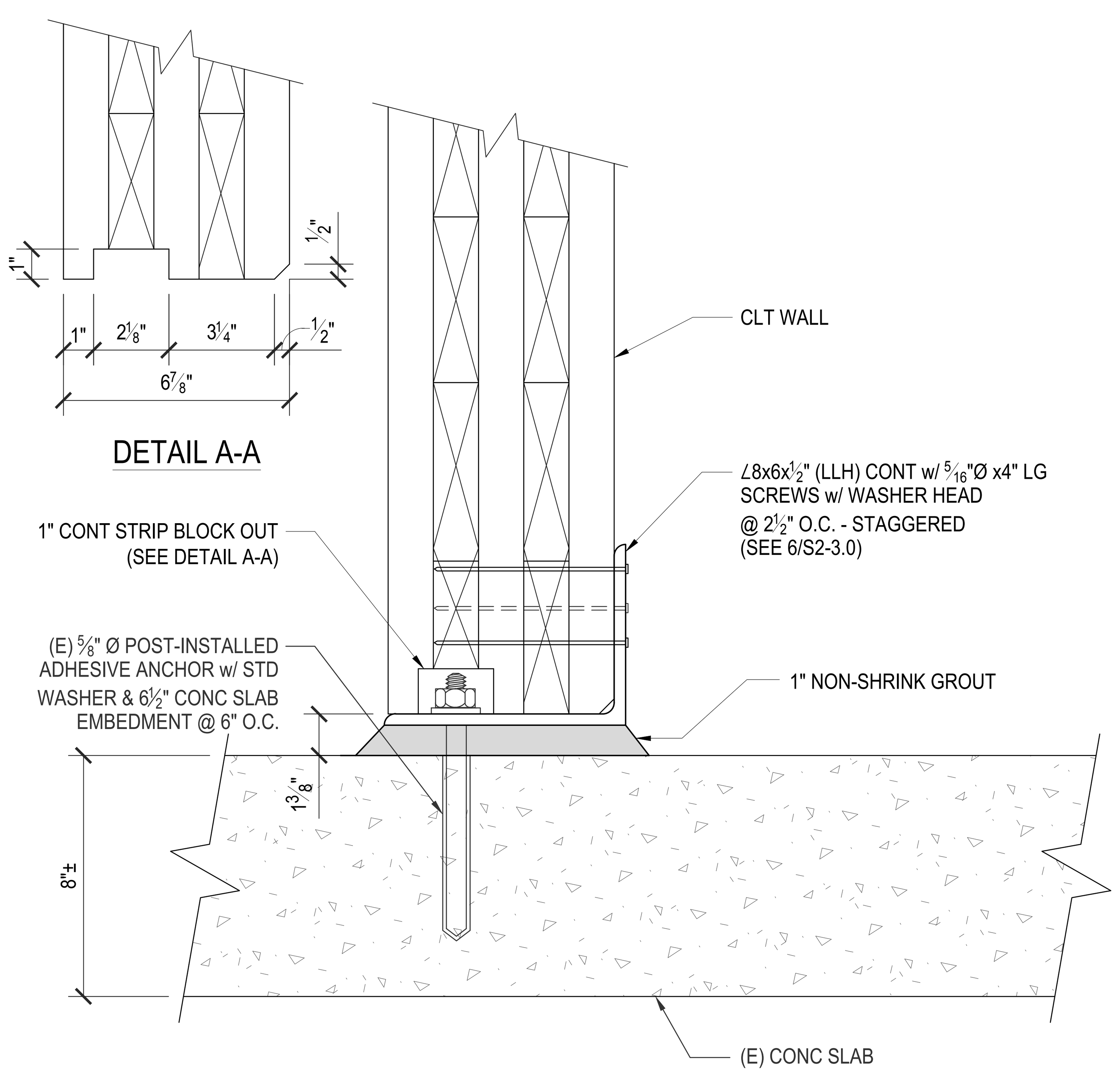

5 S2-3.0 SECTION (TYP @ FLOOR)
SCALE: 3"=1'-0"

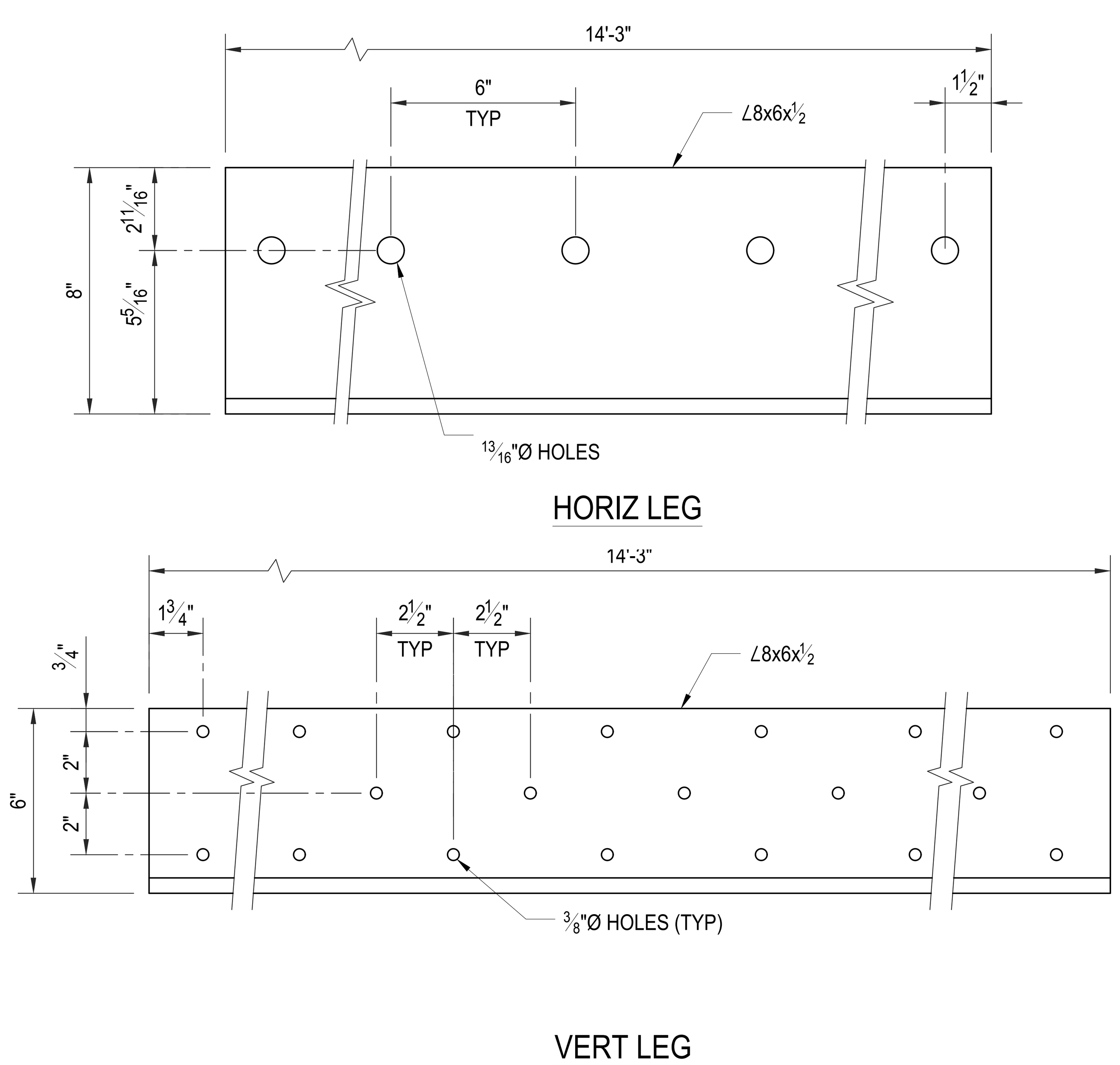

6 S2-3.0 DETAIL (PLATE SCREW SPACING)
SCALE: 3"=1'-0"

NOTE:

1. IT IS PERMISSIBLE TO RE-USE FASTENERS THAT ARE REMOVED PROVIDED THE FASTENER SHOWS NO SIGNS OF DAMAGE OR DEFORMATION FROM ITS ORIGINAL STATE.

6" 0 6" 1' 1'-6"
2" = 1'-0"

3" 0 3" 6" 1'-0"
3" = 1'-0"

K&C
Karagozian & Case
700 North Brand Blvd., Suite 700
Glendale, CA 91203-3215
Tel: 818-240-1919 Fax: 818-240-4966
www.kcse.com

Mark	Date	Appr.	Description
1	09-01-2017	MW	MISC REVISIONS
0	08-10-2017	MW	FINAL TEST ARTICLE

Revisions

PROJECT

BLAST TESTING OF LOADED MASS TIMBER STRUCTURES

SHEET TITLE

TESTS 6 & 7
DETAILS
SPECIMEN #1

DRAWN	CHECKED	APPROVED	DATE ISSUED
CJ	MW	LT	08/10/2017

JOB NO. 2396_2017
FILE NAME: S2_300_2396.DWG

SHEET NUMBER
S2-3.0
1

September 1, 2017

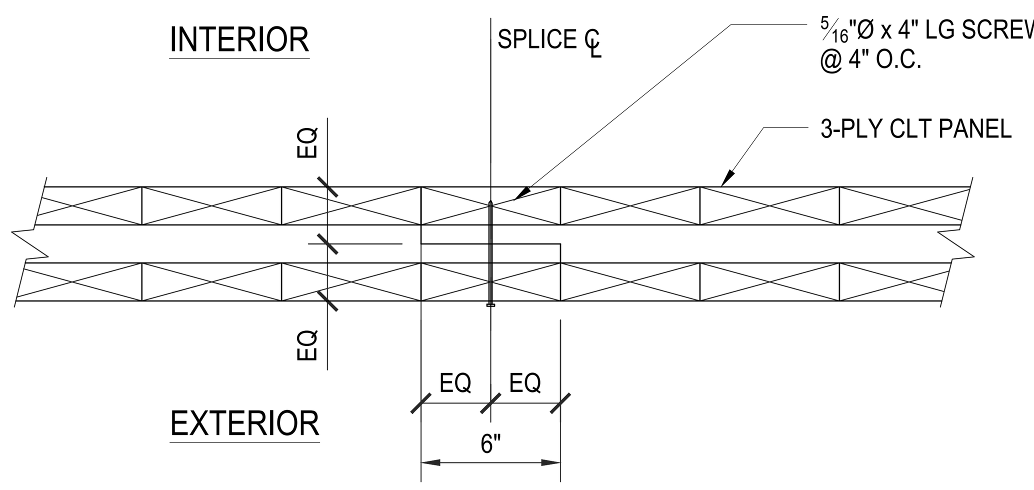

1 S2-3.1 **WALL PANEL SPLICE DETAIL**
SCALE: 2"=1'-0"

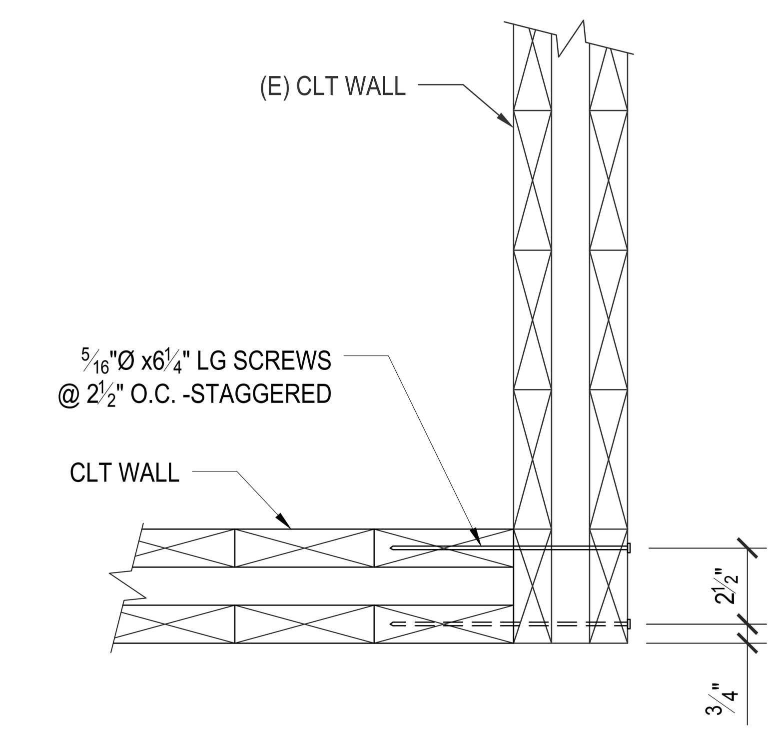

2 S2-3.1 **PLAN DETAIL (TYP @ WALL CORNER)**
SCALE: 2"=1'-0"

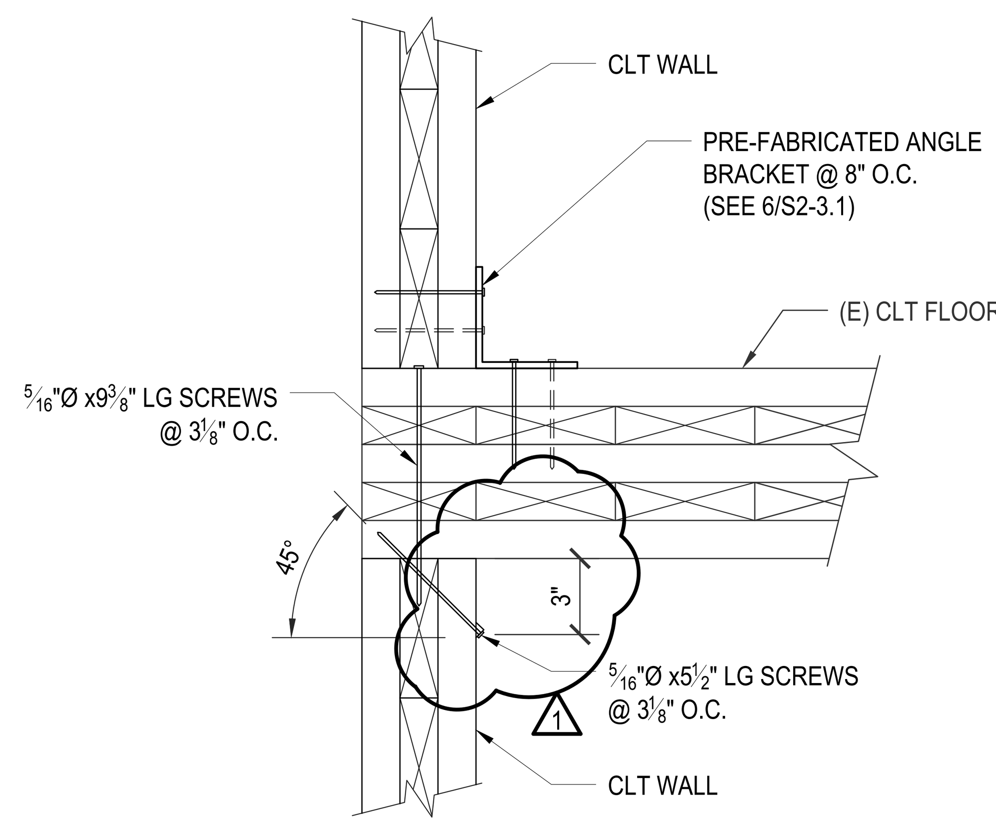

3 S2-3.1 **SECTION (TYP @ 2ND FLOOR)**
SCALE: 2"=1'-0"

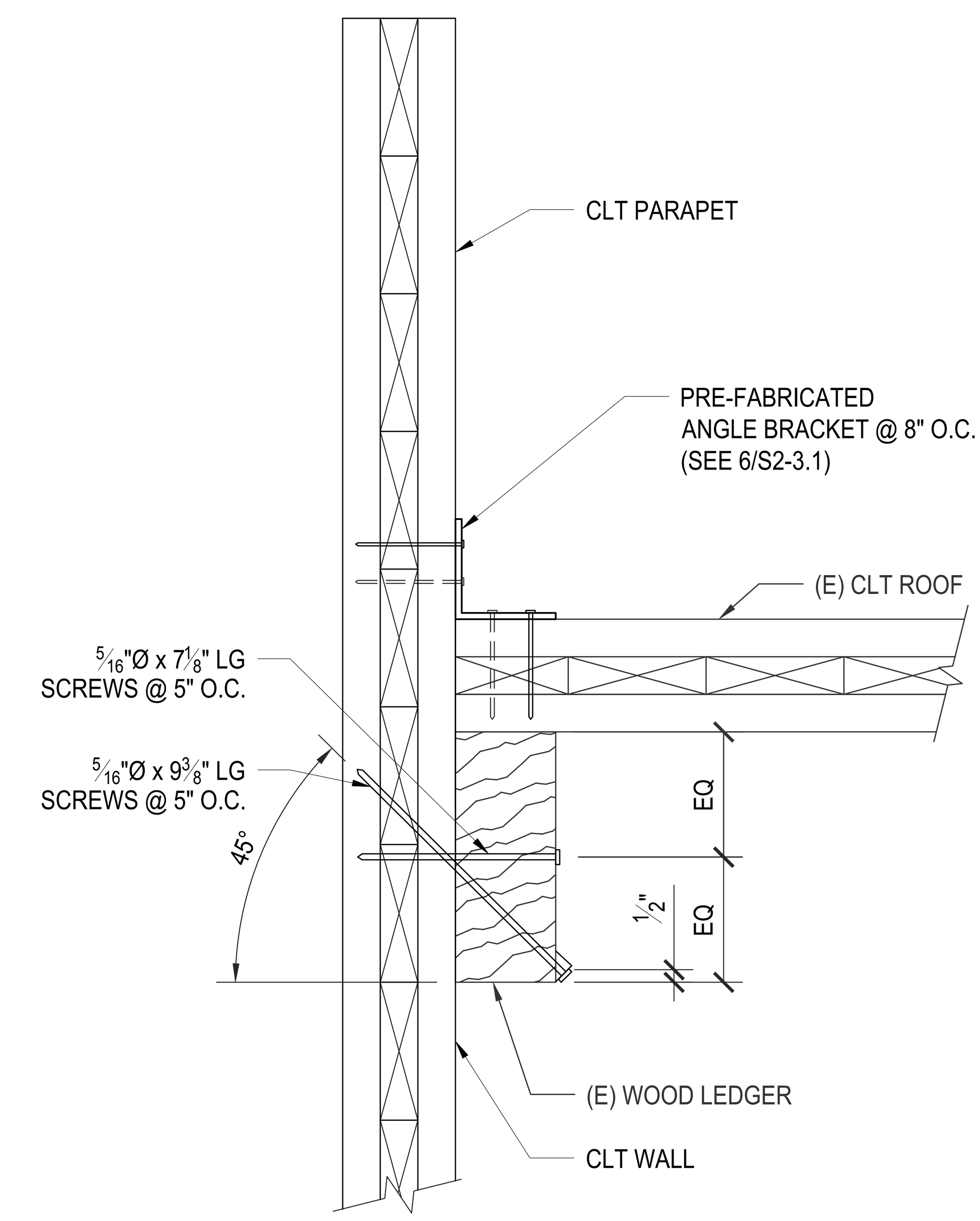

4 S2-3.1 **SECTION (TYP @ ROOF)**
SCALE: 2"=1'-0"

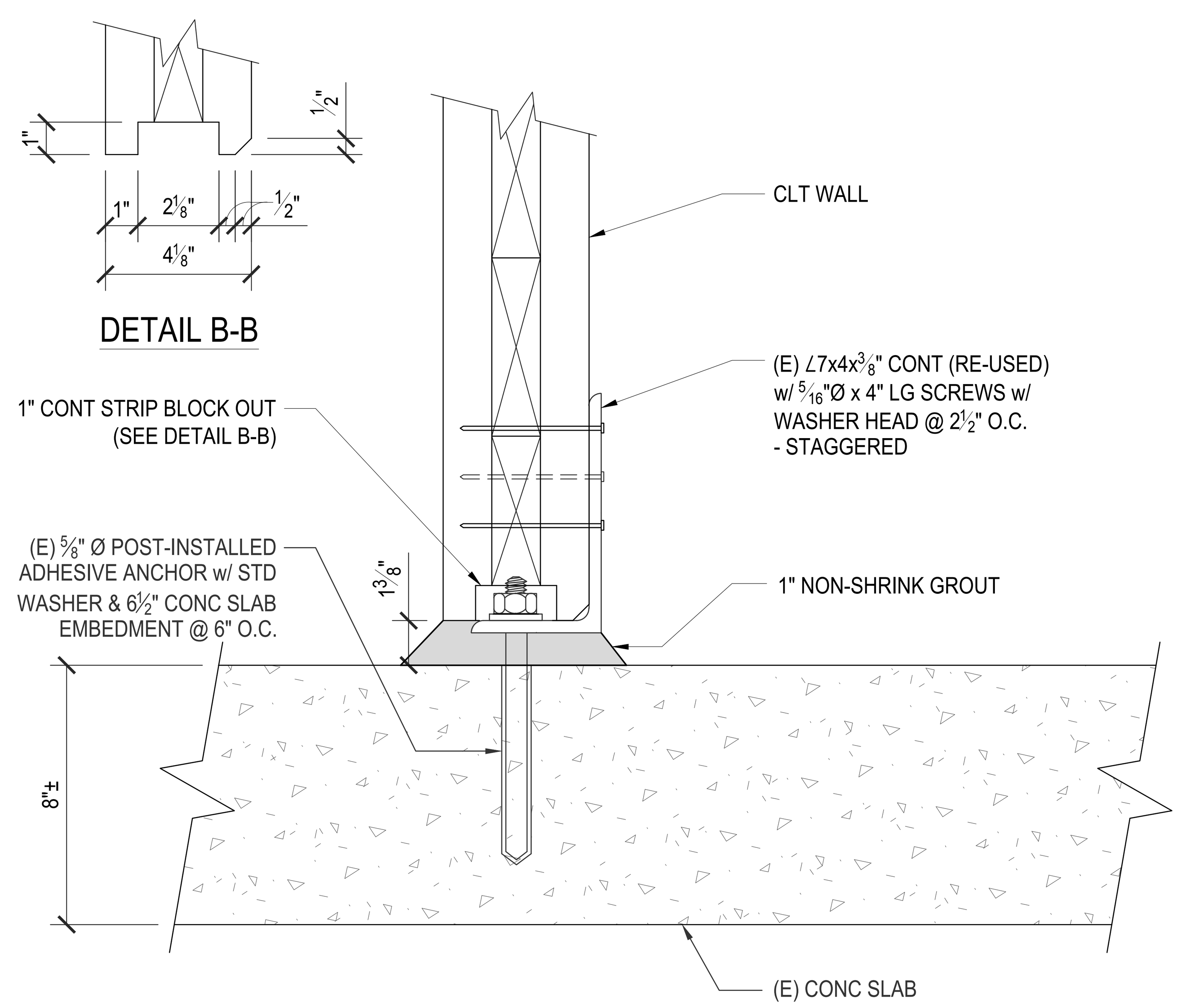

5 S2-3.1 **SECTION (TYP @ FLOOR)**
SCALE: 3"=1'-0"

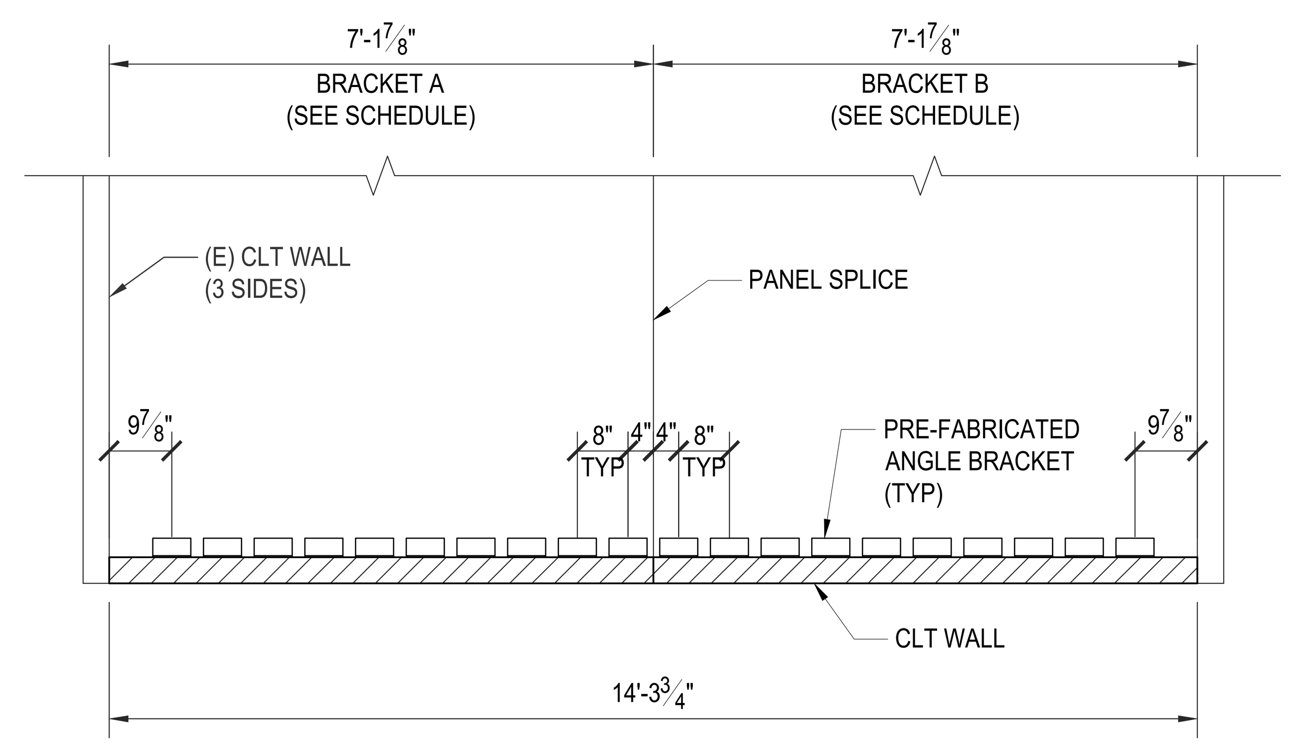

6 S2-3.1 **PARTIAL FLOOR PLAN (FRONT WALL)**
SCALE: 1/2"=1'-0"

PRE-FABRICATED ANGLE BRACKET SCHEDULE

BRACKET	TYPE	VERT LEG FASTENERS	HORIZ LEG FASTENERS	NOTES
A	SST ABR105	(10) SD10212	(14) SD10212	
B	USP HGA10	(4) WS35	(4) WS35	LLV

NOTE:

1. IT IS PERMISSIBLE TO RE-USE FASTENERS THAT ARE REMOVED PROVIDED THE FASTENER SHOWS NO SIGNS OF DAMAGE OR DEFORMATION FROM ITS ORIGINAL STATE.

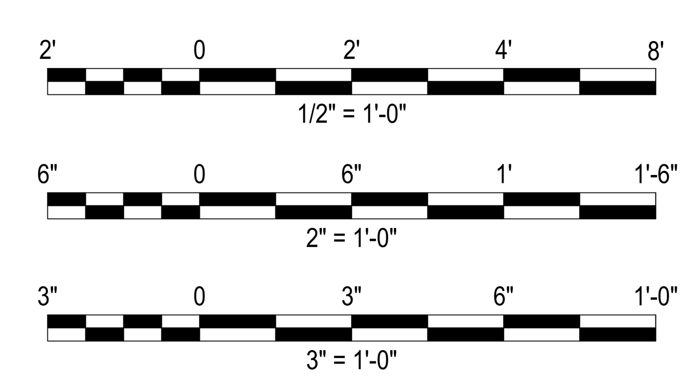

K&C
Karagozian & Case
700 North Brand Blvd., Suite 700
Glendale, CA 91203-3215
Tel: 818-240-1919 Fax: 818-240-4966
www.kcse.com

Mark	Date	Appr.	Description
1	09-01-2017	MW	MISC REVISIONS
0	08-10-2017	MW	FINAL TEST ARTICLE

Revisions

PROJECT

BLAST TESTING OF LOADED MASS TIMBER STRUCTURES

SHEET TITLE

TESTS 6 & 7
DETAILS
SPECIMEN #2

DRAWN	CHECKED	APPROVED	DATE ISSUED
CJ	MW	LT	08/10/2017

JOB NO. 2396_2017
FILE NAME: S2_301_2396.DWG

SHEET NUMBER
S2-3.1 1

September 5, 2017

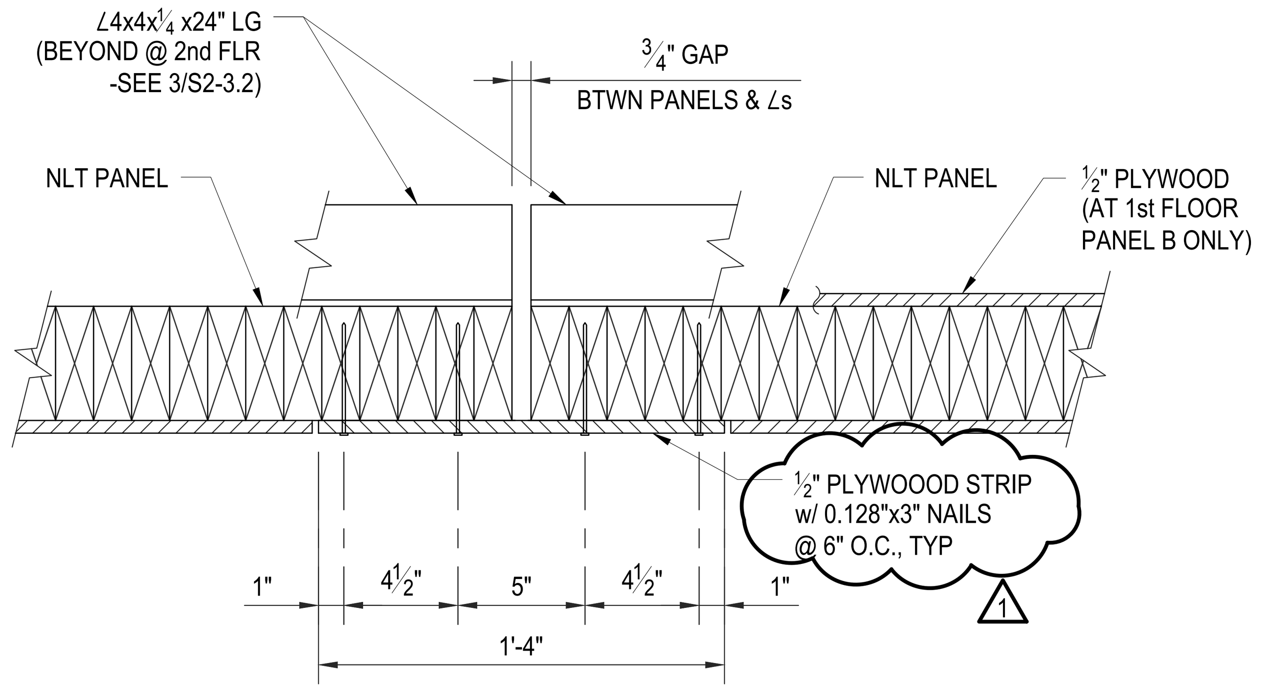

1 WALL PANEL SPLICE DETAIL
S2-3.2 SCALE: 2"=1'-0"

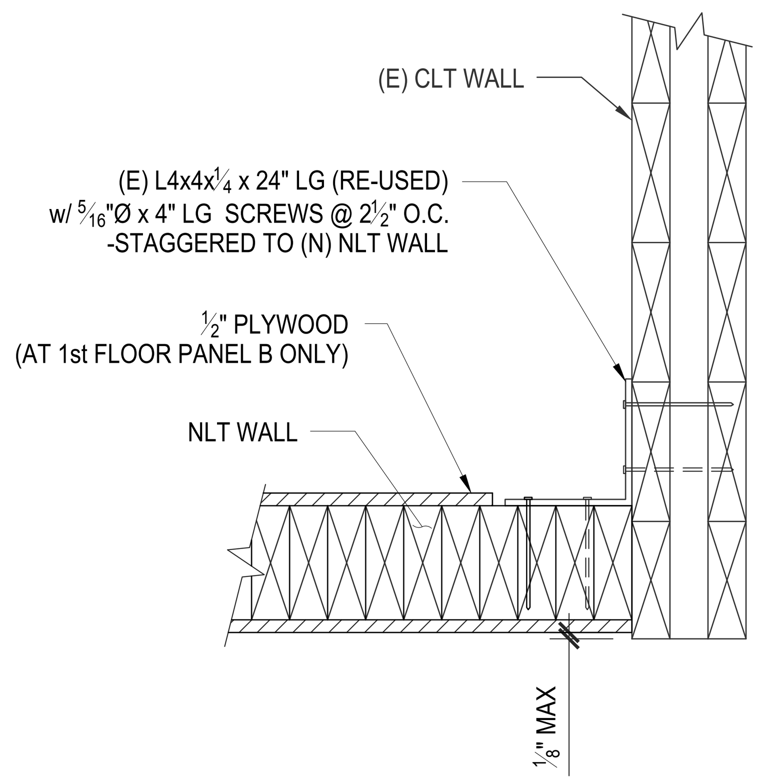

2 PLAN DETAIL (TYP @ WALL CORNER)
S2-3.2 SCALE: 2"=1'-0"

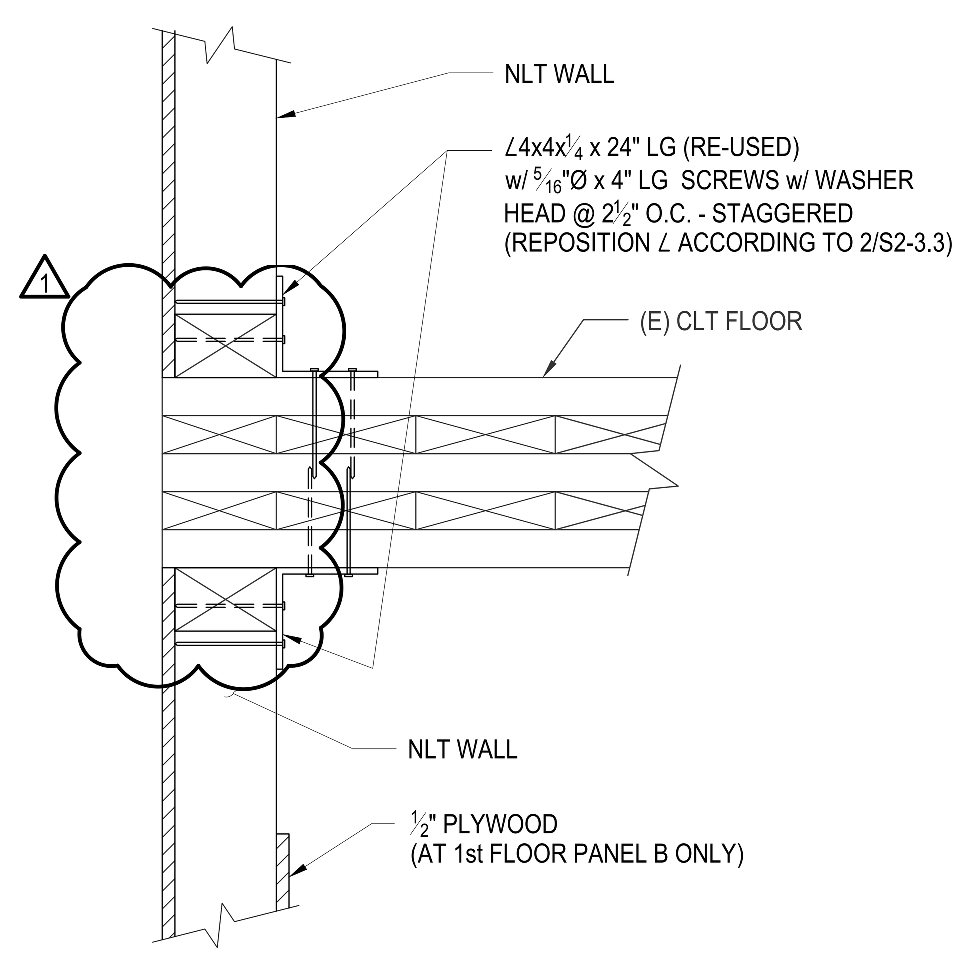

3 SECTION (TYP @ 2ND FLOOR)
S2-3.2 SCALE: 2"=1'-0"

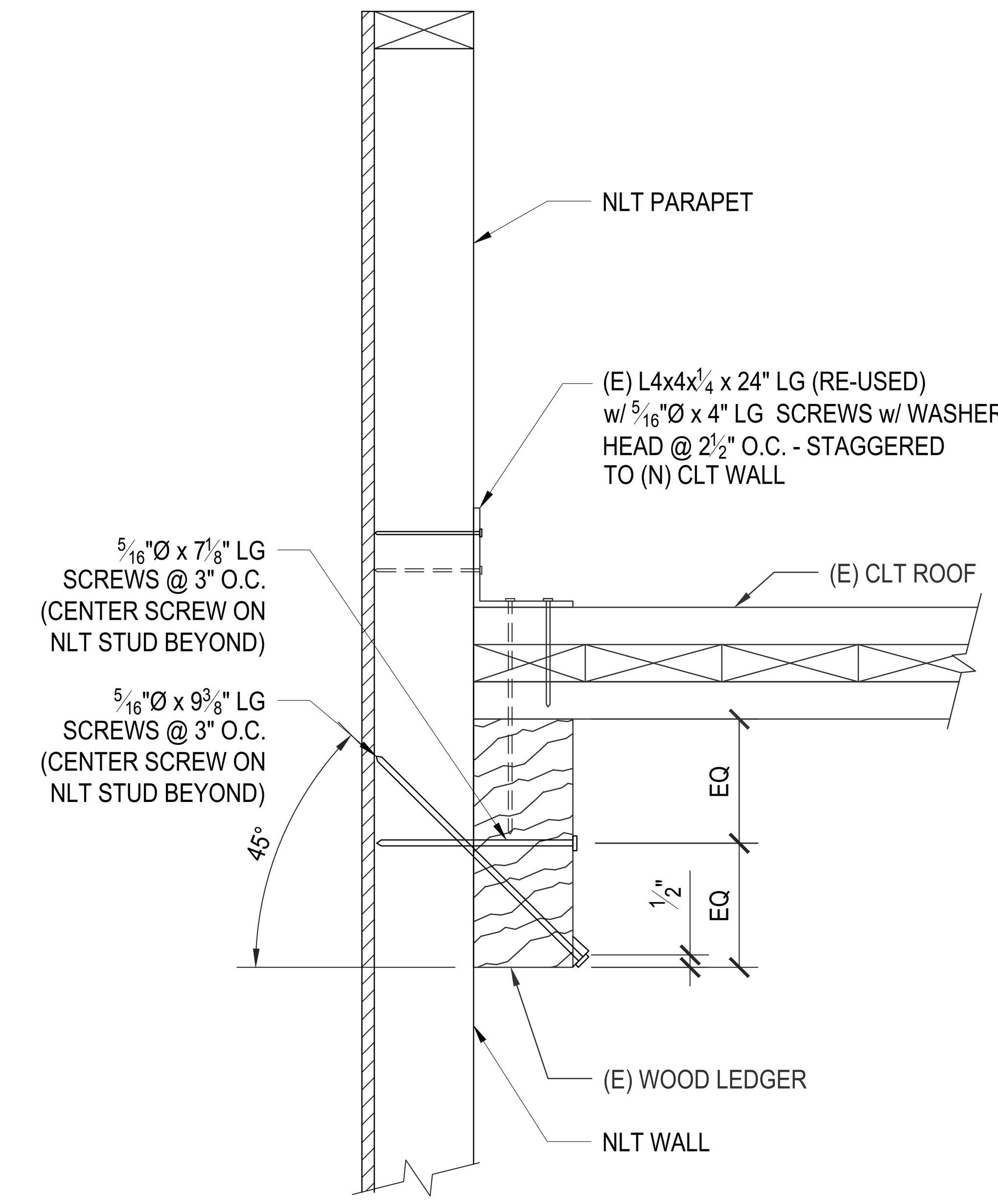

4 SECTION (TYP @ ROOF)
S2-3.2 SCALE: 2"=1'-0"

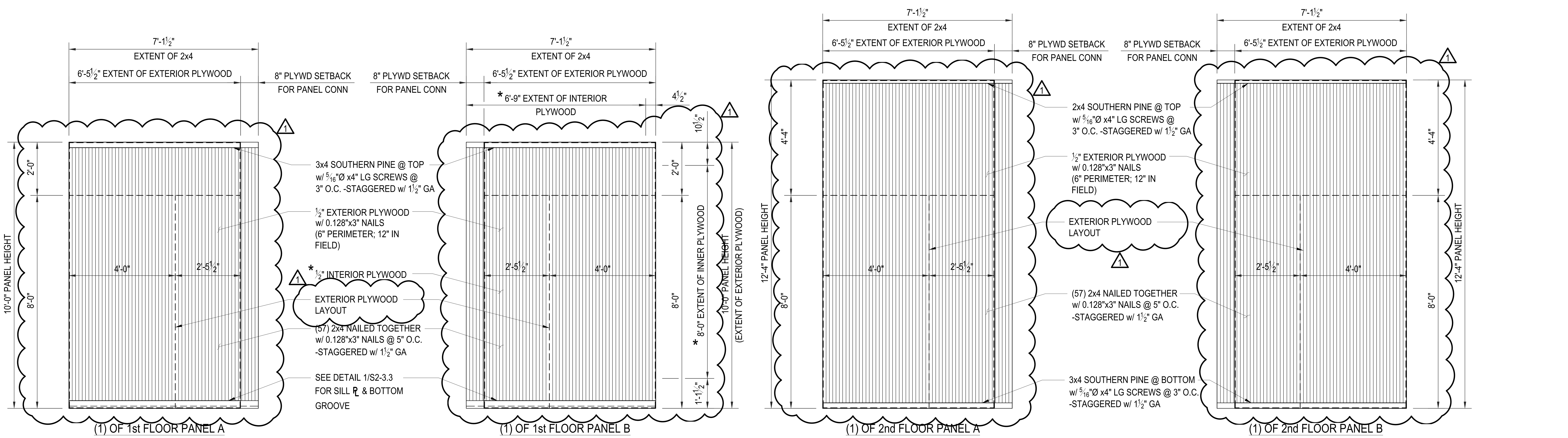

* INSTALL 1/2" PLYWOOD w/ 0.128"x3" NAILS (6" PERIMETER; 12" IN FIELD) AFTER INSTALLATION

5 PANEL DETAIL
S2-3.2 SCALE: 1/2"=1'-0"

NOTE:

1. IT IS PERMISSIBLE TO RE-USE FASTENERS THAT ARE REMOVED PROVIDED THE FASTENER SHOWS NO SIGNS OF DAMAGE OR DEFORMATION FROM ITS ORIGINAL STATE.

2' 0 2' 4' 8'
1/2" = 1'-0"

6" 0 6" 1' 1'-6"
2" = 1'-0"

K&C
Karagozian & Case
700 North Brand Blvd., Suite 700
Glendale, CA 91203-3215
Tel: 818-240-1919 Fax: 818-240-4966
www.kcse.com

Mark	Date	Appr.	Description
1	09-01-2017	MW	MISC REVISIONS
0	08-10-2017	MW	FINAL TEST ARTICLE

Revisions

PROJECT
BLAST TESTING OF LOADED MASS TIMBER STRUCTURES

SHEET TITLE
TESTS 6 & 7
DETAILS
SPECIMEN #3

DRAWN	CHECKED	APPROVED	DATE ISSUED
CJ	MW	LT	08/10/2017

JOB NO. 2396_2017
FILE NAME: S2_302_2396.DWG
SHEET NUMBER S2-3.2

September 1, 2017

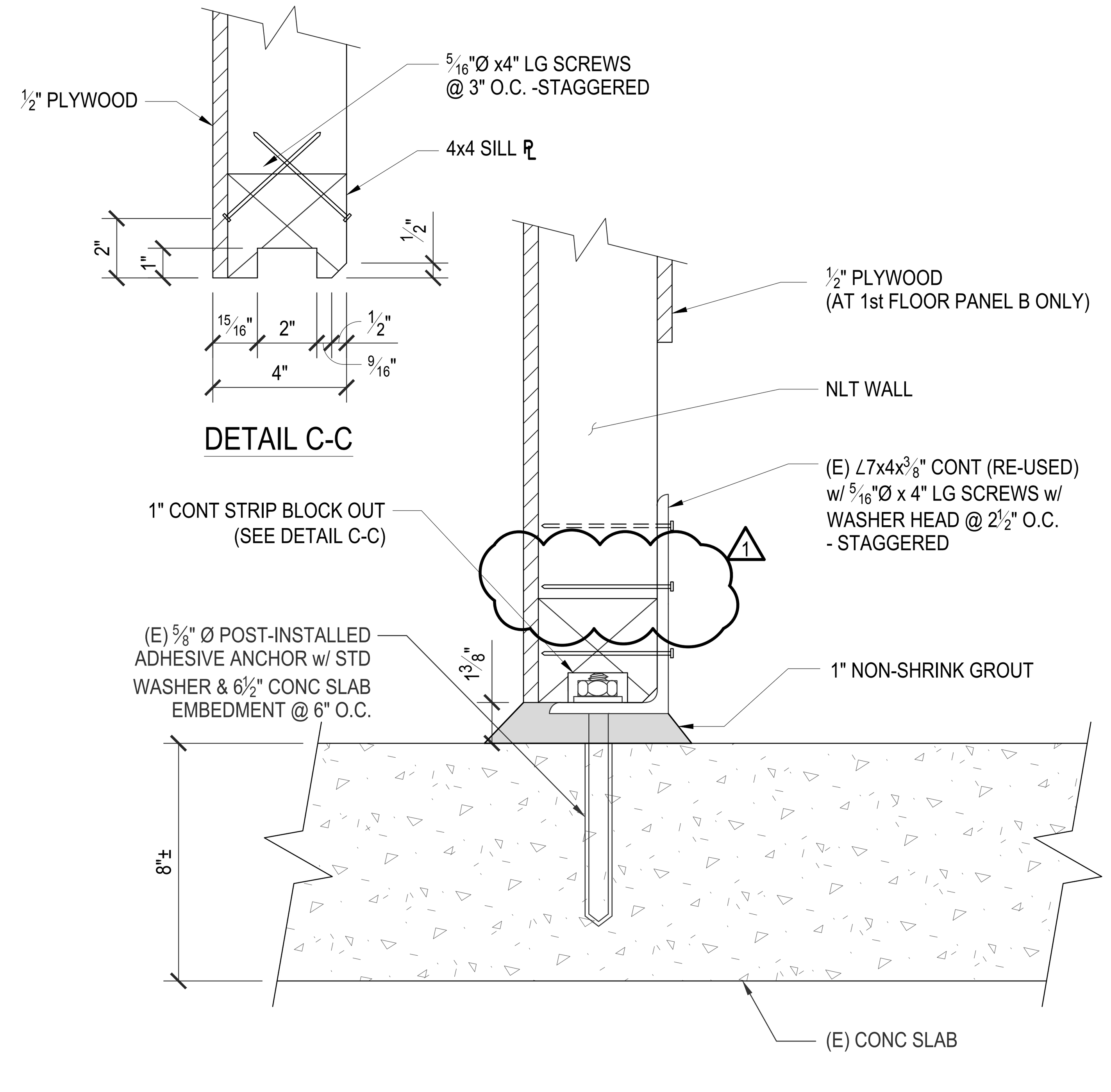

1 S2-3.3 SECTION (TYP @ FLOOR)
SCALE: 3"=1'-0"

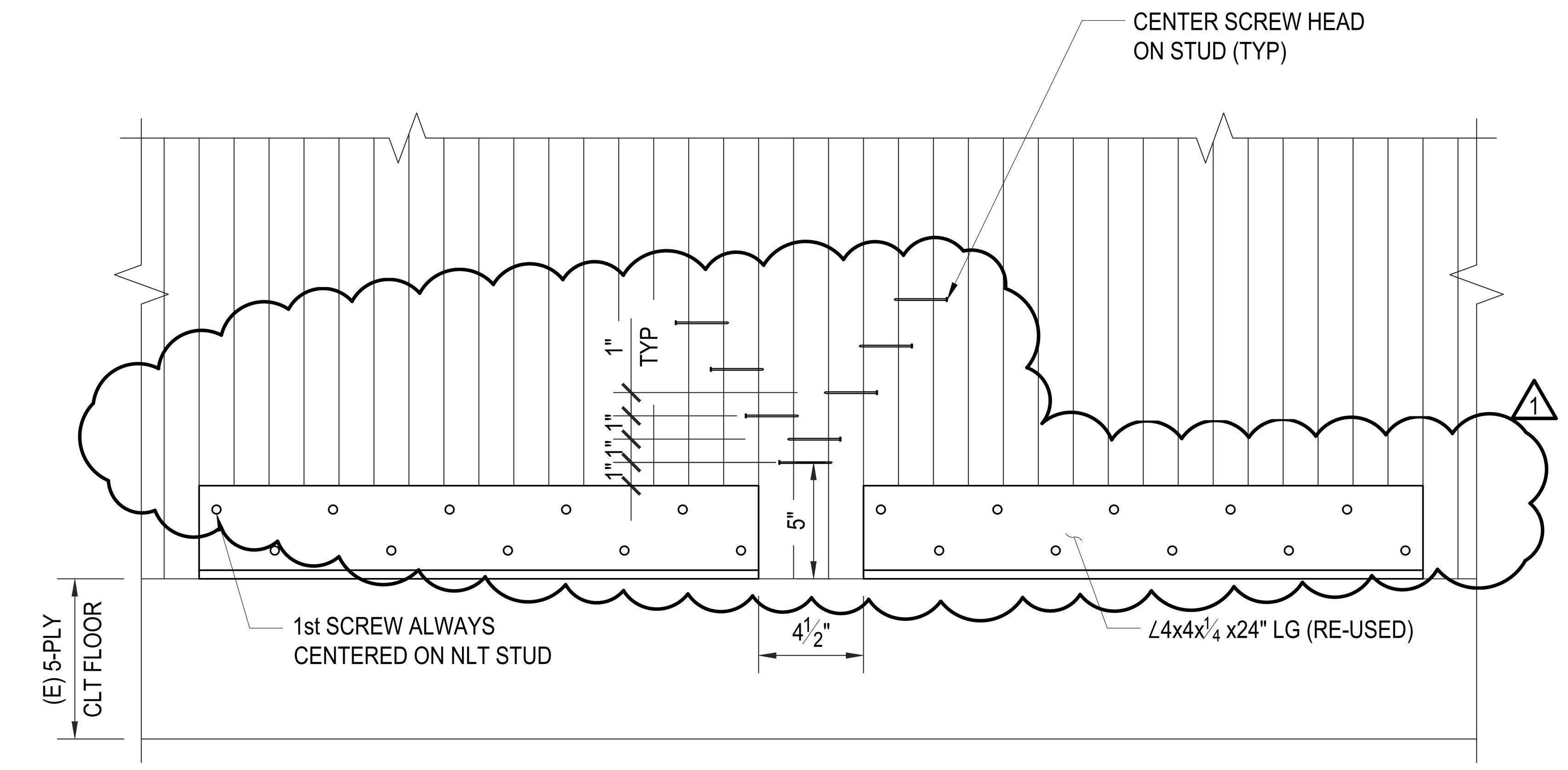

2 S2-3.3 ELEVATION DETAIL
SCALE: 2"=1'-0"

NOTE:

1. IT IS PERMISSIBLE TO RE-USE FASTENERS THAT ARE REMOVED PROVIDED THE FASTENER SHOWS NO SIGNS OF DAMAGE OR DEFORMATION FROM ITS ORIGINAL STATE.

6" 0 6" 1' 1'-6"
2" = 1'-0"

3" 0 3" 6" 1'-0"
3" = 1'-0"

K&C
Karagozian & Case
700 North Brand Blvd., Suite 700
Glendale, CA 91203-3215
Tel: 818-240-1919 Fax: 818-240-4966
www.kcse.com

Mark	Date	Appr.	Description
1	09-01-2017	MW	MISC REVISIONS
0	08-10-2017	MW	FINAL TEST ARTICLE

Revisions

PROJECT

BLAST TESTING OF LOADED MASS TIMBER STRUCTURES

SHEET TITLE

TESTS 6 & 7
DETAILS
SPECIMEN #3

DRAWN	CHECKED	APPROVED	DATE ISSUED
CJ	MW	LT	08/10/2017

JOB NO. 2396_2017
FILE NAME: S2_303_2396.DWG

SHEET NUMBER
S2-3.3

September 1, 2017

APPENDIX E

QUICK LOOK REPORT FOR ARENA BLAST TESTING

Air Force Civil Engineer Center

Integrity - Service - Excellence

Blast Resistance of Cross-Laminated Timber Construction

Casey O'Laughlin, P.E.
Research Civil Engineer, AFCEC Contractor, Jacobs SLG

Overview

- Background
- Resistance Function Development
- Full-Scale Blast Validations
  - Setup
  - Results
    - Full Scale Validation #4
    - Full Scale Validation #5
    - Full Scale Validation #6
    - Full Scale Validation #7

Background

- Cross laminated timber (CLT) is an engineered wood building system consisting of dimensional lumber oriented at right angles to one another and glued to form structural panels
- Objective of effort is the development of blast design criteria for CLT construction
- Karagozian and Case Inc. (K&C) contracted by WoodWorks and worked in conjunction with University of Maine to evaluate blast resistance of CLT panels in static laboratory conditions
- CRADA developed between Karagozian and Case Inc. and AFCEC for execution of load-tree static resistance with axial load tests and full scale blast validations

http://www.woodskyscrapers.com/cross-laminated-timber.html

Resistance Function Development

- Load tree at the Air Force Civil Engineering Center used to perform static evaluation with axial load of CLT resistance

- Parameters included panel grade, ply number, and dimensions

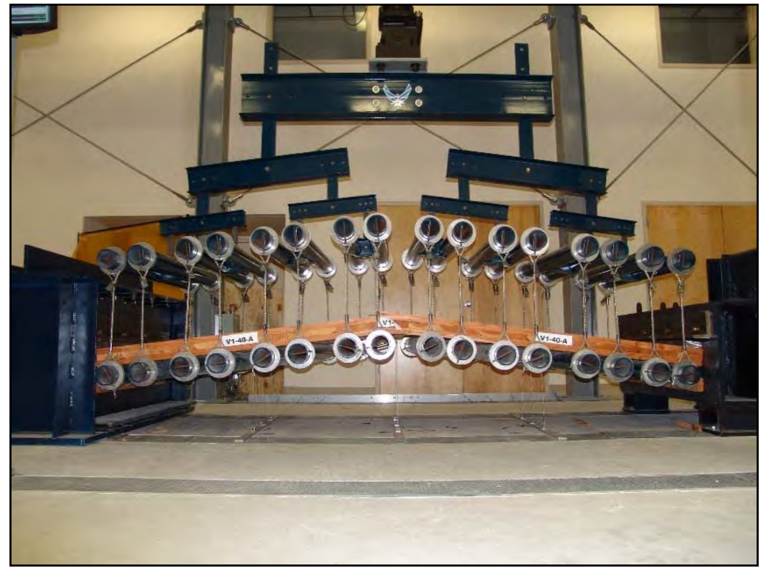

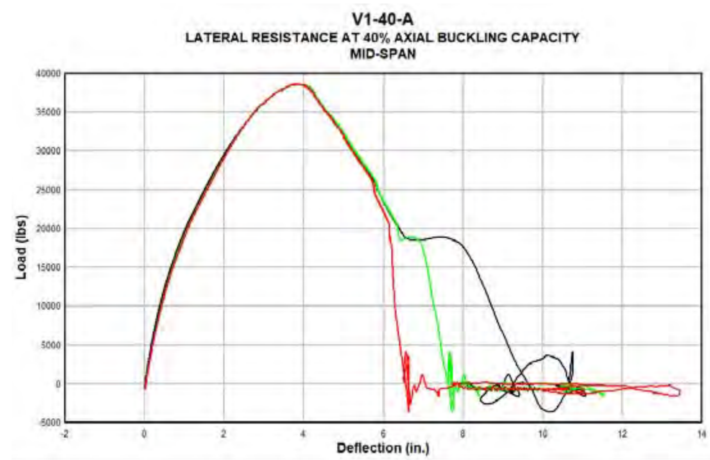

Full-Scale Blast Validations

Buildings labeled according to grade of CLT panels

Full-Scale Validation Setup

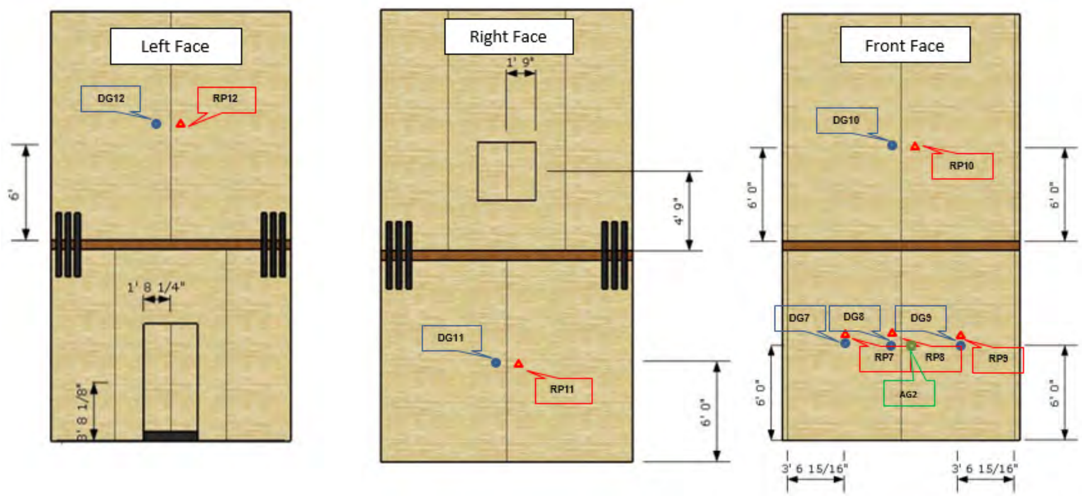

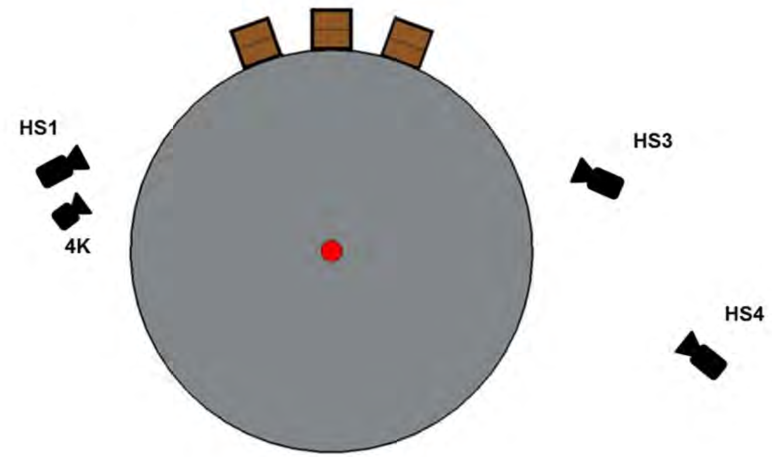

- 41 total gauges
- 18 reflected/incident pressure gauges (6 per building)
- 18 deflection gauges (6 per building)
- 2 free field incident pressure gauges
- 3 accelerometers (1 per building)
- 3 high speed cameras
- 1 4k real-time camera

Full-Scale Validation #4

Pre-test/Post-test*

*Also indicative of post-test condition.
Structures remained elastic

Validation #4 – Building V1: Front Face Reflected Pressure Gauges

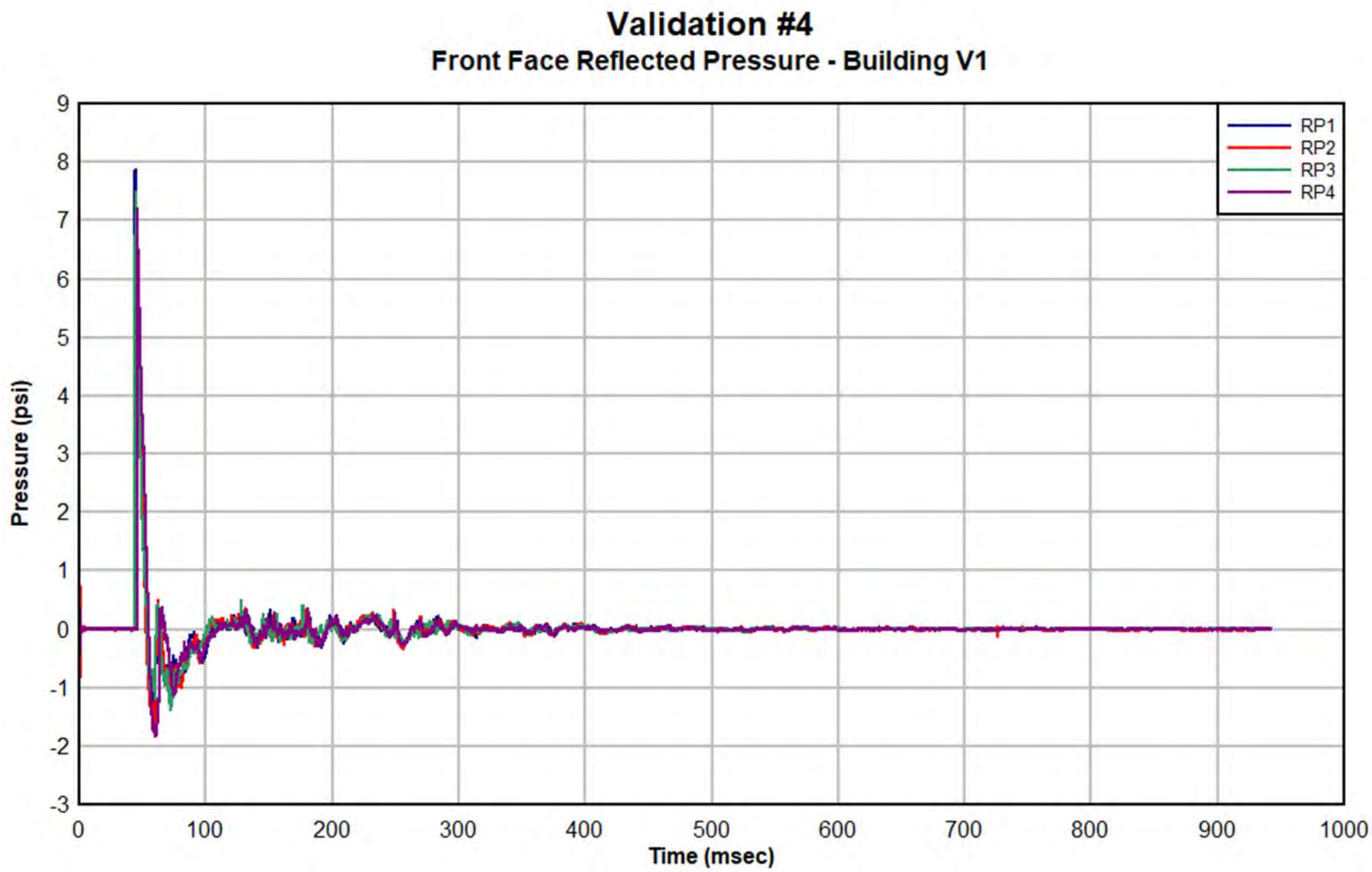

Integrity - Service - Excellence

Validation #4 – Building V1: Side Face Incident Pressure Gauges

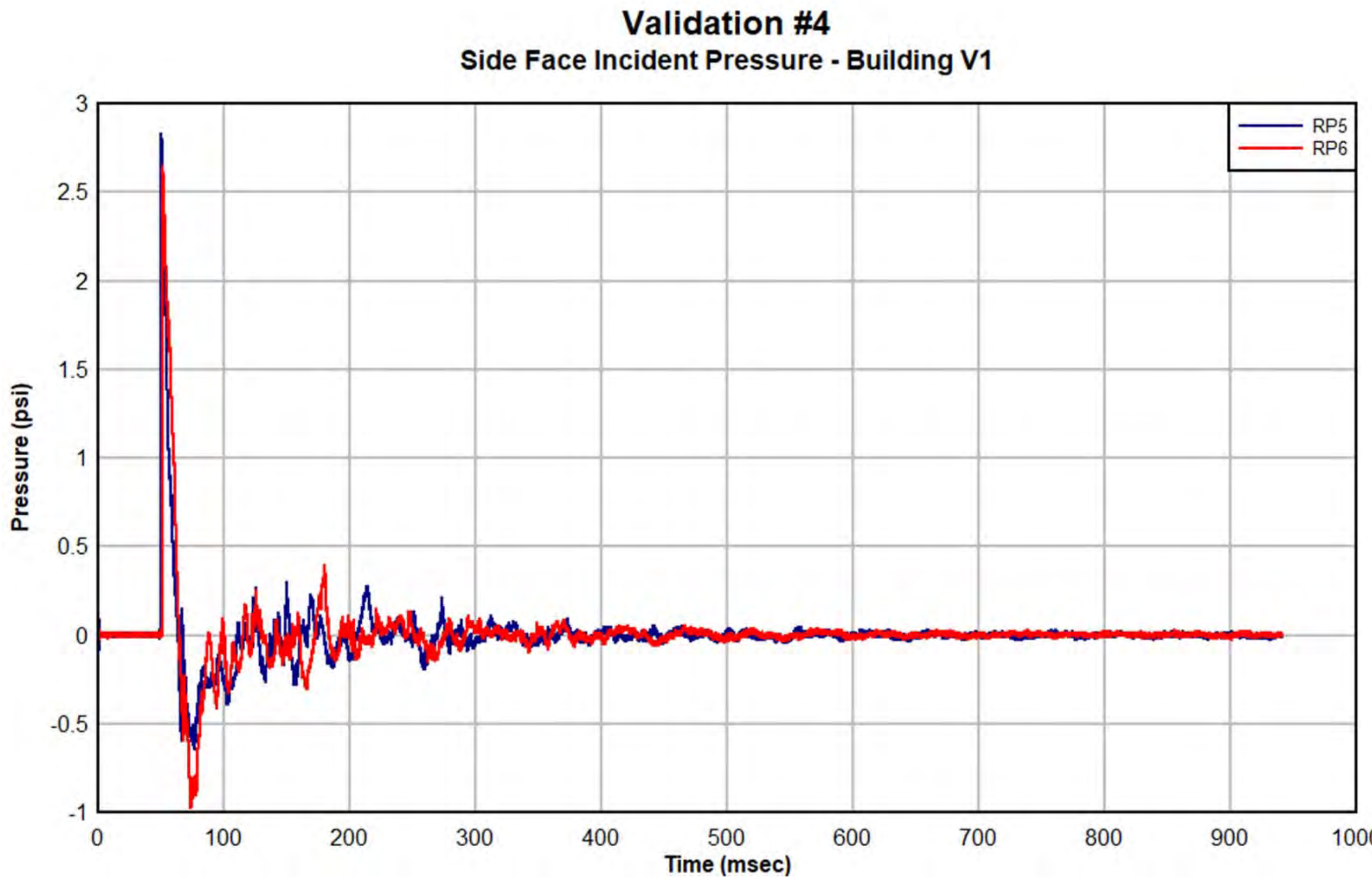

Validation #4 – Building V1: Side Face Deflection Gauges

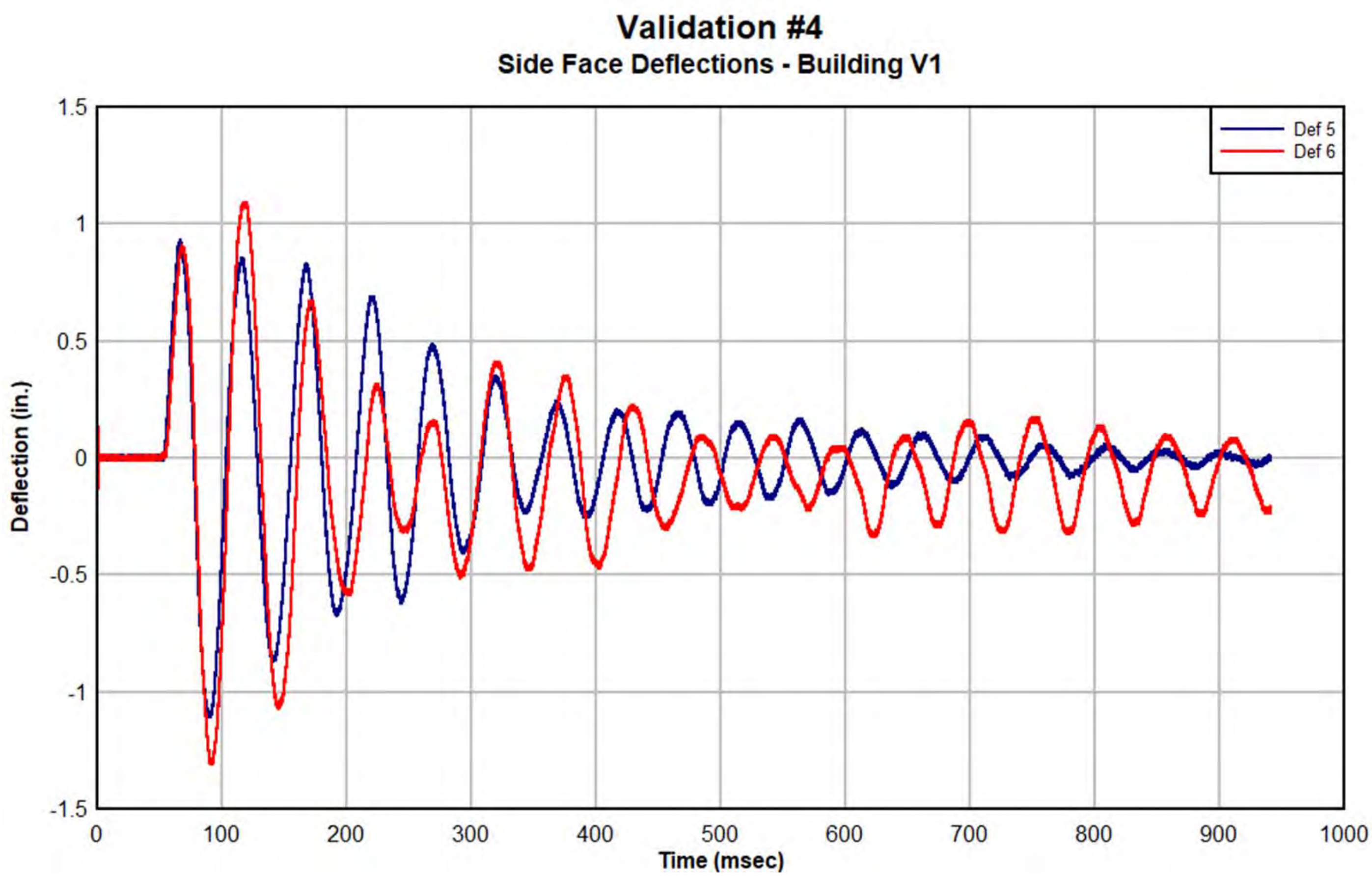

Validation #4 – Building V1: Acceleration Gauge

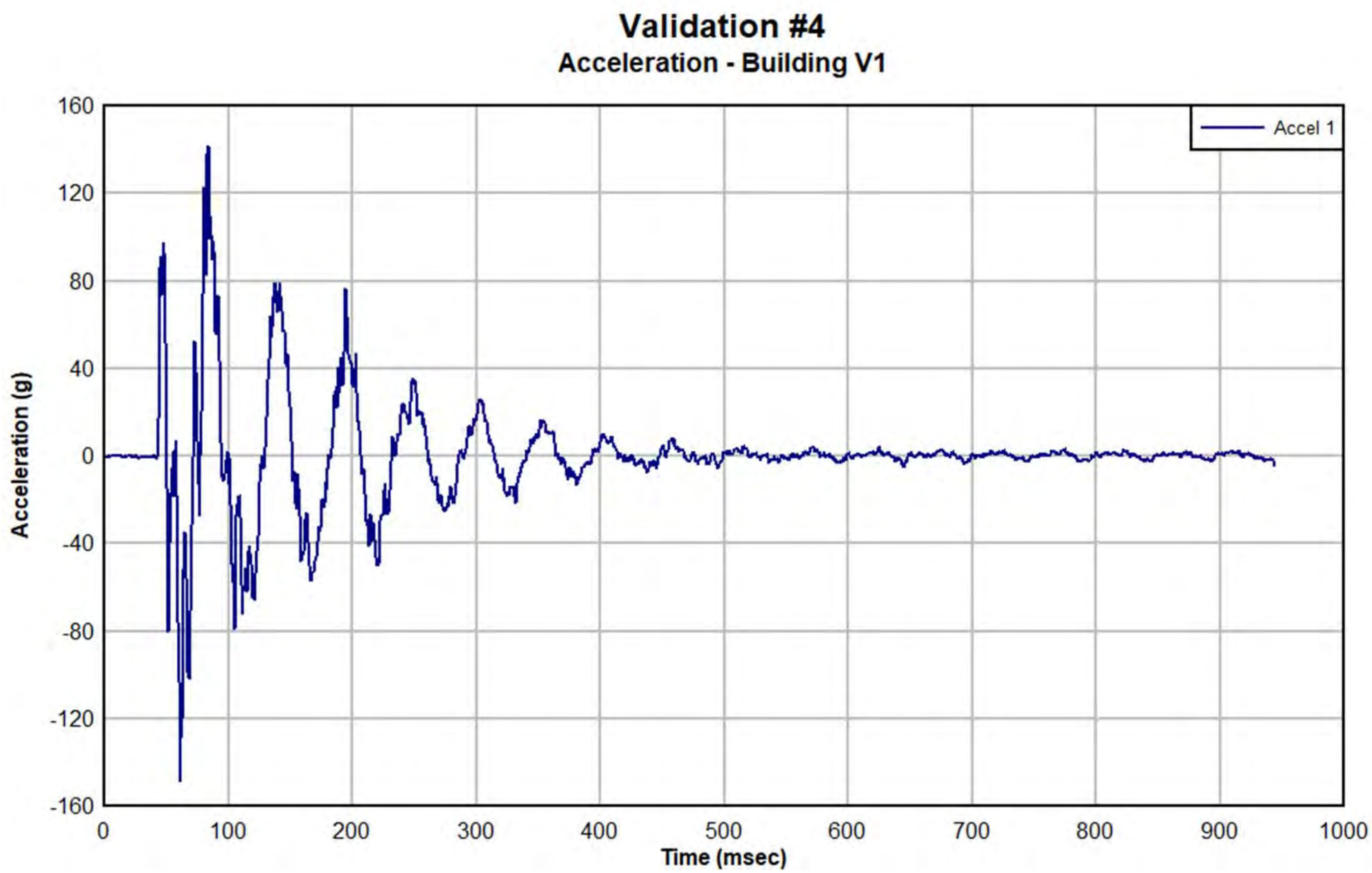

Validation #4 – Building E1: Front Face Reflected Pressure Gauges

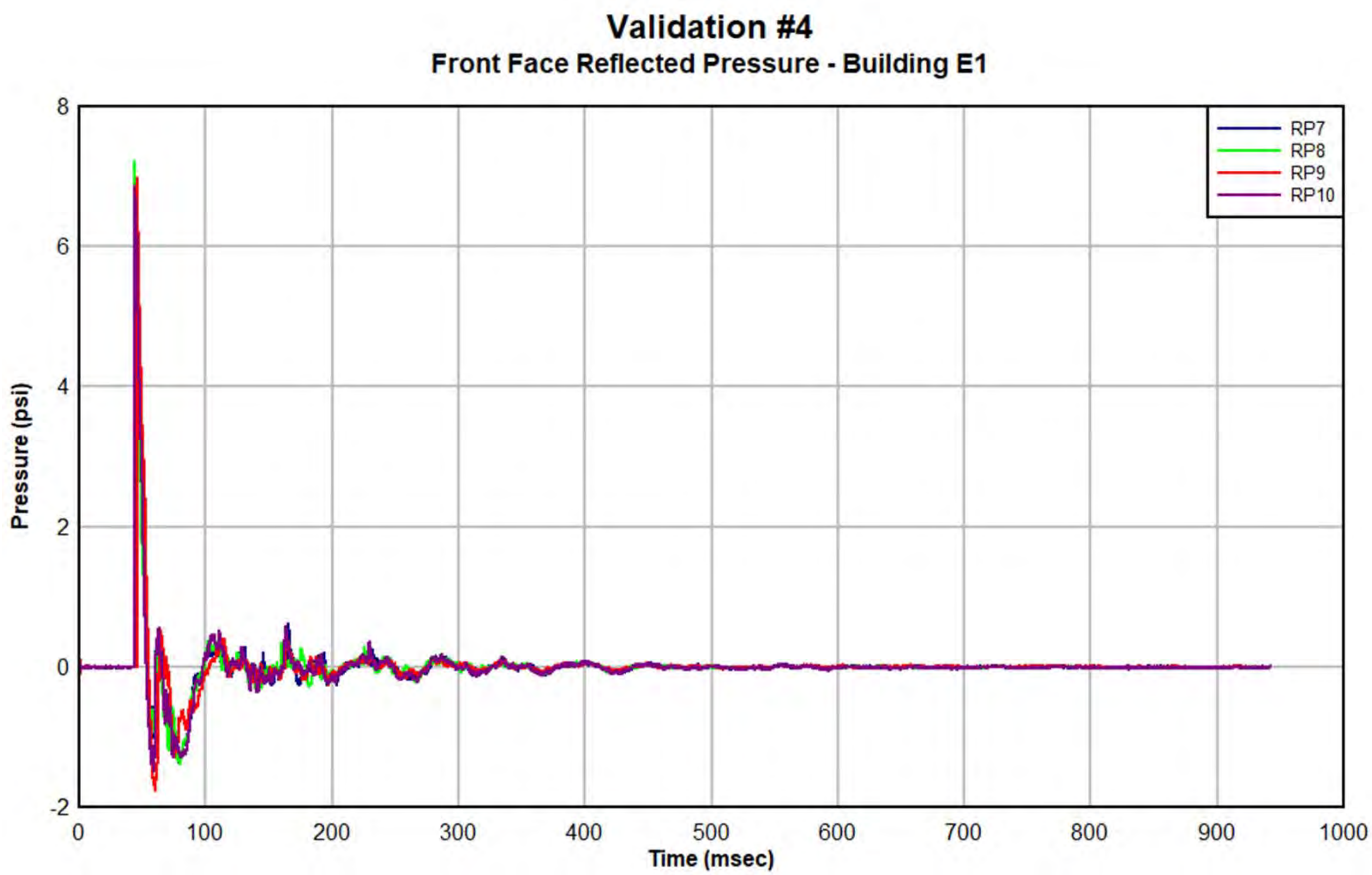

Validation #4 – Building E1: Side Face Incident Pressure Gauges

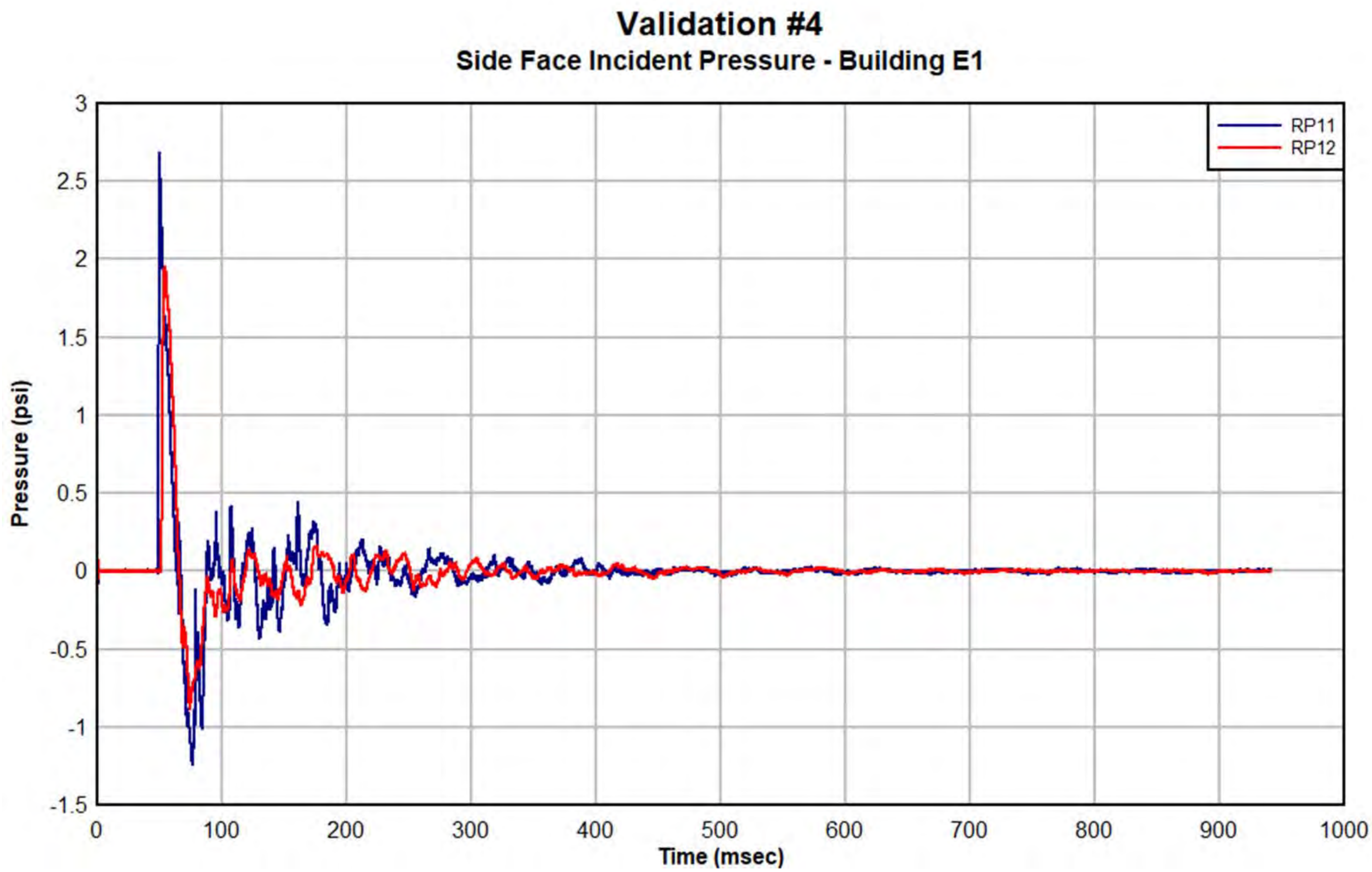

Integrity - Service - Excellence

Validation #4 – Building E1: Front Face Deflection Gauges

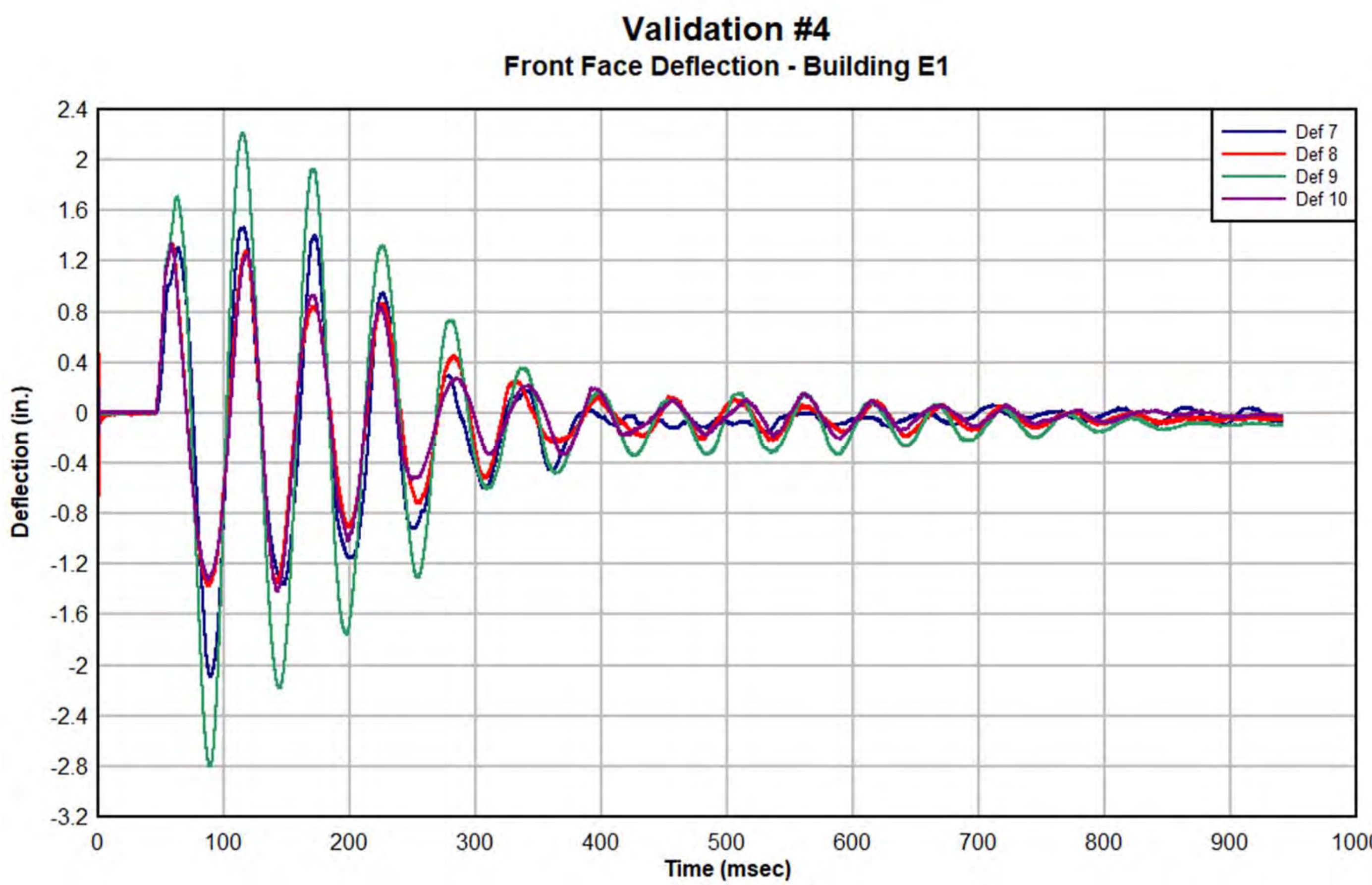

Validation #4 – Building E1: Side Face Deflection Gauges

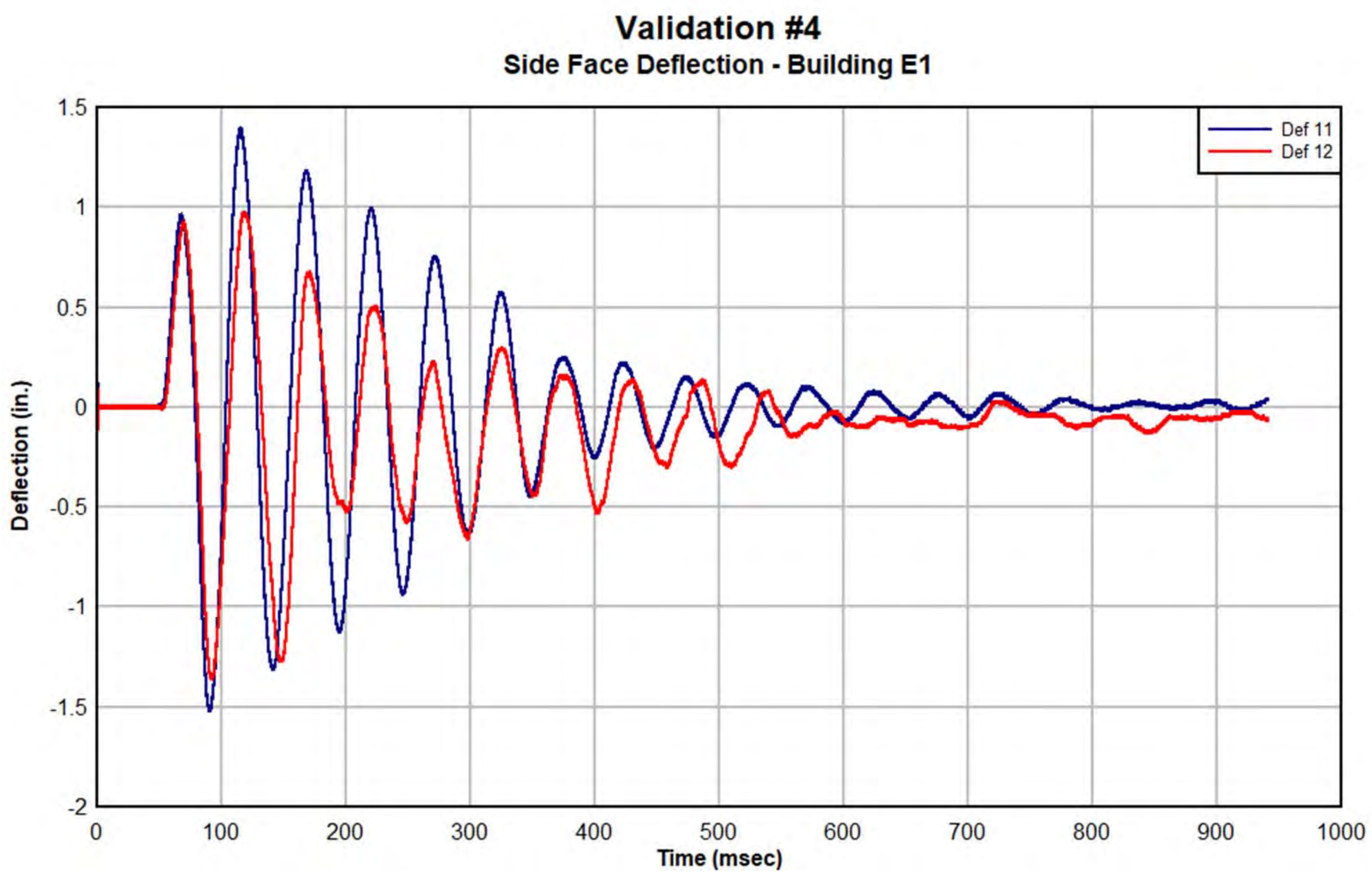

Validation #4 – Building E1: Acceleration Gauge

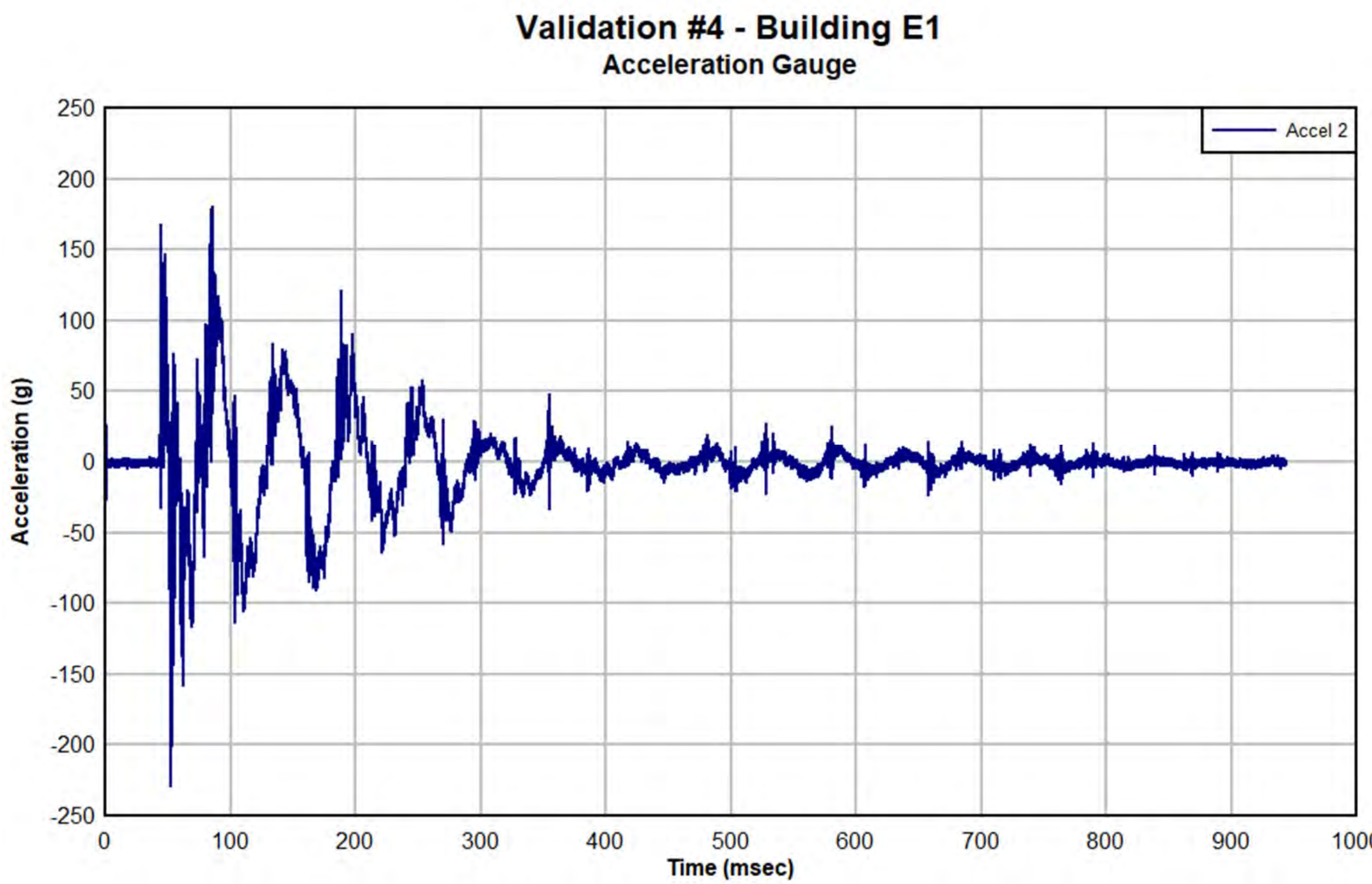

Validation #4 – Building V4: Front Face Reflected Pressure Gauges

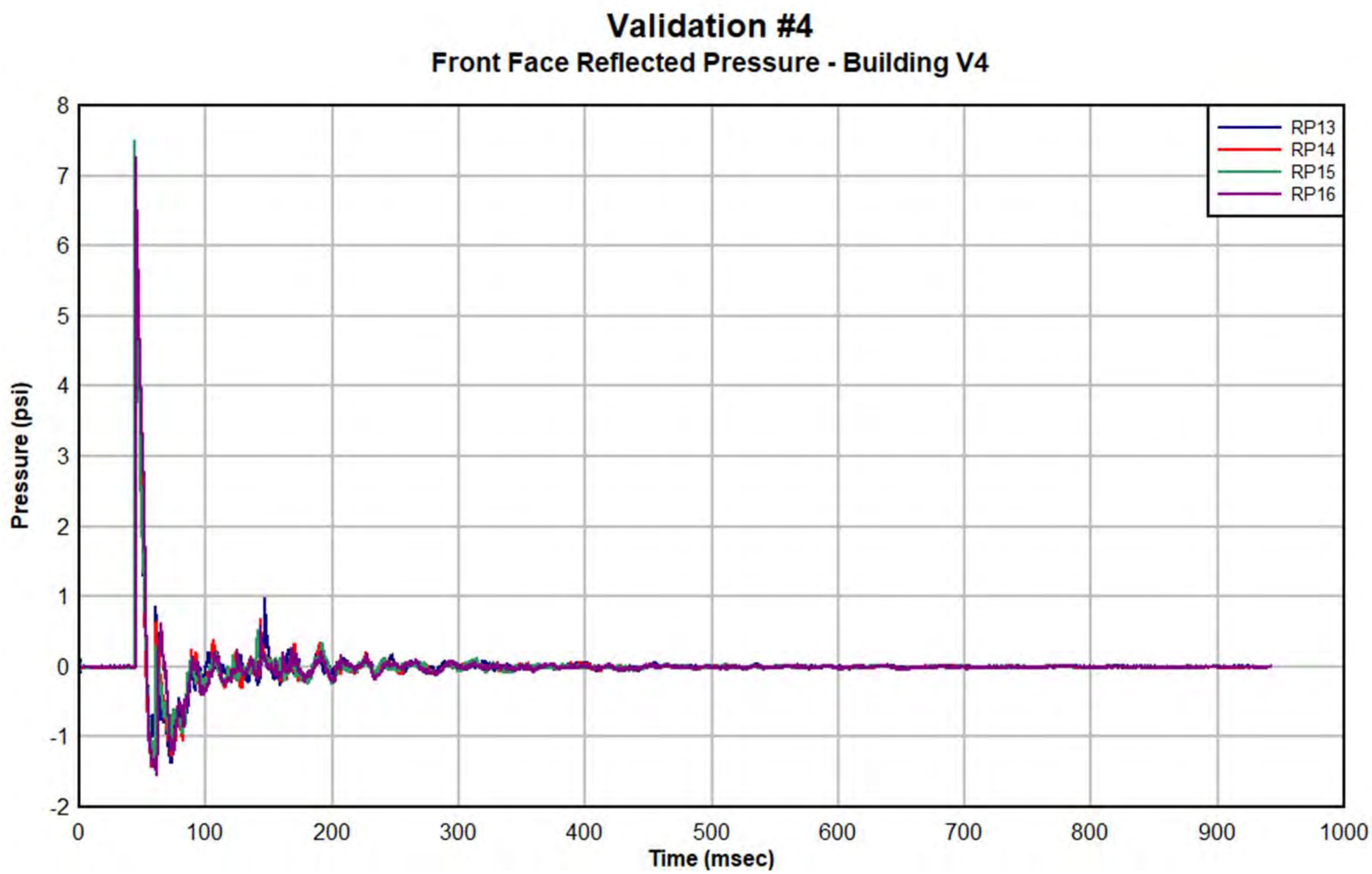

Validation #4 – Building V4: Side Face Incident Pressure Gauges

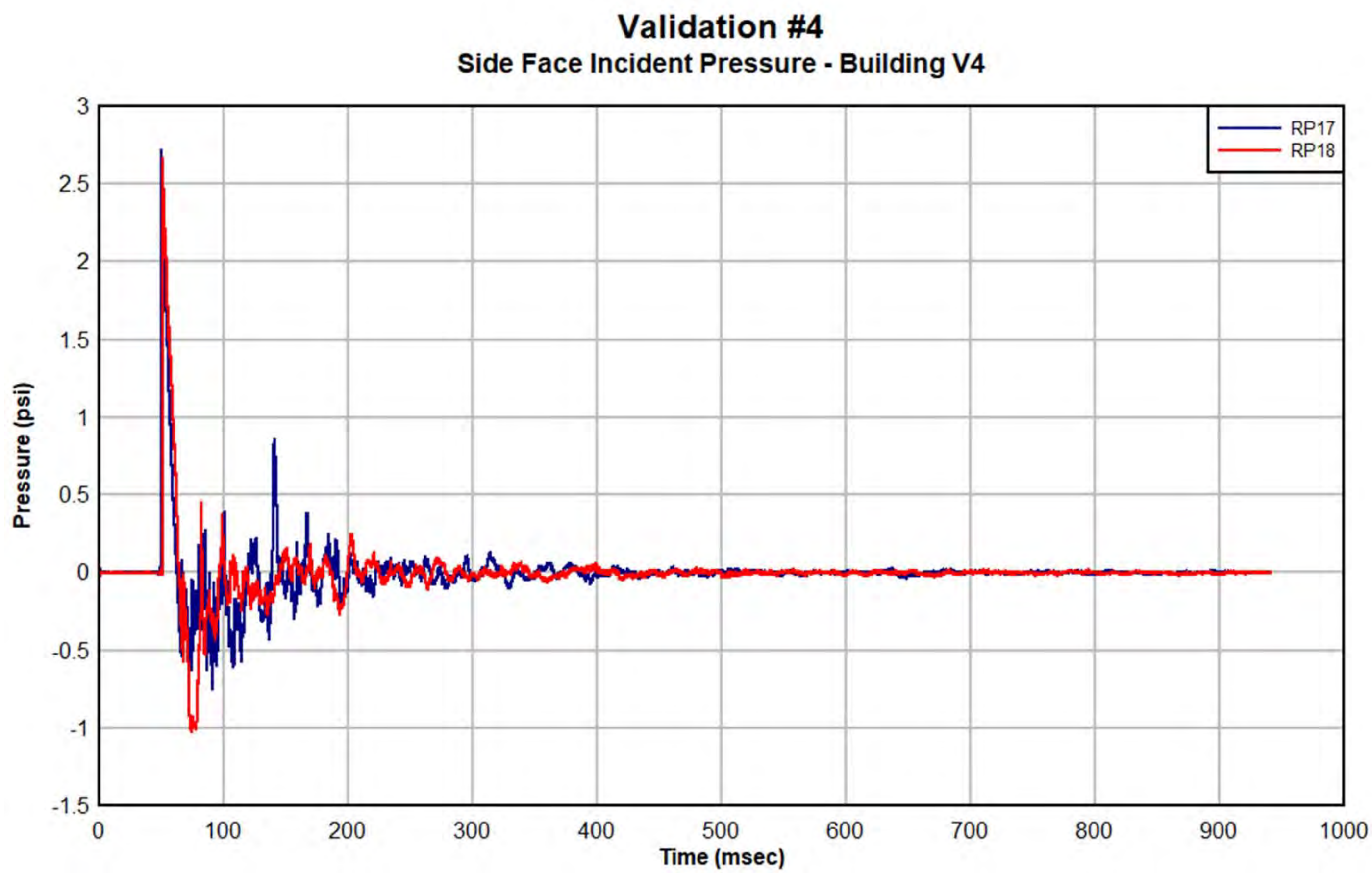

Validation #4 – Building V4: Front Face Deflection Gauges

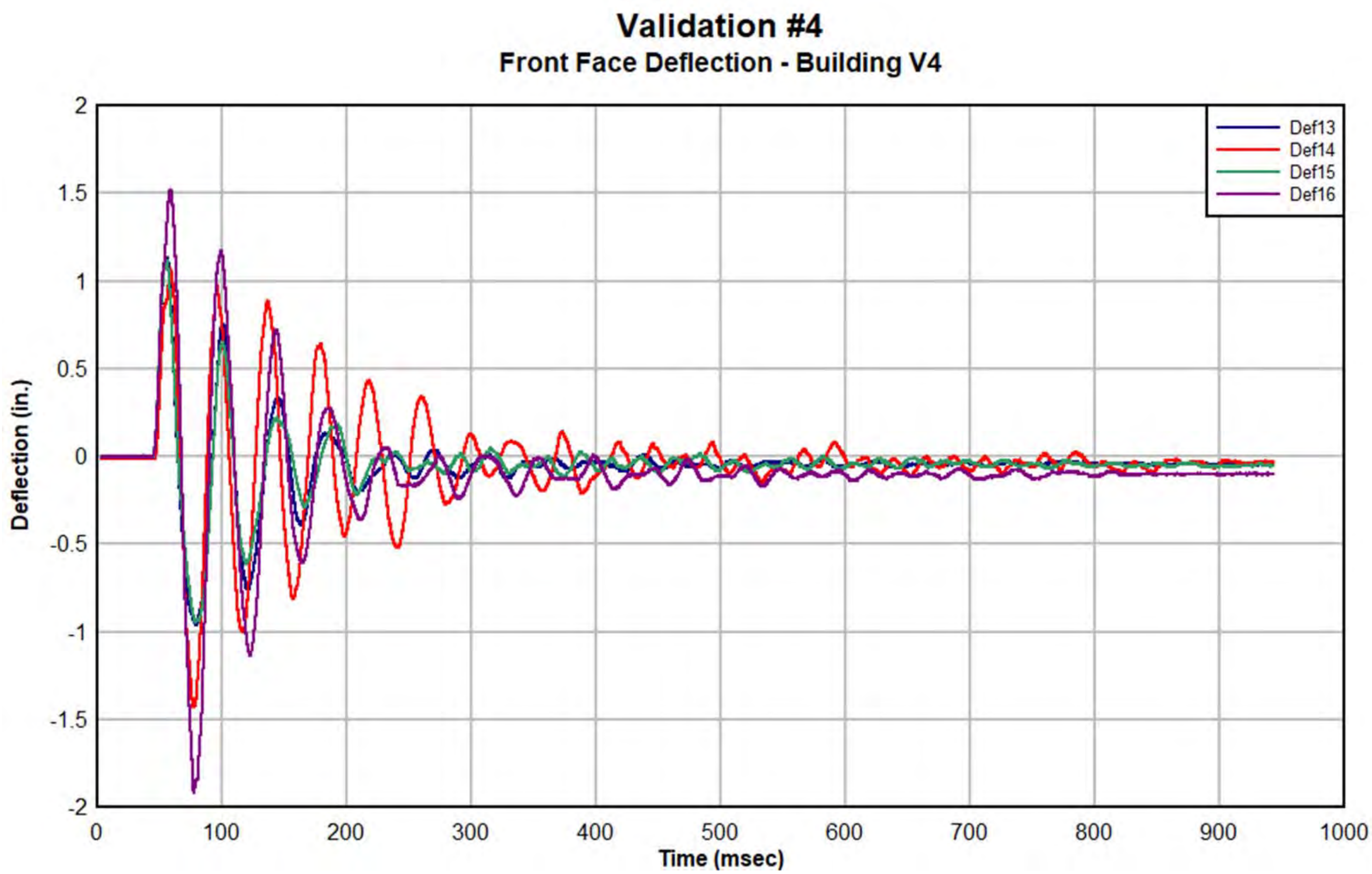

Validation #4 – Building V4: Side Face Deflection Gauges

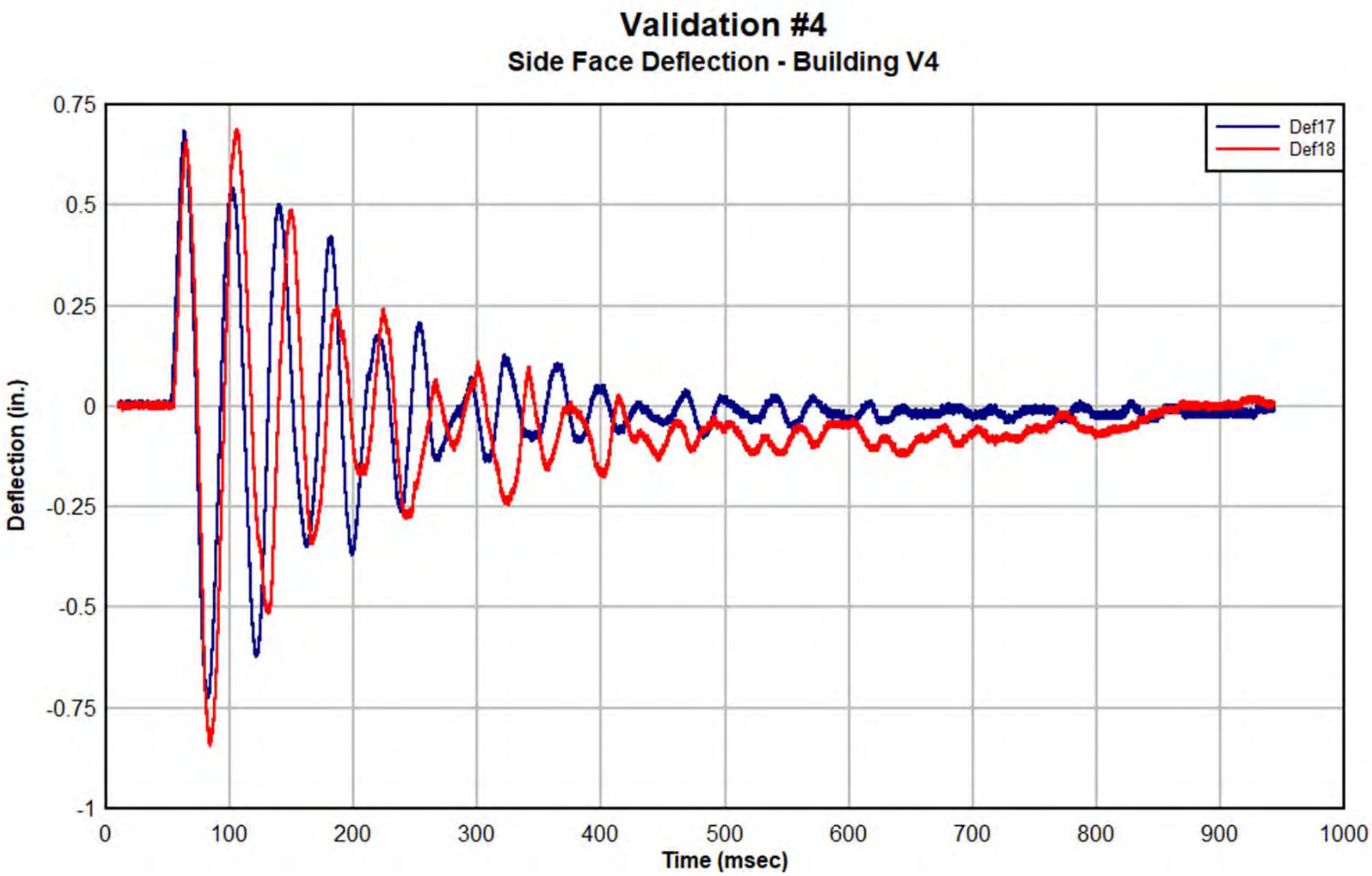

Validation #4 – Building V4: Acceleration Gauge

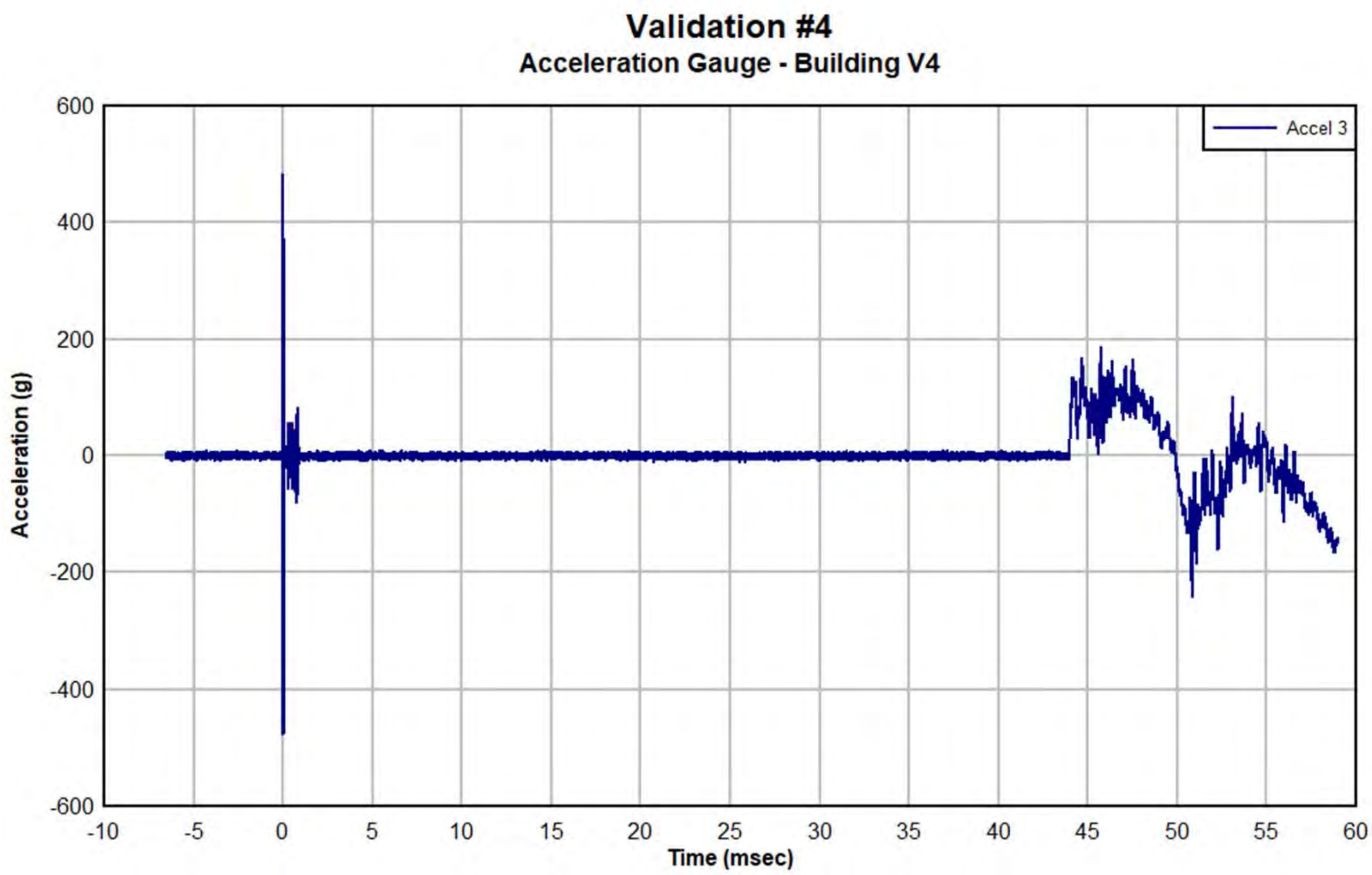

Integrity - Service - Excellence

Validation #4: Free Field Incident Pressure Gauges

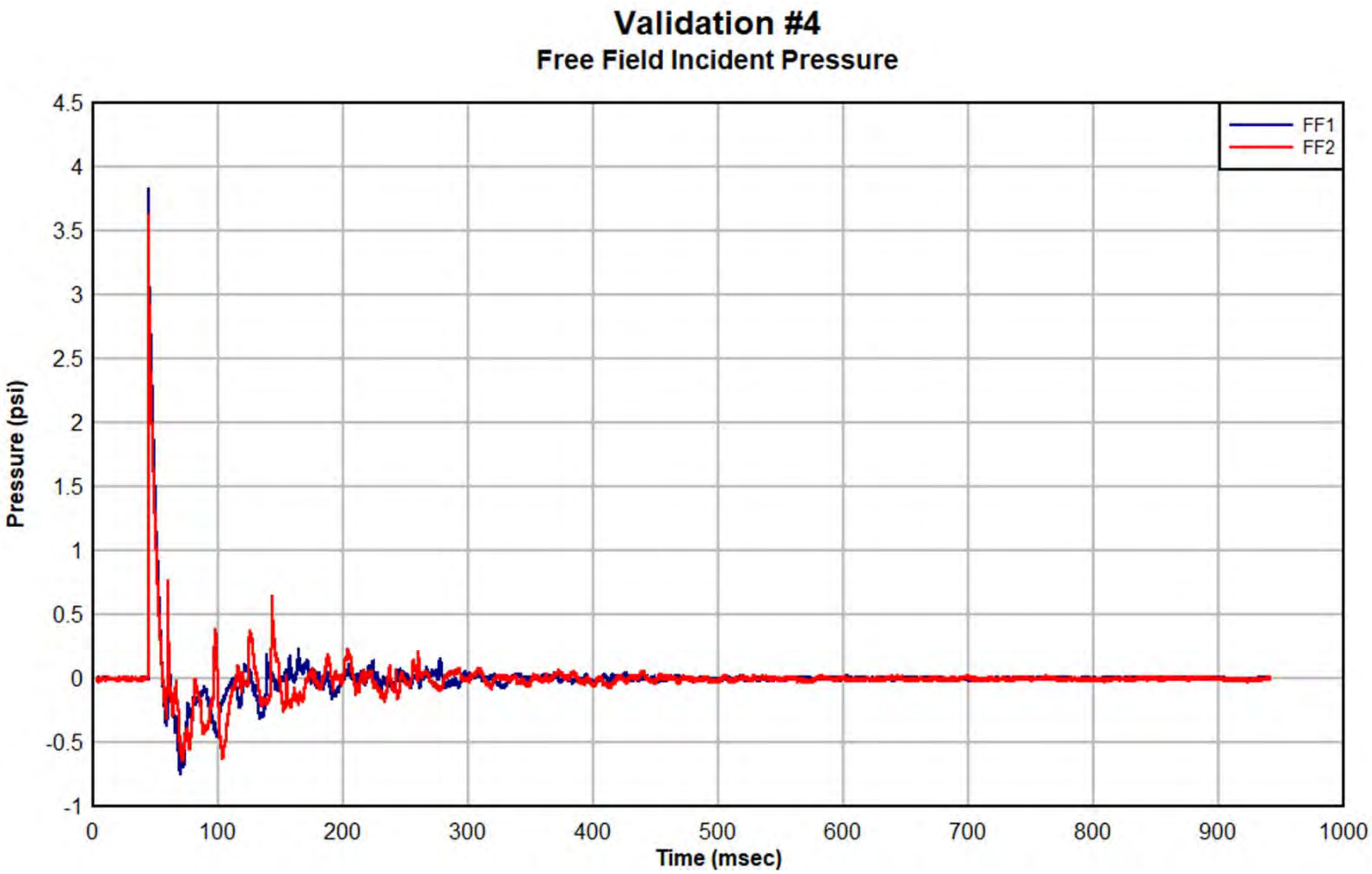

Full-Scale Validation #5

Post-test

Validation #5 – Building V1: Front Face Reflected Pressure Gauges

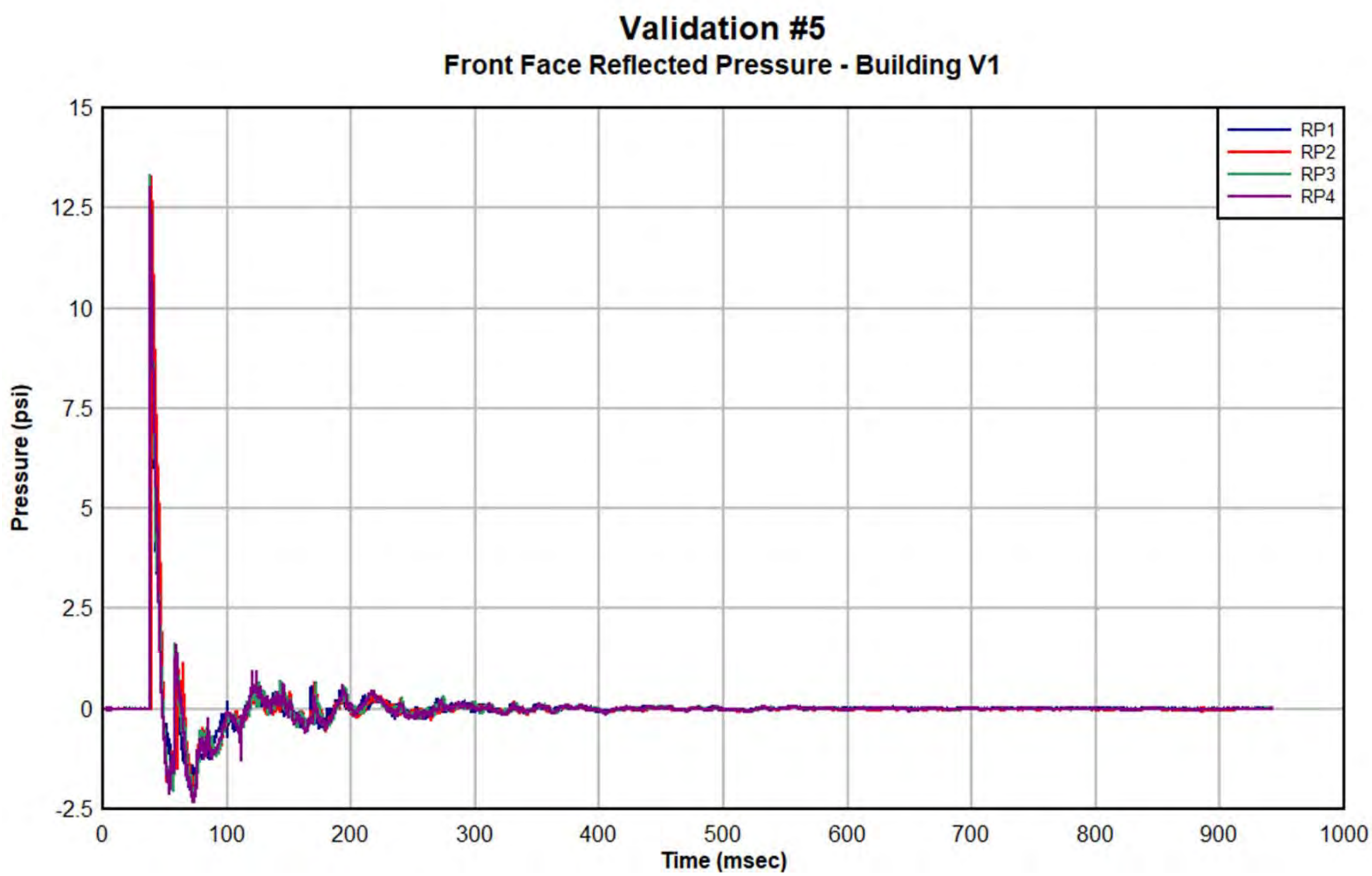

Integrity - Service - Excellence

Validation #5 – Building V1: Side Face Incident Pressure Gauges

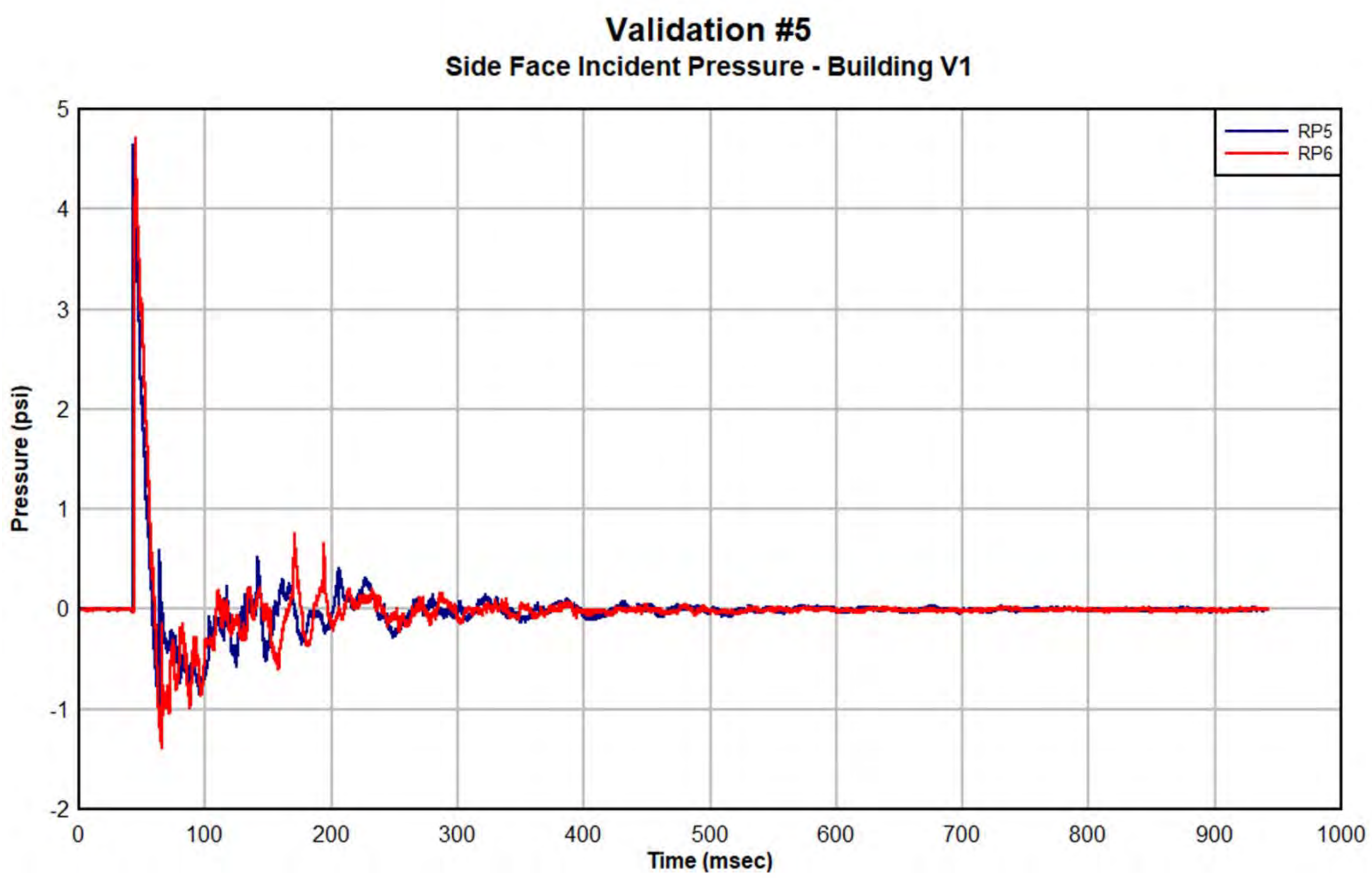

Validation #5 – Building V1: Front Face Deflection Gauges

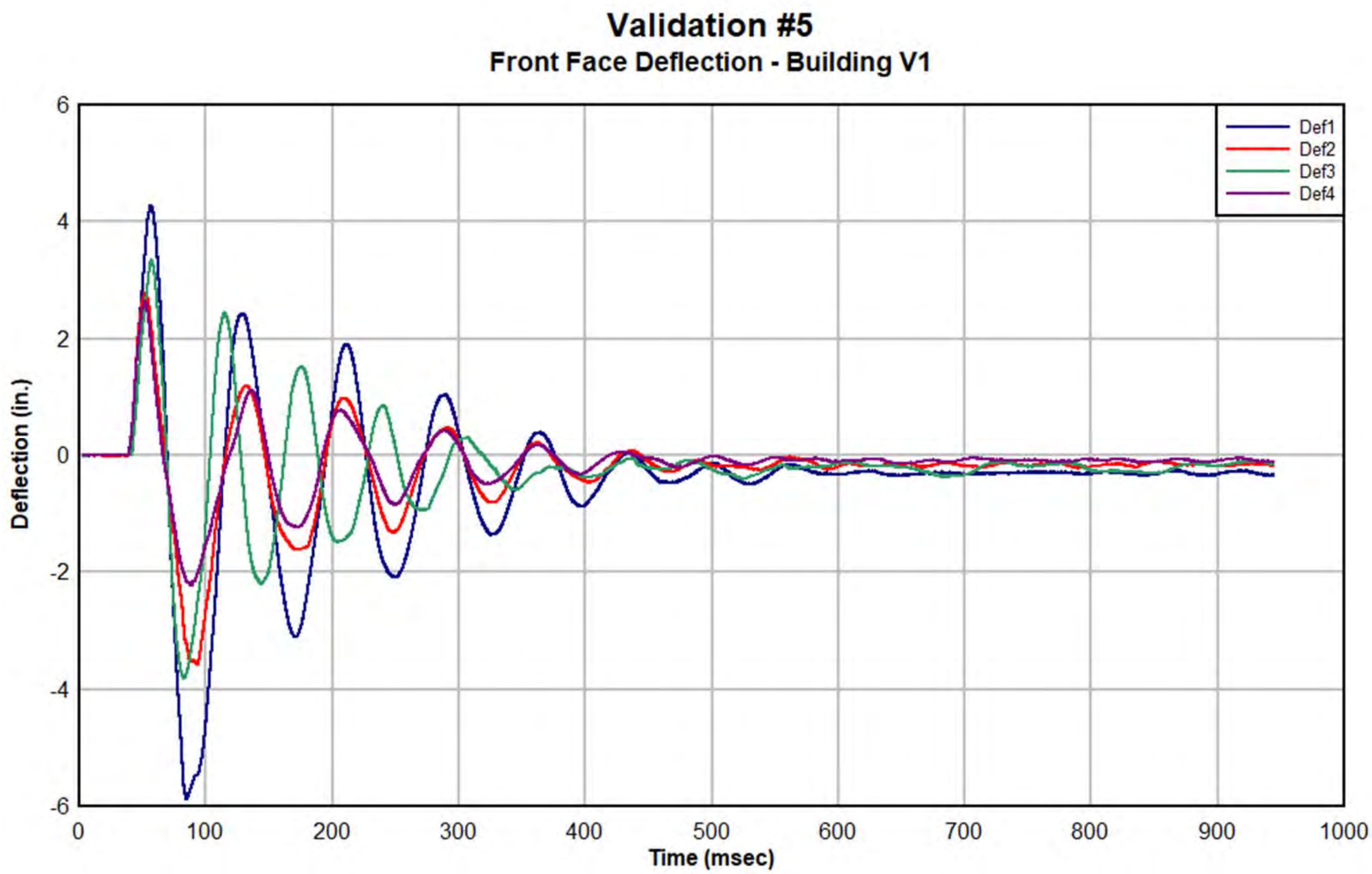

Integrity - Service - Excellence

Validation #5 – Building V1: Left Side Face Deflection Gauges

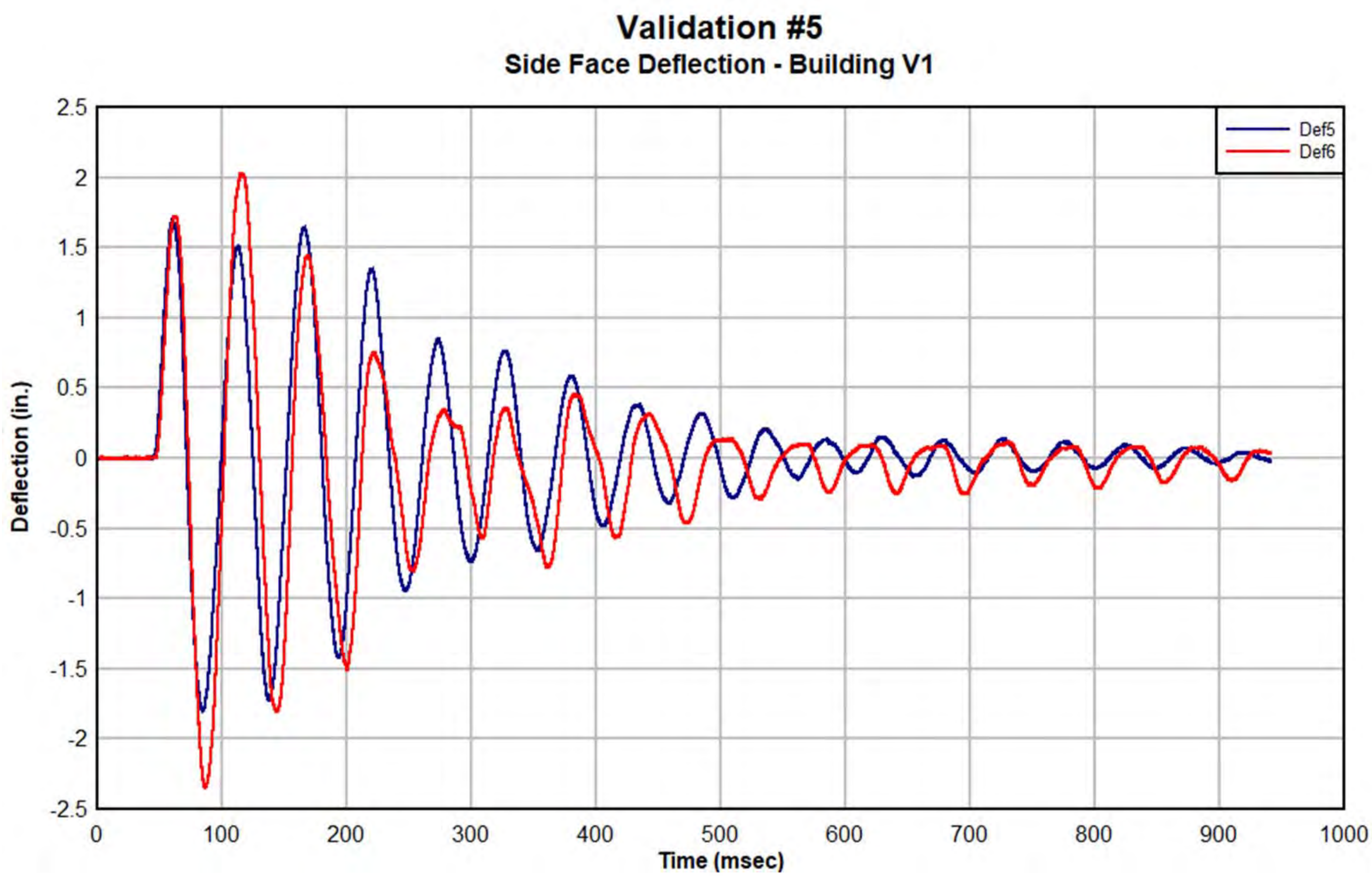

Validation #5 – Building V1: Acceleration Gauge

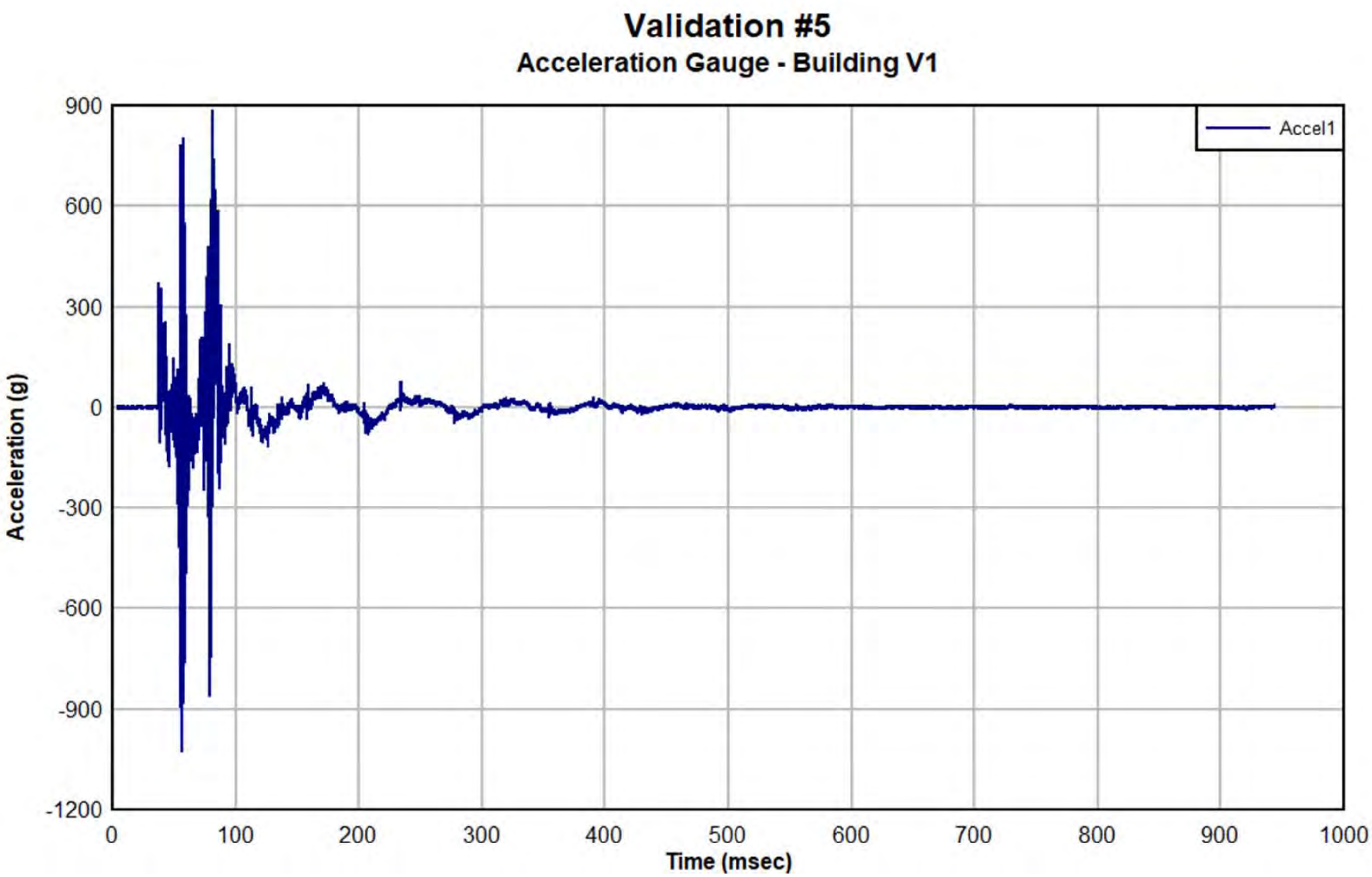

Integrity - Service - Excellence

Validation #5 – Building E1: Front Face Reflected Pressure Gauges

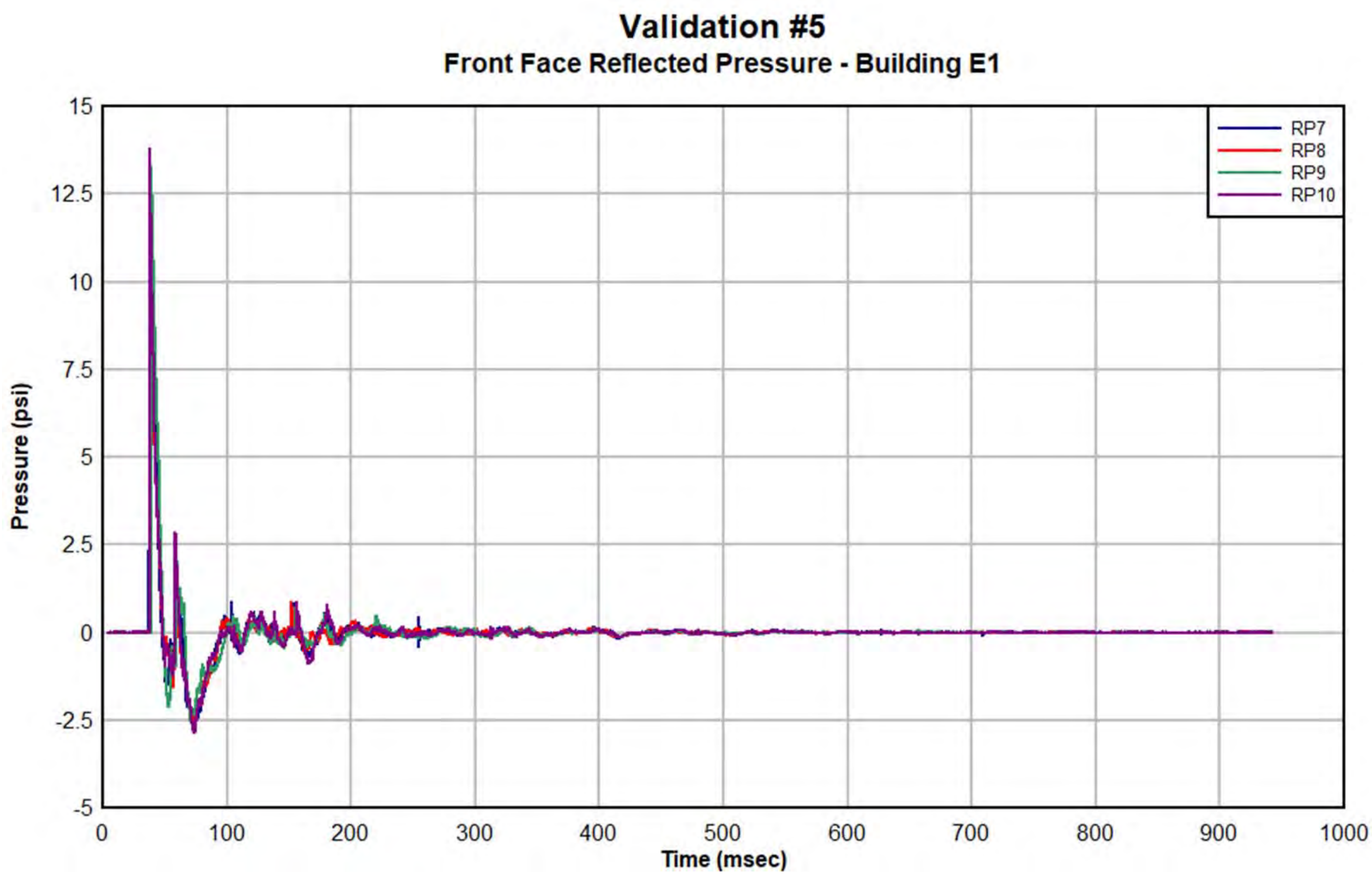

Validation #2 – Building E1: Side Face Incident Pressure Gauges

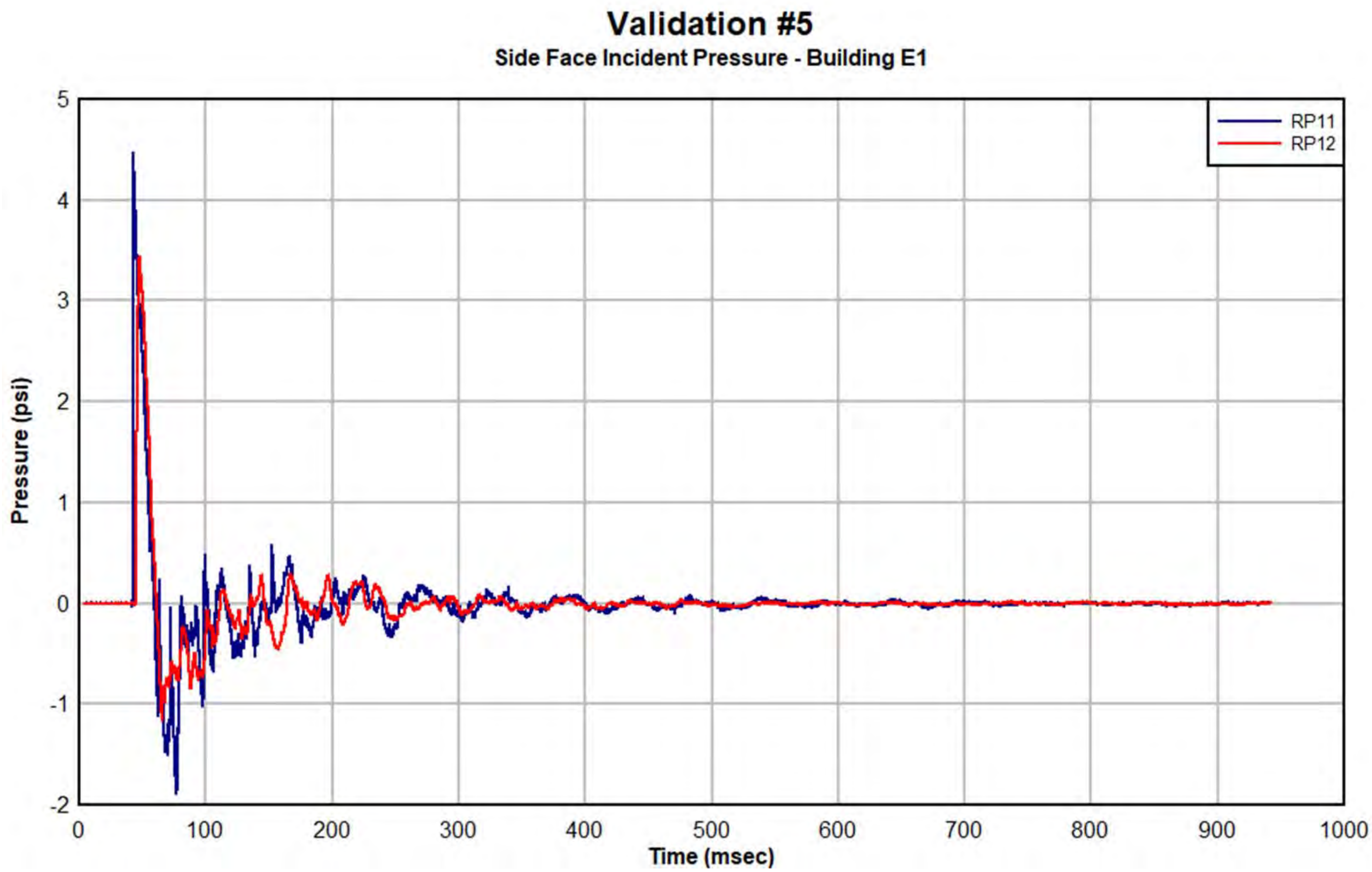

Validation #5 – Building E1: Front Face Deflection Gauges

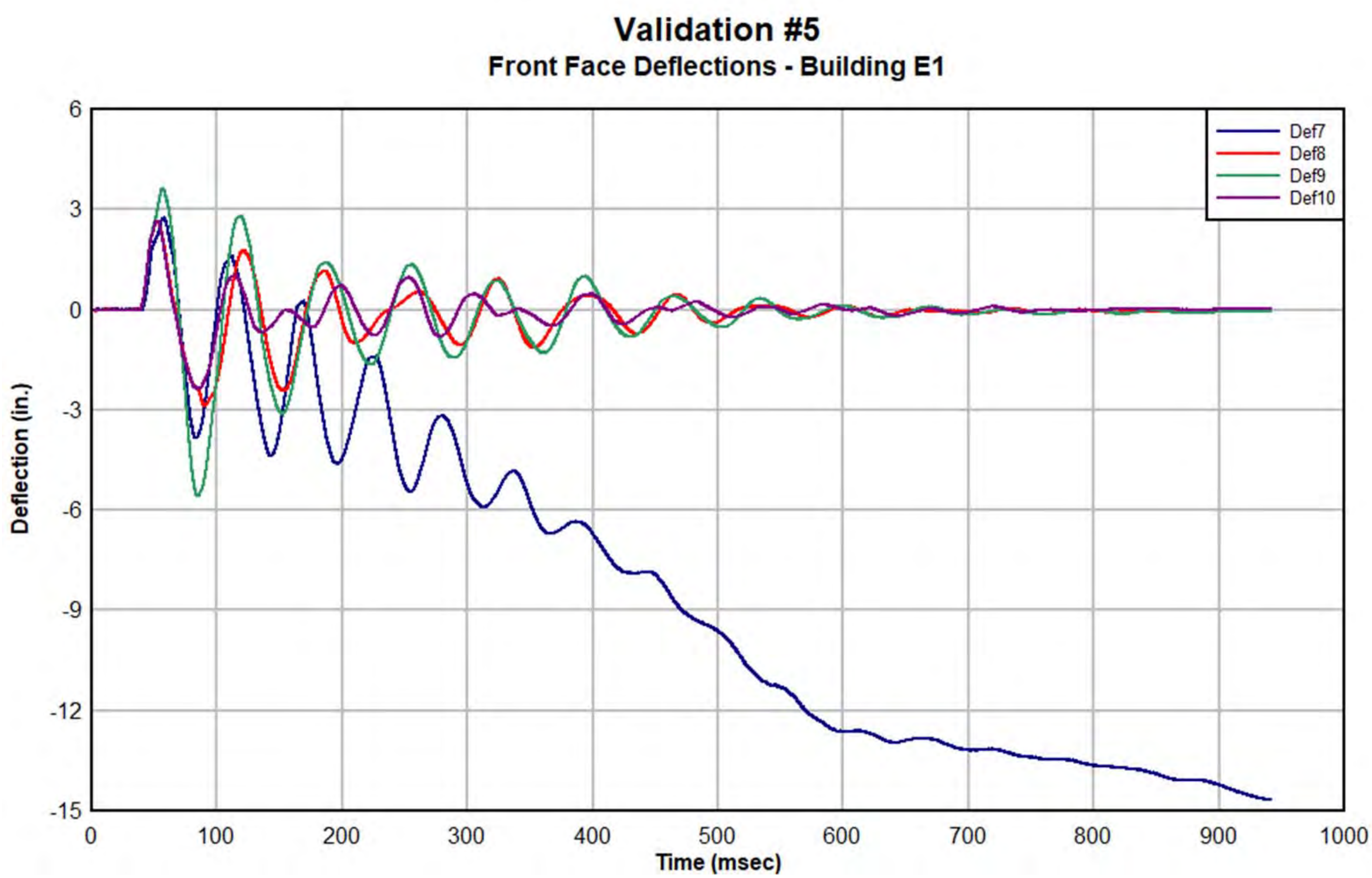

Integrity - Service - Excellence

Validation #5 – Building E1: Side Face Deflection Gauges

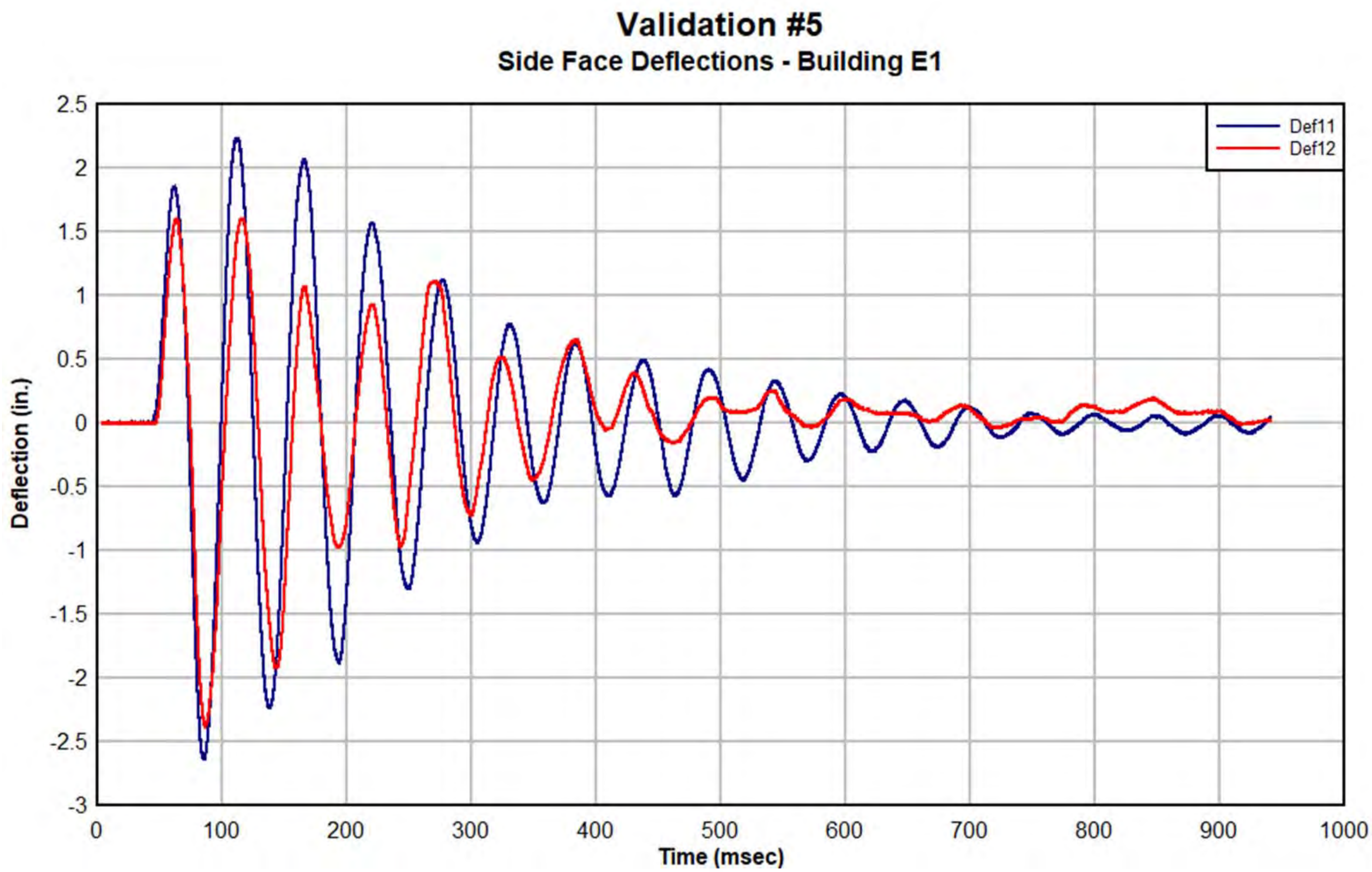

Validation #5 – Building E1: Acceleration Gauge

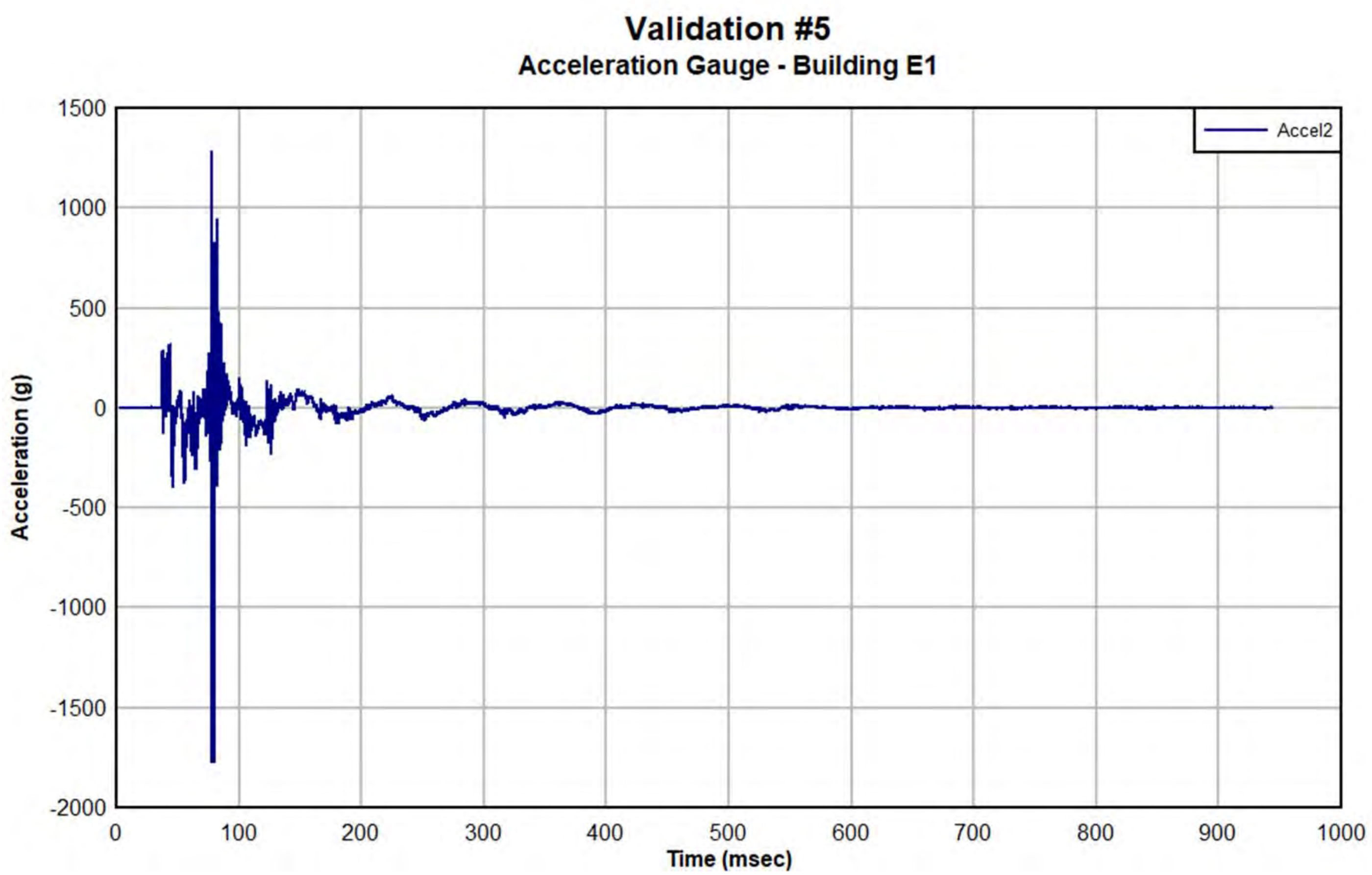

Validation #5 – Building V4: Front Face Reflected Pressure Gauges

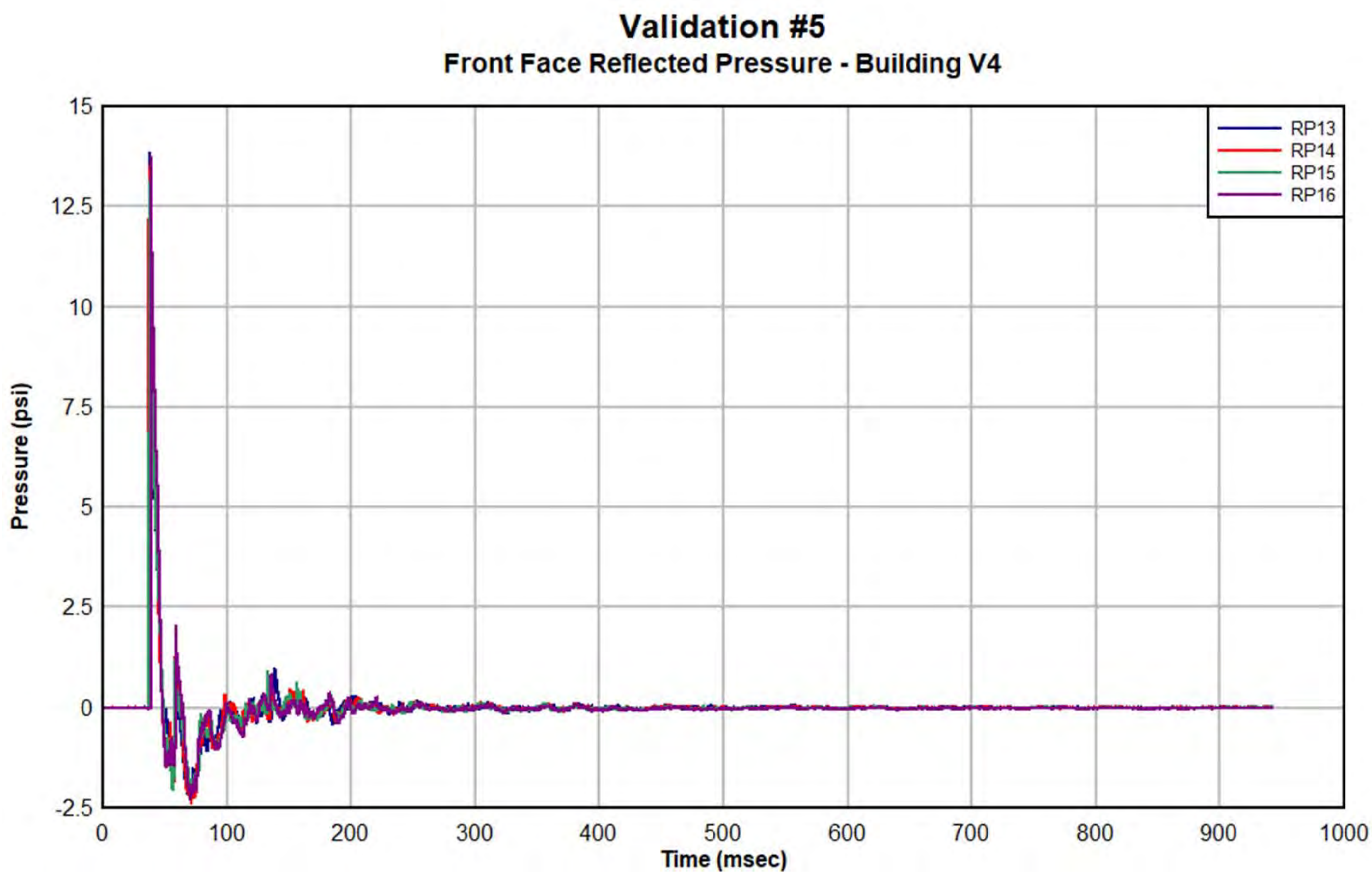

Validation #5 – Building V4: Side Face Incident Pressure Gauges

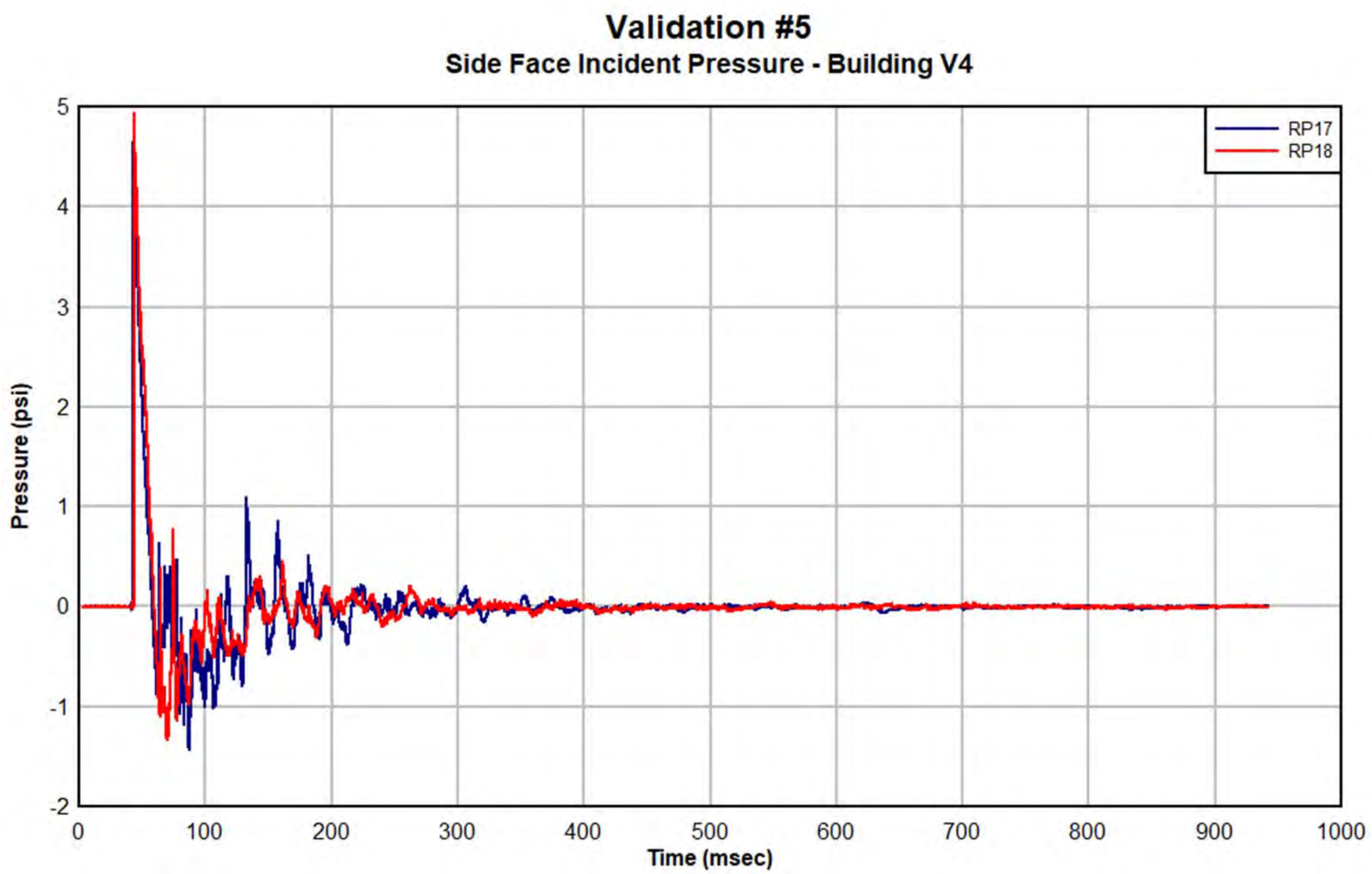

Validation #5 – Building V4: Front Face Deflection Gauges

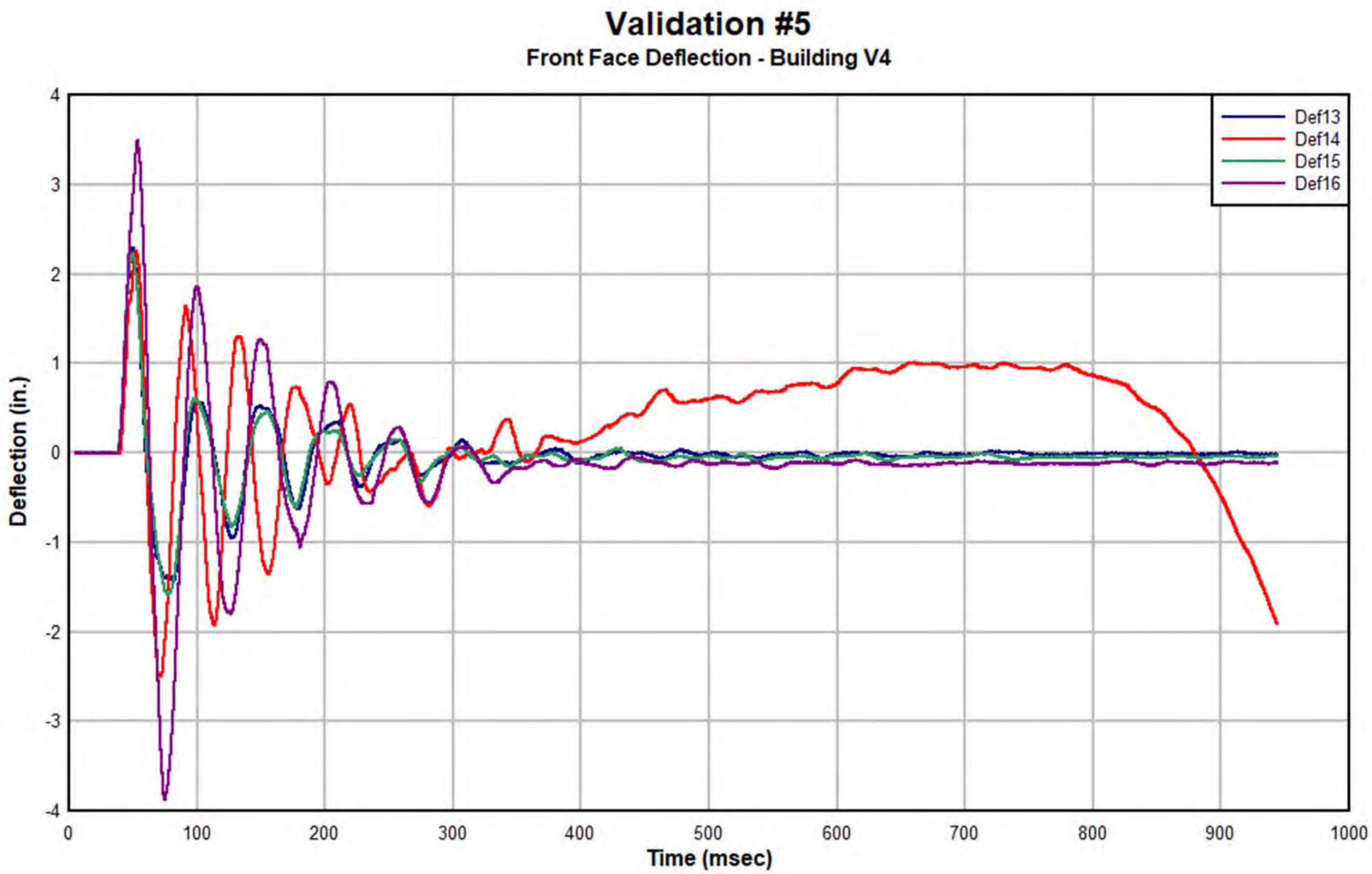

Validation #5 – Building V4: Side Face Deflection Gauges

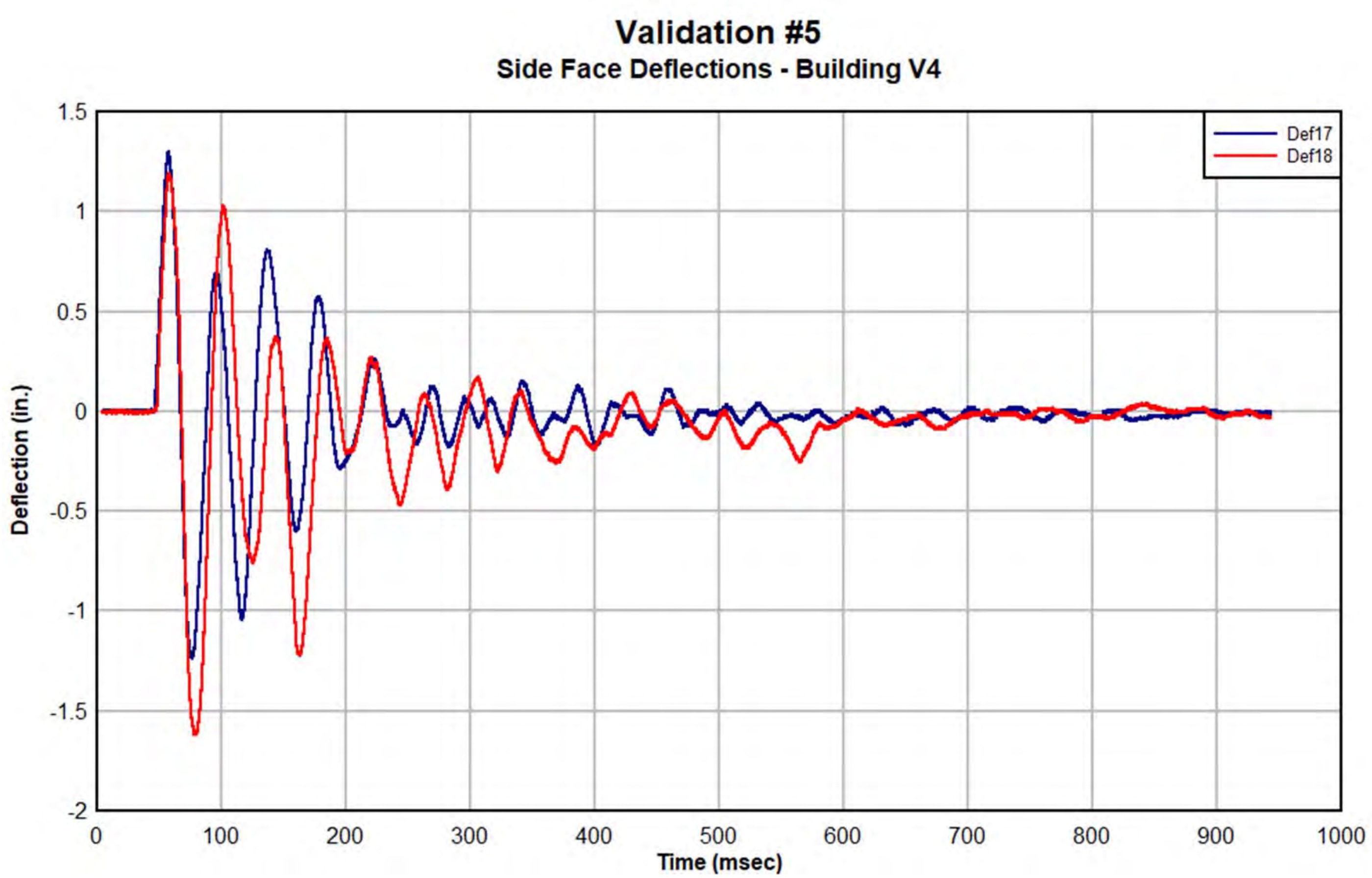

Validation #5 – Building V4: Acceleration Gauge

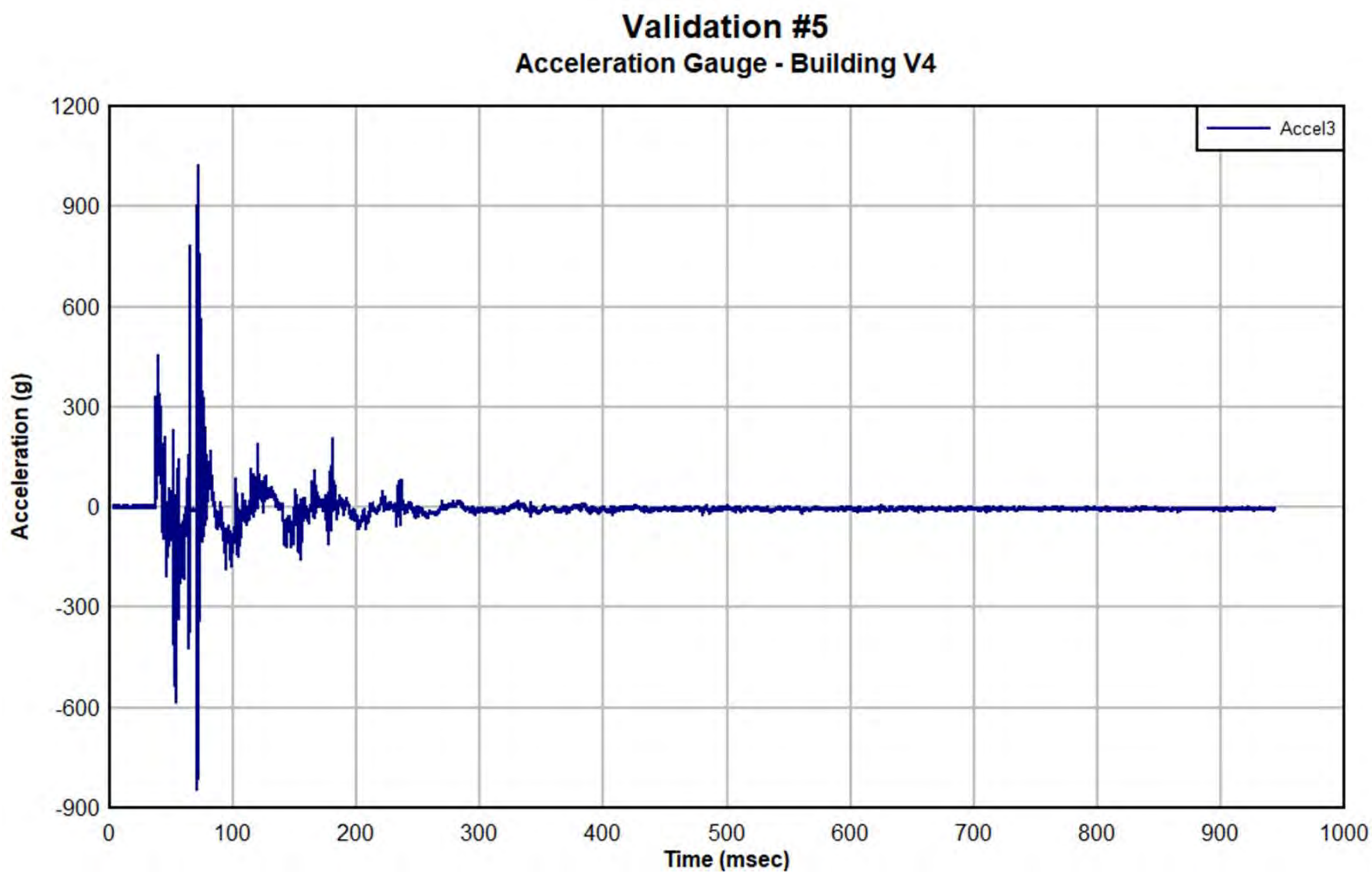

Validation #5: Free Field Incident Pressure Gauges

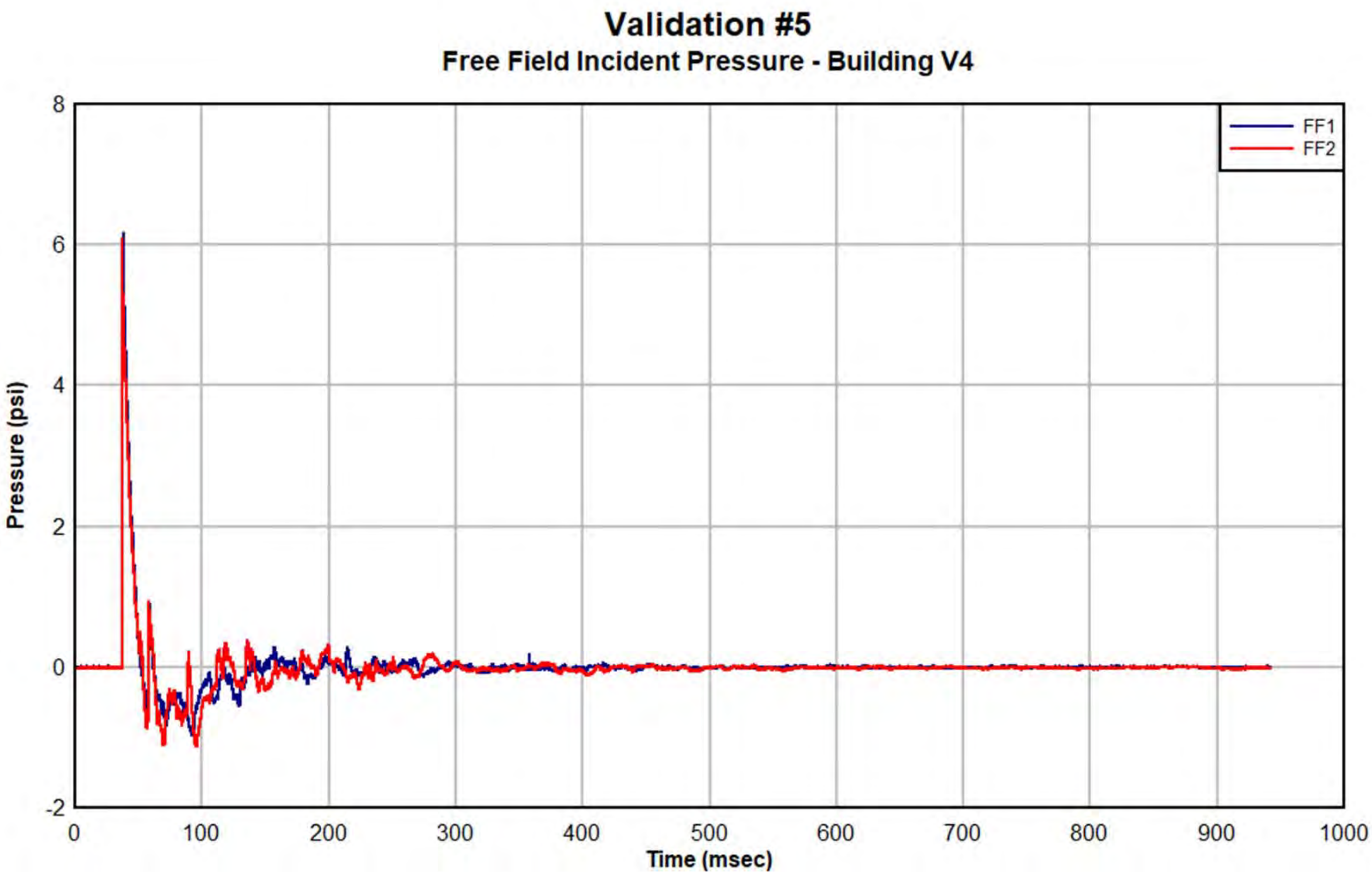

Full-Scale Validation #6

Post-test

Validation #6 – Building V1: Front Face Reflected Pressure Gauges

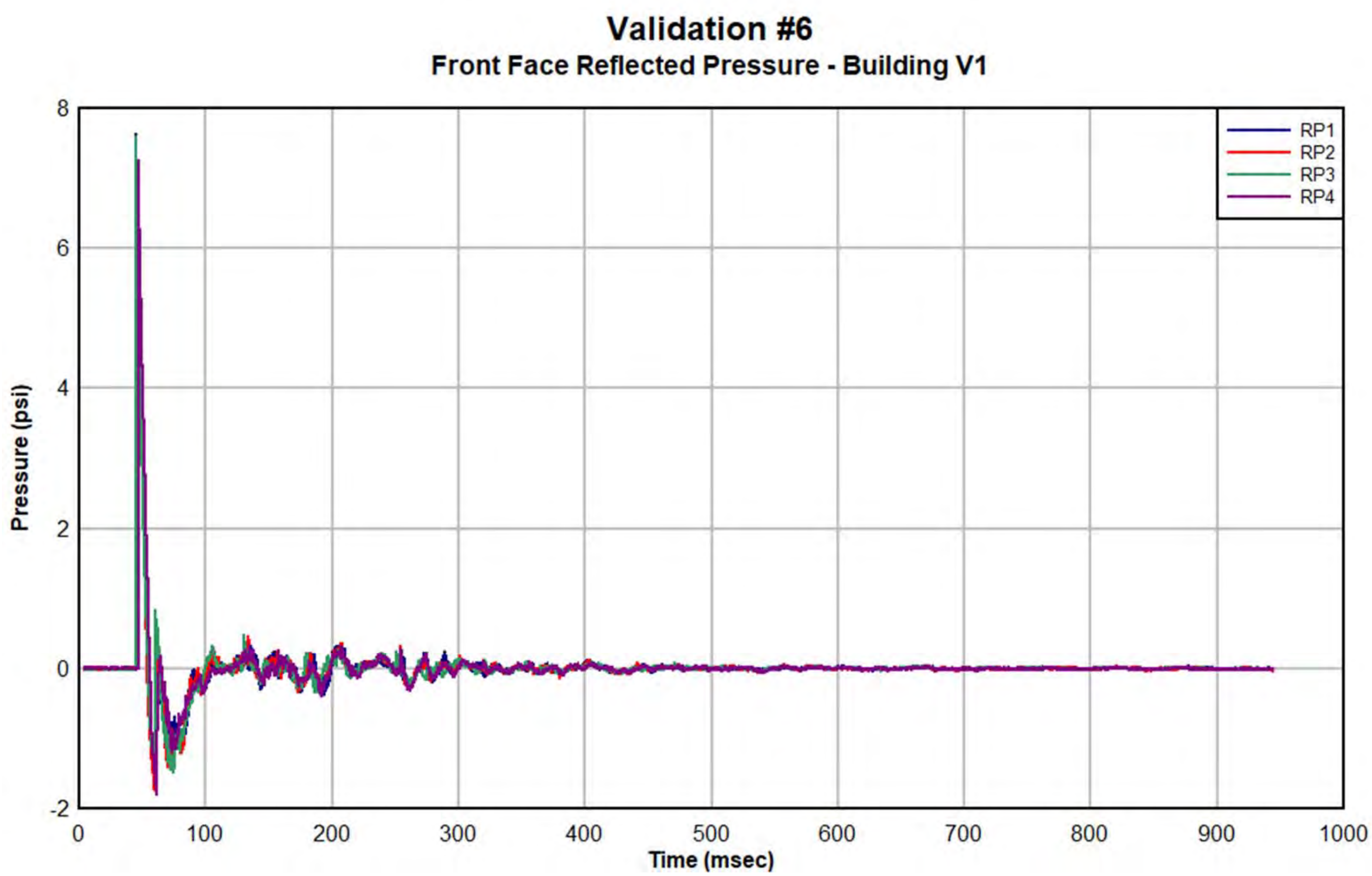

Validation #6 – Building V1: Side Face Incident Pressure Gauges

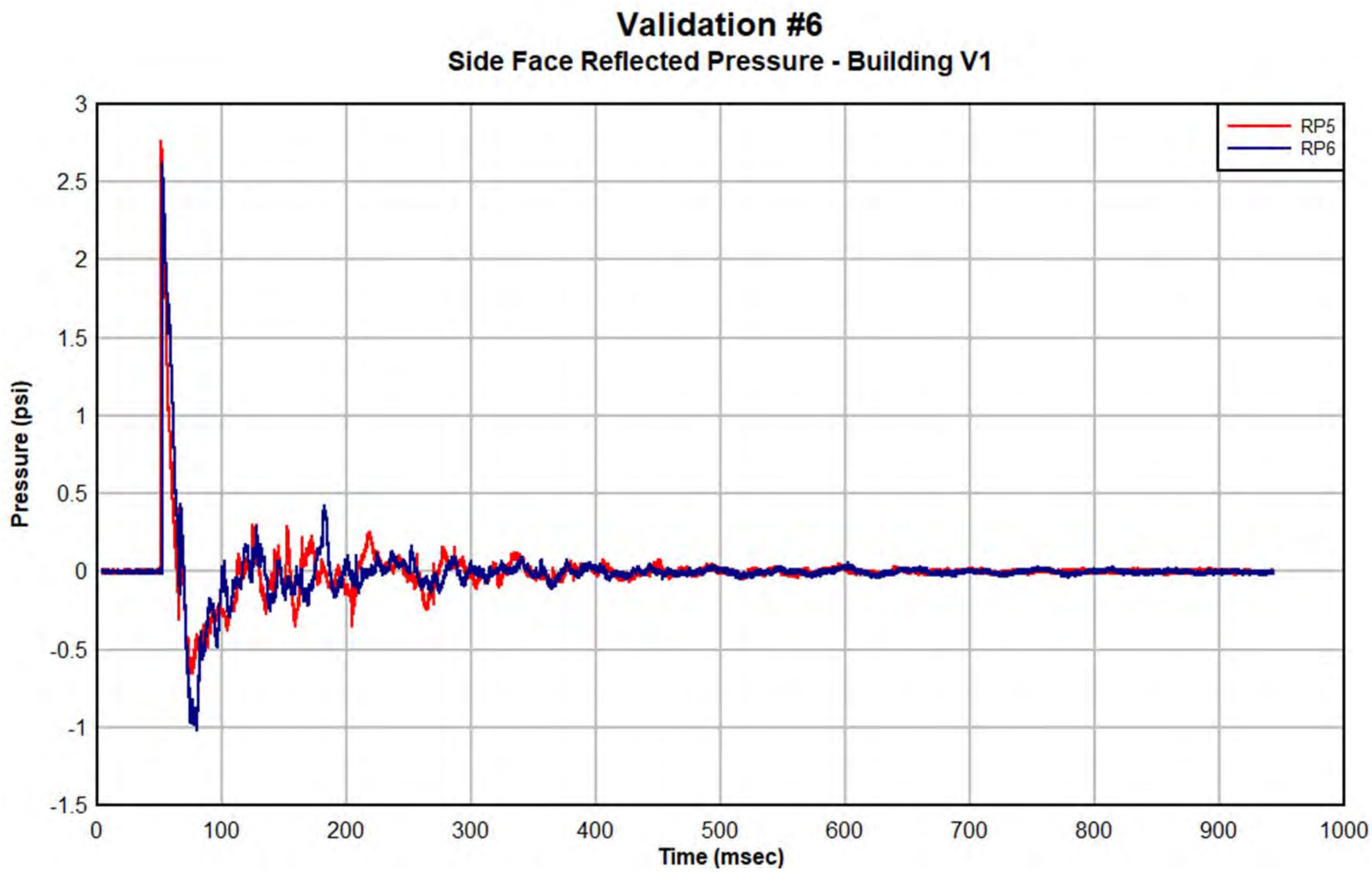

Validation #6 – Building V1: Front Face Deflection Gauges

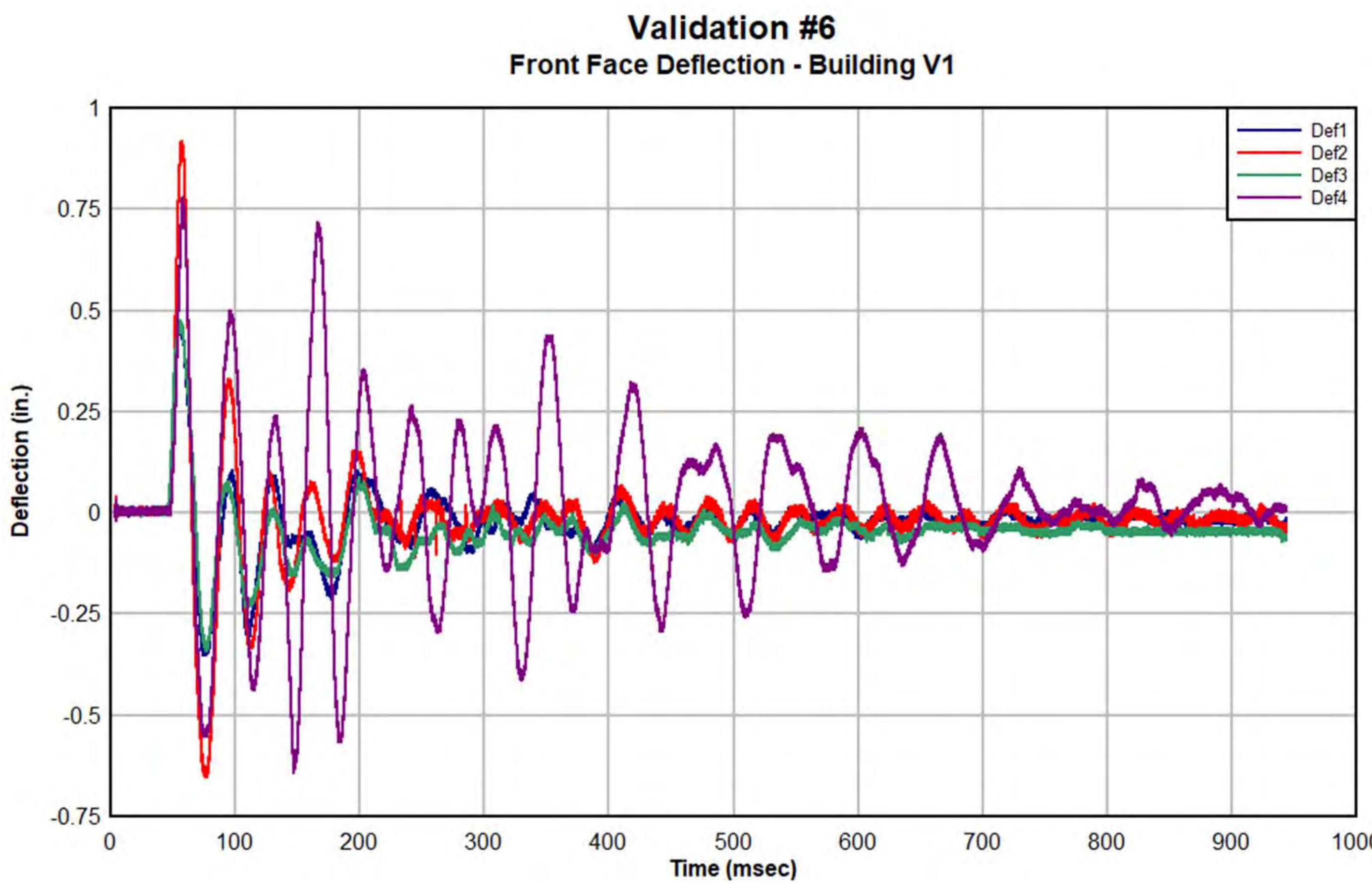

Validation #6 – Building V1: Side Face Deflection Gauges

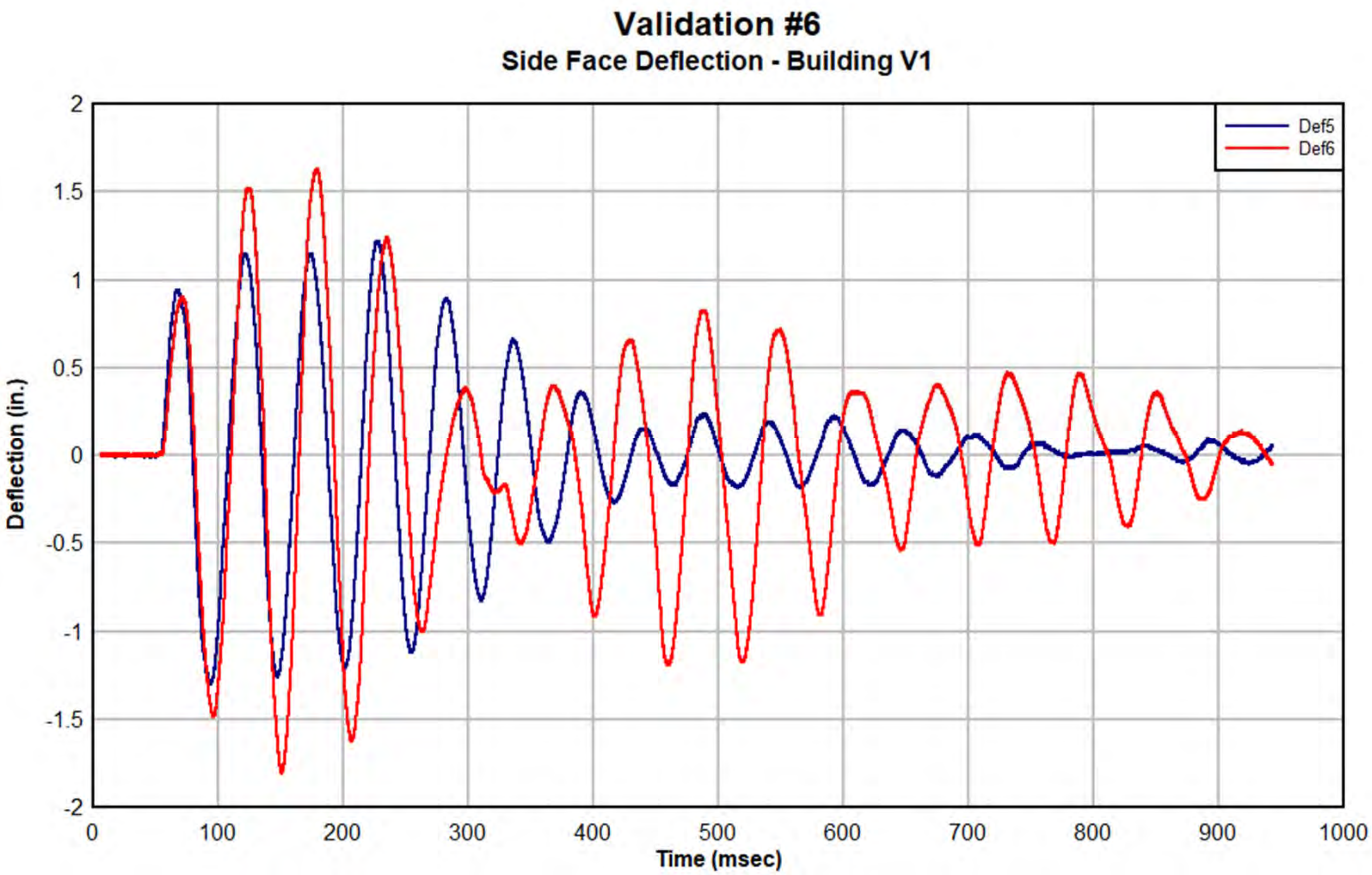

Validation #6 – Building V1: Acceleration Gauge

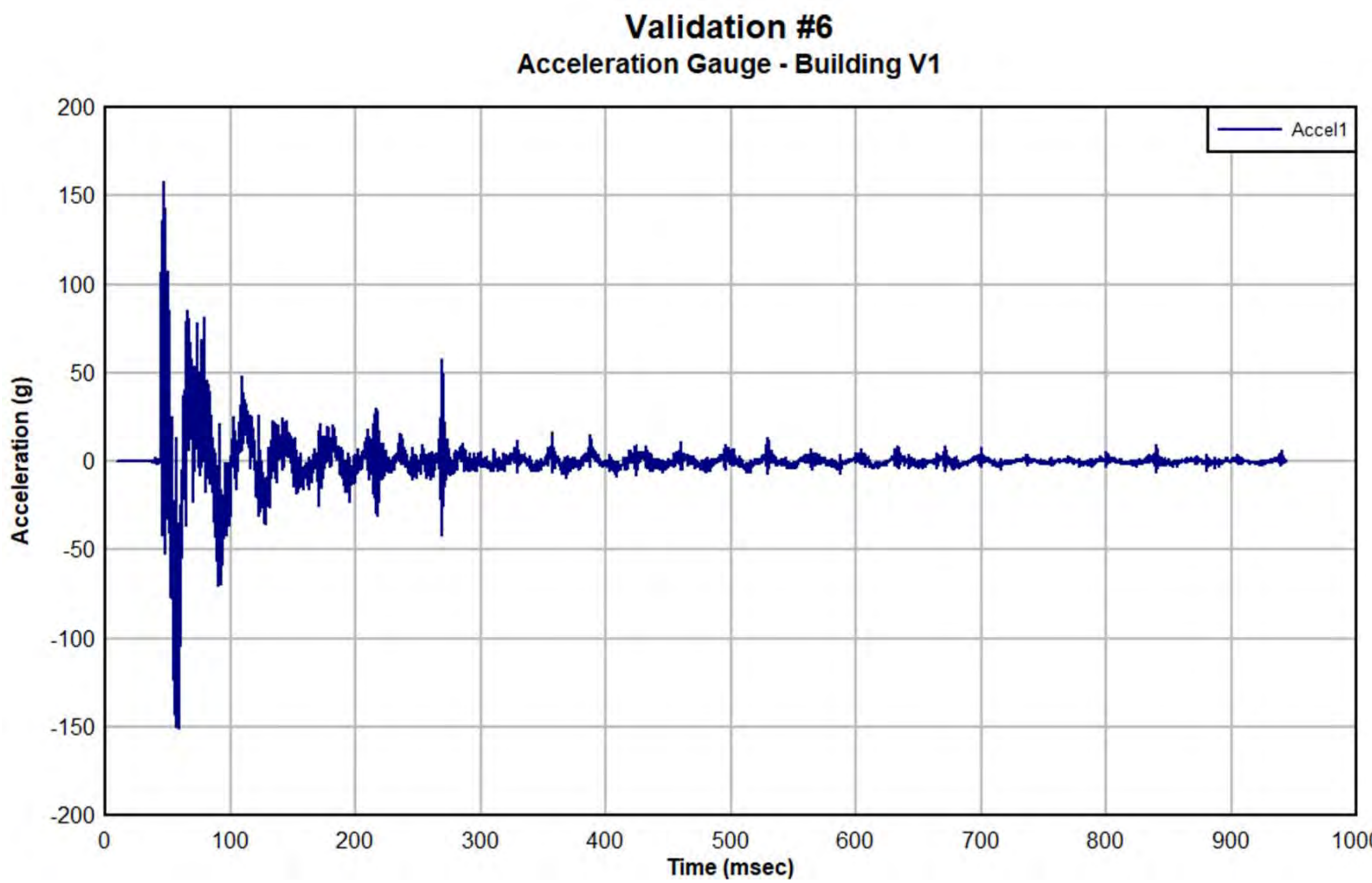

Validation #6 – Building E1: Front Face Reflected Pressure Gauges

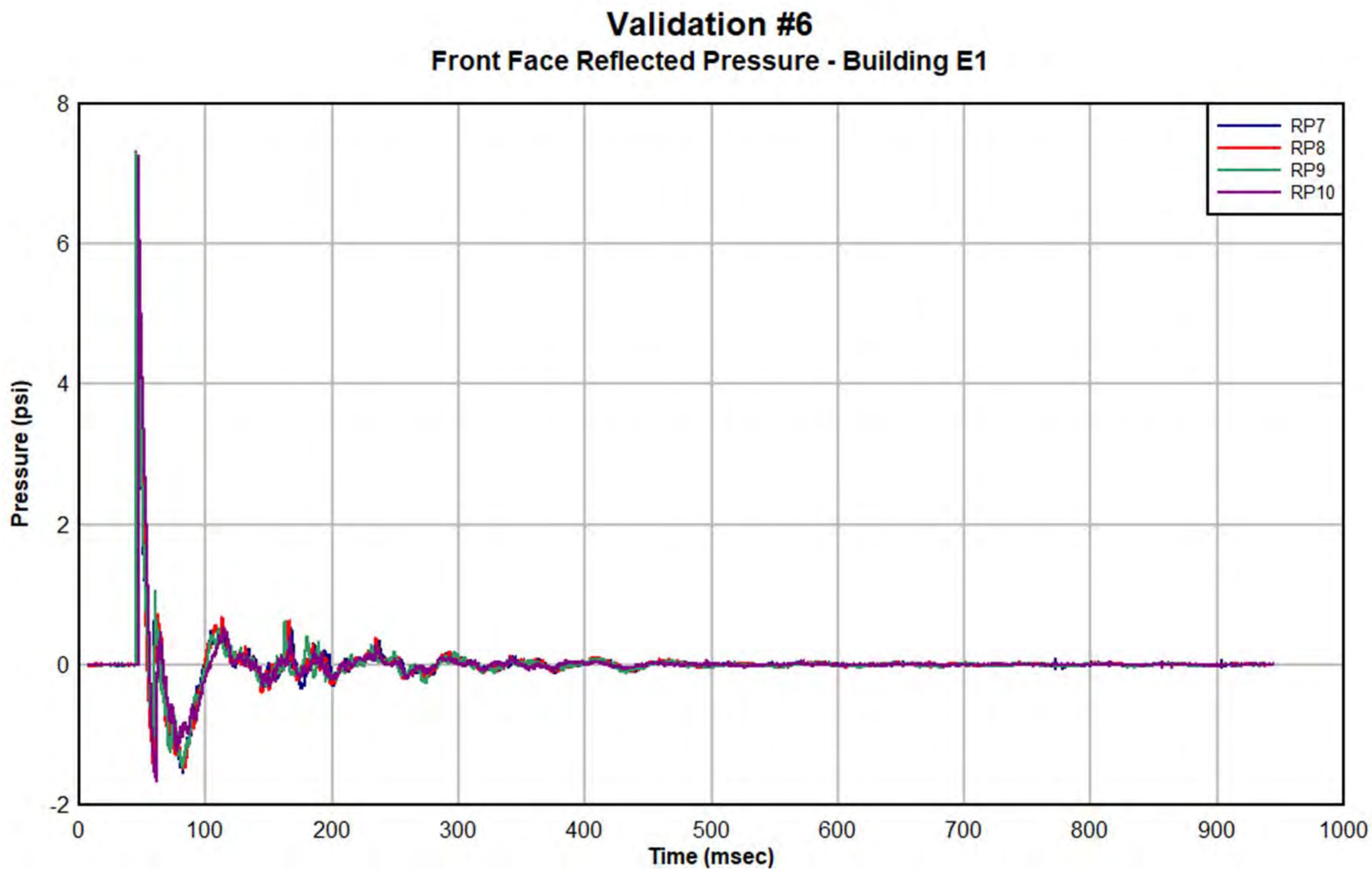

Validation #6 – Building E1: Side Face Incident Pressure Gauges

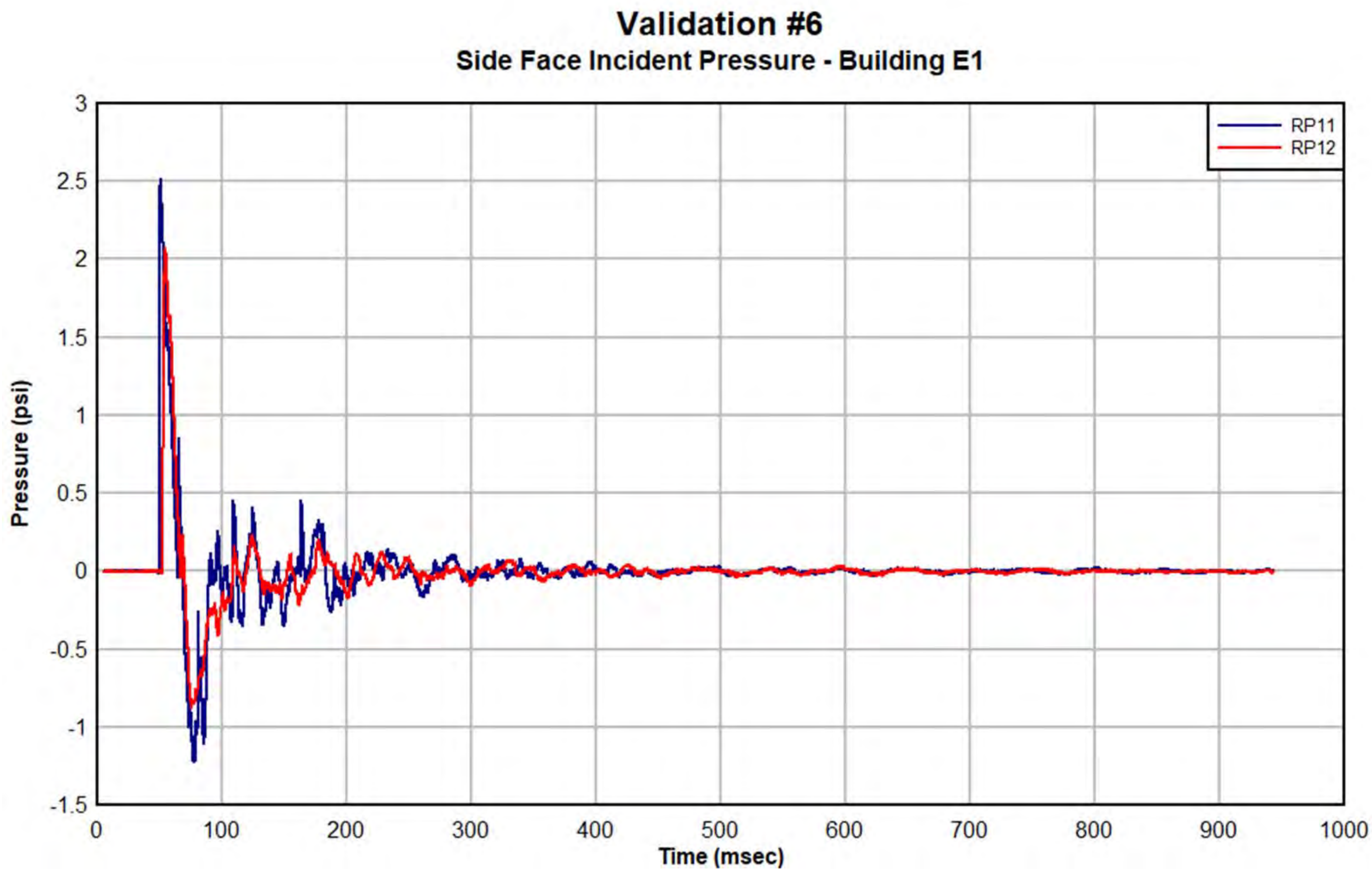

Validation #6 – Building E1: Front Face Deflection Gauges

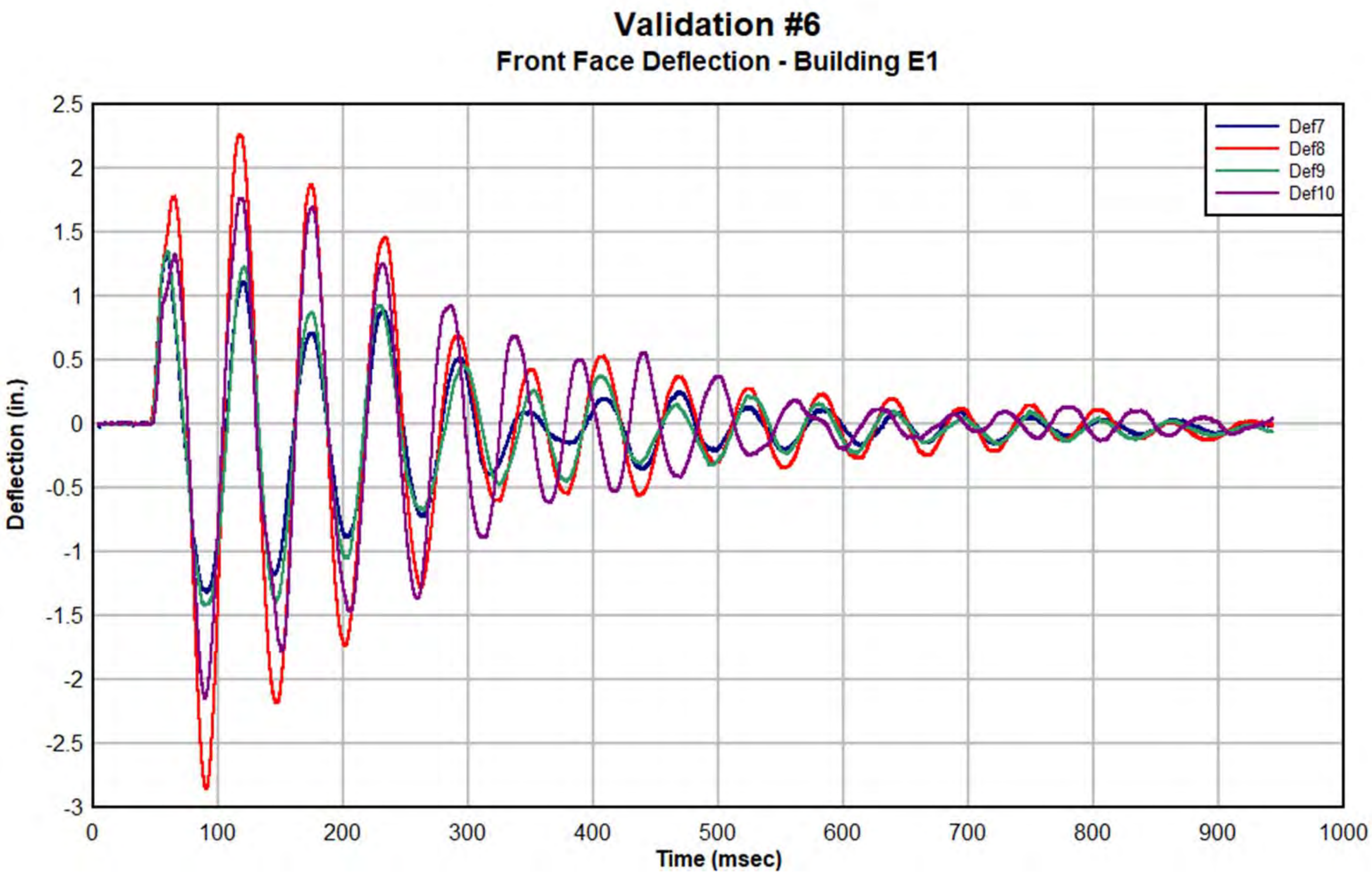

Integrity - Service - Excellence

Validation #6 – Building E1: Left Side Face Deflection Gauges

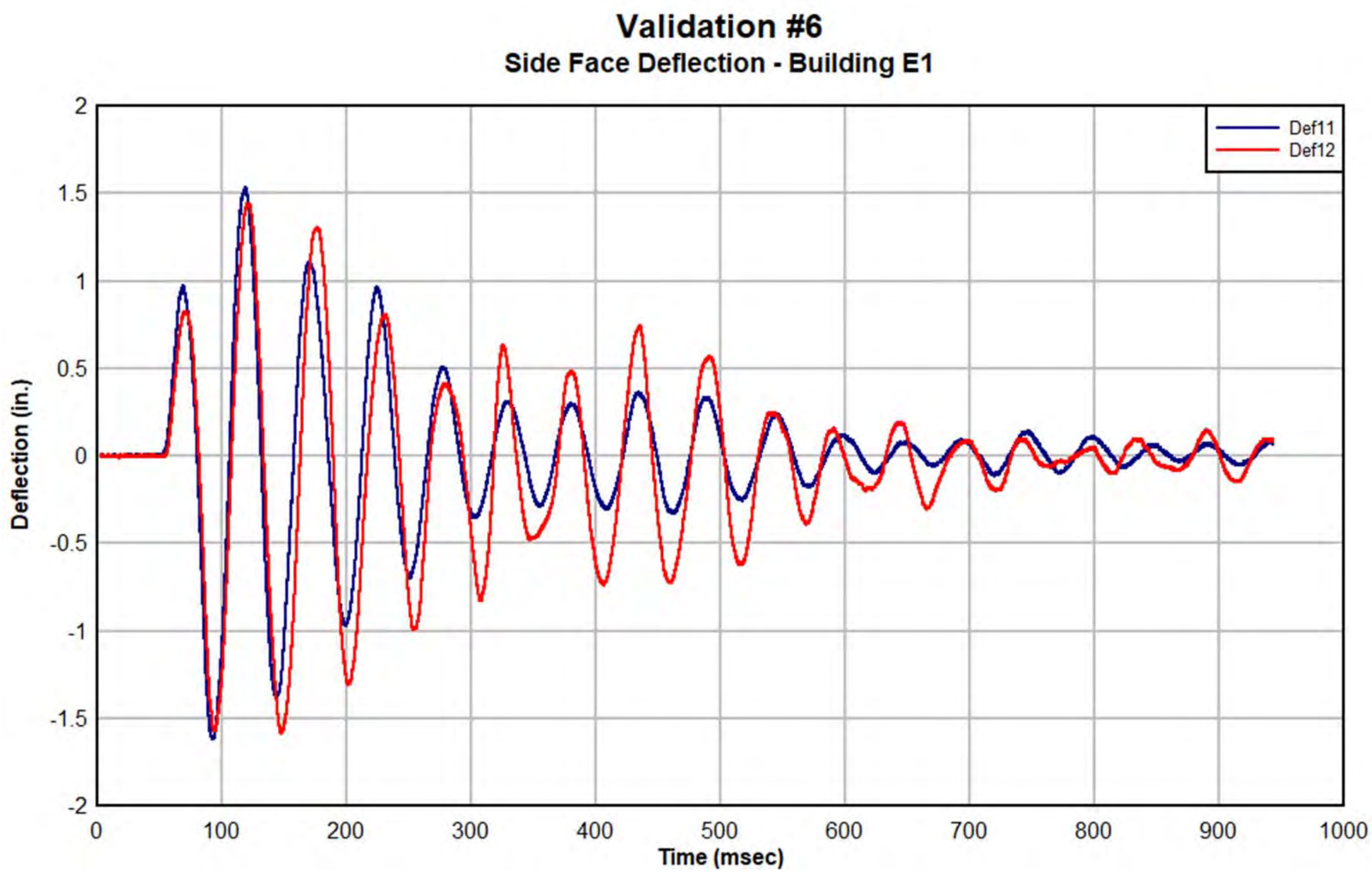

Validation #6– Building E1: Acceleration Gauge

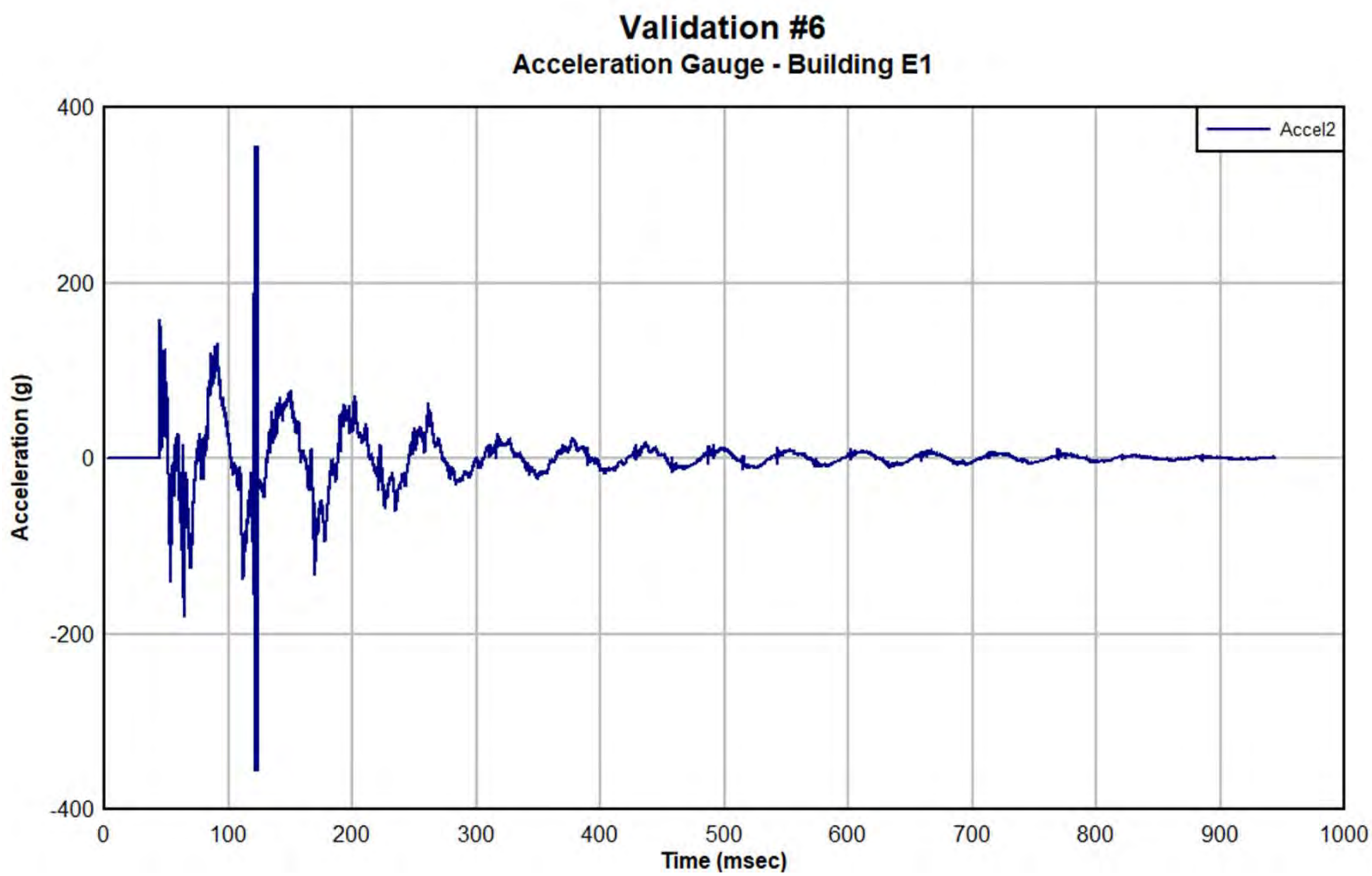

Validation #6 – Building V4: Front Face Reflected Pressure Gauges

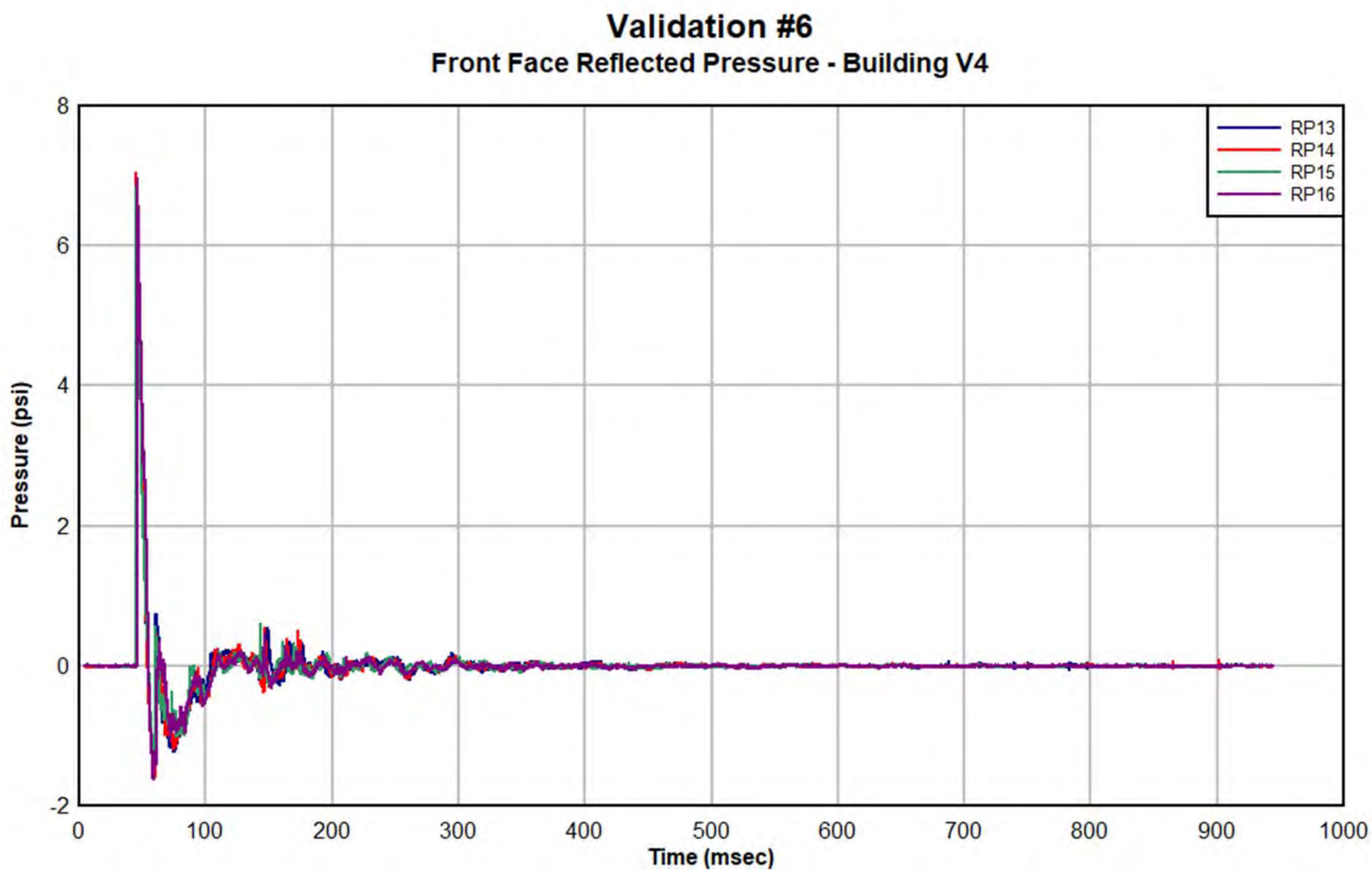

Validation #6 – Building V4: Side Face Incident Pressure Gauges

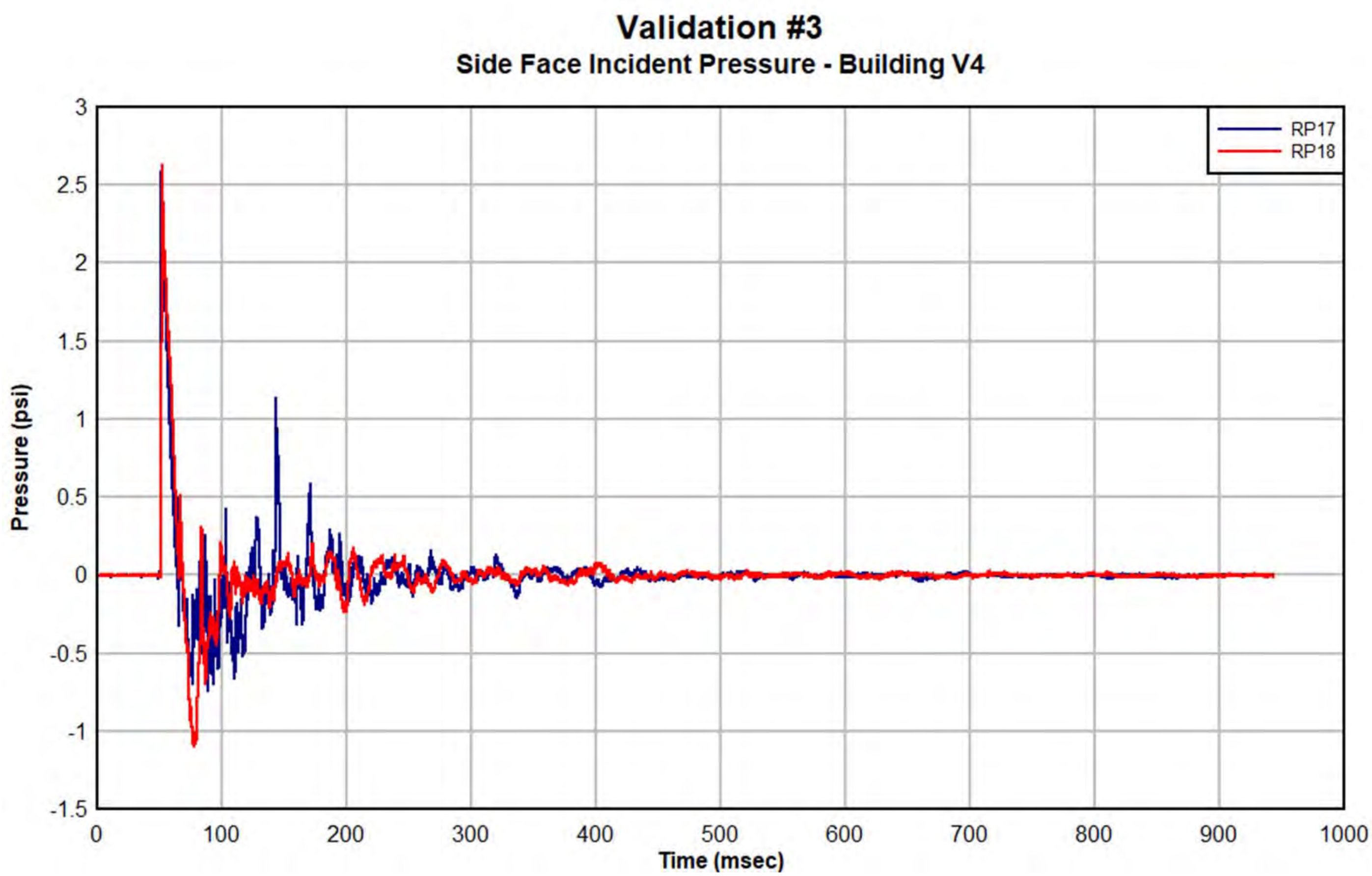

Validation #6 – Building V4: Front Face Deflection Gauges

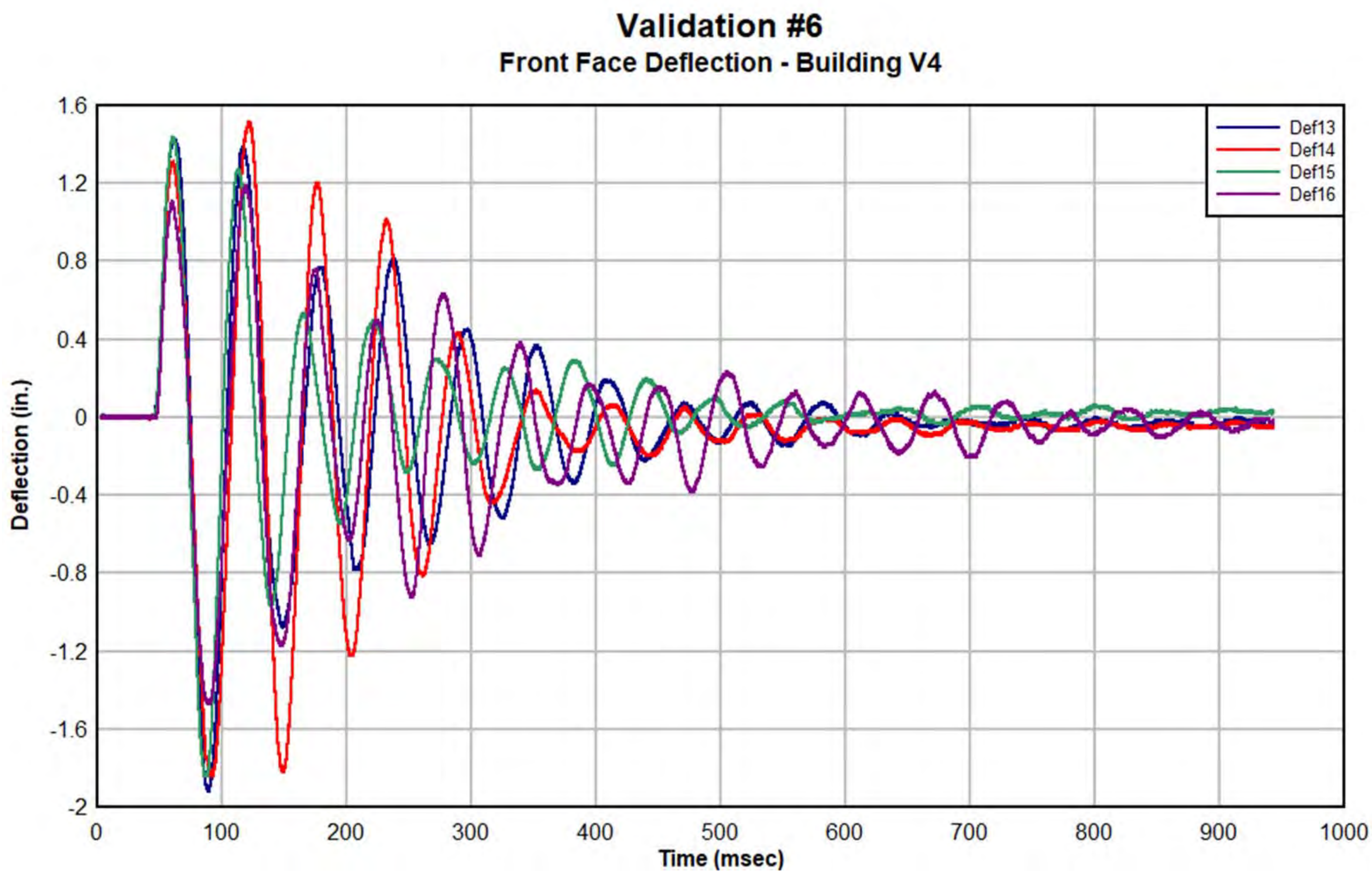

Integrity - Service - Excellence

Validation #6 – Building V4: Side Face Deflection Gauges

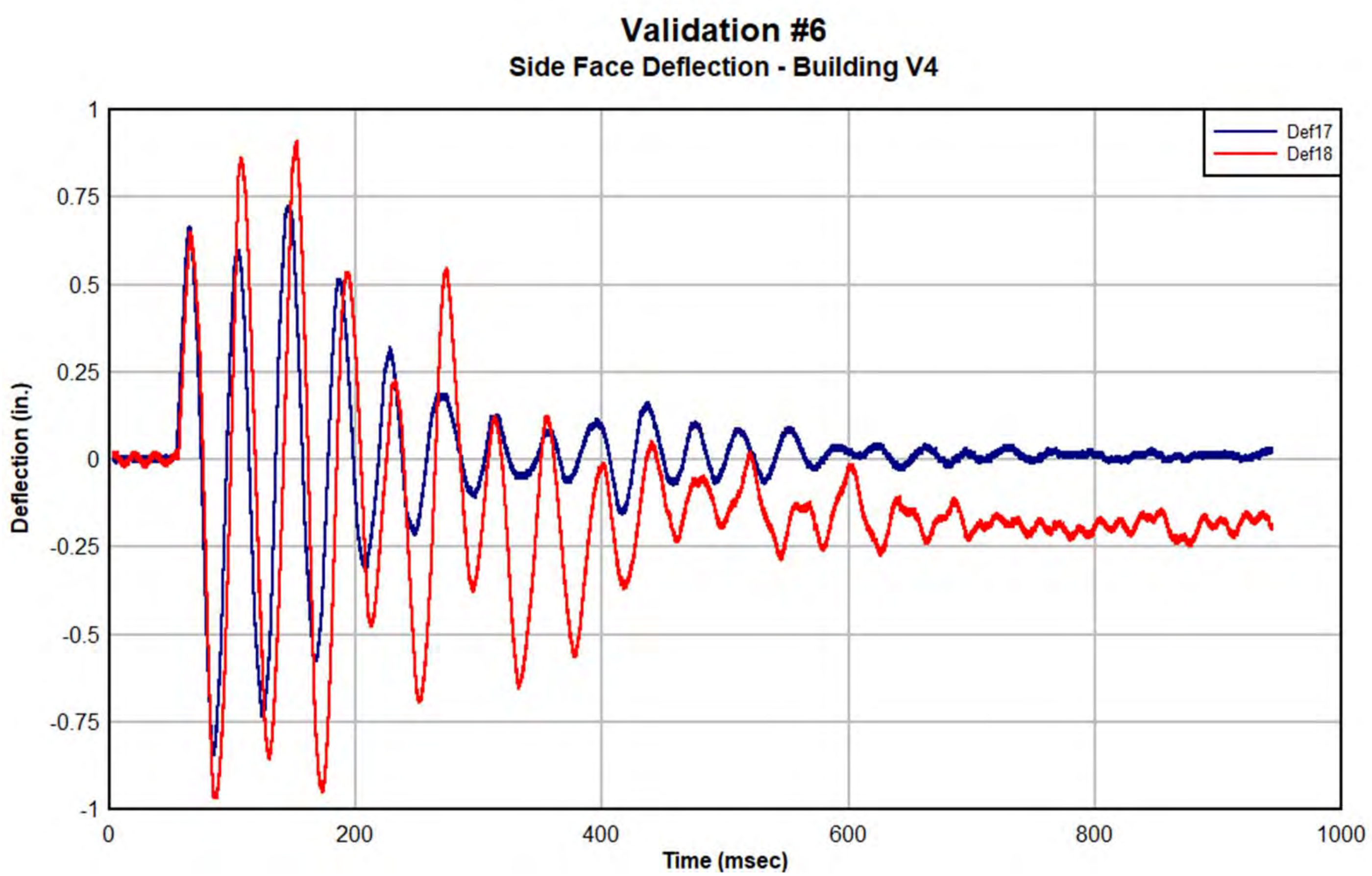

Validation #6: Free Field Incident Pressure Gauges

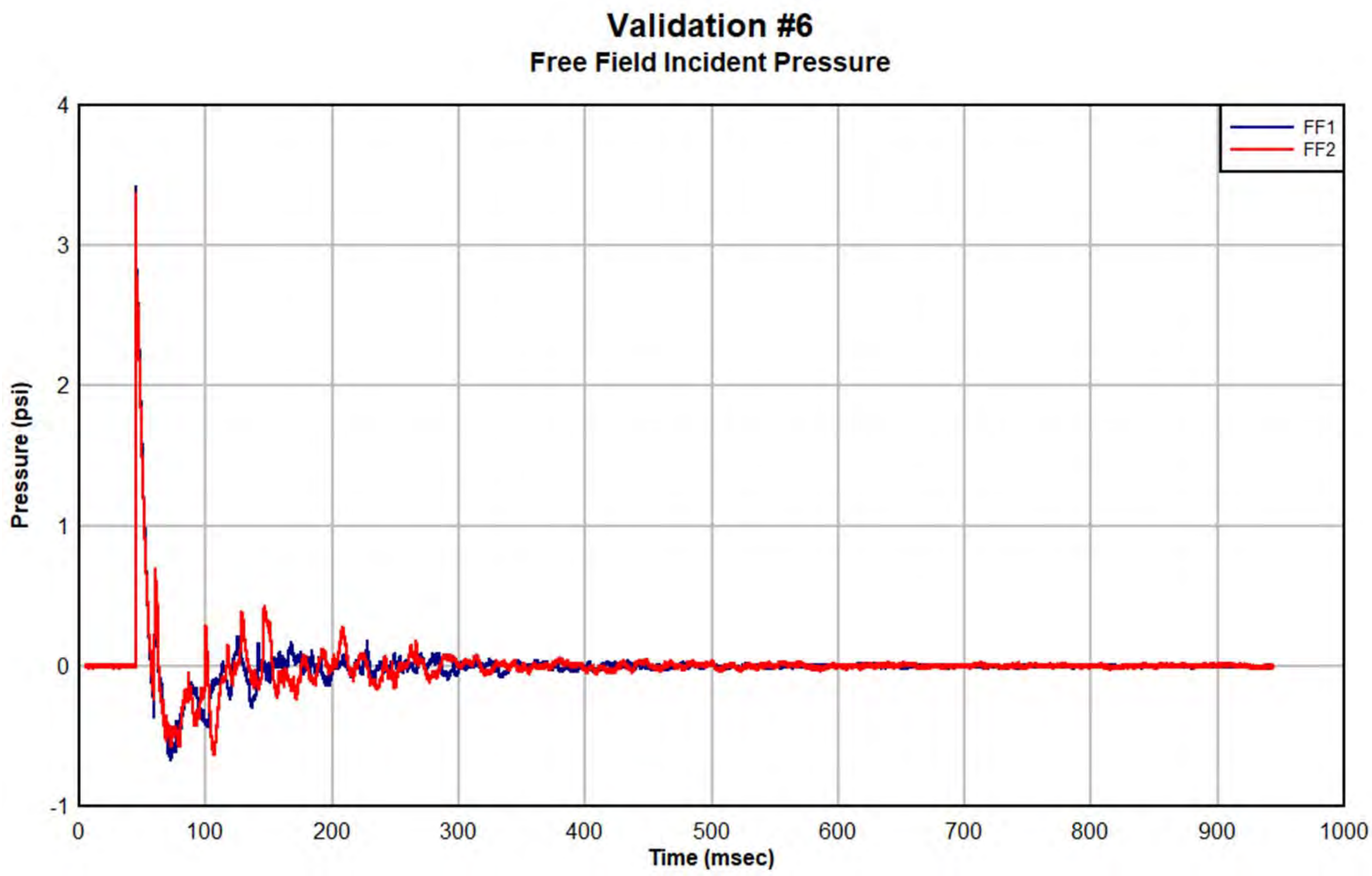

Full-Scale Validation #7

Post-test

Validation #7: Front Face Reflected

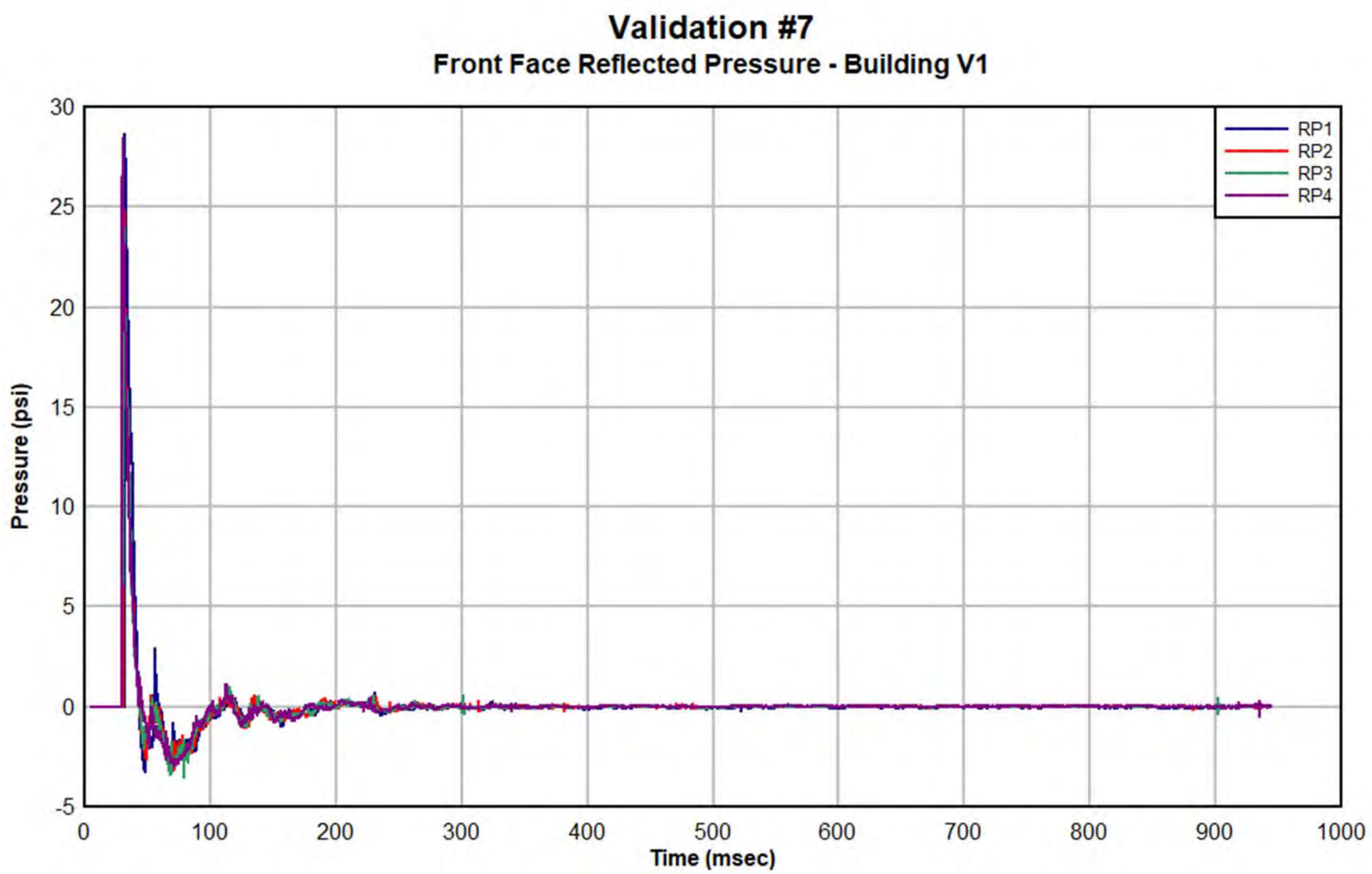

Validation #7:
Side Face Incident

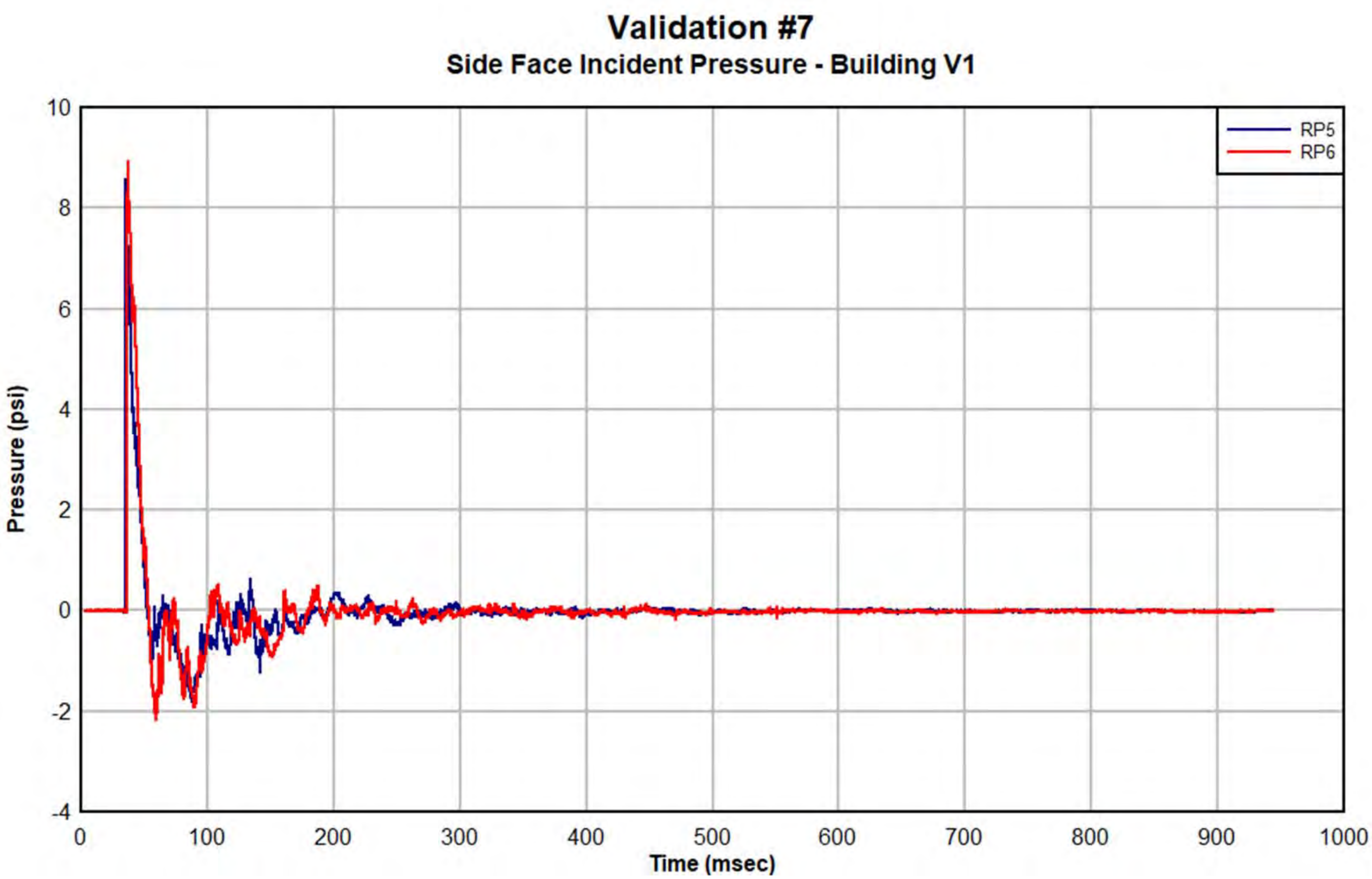

Integrity - Service - Excellence

Validation #7: Front Face Deflection

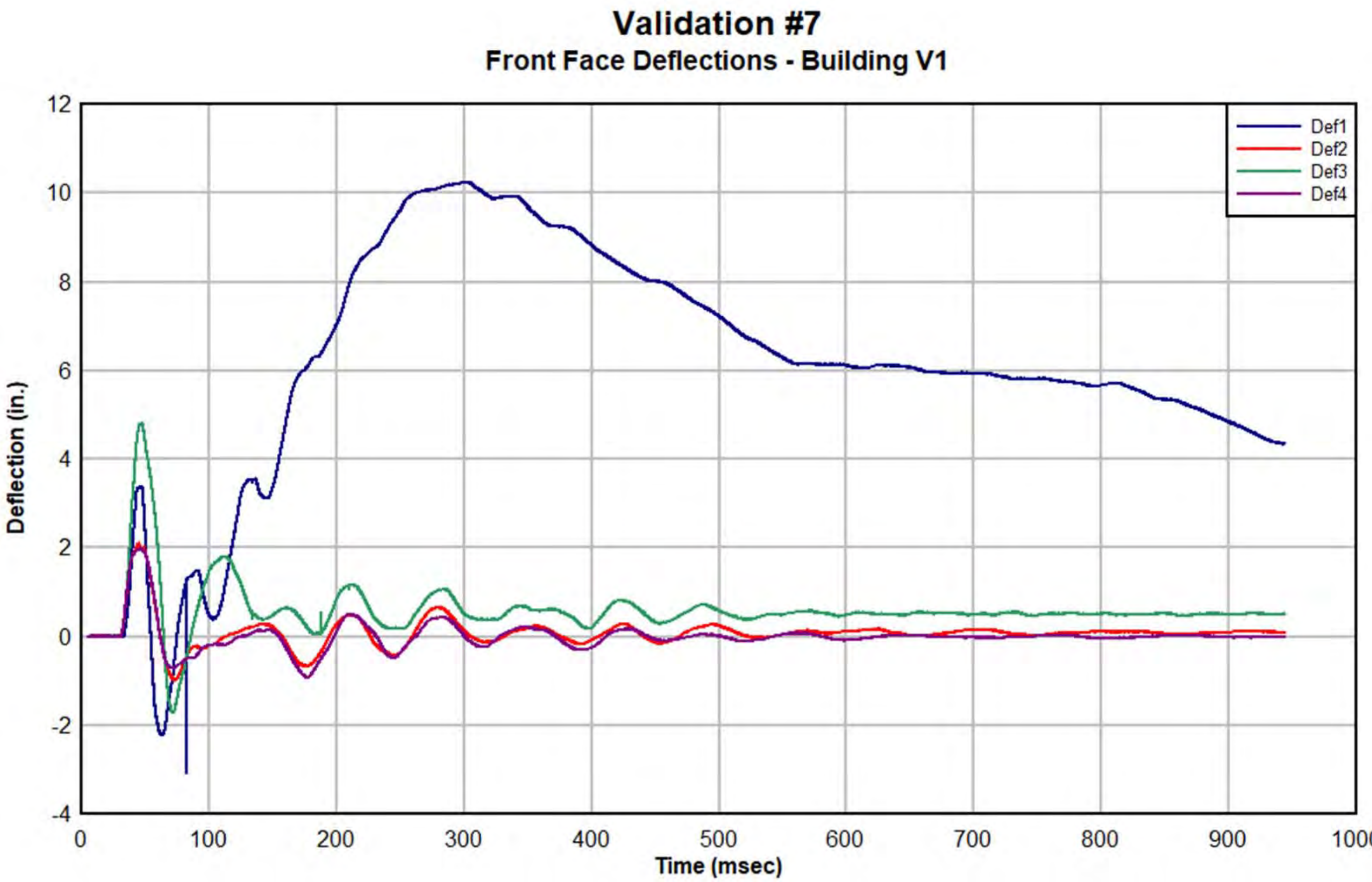

Integrity - Service - Excellence

Validation #7: Side Face Deflection

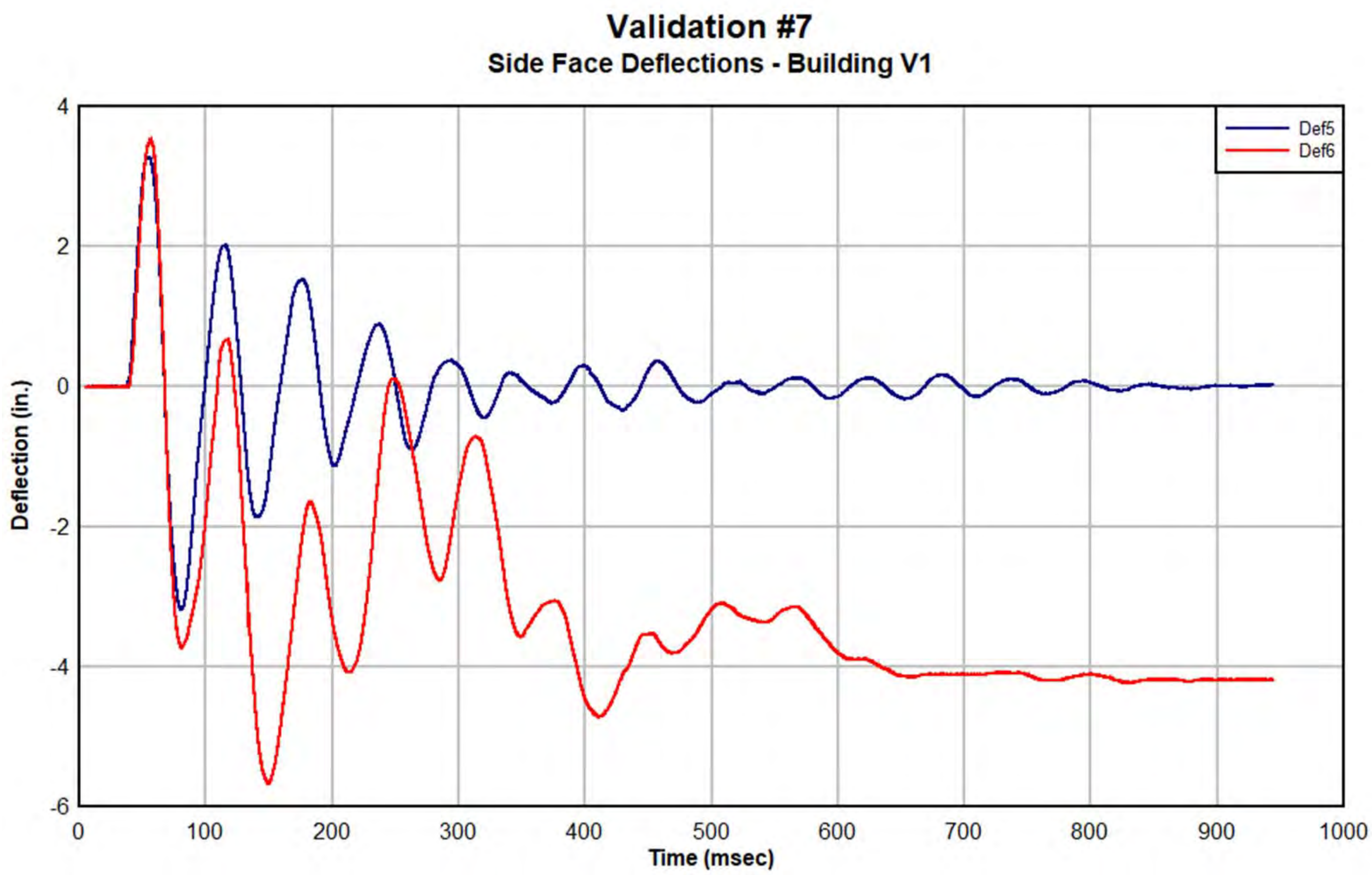

Integrity - Service - Excellence

Validation #7: Acceleration Gauge

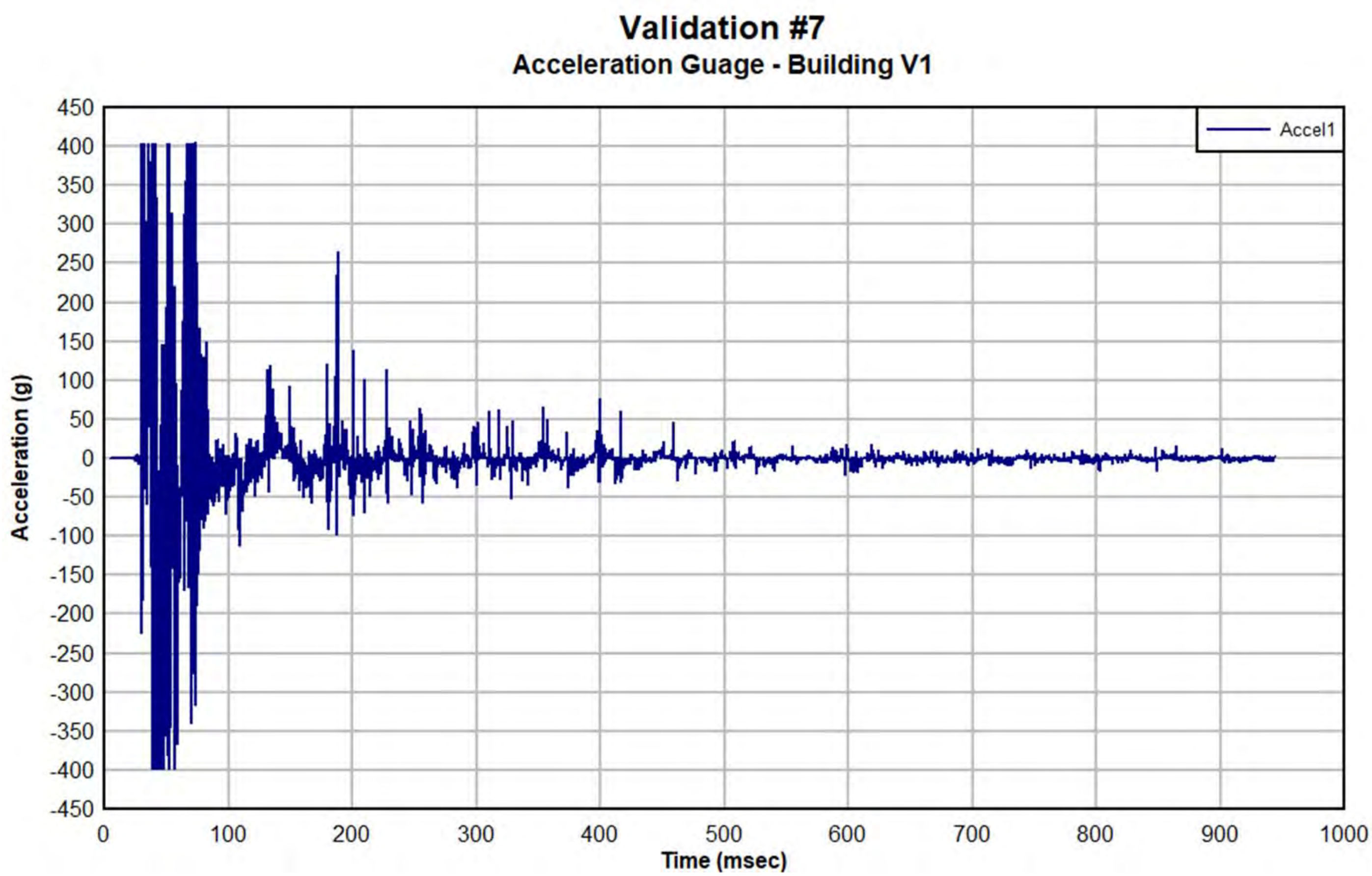

Validation #7: Free Field Incident

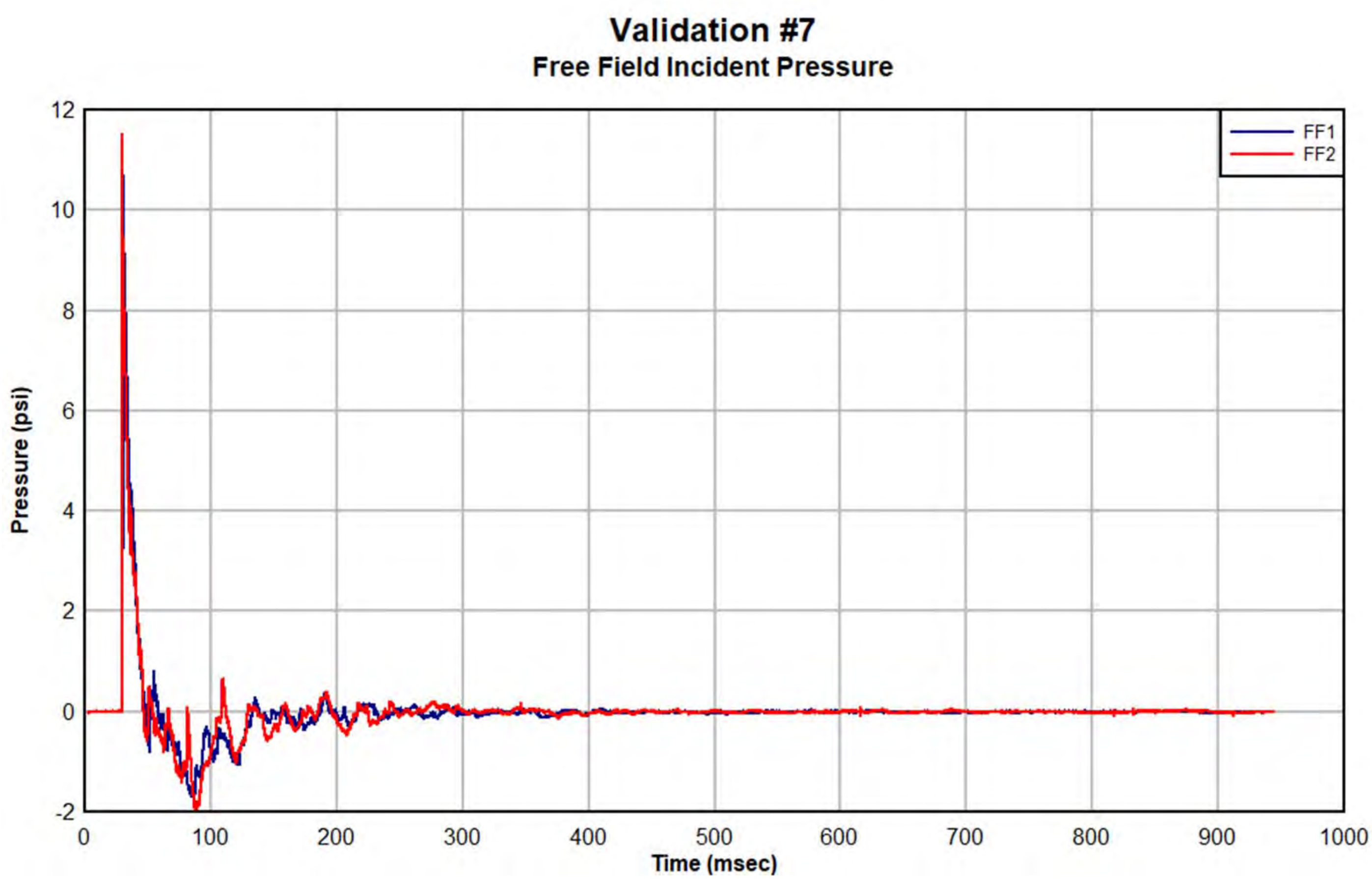

I n t e g r i t y - S e r v i c e - E x c e l l e n c e